

**OLIGOMERIC ETHYLENE GLYCOLS AS SORTING TAGS
FOR COMBINATORIAL SYNTHESIS**

by

Serhan Türkyılmaz

B.S. in Chemistry, 1996, Orta Doğu Teknik Üniversitesi, Ankara, Turkey

Submitted to the Graduate Faculty of
Arts and Sciences in partial fulfillment
of the requirements for the degree of
Doctor of Philosophy

University of Pittsburgh

2007

UNIVERSITY OF PITTSBURGH
FACULTY OF ARTS AND SCIENCES

This dissertation was presented

by

Serhan Türkyılmaz

It was defended on

July 13, 2007

and approved by

Eric J. Beckman, Professor, Department of Chemical Engineering

Toby M. Chapman, Associate Professor, Department of Chemistry

Dennis P. Curran, Professor, Department of Chemistry

Dissertation Advisor: Craig S. Wilcox, Professor, Department of Chemistry

Copyright © by Serhan Türkyılmaz

2007

OLIGOMERIC ETHYLENE GLYCOLS AS SORTING TAGS FOR COMBINATORIAL SYNTHESIS

Serhan Türkyılmaz, PhD

University of Pittsburgh, 2007

Certain problems associated with the nature of solid phase combinatorial synthesis has prompted the search for alternative methods. Among these, fluororous mixture synthesis (FMS) has emerged as a powerful method for solution phase combinatorial synthesis. In FMS each unique substrate is tagged with a perfluorinated alkane of unique length. These tagged substrates are mixed and taken through the desired synthetic steps. The final products are then subjected to fluororous chromatography. Elution order is directly proportional to fluororous tag length. Thus such fluororous tags could be regarded as sorting tags. Other classes of sorting tags which are separable under orthogonal conditions to those of fluororous tags would significantly increase the potential of this approach. In this study it has been demonstrated that oligomeric ethylene glycol (OEG) derivatives constitute a new class of sorting tags. OEG esters were separable using normal phase high performance liquid chromatography (NPLC). Separation was primarily dictated by OEG chain length with elution order being directly proportional to that length. Within those separatory regions the nature of the parent substrate played a secondary role, further improving separation. It has also been demonstrated that complexation chromatography employing silica gel containing lithium chloride further enhanced peak resolution. OEGylated (pronounced “ōēgē’lā’tēd”) analogues of benzyl alcohol have been prepared. Reversed phase high performance liquid chromatography has been found to emphasize the chromatographic nature of the parent substrate while still enabling OEG based separation. The elution order with

respect to OEG chain length was found to be the opposite of that in NPLC. Enthalpy-entropy compensation has been demonstrated for all OEG chain lengths indicating the same retention mechanism for all of the esters studied. These findings suggest that a two-tier separation approach-first RPLC then NPLC-could significantly increase the number of OEGylated substrates that can be subjected to mixture synthesis. OEGylated Evans Auxiliaries (OEG-EAs) have been prepared and applied to mixture *syn*-aldol reactions to demonstrate the synthetic utility of OEG-based sorting tags. OEGs have been found to be inert under the reaction conditions employed in the preparation of and application of OEG-EAs. The aldol products were obtained with good yield, high purity and high enantiomeric excess.

TABLE OF CONTENTS

PREFACE.....	XVIII
1.0 INTRODUCTION	1
1.1 LIQUID PHASE COMBINATORIAL SYNTHESIS (LCPS).....	2
1.2 SOLUTION PHASE COMBINATORIAL SYNTHESIS.....	6
1.2.1 Indexed Combinatorial Libraries	6
1.2.2 Combinatorial Libraries Based on Templates and Liquid-Liquid Purification 9	
1.3 FLUOROUS CHEMISTRY	11
1.3.1 Some General Issues in Fluorous Chemistry	13
1.3.2 Fluorous Catalysts, Reagents, and Scavengers.....	14
1.3.3 Fluorous Phase Tags for Reactants.....	18
1.3.4 Fluorous Mixture Synthesis Using Fluorous Sorting Tags.....	20
1.3.5 Comments on Fluorous Synthesis.....	27
2.0 OLIGOMERIC ETHYLENE GLYCOL (OEG) DERIVATIVES AS SORTING TAGS 29	
2.1 THE CASE FOR SORTING TAGS BASED ON OLIGOMERIC ETHYLENEGLYCOL.....	29
2.2 NORMAL PHASE CHROMATOGRAPHIC BEHAVIOR OF OEG ESTERS	32

2.2.1	Preparation of OEG Esters.....	32
2.2.2	NPLC Retention of OEG Esters	34
2.2.2.1	Effect of Group IA Cations on the NPLC Retention of OEG Esters....	41
2.2.2.2	The Retention Mechanism of OEG Derivatives on Silica Stationary Phases	45
2.3	OEGYLATED PROTECTING GROUPS AND THE EFFECT OF DOUBLE OEGYLATION	48
2.3.1	Design of Protecting Groups Based on Vanillic Acid	48
2.3.2	Synthetic Work	50
2.3.3	Separation of Double OEGylated Esters using NPLC and Li-TLC	54
3.0	REVERSED PHASE CHROMATOGRAPHY OF OEGYLATED ESTERS	58
3.1	GENERAL CONSIDERATIONS	59
3.2	CALCULATION OF THE PHASE RATIO (β)	64
3.3	THE QUESTION OF SILANOL ACTIVITY	65
3.4	EFFECT OF WATER CONCENTRATION ON RETENTION	69
3.5	EFFECT OF TEMPERATURE ON RETENTION	79
3.6	THE QUESTION OF ENTHALPY ENTROPY COMPENSATION.....	84
3.7	EFFECT OF LITHIUM CATIONS ON RETENTION	91
3.8	MECHANISTIC CONSIDERATIONS AND CONCLUSION.....	93
3.8.1	Effect of Mixture Injections and Hydrogen Bonding with the Stationary Phase on Retention.....	93
3.8.2	Effect of the Presence of Capping Groups on Retention Order of OEGylated Compounds	94

3.8.3	Effect of Conformational Changes of the OEG Chains on Retention	96
3.8.4	Discussion of ΔH° , ΔS° and EEC Through Comparison with Methylene Homologues	105
3.8.5	Conclusion	109
4.0	PREPARATION AND APPLICATION OF OEGYLATED EVANS AUXILIARIES	111
4.1	OBJECTIVES.....	112
4.2	PREPARATION AND ACYLATION OF OEGYLATED EVANS AUXILIARIES.....	113
4.3	ASYMMETRIC ALDOL REACTIONS USING OEGYLATED EVANS AUXILIARIES.....	118
4.4	STEREOCHEMICAL ANALYSIS OF ALDOL PRODUCTS	126
4.5	CONCLUSION.....	129
5.0	CONCLUSION AND FUTURE DIRECTIONS.....	130
6.0	EXPERIMENTAL	134
6.1	GENERAL.....	134
6.2	SYNTHETIC PROCEDURES	135
6.3	HPLC EXPERIMENTS.....	183
6.3.1	General.....	183
6.3.2	NPLC Retention of OEG Esters	185
6.3.2.1	Supelcosil Silica Column.....	185
6.3.2.2	VersaPak Silica Column.....	187
6.3.2.3	Cyclobond-I Cyclodextrin Column	188

6.3.3	Retention of DiOEGylated Esters on Silica.....	189
6.3.4	NPLC Analysis of OEGylated Aldol Adducts.....	191
6.3.5	Chiral HPLC Analysis of 132a-d.....	193
6.4	TLC EXPERIMENTS	195
6.4.1	Preparation of TLC Plates and Method of Data Acquisition.....	195
6.4.2	Determination of Salt Concentration on TLC Plates	195
6.4.3	Optimization of LiCl Concentration on TLC Plates.....	196
6.4.4	Effect of Cation Identity, and Solvent Composition on Retention of OEG Esters on Silica TLC Plates.....	197
6.4.5	Effect of LiCl on the Retention of DiOEGylated Esters.....	197
APPENDIX A.....		198
BIBLIOGRAPHY.....		200

LIST OF TABLES

Table 2-1: Percent Yields for Esterification under Various Conditions.....	34
Table 2-2: t_R , k' , N , and R_s values for the chromatogram in Figures 2-4 and 2-7.....	38
Table 2-3: Stability constants of complexes of glymes with Li^+ , and Na^+	42
Table 2-4: Separation of esters 75b-e by TLC under various conditions.....	44
Table 2-5: Chromatographic parameters for Figure 2-19.....	55
Table 2-6: R_f values for esters 89e-g , and 93a-95c on LiCl treated, and untreated silica TLC plates.....	57
Table 3-1: k' , and α values for the elution of esters 72a-75e with varying water concentrations in the mobile phase (298 K).....	71
Table 3-2: ΔG° values for the retention of esters 72a-75e	73
Table 3-3: Regression parameters for plots of ΔG° versus degree of polymerization for esters 72a-75e	74
Table 3-4: Regression parameters for plots of ΔG° versus % water (v/v) in mobile the phase for 72a-75e	76
Table 3-5: Regression parameters for $\log P$ versus $\ln k'$ plots for esters 72a-75e	78
Table 3-6: k' , and α values for esters 72a-75e between 298-318 K.....	80

Table 3-7: ΔH° , ΔS° , and $T\Delta S^\circ$ (at 298 K) values from the Van't Hoff plots of esters 72a-75e .	.81
Table 3-8: ΔH_{EG}° , ΔH_S° , ΔS_{EG}° , and ΔS_S° values for 72a-75e obtained from ΔS_S° versus DP and ΔH° versus DP plots.	83
Table 3-9: Regression parameters of ΔH° versus ΔG° plots and Θ values for esters 72a-75e .	87
Table 3-10: Θ ranges for esters 72a-75e obtained through the <i>t</i> -test at the 95 % confidence level.	90
Table 3-11: ΔH^0 , ΔS^0 and T_c values for some methylene homologues and compounds with structural similarity.	107
Table 4-1: Chromatographic parameters for the peaks in Figure 4-12.	124
Table 4-2: Optical Rotation and spin-spin coupling values for 131a-132d .	127
Table 4-3: Relevant chromatographic data for the chromatograms in Figures 4-15.	129
Table 6-1: t_R (retention time), k' (retention factor), N (number of theoretical plates), R_s (resolution factor), and symmetry values for the chromatogram obtained with the 5 μ Supelcosil column.	186
Table 6-2: Standard deviation for retention times of OEG esters 72b-75e on the Supelcosil column.	187
Table 6-3: t_R , k' , N , R_s , W_A , $w_{1/2}$, and symmetry values for the chromatogram obtained with the Alltech/Applied Science 10 μ , 300 x 4.1 mm VersaPak silica column.	188
Table 6-4: t_R , k' , R_s , N , and symmetry values for the chromatogram in Figure 6-4.	191

Table 6-5: Determination of elution order of 89e-g , and 93a-95c through averaging of a number of HPLC experiments.	191
Table 6-6: Chromatographic parameters for the peaks in Figure 6-5.....	192
Table 6-7: Chromatographic parameters for the chiral separation of 132a-d	193
Table 6-8: Salt concentrations on TLC plates.....	196
Table 6-9: Optimization of [LiCl] for optimum separation of OEG esters.	196
Table 6-10: Separation of esters 75a-d by TLC under various conditions.....	197
Table 6-11: R _f values, standard deviations, and % standard deviations for esters 89e-g , and 93a-95c on silica TLC plates dried after immersion into 0 M, and 2.6 M aqueous LiCl solutions.	197

LIST OF FIGURES

Figure 1-1: Some supports used in LPS and LCPS.	3
Figure 1-2: Synthesis (A) and recursive deconvolution (B) of a hypothetical 27-member tripeptide library.....	4
Figure 1-3: Parallel synthesis of aminobenzimidazole using MPEG as a soluble polymer support.....	5
Figure 1-4: Preparation and assay of 54 carbamates using the ICL method.	7
Figure 1-5: Preparation and assay of a 42-member ICL of (-)-stipiamide analogues.	8
Figure 1-6: Preparation of a 27-member combinatorial library based on a template and purification via acid/base extraction.....	10
Figure 1-7: Some templates used in template based synthesis.	11
Figure 1-8: Temperature dependence of the solubility of <i>c</i> -C ₆ F ₁₁ CF ₃ (PFMC) in a mixture of <i>n</i> -hexane and toluene.....	14
Figure 1-9: Some strategies in fluorous synthesis.	15
Figure 1-10: Examples of reactions employing fluorous reagents.	16
Figure 1-11: Some fluorous reagents and catalysts.	18
Figure 1-12: Some fluorous protecting groups.....	20
Figure 1-13: The FMS strategy.....	21

Figure 1-14: Retention of some fluorinated substrates on FRP silica and C18 stationary phases.	22
Figure 1-15: FMS of mappicine derivatives.	23
Figure 1-16: Chromatogram of 4 fluorous sorting tag bearing mappicine derivatives on FRP silica.	23
Figure 1-17: Separation of 12 acrylate-thiol conjugate addition products on FRP silica.	24
Figure 1-18: FMS preparation of discodermolide analogues.	25
Figure 1-19: FMS of tripeptides.	27
Figure 2-1: Comparison of the efficiencies of tagged mixture synthesis and parallel mixture synthesis.	31
Figure 2-2: OEG esters used in HPLC studies.	33
Figure 2-3: ¹ H-NMR spectrum for ester 73c	34
Figure 2-4: Chromatogram for esters 72b-e , 73c-e , 74c-e , 75b-e , and 76b-e	36
Figure 2-5: Real-time UV/Vis spectra for 72b-e , 73c-e , 74c-e , 75b-e , and 76b-e	36
Figure 2-6: Isocratic elution of 72b-e	39
Figure 2-7: Retention of OEG esters 72b-76e on a VersaPak column.	40
Figure 2-8: TLC results for esters 75b-e . Plates were immersed in 0, 1.3, 2.6, 3.9, and 5.2 M aqueous LiCl solutions and dried prior to analyte application and development with EtOAc.	44
Figure 2-9: Equilibria affecting OEG ester retention on silica.	45
Figure 2-10: Dipole moments for methyl esters 72-76a.	47
Figure 2-11: Dipole moment versus relative retention time plots for peaks within each separatory region 1-4 (A-D) for the chromatogram in Figure 2-4.	47
Figure 2-12: Rethrosynthetic strategy for sorting tags based on vanillic acid.	49

Figure 2-13: Effect of preorganization on the ion binding ability of some OEG derivatives.	50
Figure 2-14: Preparation of 87b-d and 89a-g	51
Figure 2-15: Preparation of 79a-d and 78a-d	52
Figure 2-16: Employment of 78a-d in the mixture synthesis of stereoisomers of murisolin.	52
Figure 2-17: Preparation of 90a-d , 91a , and 91c	53
Figure 2-18: Preparation of 93a-c , 94a-c , and 95a-c	54
Figure 2-19: Chromatogram for the elution of a mixture of double OEGylated esters.	55
Figure 2-20: Retention times for 89e-g , 93a-c , 94a-c , and 95a-c	55
Figure 3-1: Esters employed in RPLC studies.	59
Figure 3-2: A. Types of surface silanols in silica. B. CPK model of TMS derivatized silica. ⁸ C. Structure of a typical TMS-capped C18 column.	66
Figure 3-3: Elution of phenol and aniline on a Microsorb MV C18 column.	67
Figure 3-4: Expected shapes of $\ln k'$ versus $\Psi(A)$ and Van't Hoff (B) plots under conditions where significant silanol activity is present.	69
Figure 3-5: Chromatograms for esters 75b-e for different mobile phase water concentrations (298 K).	70
Figure 3-6: $\ln k'$ versus mobile phase water concentration plots for esters 72a-75e (298 K).	72
Figure 3-7: Plots of ΔG° versus degree of polymerization for esters 72a-75e	75
Figure 3-8: Plots of ΔG° versus % water (v/v) in the mobile phase for esters 72a-75e	76
Figure 3-9: $\log P$ versus $\ln k'$ plots for esters 72a-75e	77
Figure 3-10: Effect of temperature on the retention of esters 75b-e	79
Figure 3-11: Van't Hoff plots for esters 72a-75e	81
Figure 3-12: Plots of ΔH° versus ΔS° for esters 72a-75e	85

Figure 3-13: ΔH° versus ΔG° plots for esters 72a-75e	87
Figure 3-14: Convergence of Van't Hoff plots for esters 72a-75e at Θ	89
Figure 3-15: The effect of LiCl on the retention of esters 72a-e	92
Figure 3-16: Elution orders of a number of capped and uncapped OEGs.....	96
Figure 3-17: The anti and gauche conformers of DME as suggested by theoretical work.....	98
Figure 3-18: Most stable conformers of DME and the experimental methods that can be used to determine them.....	99
Figure 3-19: Hydrogen bonding structures that may stabilize the gauche configuration around the C-C bond (A-C) and various conformations of OEGs (D-F).....	101
Figure 3-20: Van't Hoff plots for 72a-e and mono-capped OEGs.....	104
Figure 3-21: ΔH° versus DP and ΔS° versus DP plots for 72b-76e	105
Figure 3-22: Loss of water from an EG unit upon interaction with the stationary phase.....	108
Figure 4-1: Hypothetical transition states for the Evans aldol reaction.....	112
Figure 4-2: The strategy employed in this study.....	112
Figure 4-3: Some synthetic routes for the preparation of 103b	114
Figure 4-4: Preparation of 103a and 103b	115
Figure 4-5: Preparation of 114a-d and 115a-d	117
Figure 4-6: Poor yields obtained from the <i>syn</i> -aldol reactions of 115a using 1.1 eq Bu ₂ OTf...	119
Figure 4-7: Protolysis of the B-C bonds in boranes.....	120
Figure 4-8: Preparation of Et ₂ BOTf and Bu ₂ BOTf.....	120
Figure 4-9: Open and closed transition states in Bu ₂ BOTf promoted aldol reactions.....	121
Figure 4-10: Effect of equivalents of Bu ₂ BOTf on the % conversion of 115a	122
Figure 4-11: Optimized yields for Evans aldol reactions of 115a-d	123

Figure 4-12: Chromatogram and real-time UV-Vis spectrum for a mixture of 116a-d .	124
Figure 4-13: Hydrolysis of 116a-d and preparation of methyl esters from 131a-d .	125
Figure 4-14: Coupling constants for <i>syn</i> - and <i>anti</i> -aldol products.	126
Figure 4-15: Chromatograms for a sample consisting of an equimolar mixture of 132a-b (A), a sample consisting of 132a (B), a sample consisting of 132b (C), a sample consisting of an equimolar mixture of 132c-d (D), a sample consisting of 132c (E), and a sample consisting of 132d (F).	128
Figure 6-1: Definition of terms t_R , t_M , W_A , and $w_{1/2}$.	185
Figure 6-2: Chromatogram for samples 72b-76e on an Astec Cyclobond-I column.	189
Figure 6-3: Retention times for diOEGylated vanillic acid derivatives.	190
Figure 6-4: (Left) Elution of a mixture of 89e-g , and 93a-95c . (Right) Real-time UV-Vis spectra of the peaks.	190
Figure 6-5: Chromatogram for a mixture of 10^{-3} M each of 132a-d .	192
Figure 6-6: Chromatograms and real-time UV-vis spectra for a sample containing approximately equimolar amounts of 132a-b (A, A'), for a sample of 132a obtained as a product of the synthetic work (B, B'), and for a sample of 132b obtained as a product of the synthetic work (C, C').	194
Figure 6-7: Chromatograms and real-time UV-vis spectra for a sample containing approximately equimolar amounts of 132c-d (A, A'), for a sample of 132c obtained as a product of the synthetic work (B, B'), and for a sample of 132d obtained as a product of the synthetic work (C, C').	194

PREFACE

I would like to thank to Dr. Craig S. Wilcox for his expert guidance, kindness, endless patience, and support during my Ph.D. studies. His insight into and understanding of chemical phenomena are truly exceptional, and I have greatly benefited from them. He will be a role model whom I will always look up to.

I would like thank to Dr. Dennis P. Curran for helpful discussions and his support. I have benefited from discussions with Dr. Stephen G. Weber and would like to thank him as well. Past and present Wilcox group members have been great colleagues and I would like to thank them for their help and discussions on chemistry and politics. In particular I would like to thank to Dr. Cesar Raposo, Dr. Comfort M. Nkambule, Dr. Janet Asper, and Michael Martucci.

Last, but not least, I would like to thank to my wife Ayla for being a bright star on a cold, dark, and long winter night. Seni seviyorum.

This dissertation is dedicated to my parents, my wife Ayla, and soon-to-be son Ali Uğur.

1.0 INTRODUCTION

Since its invention by Merrifield, solid phase organic synthesis (SPOS) has been expanded in scope beyond peptide synthesis.¹ The use of insoluble polymeric beads as supports facilitates syntheses by rendering the substrates insoluble and thus reducing the purification process to simple filtration. This seminal technique has revolutionized the synthesis of large libraries of structurally diverse compounds. High throughput generation of libraries has been achieved through parallel synthesis, the split, and the split-and-mix strategies, the latter being enabled by the encoding of each bead with an identifying tag.^{2, 5c} Using this method peptide libraries containing millions of compounds have been prepared.^{3a, b}

While SPOS has unique advantages, it also has shortcomings. By definition reactions in SPOS are performed under heterogeneous conditions which complicate the kinetics of those reactions as well as rendering some substrates inaccessible to reagents employed. Reactions that require extremes of pressure, temperature, or other conditions that are not compatible with the solid supports, and/or with the linkers employed can not be used in SPOS. Loading capacities of polymeric beads are low, thus scaling is a significant problem, and only minute quantities of product are obtained. Reactions that create side products, or are not high yielding, significantly reduce the purity of compounds, which in turn makes the characterization, purification, and screening of products complicated. Since the substrates are bound to insoluble polymeric beads monitoring of reaction progress, and characterization of products without liberating them from the supports requires specialized techniques, and expensive equipment. SPOS equipment is highly dedicated, and expensive. This makes SPOS not feasible when smaller libraries are

needed (the trend in the drug discovery process has shifted towards small, focused libraries), or when library generation is done in laboratories with limited financial resources.⁴

Alternative methods which eliminate the problems stated above, yet still accelerate the library generation are thus very useful in addressing certain needs. A number of approaches have been developed. The remainder of this chapter will summarize some of the progress that has been made in this area.

1.1 LIQUID PHASE COMBINATORIAL SYNTHESIS (LCPS)

The supports employed in LPS (liquid phase synthesis), and LPCS are polymers that are soluble under some conditions, and not under others.^{4a-b} This way some of the problems in SPOS arising from heterogeneous reaction conditions are avoided. Additionally removal of excess reagents can be achieved by precipitating the support (and *thus the bound substrates*) in solvents in which it is not soluble followed by simple filtration.^{4a-b, 5a} A number of polymers including MPEG (poly(ethyleneglycol) ω -monomethyl ether. **1**), PVA (polyvinylalcohol, **2**), polyacrylic acid (**3**), PEG (polyethylene glycol) derivatized with 3,5-diisocyanatobenzyl chloride (**4**), and polyacrylamide (**5**) have been used in LCPS (Figure 1-1).⁴ Recently ionic liquids were introduced as supports for LPS, and LCPS, although syntheses employing them are referred to as Ionic-Liquid Supported Synthesis (ILSS).⁶ Dendrimer supported organic synthesis is a technique related to LCPS, and offers certain distinct advantages like high loading capacity, and the possibility of purification using size exclusion chromatography.^{4a-b,5b} Soluble polymers, particularly MPEG have been successfully applied to the syntheses of a number of substrates including polysaccharides, oligopeptides, oligonucleotides, and azatides.^{8a, b, c, d, e}

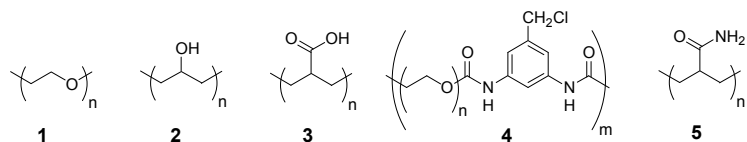


Figure 1-1: Some supports used in LPS and LCPS.

An impressive example of the application of LCPS is Erb, Janda, and Brenner's preparation of a 1024-member library of pentapeptides using MPEG as the soluble polymer support with the aim of obtaining a peptide that would efficiently bind to a β -endorphin antibody.⁷ Since a split-pool strategy was used to maximize diversity, a method for the identification of the active products was needed. While the application of identifying tags might be beneficial in SPOS, LCPS does not (for obvious reasons) allow the use of them. Thus another approach, termed "recursive deconvolution", (RD) was utilized which was originally developed for SPOS to eliminate the need for identifying tags.⁹

The strategy employed by Erb *et al.* is depicted in Figure 2. Assume a 27-member tripeptide library made from amino acids A, B, and C is desired. A, B, and C are attached to MPEG, some of each resin-bound amino acid is put aside as a partial library 1 (p(1)). The rest is mixed, and separated into 3 samples, each being reacted with A, B, and C. Some of each newly obtained pool of compounds is saved as partial library 2 (p(2)), the rest is mixed, and separated into 3 samples. These samples are reacted again with either A, B, or C. The final products are now in 3 pools containing 9 tripeptides each. Now RD can be applied. Each pool is assayed. Assume that the MPEG-N₁N₂A (where N₁, and N₂ are the amino acids in the active tripeptide whose identity is unknown at this stage) pool shows the desired activity. Since the final amino acid's identity is known, each of the partial libraries p(2) can now be reacted with A,

and assayed. Assume that the MPEG-N₁-AA pool shows the desired activity. Thus N₂ has been established as A. The partial libraries p(1) are now reacted with amino acid A, to give a positive for the tripeptide AAA. Using this strategy Erb *et al.* have found that the pentapeptide NH₂-Tyr-Gly-Gly-Phe-Leu was a good binder of a β -endorphin antibody. In a similar fashion the workers have also prepared, and identified the active member of a arylsulfonamide library.⁷

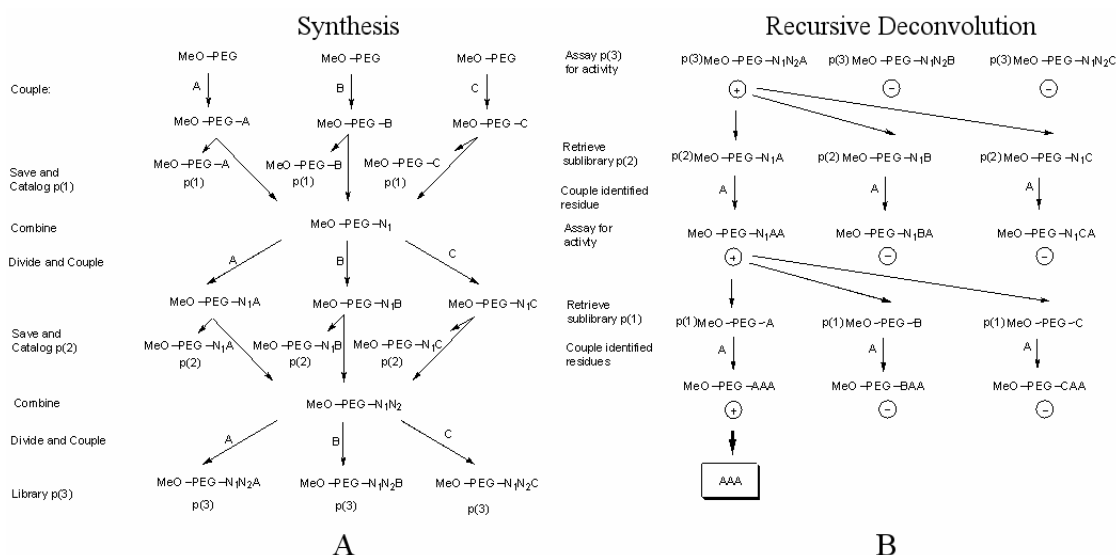


Figure 1-2: Synthesis (A) and recursive deconvolution (B) of a hypothetical 27-member tripeptide library.⁴

A simpler approach to LCPS is parallel synthesis. Huang, and Sung have prepared a 16-member library aminobenzimidazoles in parallel using MPEG as the soluble polymer support.^{10a} Treatment of MPEG supported 4-fluoro-3-nitrobenzoate (**6**) with the corresponding primary amine, and subsequent reduction afforded **7** (Figure 1-3). The MPEG supported *o*-phenylenediamines (**7**) were then subjected to a one-pot cyclodesulfurization by DICDI mediated reaction with the corresponding isothiocyanates, and subsequent treatment with NaOCH₃/MeOH to afford the desired 2-(arylamino)benzimidazoles (**8**). Purification of the products was accomplished by washing upon precipitation of the support. It was possible to monitor reaction

progress while the substrates were bound to the MPEG support. The purities of the products upon liberation from the support were 80-99%. Other libraries generated through parallel LPS include the syntheses of 1,4-benzodiazepine-2,5-diones (MPEG), and [1,4]Oxazepine-7-ones via the Baylis-Hillman Reaction (MPEG, split synthesis).^{10b, c}

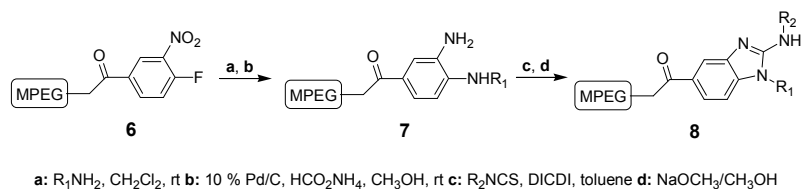


Figure 1-3: Parallel synthesis of aminobenzimidazole using MPEG as a soluble polymer support.

LPS, and LCPS have certain advantages over SPOS, as these and many more studies found in the literature, suggest. The chemist has the ability of having the support, and thus the substrates attached to it in solution, or as a precipitate, and thus removal of excess, and used reagents can be achieved by simple filtration in many cases. Solution phase reaction conditions can be used in most cases, and most solution phase reactions that are not compatible with SPOS can be employed in LCPS, and LPS. It is possible to follow reaction progress, and characterize products while they are still bound to the support using spectroscopic techniques that are employed in solution phase chemistry. Many kinds of supports are available which increases the range of chemistry that can be done using LCPS. Clear disadvantages exist as well. Split-and-mix syntheses of libraries is very difficult, and is enabled by few methods like RD. RD is cumbersome, and can only be applied to small, or medium sized libraries. Practical library generation strategies can be assumed to be limited to parallel and split syntheses.

1.2 SOLUTION PHASE COMBINATORIAL SYNTHESIS

SPCS can be defined as any combinatorial synthesis method that does not involve substrates attached to solid or soluble polymeric supports. Methods used in SPCS include parallel solution synthesis, indexed combinatorial libraries, template-based libraries, solution phase libraries purified by liquid-liquid extraction, various solution syntheses that involve solid phase reagents, resin capture, or polymeric reagents, and fluororous tags.^{5b} Some of these methods will be discussed briefly in the following sections.

1.2.1 Indexed Combinatorial Libraries

While Indexed Combinatorial Libraries (ICLs) could be regarded as Spatially Addressable Combinatorial Libraries, the former differ from the latter in that they do not rely on a solid support, that mixtures of compounds are synthesized, and that the spatial location of the active substrate is on a multi-dimensional imaginary matrix established through screening the library for products that exhibit the desired activity.¹¹ Assuming an active compound in a library which is obtained through the binary reaction of two subunits (subunits A, and B with a basis set of 6 each) needs to be identified, then such a task would require 36 reactions, and 36 assays using conventional synthesis. In the ICL approach one subunit (i.e. A₁) is held constant, and reacted with a mixture of the corresponding subunits (i.e. B₁₋₆). The same is done for each of the other A subunits, then each B subunit is reacted with a mixture of A₁₋₆ in the same fashion. Thus, in 12 reactions each final product is synthesized twice. The product mixtures are then assayed noting which subunit was held constant. Assuming that these assays give maxima for the reaction of A₃

with B₁₋₆, and B₅ with A₁₋₆, then it is concluded that A₃B₅ is the compound that has maximum activity.

Pirrung and Cheng have prepared an ICL of 54 carbamates in order to identify an inhibitor of the electric eel acetylcholinesterase. Using a basis set of 9 alcohols, and 6 isocyanates 54 different carbamates (each being synthesized twice) were obtained distributed as mixtures of varying composition in 15 different sets (9 sets of 6 carbamates, and 6 sets of 9 carbamates).¹² Screening, and data analysis revealed O-succinimidyl *N*-methyl carbamate (**9**) as the most potent acetylcholinesterase inhibitor ($1/IC_{50} = 1497 \text{ M}^{-1}$). Application of ICL in this particular case resulted in a 3.6-fold increase in the efficiency of the synthesis, and assay of the products (Figure 1-4).

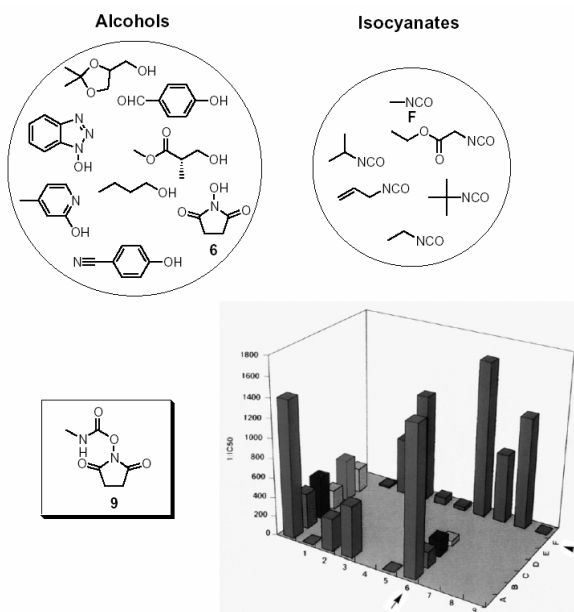


Figure 1-4: Preparation and assay of 54 carbamates using the ICL method.^{12b}

An interesting study has been reported by Andrus, Turner, Sauna, and Ambudkar that demonstrates one inherent weakness of ICLs; namely the limitations of assays of mixtures of

compounds.^{13a, b} Andrus *et. al.* have prepared a 42-member ICL of polyenes based on (-)-stipiamide, which is a compound shown to reverse multidrug resistance. A subset consisting of 6 groups was used for R, and a subset consisting of 7 groups was used for R' (**10**). 13 sets (6 groups with 7 members each, and 7 groups with 6 members each) of (-)-stipiamide analogues were prepared, and assayed using adriamycin resistant MCF7-adrR human breast cancer cells with concomitant employment of adriamycin. While **11** was in fact the most effective ($ED_{50} = 1.45 \mu\text{M}$) ICL member, while the 2 dimensional activity matrix suggested a different compound as the most potent (Figure 1-5). This is a common problem with assays of compound mixtures (*or single compounds with high impurity levels*), and demonstrates a built-in limitation of the ICL method. The root causes for this problem might be favorable or unfavorable drug-drug interactions, particularly if the receptor has multiple binding sites.

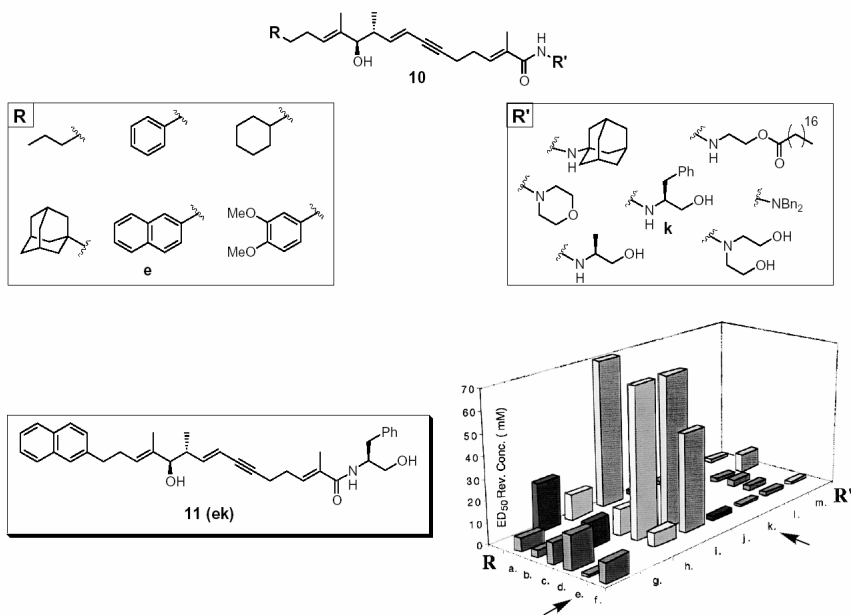


Figure 1-5: Preparation and assay of a 42-member ICL of (-)-stipiamide analogues.^{13c}

The problem associated with assays of mixtures of compounds is not the only limitation of ICLs. Library size is limited as well, since the number of sets that need to be prepared for a 2-dimensional matrix is the product of the basis sets of each dimension. This problem gets worse if the number of dimensions is increased. The possibility of false positives in the assays also increases under such conditions. While there are certain limitations associated with ICLs, this methodology could still be useful in many cases.

1.2.2 Combinatorial Libraries Based on Templates and Liquid-Liquid Purification

Boger, Tarby, Myers, and Caporale have reported the synthesis of a 27-member library based on a core structure that can be derivatized at 3 positions, and purified by acid/base extraction.¹⁴ N-protected anhydride **12** offers 3 points where derivatization through amide/ester/thioester formation is possible (only amides were prepared in this particular case), and the intermediates can be purified by acid/base extraction as they bear carboxylic acids, and/or amines. Additionally **12** is very rigid, and when fully extended can be regarded as a Gly-Xxx mimic.

Anhydride **12** was reacted with 3 amines in parallel to give **13a-c**, the products were purified, and each product was split into 3 groups, each was carried onto the next step. Each group of products **13a-c** were reacted with the second set of amines in parallel to give 9 products (**14a-i**), which were purified via acid/base extraction, deprotected, split into groups, each group reacted with a 3 member set of carboxylic acids to give 27 individual products (**15a-u**, Figure 1-6). Overall yields varied from poor to good (3-89 %), but the purity of the products was very good (90-95%).

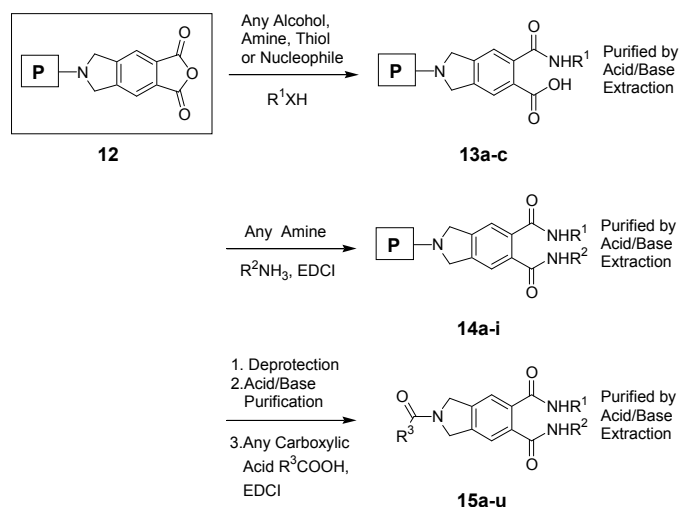


Figure 1-6: Preparation of a 27-member combinatorial library based on a template and purification via acid/base extraction.¹⁴

Cheng, Comer, Williams, Myers, and Boger have reported a similar study employing an anhydride based template (**17**) that could be derivatized at 3 positions.¹⁵ The intermediates, and products can also be purified by acid/base extraction. A 39-member library (**18**) was generated through EDCI (1-(3-dimethylaminopropyl)-3-ethylcarbodiimide hydrochloride), and PyBOP (1-yl-oxytripyrrolidinophosphonium hexafluoride) mediated amide formation (Figure 1-7). Yields were in the 9-84 % range (average 61%), and purity was ≥ 90 % for all compounds. In the same paper the successful preparation of a 1014-member library based on **17** was also reported. In similar studies libraries based on 9,9-dimethylxanthene tetracarbonyl chloride (**19**, 65341-member library), and cubane tetracarbonyl chloride (**20**, 11191-member library) were reported (Figure 1-7).^{16a, b} Purification in these cases was accomplished by washing with citric acid, and bicarbonate solutions. Obviously the analysis, and bioassay of these huge libraries were very problematic, extensive resynthesis was required for active compound determination, and significant amounts of false positives were observed.

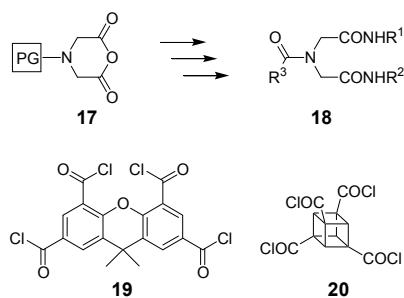


Figure 1-7: Some templates used in template based synthesis.

1.3 FLUOROUS CHEMISTRY

Perfluorinated alkanes have been known for well over 60 years (for instance they have been used for the purification of uranium during the Manhattan Project)^{17a}, and they possess unique qualities.^{17a-f, 18} These properties include chemical inertness, thermal stability, temperature dependent low solubility, or practical insolubility in common organic solvents, and water, volatility, non-toxicity, and inflammability. Low solubility of perfluorinated alkanes in conventional solvents, which can be regarded as a result of the reduced Van der Waals forces due to the low polarizability of fluorine, is the key property which make them attractive for organic synthesis, and combinatorial organic synthesis.

The fluoruous phase may be regarded as a fifth phase to complement the organic, aqueous, solid, and gas phases which are employed in organic synthesis. One can imagine reagents, catalysts, and reactants bearing perfluorinated groups which could facilitate the partitioning of these into the fluoruous phase, and thus allow for easy purification of reactions. Such fluoruous syntheses could be regarded as being similar to solid phase synthesis in the sense that the products, catalysts, or reagents would be in, or could be partitioned into a phase that

renders them easily separable from the organic, and aqueous phases utilized in the reactions, and workups. But at the same time fluorous synthesis would still retain the beneficial qualities of solution phase synthesis.

The possibility of fluorous synthesis has been realized. The first example of a fluorous reaction can be regarded as the invention of fluorous biphasic catalysis by Horváth, and Rábai.^{19a-b, 17a} In this study a hydroformylation catalyst bearing highly fluorinated ligands ($\text{HRh}(\text{CO})\{\text{P}[(\text{CH}_2)_2(\text{CF}_3)_5\text{CF}_3]_3\}_3$) was prepared, and it was observed that this catalyst was soluble in fluorous solvents, but not in others. Hydroformylation of alkenes in a biphasic system (alkenes in the organic phase, catalyst in the fluorous phase) was performed successfully.^{17a, 19a-b} This study made use of the mutual solubility of perfluoromethylcyclohexane (PFMC), and toluene at elevated temperatures.

While this new area of chemistry has been started by others, the application of fluorous synthesis to many aspects of organic and organic combinatorial chemistry has been pioneered by the Curran group of the University of Pittsburgh Department of Chemistry and the affiliated startup company Fluorous Technologies, Inc., with well over 100 reports published in just 10 years starting from 1996.

The following sections will examine fluorous chemistry in three categories: i. Fluorous reagents, catalysts, and scavengers; ii. Fluorous phase tags for reactants; iii. Fluorous Mixture Synthesis (FMS) through fluorous sorting tags. The emphasis will be on FMS, as this area is directly related to the subject of this dissertation

1.3.1 Some General Issues in Fluorous Chemistry

One common aspect that is relevant to all categories of fluorous synthesis is the solubility issue of highly fluorinated compounds. Attachment of perfluorinated groups facilitates partitioning of these into fluorous solvents. But associated with this benefit is also a drawback; namely reduced solubility, or insolubility of these in organic solvents. Should the solubility of these compounds in regular organic solvents be too low, heterogeneous reaction mixtures result, and this is accompanied with the disadvantages of such reaction conditions. This is a particularly significant problem with the earlier “heavy fluorous” compounds ($\geq 60\%$ fluorine content by weight). This issue has been resolved with three approaches. The first is heating the solution to facilitate phase mixing (Figure 1-8).^{19a-b} The second has been the use of a solvent that is part organic, and part fluorous; namely benzyltrifluoride (BTF, $C_6H_5CF_3$).^{20a} The third approach is the use of “light fluorous” groups ($\leq 40\%$ fluorine content by weight). But the third approach, in turn, creates a problem with the solubility of these compounds in fluorous solvents, thus makes fluorous liquid-liquid extraction (F-LLE) impractical. This problem has been solved by the reintroduction of fluorous reversed phase (FRP) silica, and its employment in solid phase extraction (Fluorous Solid Phase Extraction. F-SPE).^{20c-d}

Another occasional problem is the change in reactivity of some compounds upon attachment of perfluorinated groups. The strongly electron withdrawing nature of these groups renders some of these compounds poorly reactive, or completely unreactive. This issue has been resolved by introducing methylene spacers between the perfluorinated groups, and the point of their attachment to the substrate, and by using microwave radiation to quickly heat, and speed up the reactions.^{19a-b, 20c}

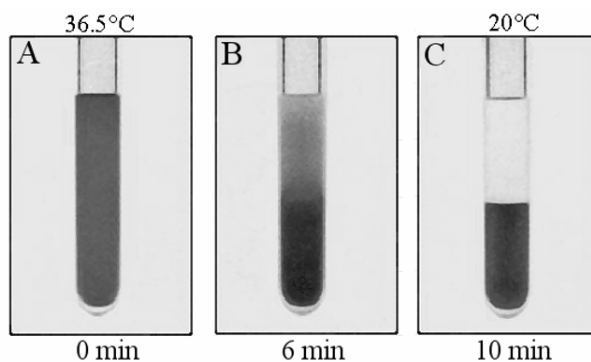


Figure 1-8: Temperature dependence of the solubility of $c\text{-C}_6\text{F}_{11}\text{CF}_3$ (PFMC) in a mixture of n -hexane and toluene (The color is due to a highly fluorinated dye that partitions into the fluorous phase upon cooling to room temperature.).^{19b}

Yet another issue is the use of standard abbreviations, language, and definitions employed in fluorous synthesis. Thus the adjective fluorous has been defined as “*of, relating to, or having the characteristics of highly fluorinated saturated organic materials, molecules, or molecular fragments. Or, more simply (but less precisely), ‘highly fluorinated’ or, ‘rich in fluorines’, and based upon sp^3 -hybridized carbon.*”^{17c} Some procedures, and substances have been implied to be fluorous by the prefix “F-“, for instance F-SPE for fluorous solid phase extraction, and F-HPLC for HPLC employing fluorous silica gel. The identity of perfluorinated groups, and associated methylene spacers have been denoted by the symbol R_xH_y , where x is the number of $-\text{CF}_2-$, and $-\text{CF}_3$ groups, and y is the number of $-\text{CH}_2-$ groups.

1.3.2 Fluorous Catalysts, Reagents, and Scavengers

A large number of catalysts, reagents, and scavengers have been transformed into fluorous ones, thus a wide range of reactions employed classic organic solution phase syntheses are now available in the “parallel universe” of fluorous synthesis. The general schemes under which these synthetic tools have been applied are depicted in Figure 1-9.

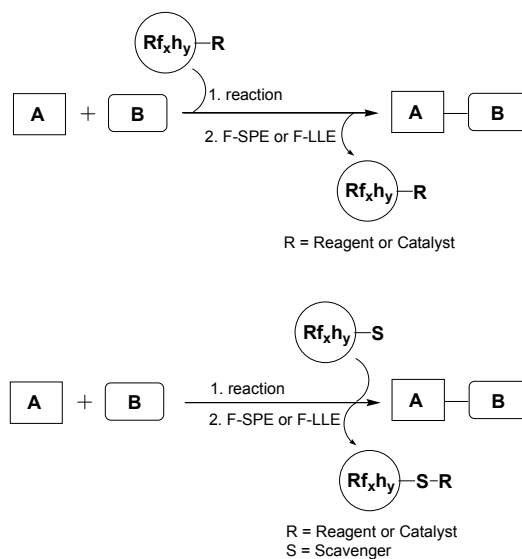


Figure 1-9: Some strategies in fluororous synthesis.

The Curran group worked extensively on the fluororous reactions of stannanes, because the organic versions of these reagents are hard to remove from reaction mixtures. The first example of such a fluororous reagent was $(Rf_6h_2)_3SnH$ (**21a**, Figure 1-10, A).^{20a} The reduction of 1-bromoadamantane (**22**) to adamantane (**23**) did not proceed well using **21a** in toluene/ PFMC, or benzene as solvents.^{19a} However it was observed that employment of pure PFMC resulted in the desired reduction with 72 % yield of adamantane. Thus it was concluded that homogenous reaction conditions were required to prevent the early termination of the radical chain propagation. The reduction was further improved using BTF/*tert*-butanol as the solvent, catalytic amounts of **21a**, and $NaCNBH_3$ as the stoichiometric co-reductant to give a 95% yield of pure adamantane after removal of catalyst **21a** using F-LLE, which was recovered as the corresponding bromide (**21b**) in good purity, and could be reused with, or without activation with $LiAlH_4$. Fluororous allylstannane **24** was reacted neat with a number of aldehydes (**25**) to yield the corresponding allylalcohols (**26**) in moderate to good yields upon removal of excess **24**, and the used-up reagent using F-LLE (with FC-72, fluorohexanes), or F-SPE using FRP silica

(Figure-1-10, B).^{20b} In another study Stille couplings were performed where fluoros phenylstannane (**27**) was reacted with *p*-bromomethylphenylketone (**28**), among others, to give the desired product (**29**) in very good yield, and biphenyl (**30**) as the homocoupling side product (Figure 1-10, C).^{21a} The catalyst was PdCl₂(PPh₃)₃, the solvent was THF, and LiCl was used to improve yields (CuI was employed to suppress formation of the homocoupling product with some other substrates.). In a related study it was found that microwave radiation significantly improved the yield of these couplings.^{21b-c} In yet another stannane related study, various perfluorinated allylic compounds were obtained in good to excellent yields through the reaction of regular allyltin reagents with perfluoroalkyl iodides using AIBN in hexane, and subsequent purification by F-SPE.^{20c}

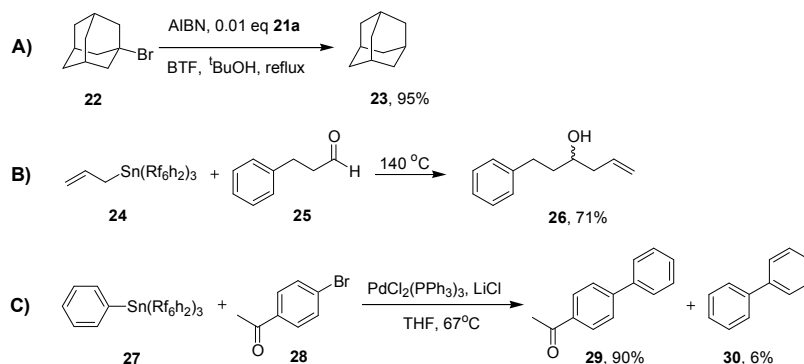


Figure 1-10: Examples of reactions employing fluoros reagents.

Fluorous phosphines (PhPf₆h₂)₂PPh (**33**), (PhPf₈h₂)PPh₂ (**34**), and fluoros DEAD (^FDEAD) analog Pf₆h₂OC(O)N=NCOOPf₆h₂ (**35**) were prepared, and applied to Mitsunobu reactions with good yields (Figure 1-11, A).^{22a} The fluoros phosphine oxides, and fluoros

hydrazine were easily removed by F-SPE (and could be recycled) or F-LLE to afford the desired products with good purity.^{22b} The addition order of the reactants, and reagents was found to be important to the reaction outcome. In later studies it was observed that **35** gave poor results with some hindered substrates. Thus a ^FDEAD with propylene spacers, and another one with only one fluorine arm were prepared, and these reagents remedied the reactivity problems while still being separable by F-SPE.^{22c} A number of phosphines with varying fluorine content were prepared, and found to exhibit reactivities similar to regular triphenylphosphine in oxidation, alkylation, and Staudinger reactions.^{22d} Various fluorine aryl iodides, and hypervalent iodine compounds were prepared, and applied to the oxidation of hydroquinones, with purification being done using F-LLE.^{22e} A fluorine Lawesson's reagent (**38**) has been used for the preparation of compounds such as thioamides, thiophenes, and thiazoles followed by purification with F-SPE (Figure 1-11, B).^{22f} A number of fluorine, or fluorine ligand bearing catalysts have also been prepared including a fluorine phosphine ligand (F-dppp, **42**) bearing catalyst for Heck vinylation with enamides (Figure 1-11, C), a fluorine Grubbs-Hoveyda catalyst (**44**) for alkene metathesis, a fluorine imidazolidinone based organocatalyst (**45**) for Diels-Alder reactions, and a fluorine diphenylprolinol silyl ether organocatalyst (**46**) for enantioselective aldehyde-nitroolefin Michael addition reactions.^{22g-j} A fluorine amine (HN((CH₂)₃Si(Rf₆H₂)₃)₂) was used as a scavenger for excess isocyanate during the parallel solution synthesis of a 9-member urea library to afford the products in good purity.^{22k}

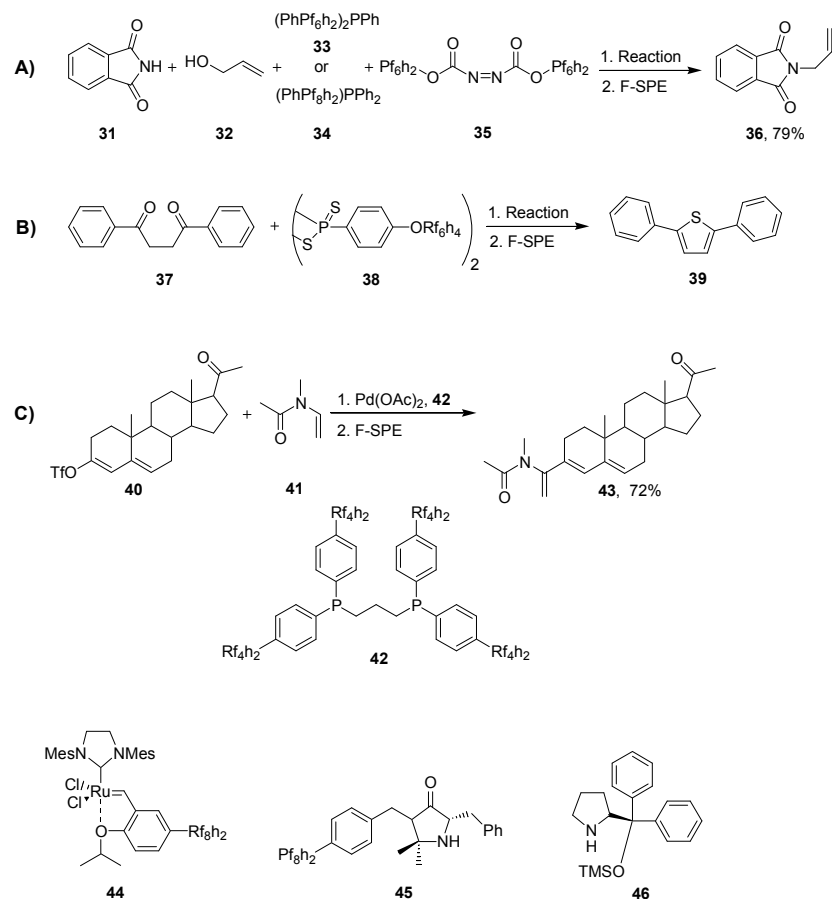


Figure 1-11: Some fluororous reagents and catalysts.

1.3.3 Fluorous Phase Tags for Reactants

A strategic alternative to reagent tagging would be the tagging of reactants. Through reactant tagging it would be possible to purify the product by F-LLE, or F-SPE, and have excess, or spent reagents remain in the organic, or aqueous phase. It would be advantageous to have fluororous protecting groups, as these would solve the protecting group, and phase tag problems simultaneously.

A number of fluororous protecting groups for alcohols have been reported. A fluorinated silyl group ($\text{BrSi}(\text{Rf}_6\text{h}_2)_3$) was prepared, and a small library of isoxazolines was prepared from

the reaction of substituted nitrile oxides, and fluorous silyl protected allyl, and propargyl alcohols.^{23a-b} Protection, and deprotection could be carried out under regular conditions, and F-LLE (with FC-72) afforded the desired products in good yield, and purity. An interesting application of such fluorous silyl protecting groups has been their employment in the “cap-tag” method as applied to the solid phase synthesis of oligosaccharides.^{23c} Using this method unreacted carbohydrates were tagged with a fluorous silyl group (TfO(ⁱPr)₂SiRf₈h₂) after each synthetic step, and removed via F-SPE upon liberation of the products from the solid support to afford the desired products in higher purity. The Bfp (**47**) group is another fluorous protecting group developed for employment in carbohydrate chemistry.^{23d} A fluorous version (^FMOM, **48**) of the methoxymethyl protecting group has also been reported.^{23e} Protection-deprotection sequences using ^FMOM were performed with yields varying between 60%, and 90% over those 2 steps (Figure 1-12).

Fluorous protecting groups for amines have also been developed. A fluorous analogue of the Boc protecting group (^FBoc, **49**) has been prepared and protection/deprotection was found to work well using standard conditions. ^FBoc was applied to the parallel synthesis of 16- and 96-member libraries of amides.^{23f} A perfluorinated group bearing benzyloxycarbonyl protecting group (**50**) has been reported.^{23g} A dipeptide library was prepared using a fluorous Fmoc (f-Fmoc, **51**) protecting group and purification was done using F-SPE.^{23h} A 27-member library of biaryl sulfonamides, and a 18-member library of biaryl carboxamides was prepared using acid-labile fluorous protecting group **52**, which was attached to the amines through reductive amination, and the products could be purified through F-SPE (Figure 1-12).²³ⁱ

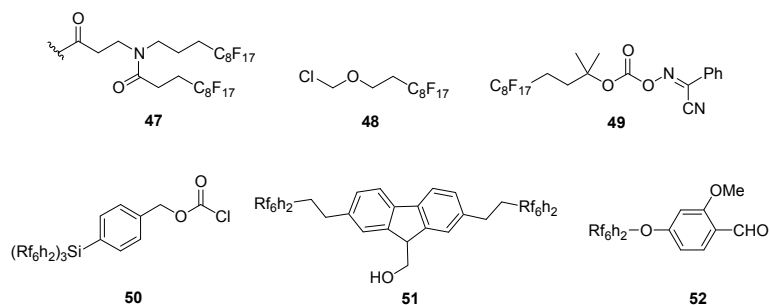


Figure 1-12: Some fluorinated protecting groups.

1.3.4 Fluorous Mixture Synthesis Using Fluorous Sorting Tags

Analytes forming homologous series, particularly methylene homologues, have been studied extensively since the advent of HPLC.^{24a} These tend to elute in an orderly fashion, the elution order is dictated by the number of homologous groups a molecule has, and by the nature of the stationary phase employed in the chromatographic system.^{24a,b} The elution time increases as the number of methylene groups of a substrate increases. The free energy associated with this retention increases linearly with increasing chain length, thus retention times tend to increase exponentially as chain length increases.

Perfluorinated alkanes of varying chain lengths can be regarded as forming a homologous series. Curran recognized that substrates could be tagged with perfluorinated alkane chains, reacted as a mixture, and later separated by chromatography. Thus those perfluoroalkanes would act as *sorting tags* for the substrates, and such a synthesis could be termed “fluorous mixture synthesis” (FMS, Figure 1-13). This synthetic strategy could speed up the synthetic process as the number of reactions that need to be carried out would be less than the number of reactions that would be required were those substrates synthesized in parallel. The only thing that would be needed is a chromatographic medium that has retention selectivity for

perfluoroalkanes. The purifications carried out using F-SPE would suggest that FRP silica could be such a medium.

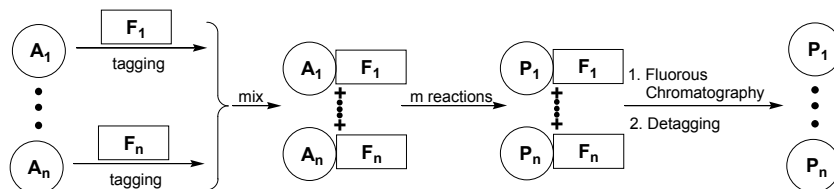


Figure 1-13: The FMS strategy.

First generation fluorous chromatographic stationary phases were made of lithium amalgam treated teflon, and were not very effective. Second generation stationary phases were prepared by exchange of $-OH$ groups on the surface of silica with fluorines. These columns had very short lifetimes. The third generation fluorous stationary phases were made by alkylating the surface of silica with Rf_8h_2 .^{25a-b} These columns were quite stable, and this technology is still being used in the preparation of contemporary FRP silica based columns.

These columns have been employed in the analysis of (among others) biologically important molecules such as proteins, and a variety of small molecules such as aromatic amines, phenols, and aromatic acids. More importantly it was observed early on that fluorinated compounds were retained based on their fluorine content, the more fluorines present, the longer the retention time.^{25b, 26a-c} For instance for benzene (**53a**) and fluorinated benzenes **53b-g** it was observed that retention on FRP silica increased with fluorine content and that better resolution was attainable than on C18 stationary phases (Figure 1-13).^{26b} Moreover addition of trifluoroethanol to the mobile phase caused the resolution to completely disappear and all

substrates eluted at the same time.^{26b} These findings suggest that the fluorine content of molecules is the primary factor that affects the energetics of the retention process on FRP silica.

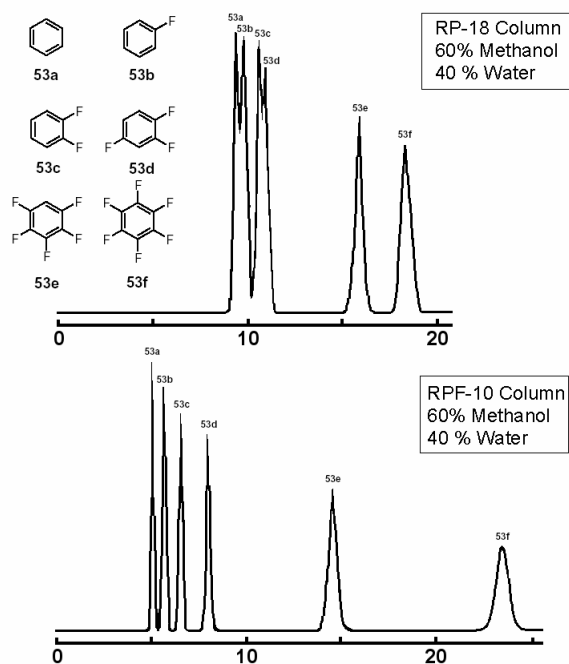


Figure 1-14: Retention of some fluorinated substrates on FRP silica and C18 stationary phases.^{26d}

These observations suggest that substrates that have perfluorinated groups attached to them could be used as sorting tags and that FMS is possible. Furthermore, the elution order of the substrates would give information about their identities. This is indeed the case. Luo, Zhang, Oderaotshi, and Curran initially applied FMS to the “quasiracemic” synthesis of the two enantiomers of mappicine. Quasiracemic synthesis is the simultaneous synthesis of enantiomers as a separable mixture. This strategy was subsequently applied to the split synthesis of a 100-member library of mappicine derivatives. 4 alcohols were individually silylated with fluorous tags of differing lengths ($-C_4H_9$, $-C_6F_{13}$, $-C_8F_{17}$, and $-C_{10}F_{21}$), mixed, and separated into 5 portions. Each portion was reacted with a different propargyl bromide. The

resulting mixtures were separated into five portions each (five portions with a mixture of 4 compounds each). Each portion was reacted with 5 different isonitriles to give a 100 mappicines (99 of those were formed) upon fluoros chromatography and detagging (Figures 1-14 and 1-15).^{27a} Subsequently an impressive 560-member mappicine library was also constructed.^{27b}

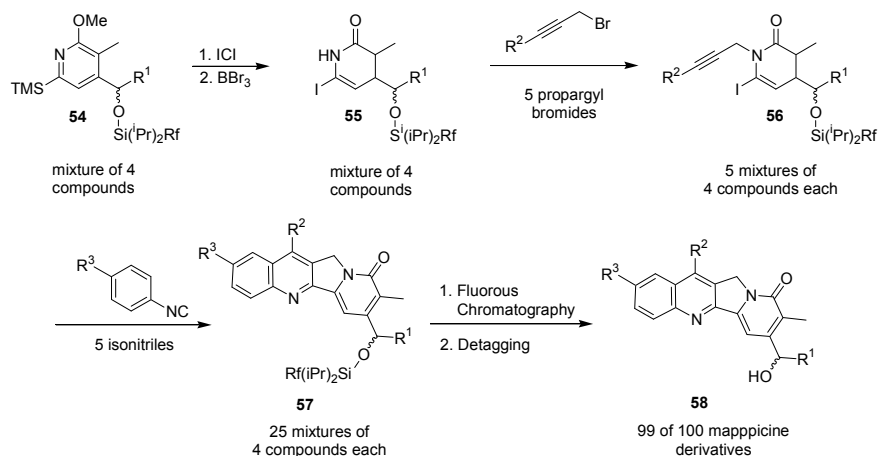


Figure 1-15: FMS of mappicine derivatives.

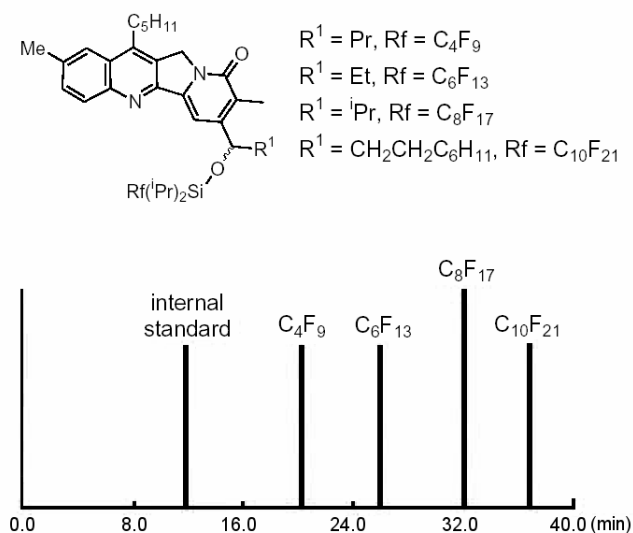


Figure 1-16: Chromatogram of 4 fluoros sorting tag bearing mappicine derivatives on FRP silica.^{27d}

An important facet of chromatographic demixing in FMS was demonstrated by Curran, and Oderaotshi.^{27a, c} The authors prepared libraries of compounds obtained from NEt_3 mediated conjugate addition of various thiols to 3 different acrylate esters of fluorinated benzyl alcohols bearing perfluoroalkane groups of differing lengths ($-\text{C}_6\text{F}_{13}$, $-\text{C}_8\text{F}_{17}$, $-\text{C}_{10}\text{F}_{21}$). Three libraries of 12 members each were prepared from 4 thiols, and 3 fluorinated acrylate esters. The method used in the preparation of these libraries was the same as the one used in the mappicine study described above. When all 12 members of one library were mixed, and subjected to chromatography on FRP silica it was observed that separation was primarily based on the length of the fluorinated chain, but that the substrate structure had also an effect on the retention time. 7 of the 12 compounds exhibited baseline separation, and the rest eluted with partial overlap (Figure 1-16). This observation suggests that it would be possible to do FMS without the need for splitting (more than one product could be tagged with the same sorting tag), that all products could be made in one pot, and demixed with just one chromatographic separation. Thus a 9-member library was constructed through the reaction of 3 thiols, and 3 fluorinated acrylate esters. 7 of the 9 products could be separated on FRP silica followed by C18 chromatography.

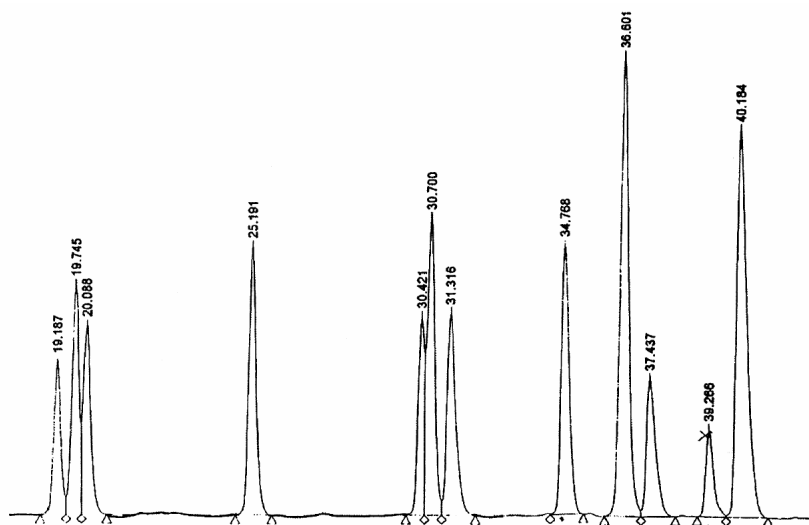


Figure 1-17: Separation of 12 acrylate-thiol conjugate addition products on FRP silica.^{27c}

Curran, and Furukawa have reported the preparation of 4 truncated analogues of the anticancer agent (+)-discodermolide using fluororous *p*-methoxybenzyl (^FPMB) sorting tags.^{28a} Starting from a mixture of **59a-d**, which were made as individual compounds, 8 consecutive reactions were performed to give 4 analogues of (+)-discodermolide. Thus 24 synthetic steps were saved by using FMS instead of classic parallel synthesis. It was possible to characterize each intermediate using LCMS and LCNMR. The final products were easily separable by chromatography on FRP silica (Figure 1-17). FMS has also been applied to the syntheses of libraries, and stereoisomers of targets such as pyridovericin, (-)-dictyostatin, hydantoin, passifloricin, lagunapyrone B, and the Pinesaw fly sex pheromones.^{28b-g} The synthesis involving the preparation of a library of hydantoin is particularly interesting as it involves a mixture synthesis where the number of substrates that were tagged was larger than the number of tags. Retention differences of the parent substrates were exploited to achieve this. This approach has been termed “redundant tagging”.^{28d}

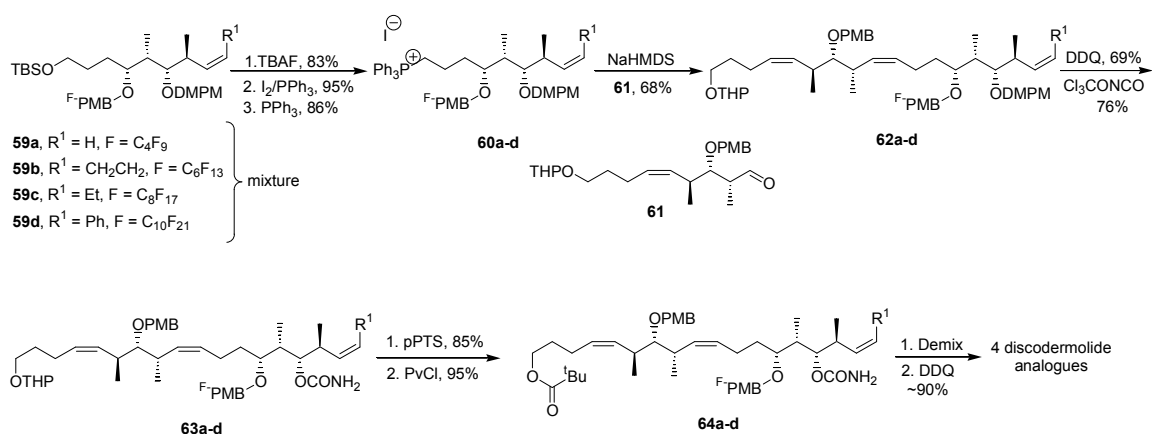


Figure 1-18: FMS preparation of discodermolide analogues.

Wang, Nelson, and Curran have recently reported the synthesis of a 27-member tri- β -peptide library through FMS employing only one fluororous tag.^{29a} The fluororous tag used was one of the ^FPMB tags (p-C₈F₁₇(CH₂)₃OC₆H₄CH₂-) employed in the (+)-discodermolide study discussed earlier.^{28a} Library generation was done using the split synthesis strategy. The β -amino acids employed were synthesized using the β -azido acid approach reported by Nelson, Spencer, Cheung, and Mamie.^{29b} The mixed β -lactones (**65a-c**) were prepared using the AAC reaction, and opened using NaN₃ to give the β -azido acids (**66a-c**) in excellent yield.^{29c} EDCI/DMAP mediated esterification with ^FPMBOH, and purification with F-SPE was followed by reduction of the azides using a Staudinger procedure involving PPh₃, and microwave radiation to give the fluororous esters β -amino esters **67a-c** upon F-SPE purification.^{29d} The mixture comprised of **67a-c** was split into 3 portions, and each portion was coupled with a different β -azido acid using EDCI/DMAP to give **68aa-cc**, followed by F-SPE. Each of the three mixtures was split into three portions, and the cycle was repeated to give 9 mixtures of 3 compounds (**69aaa-ccc**) each after F-SPE. Hydrogenation gave the tri- β -peptides (**70aaa-ccc**) with yields varying between 33% and 100% over 3 steps. Chromatography on FRP silica, and C18 gave 26 out of 27 of the desired tri- β -peptides in good purity (Figure 1-18). In all, 34 synthetic steps were saved with respect to the classic parallel synthesis approach.

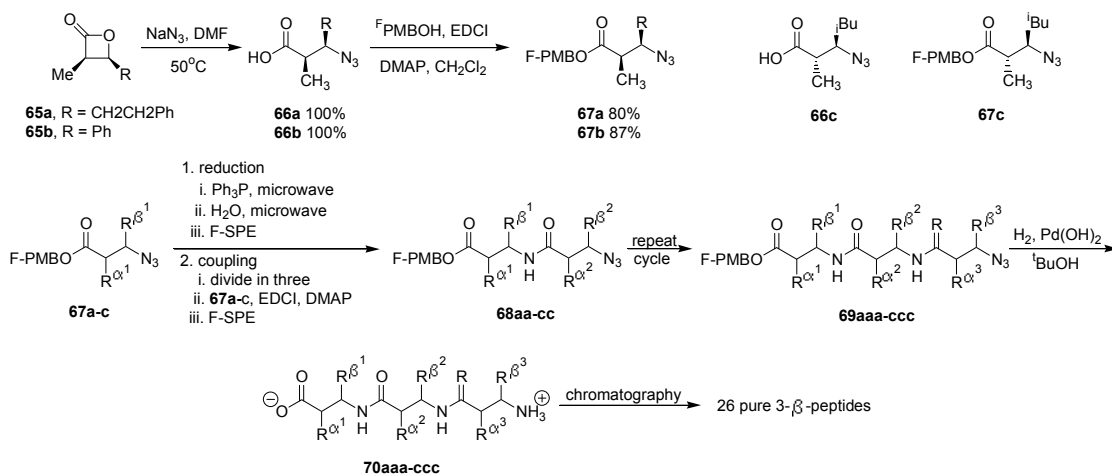


Figure 1-19: FMS of tripeptides.

1.3.5 Comments on Fluorous Synthesis

These studies, and many more not mentioned here show that fluorous synthesis is a powerful method for parallel and combinatorial synthesis. Since product purification can be done using F-SPE in most cases this method lends itself to automation, and instrumentation employed in solution phase synthesis can be used to monitor reactions, and characterize products without the need for removing the fluorous tag. Fluorous reagents, and catalysts can be easily removed from reaction mixtures, and recycled in many instances. With the advent of F-SPE the need for costly fluorous solvents has been-to a large extent-eliminated. The intoxicity, and inflammability of perfluorinated alkanes makes fluorous synthesis safe, and environmentally benign.

Fluorous mixture synthesis is particularly useful, as large numbers of compounds can be prepared using the split synthesis method. Even mixture synthesis where more than one substrate is tagged with one kind of sorting tag is possible. A new class of sorting tags separable under conditions orthogonal to conditions for the separation fluorous compounds would certainly

extend the potential of combinatorial chemistry in the solution phase further, as these two classes of sorting tags could be used together.

2.0 OLIGOMERIC ETHYLENE GLYCOL (OEG) DERIVATIVES AS SORTING TAGS¹

The objectives of the studies outlined in this chapter are: i. Determination of the utility of OEG derivatives as sorting tags for mixture synthesis. ii. Investigation of the factors that affect the separatory efficiency of OEG derivatives on a number of different chromatographic media. iii. Preparation of protective groups bearing only OEG subunits, and of those bearing OEG, and fluororous subunits simultaneously. iv. Investigation of the potential of double OEG tagging as a means for mixture, and cross-reaction mixture synthesis.

2.1 THE CASE FOR SORTING TAGS BASED ON OLIGOMERIC ETHYLENEGLYCOL

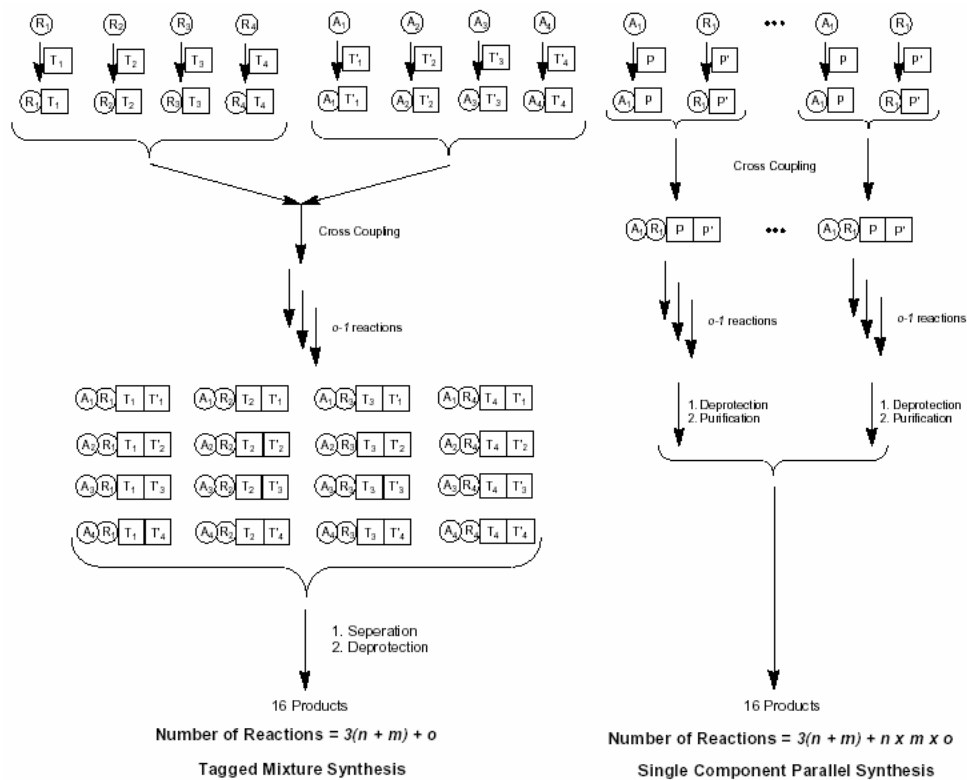
As the work on fluororous sorting tags (Chapter 1) demonstrates, such tags can be very useful in parallel and mixture synthesis. But having only one class of sorting tags puts limitations on the utility of this synthetic strategy. The number of homologous perfluorinated tags is limited, and mixture synthesis involving more substrates than tags (redundant tagging, section 1.3.4) can be difficult, especially if the products attached to one tag are not separable by

chromatographic means. Different classes of sorting tags separable under conditions that are orthogonal to those of perfluorinated tags would help overcome these limitations.

One obvious way a new class of sorting tags would be useful is by increasing the number of reactions that can be run as a mixture. If both classes of tags are used as a mixture, then the number of reactions that can be run simultaneously would be the sum of the number of distinct tags in each class. If tags are developed that incorporate both classes of sorting elements, the number of reactions that can be run as a mixture is the product of the number of distinct tags in each class. This kind of tagging can be called *Chimeric tagging*. This argumentation assumes that each final product would have a unique combination of the two sorting tags. Applying the redundant tagging strategy, the number of reactions that can be run simultaneously increases even more. Obviously split synthesis can also be applied.

A new class of sorting tags would also allow for the mixture synthesis that requires the cross-reaction of two groups of substrates. Let's assume that a cross reaction is required between two sets of 4 reactants each (A_1 - A_4 , and R_1 - R_4). If protection and deprotection are required before, and after the reaction, and both protecting groups can be cleaved in one step, the number of reactions required to obtain the 16 desired products (A_1R_1 - A_4R_4) by one component parallel synthesis would be 40. The same products could be obtained in only 25 reactions through cross-reaction mixture synthesis using a different class of sorting tag (T_1 - T_4 , T'_1 - T'_4) for each set of reactants. (Figure 2-1). This would correspond to a 160% increase in synthetic efficiency. To generalize this concept, for n reactants in one set, m reactants in the other set, and o reactions (one cross-reaction + subsequent reactions of the cross-coupled products), single component parallel synthesis would require $(o \cdot m \cdot n + 3(m+n))$ reactions, whereas the tagged mixture synthesis would require only $(o + 3(m+n))$ reactions. This generalization is only valid

under the conditions stated above. Obviously the number of chromatographic separations required would be less for tagged mixture synthesis, assuming that the single component reaction products require chromatographic purification as well. The increase in reaction efficiency would increase dramatically if more than one synthetic step would be required.



n	m	o	Parallel Synth. # of Rxns.	Mixture Synth # of Rxns.
4	4	1	40	25
4	4	2	56	26
4	4	3	72	27
4	4	4	88	28
5	5	1	55	31
5	5	2	80	32
5	5	3	105	33
5	5	4	130	34

Figure 2-1: Comparison of the efficiencies of tagged mixture synthesis and parallel mixture synthesis.

Sorting tags should exhibit certain qualities to be useful in organic synthesis. They should be readily available at a reasonable cost. They should be polymeric, and there should be an exponential relationship between polymer length, and retention time on chromatographic media (*isocratic elution*). That is, they should form a homologous series. They should be chemically inert, and not interfere with the analysis of the product.

There are few classes of compounds that satisfy all, or most, of the requirements stated above. Derivatives of oligomers of ethyleneglycol (OEGs), **71**, have the potential to be a new class of sorting tags. They are relatively cheap, can be expected to be stable under most reaction conditions MPEG supports are stable, introduce little interference with the analysis of the products, and are polymeric. The main questions that need to be asked are whether OEGs have sufficient separatory power to be used as sorting tags and whether they can be separated under orthogonal conditions with respect to fluoruous tags.

2.2 NORMAL PHASE CHROMATOGRAPHIC BEHAVIOR OF OEG ESTERS

2.2.1 Preparation of OEG Esters

To determine whether or not OEGs have sufficient separatory power to be useful as sorting tags 25 OEG bearing esters (**72a-76e**) were prepared (Figure 2-2). The esters have been chosen such that their polarities are similar since under such conditions tagged mixture synthesis would be most useful. The methyl esters would provide a reference point. While they were not employed in the normal phase HPLC (NPLC) work, they proved to be useful in the reversed phase HPLC (RPLC) work.

The methyl esters were prepared through methylation with CH_2N_2 , and the yields were quantitative. Initial attempts at making the OEG esters using SOCl_2 /benzotriazole/TEA, commercial benzoyl chloride/TEA, and SOCl_2 /TEA afforded them in poor to moderate yields (24-69%).^{3a-b} EDCI/DMAP on the other hand afforded the desired esters in good yields (Table 2-1). These esters can be prepared as mixtures, or individually with similar yields. The mixture preparation could be viewed as the first example of a mixture synthesis using OEG derivatives. It should be pointed out OEG derivatives have an NMR fingerprint (4.5-3.2 ppm in $^1\text{H-NMR}$, Figure 2-3), which might interfere with the characterization of some OEG-bound substrates, but this is not expected to prohibit OEG tag use because often analytically important hydrogen resonances lie outside this region.

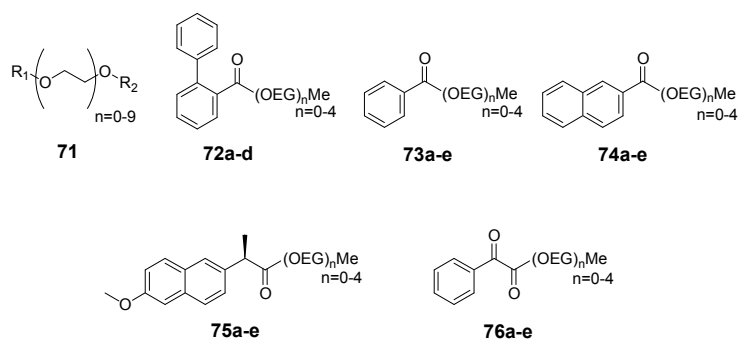
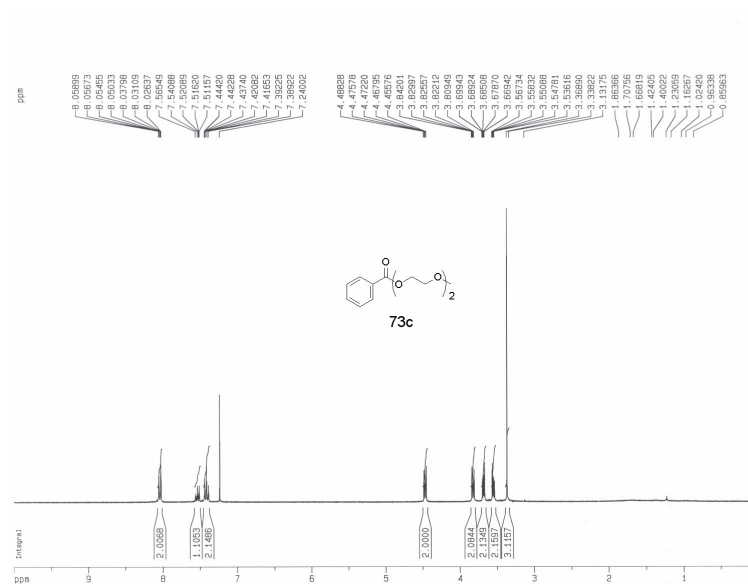


Figure 2-2: OEG esters used in HPLC studies.

Table 2-1: Percent Yields for Esterification under Various Conditions

	a	b	c	d	e
72	99	91 ^a (24) ^a	94 ^a (52) ^b	95 ^a (42) ^b	92 ^a (43) ^b
73	99	93 ^a (67) ^c	94 ^a (66) ^c	96 ^a (63) ^c	92 ^a (65) ^c
74	99	95 ^a	98 (63) ^c	96 (32) ^c	93 (56) ^c
75	99	95 ^a (63) ^b	96 ^a (60) ^b	97 ^a (50) ^b	95 ^a (52) ^b
76	99	61 ^a (69) ^b	58 ^a (66) ^b	43 ^a (45) ^b	46 ^a (54) ^b

^aEDCI/DMAP. ^bSOCl₂/benzotriazole/TEA. ^ccommercial benzoyl chloride/TEA. ^dSOCl₂/Heat/TEA.

**Figure 2-3:** ¹H-NMR spectrum for ester **73c**.

2.2.2 NPLC Retention of OEG Esters

Depending on the nature of the stationary phase, a number of interactions between the substrates, the mobile, and stationary phases are responsible for retention in chromatography. Among these can be hydrophilic, and hydrophobic interactions, partitioning between the stationary, and mobile phases, hydrogen bonding, π -acidic/ π -basic interaction, and inclusion complexation.^{2a-d}

The separatory power of the OEGs was tested by examining the normal phase HPLC (NPLC) retention of OEG esters **72a-76d**. A mixture containing 18 of these 25 esters was prepared (the methyl esters, **73b**, and **74b** were not used), and separation was tested on several silica NPLC columns. The preparation and separation of such a mixture can be regarded as being the logical equivalent of a mixture synthesis involving Excess Substrate Tagging (EST, our term for redundant tagging). We considered such an experiment to be sufficient as the proof-of-principle for mixture synthesis involving OEG-based sorting tags.

In a single pass on a NPLC silica column (5 μ Supelcosil), 17 of the 18 esters were separated (Figure 2-4). **73c** completely overlapped with **72c**, and **73e** partially overlapped with **74e**. Identification of individual peaks was accomplished by comparing the retention times of pure compounds to the retention times of components in the mixture, and by analyzing the real-time UV-Vis spectra of the component peaks (Figure 2-5).

As can be seen in Figure 2-4, the separation of the esters is dominated by the degree of polymerization (DP) of their OEG portions, and the chromatogram can be separated into four major separatory regions based on the DP of the OEG portions of the molecules. Within each separatory region, esters elute in the same order ($t_{72} < t_{73} < t_{74} < t_{75} < t_{76}$) based on the nature of the parent methyl ester. Thus separation is a function of both the DP of the OEG group, and the nature of the substrate attached to it. The fact that conditions required to separate the 4 OEG regions does not obliterate the separation within each separatory regions is an important finding, as this would enable mixture syntheses with more than one kind of substrate attached to OEG groups with the same DP (EST, or redundant tagging).

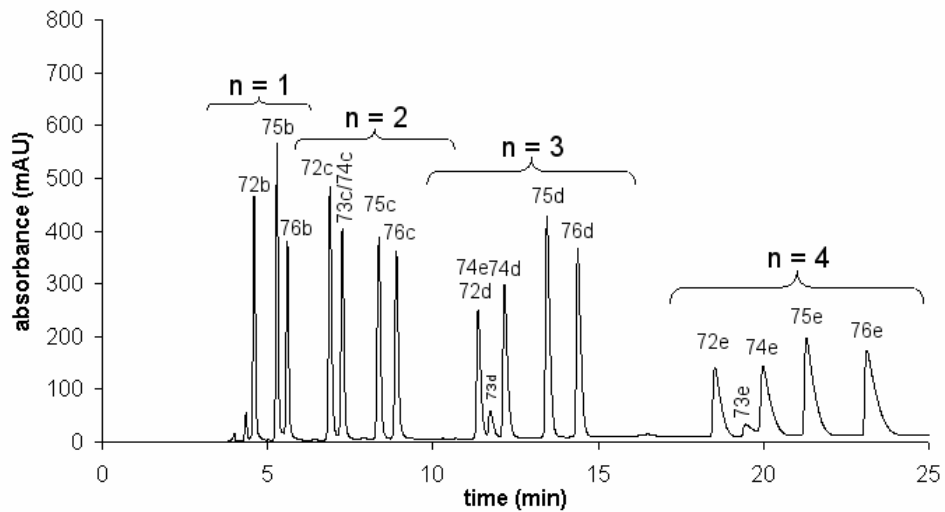


Figure 2-4: Chromatogram for esters 72b-e, 73c-e, 74c-e, 75b-e, and 76b-e.

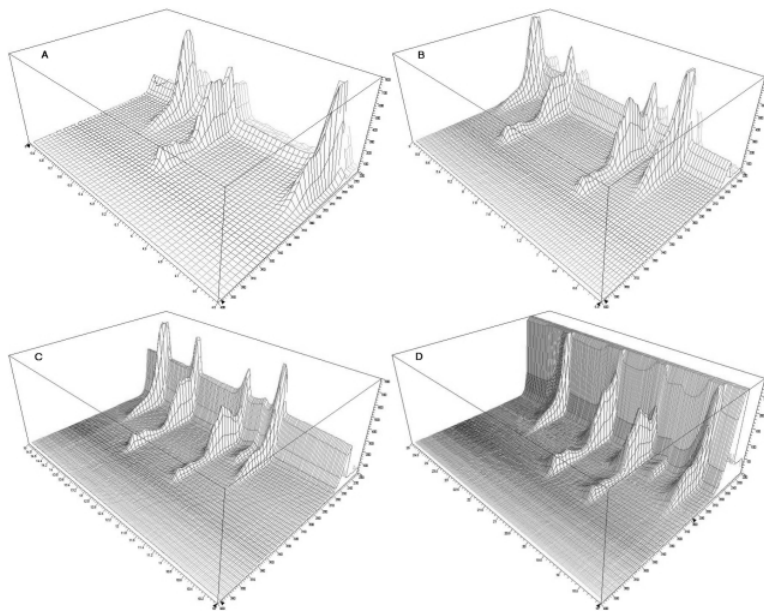


Figure 2-5: Real-time UV/Vis spectra for 72b-e, 73c-e, 74c-e, 75b-e, and 76b-e..

The chromatographic parameters for the chromatogram in Figure 2-5 (Table 2-2), t_R (retention time), k'_A (retention factor), N (number of theoretical plates), and R_s (resolution factor) can be calculated using (1)-(3)

$$k'_A = \frac{t_R - t_M}{t_M} \quad (1)$$

$$N = \frac{5.55t_R^2}{w_{1/2}^2} \quad (2)$$

$$R_s = \frac{2[(t_R)_B - (t_R)_A]}{W_A + W_B} \quad (3)$$

where t_R is the retention time for the solute, t_M is the retention time for the mobile phase (i.e. dead volume for the column), $w_{1/2}$ is the peak width at half height, R_s is the resolution between adjacent peaks, and W_A is the peak width at baseline for solute A. Examination of the data in Table 2-2 and inspection of the peaks in Figure 2-4 demonstrate baseline or near-baseline separation ($R_s \geq 1.5$ indicates baseline separation) and good peak symmetry for all the peaks, with the exception of **73c**, which completely overlapped with **74c**. These findings suggest that using preparatory scale HPLC meaningful quantities of OEG tagged substrates could be separated with acceptable purity. Separation can be further enhanced by the employing higher efficiency columns.

The chromatogram in Figure 2-4 was obtained using gradient elution. The separatory power of OEGs becomes more apparent when OEG esters are subjected to isocratic elution.

When esters **72a-d** were subjected to isocratic elution on the same column, it was observed that the separation between the peaks increased dramatically (Figure 2-6). This would suggest that a relatively large number of substrates, particularly nonpolar ones could be tagged with OEGs of the same DP value. It should be noted that there was an exponential relationship between the DPs of esters **72a-d**, and their respective t_R (and similarly k') values. While this might seem peculiar at first glance, it is in fact the result of the capacity factor-free energy of retention relationship (4) in HPLC (see Chapter 3).

$$\ln k' = \ln \beta - \frac{\Delta G^o}{RT} \quad (4)$$

Table 2-2: t_R , k' , N, and R_s values for the chromatogram in Figures 2-4 and 2-7.

		b*	c*	d*	e*	b**	c**	d**	e**
72	t_R	4.56	6.89	11.37	18.53	5.44	8.74	13.84	20.32
	k'	0.75	1.65	3.37	6.13	1.09	2.36	4.32	6.82
	N	26100	27700	43000	35300	8000	5900	14800	15100
	R_s	- ^a	8.71	12.11	15.95	- ^a	4.56	5.61	5.30
73	t_R	- ^b	- ^c	11.74	19.45	- ^b	- ^c	- ^d	- ^e
	k'	- ^b	- ^c	3.52	6.48	- ^b	- ^c	- ^d	- ^e
	N	- ^b	- ^c	33500	34100	- ^b	- ^c	- ^d	- ^e
	R_s	- ^b	- ^c	1.57	2.52	- ^b	- ^c	- ^d	- ^e
74	t_R	- ^b	7.26	12.16	19.99	- ^b	9.22	14.76	21.76
	k'	- ^b	1.79	3.68	6.69	- ^b	2.55	4.68	7.37
	N	- ^b	30800	42400	27300	- ^b	10100	10600	9800
	R_s	- ^b	2.17	1.57	0.96	- ^b	1.06	1.63	1.65
75	t_R	5.28	8.36	13.45	21.30	6.55	10.66	16.25	23.05
	k'	1.03	2.22	4.17	7.19	1.52	3.10	5.25	7.86
	N	28400	37700	55600	31500	9400	13200	16700	16800
	R_s	5.28	6.04	4.60	2.18	3.76	3.20	2.57	1.41
76	t_R	5.60	8.90	14.39	23.13	6.82	10.99	16.93	24.23
	k'	1.15	2.42	4.53	7.90	1.62	3.23	5.51	8.32
	N	27600	35300	63700	30400	9400	12600	18700	15100
	R_s	2.32	2.85	3.54	3.21	0.84	0.68	1.23	1.41

*Sulpelcosil (Figure 2-4). **VersaPak (Figure 2-7). ^a R_s is defined with respect to the precedent peak.
^bNot present in sample. ^cOverlaps with **72c**. ^dOverlaps with **74d**. ^eOverlaps with **74e**.

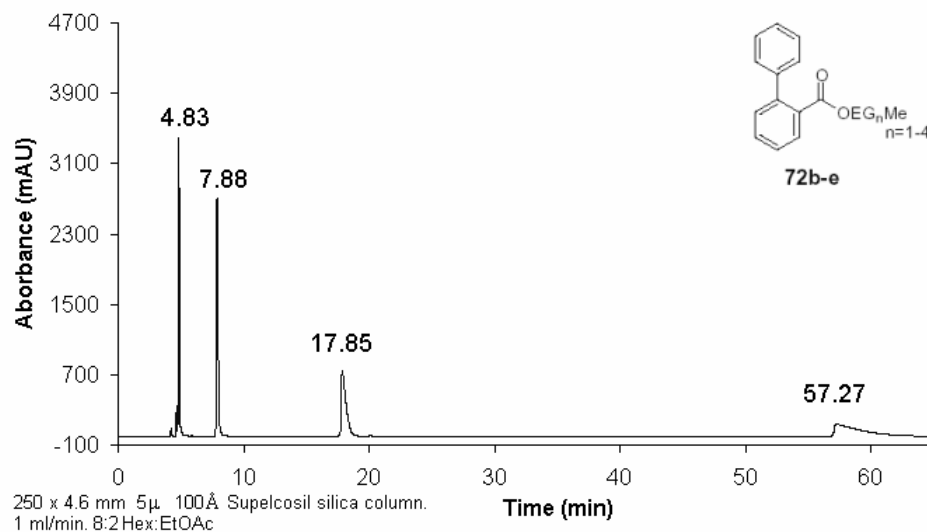


Figure 2-6: Isocratic elution of **72b-e**.

Normal phase HPLC analysis of a mixture of esters **72b-76e** has also been done using a 10µ VersaPak silica column (Figure 2-7). The conditions optimized for the 5µ Supelcosil column were used on the VersaPak column. Total elution time was approximately the same for the two silica columns. As Figure 2-7 demonstrates, separatory region structures, and elution orders were the same with the VersaPak column as with the Supelcosil column. However the resolution of the peaks was weaker, and column efficiency (quantified as *N*) was lower (Table 2-2). Complete overlap was observed between the pairs **72c-73c**, **73d-74d**, and **73e-74e**. However, peak symmetry seems to be better for the VersaPak column, particularly for late eluting substrates. The relatively poor performance of the VersaPak column might be due to its larger particle size, which could make the column less efficient. The absence of column-specific elution optimization might also be a factor. Since the efficiency of the column was not determined before the experiments, deterioration in the column efficiency might also be a factor.

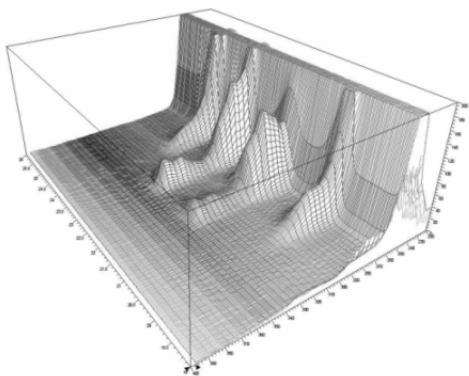
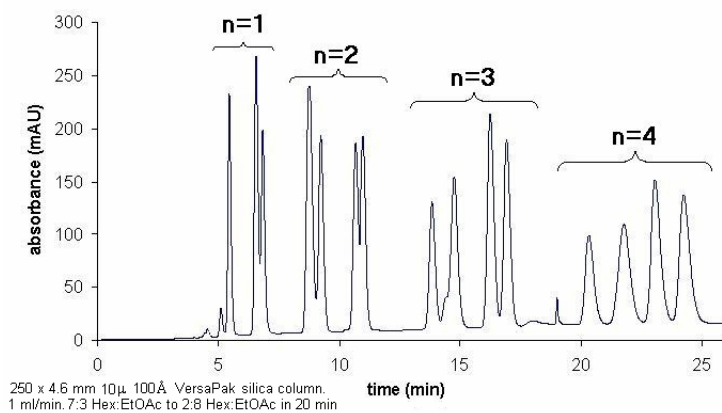


Figure 2-7: Retention of OEG esters **72b-76e** on a VersaPak column.

We postulated that under normal phase conditions a large portion of the separatory power of OEGs might be the result of hydrogen bonding with the stationary phase, and therefore the separation of the esters **72b-76e** on a 5 μ Cyclobond I column under normal phase conditions was also investigated. Apart from their hydrogen bonding capability, cyclodextrin stationary phases have the added benefit of potential inclusion complexation with aromatic portions of solutes. Such interactions could further improve the separation of substrates, although this is not expected to play an important role under normal phase conditions. While the natures of silica and cyclodextrin stationary phases are significantly different, potential hydrogen bonding between the substrates, and the stationary phase is a common quality. Polar interactions would be expected to play a lesser role. The elution order of the esters observed on silica stationary phases

was retained on the cyclodextrin column, with the exception of **73c-73e** which moved to the first position within the OEG DP based separatory regions. Significant band broadening of the peaks resulted in poor resolution. However the observation that both silica and cyclodextrin stationary phases separate these esters in a similar fashion lends credibility to the hypothesis that hydrogen bonding is an important factor contributing to the efficiency of OEG derivatives as sorting tags.

2.2.2.1 Effect of Group IA Cations on the NPLC Retention of OEG Esters

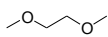
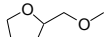
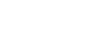
The accidental discovery of crown ethers, and their cation binding properties, led to a renewed interest in such properties of glymes, and their aromatic group bearing derivatives, commonly referred to as podands.⁴ This interest is in part due to the lower cost, and synthetic availability of these open-chain structures. The nature and structure of glyme-metal complexes, and analogous structures have been investigated in detail.⁵

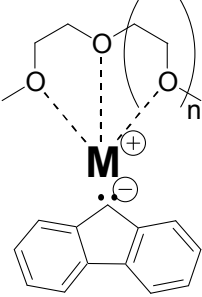
One striking difference between crown ethers and their glyme counterparts is the difference in their metal binding ability. For instance the K^+ complex of cyclohexyl-15-crown-5 has a K_s (stability constant) that is $\sim 10^4$ times larger than that of pentaglyme. Similarly, there is a three orders of magnitude difference in the K_s values between the Na^+ complexes of these two.⁶ This difference in K_s values is attributed to the “macrocyclic effect”, which is a result of entropy factors associated with the reorganization of the O donor groups around the substrate, thermodynamic parameters, and changes in solvation around the ligand upon complexation.^{7a-c}

Smid and coworkers have investigated the nature and properties of glyme-cation complexes extensively.^{8a-e} Chan, Wong, and Smid have studied the binding of various glymes (DP = 1-7) with fluorenyl lithium, sodium, and potassium in solvents such as dioxane, THF, and THP.^{8a} Fluorenyl salts have strong absorbances which change upon variations in their

aggregation states, and ion separation (i.e. contact ion pair vs. solvent separated ion pair). The workers have found that the stability constants (K_s) of glyme-separated ion pairs of fluorenyl alkali salts increased with increase in the DP of glymes (Table 2-3). The authors note that no significant increase in Li^+ binding was observed with glymes having a DP larger than 5. However, for Na^+ it was found that stability constants of the complexes increased as the DP increased. Similar observations have been made with potassium cations as well.

Table 2-3: Stability constants of complexes of glymes with Li^+ and Na^+ .

Glyme	K_s $M^+ = \text{Li}^+$	K_s $M^+ = \text{Na}^+$
	0.055	-
	0.25	-
	3.1	1.4
	130	9.0
	240	170
	-	450
	-	800



The observations of Smid *et al.* prompted us to study the effect of group IA cations on the retention of OEG esters on silica stationary phases. We anticipated that additions of group IA cations to the chromatographic medium would increase the retention times, and peak resolution of OEGylated molecules. To test this a number of TLC plates were prepared by immersing standard analytical silica plates in aqueous solutions of different salts and then drying the plates

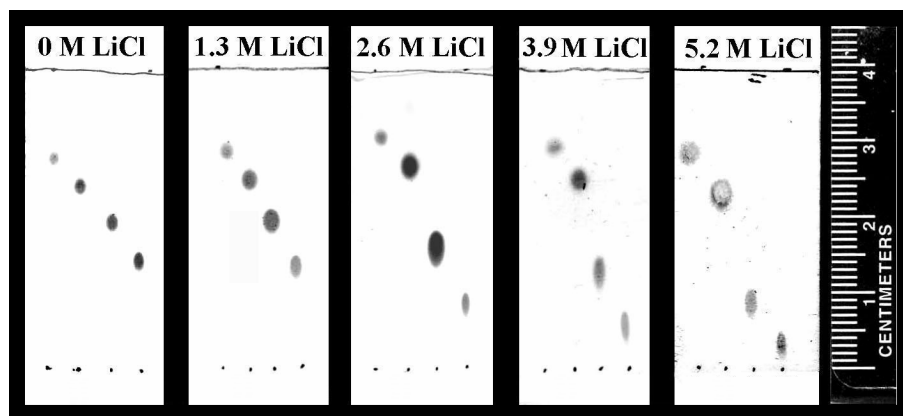
at 150 °C. Visualization of developed TLC plates was done by examination under UV light and CAM (cerium ammonium molybdate) staining. Salt densities on plates (mol/cm^2) were determined by weighing the silica on the plates before and after treatment with aqueous solutions of group IA salts.

Using a number of different eluents the R_f values for **75b-f** on these lithium salt treated (Li-TLC), and untreated TLC plates were recorded (Table 2-4, Figure 2-8). It was found that the highest improvement in separation was obtained for a $8.73 \times 10^{-5} \text{ mol}/\text{cm}^2$ concentration of Li^+ (entries 1-6). The retarding effect is larger for the longer OEGs **75d-e** than for the shorter tagged esters **75b-c**. The comparative lack of effect of Na^+ and K^+ salts (entries 6-7) agrees with the known K_s values for OEG/ Li^+ and OEG/ Na^+ complexes.^{8a} Both DME and THF caused the esters to elute closer to each other (entries 9-14). This is probably due to competition of the mobile phase with the OEG esters for hydrogen bonding sites on the surface of the stationary phase (i.e. silanol groups and adsorbed water). The presence of a soluble Li^+ salt (LiClO_4) in the mobile phase caused **75d-e** to elute relatively faster while the modification in the mobile phase had no apparent effect on the R_f values for **75a-b**. This could mean that the OEG-lithium complexes elute faster than free OEG ligands in the presence of mobile phases containing soluble lithium salts. This is probably a result of the increased mobile phase affinity of these OEGylated esters upon complexation with LiClO_4 . All of these observations suggest that the presence of lithium salts in the stationary and/or mobile phases can be used to improve the separation of OEG bearing substrates on silica.

Table 2-4: Separation of esters **75b-e** by TLC under various conditions.

Entry	[M ⁺] (mol/cm ²) ^a	5a ^{b,h}	5b ^{b,h}	5c ^{b,h}	5d ^{b,h}	Eluent
(1)	0	0.70	0.60	0.46	0.34	EtOAc
(2)	1.72 x 10 ⁻⁵ (Li ⁺)	0.75	0.64	0.33	0.18	EtOAc
(3)	3.73 x 10 ⁻⁵ (Li ⁺)	0.76	0.63	0.34	0.19	EtOAc
(4)	6.63 x 10 ⁻⁵ (Li ⁺)	0.70	0.6	0.34	0.16	EtOAc
(5)	8.73 x 10 ⁻⁵ (Li ⁺)	0.71	0.59	0.22	0.11	EtOAc
(6)	1.09 x 10 ⁻⁴ (Li ⁺)	0.70	0.59	0.22	0.10	EtOAc
(7)	8.9 x 10 ⁻⁵ (Na ⁺)	0.75	0.63	0.48	0.38	EtOAc
(8)	6.1 x 10 ⁻⁵ (K ⁺)	0.78	0.68	0.53	0.33	EtOAc
(9)	0	0.50	0.29	0.15	0.08	^c
(10)	8.73 x 10 ⁻⁵ (Li ⁺)	0.56	0.34	0.08	0.03	^c
(11)	8.73 x 10 ⁻⁵ (Li ⁺)	0.59	0.48	0.30	0.20	^d
(12)	8.73 x 10 ⁻⁵ (Li ⁺)	0.78	0.75	0.68	0.62	DME
(13)	8.73 x 10 ⁻⁵ (Li ⁺)	0.58	0.45	0.23	0.11	^e
(14)	8.73 x 10 ⁻⁵ (Li ⁺)	0.64	0.58	0.50	0.39	THF
(15)	0	0.73	0.65	0.51	0.38	^f
(16)	0	0.75	0.64	0.61	0.58	^g
(17)	3.73 x 10 ⁻⁵ (Li ⁺)	0.78	0.65	0.43	0.30	^g

^aConc. of metal ions on the surface of the TLC plate. ^bR_f values. ^c1:1 EtOAc:Hex. ^d1:1 DME:Hex. ^e1:1 THF:Hex. ^f0.1 M LiClO₄ in EtOAc. ^g1 M LiClO₄ in EtOAc. ^hVariation in R_f values was ± 0.05.

**Figure 2-8:** TLC results for esters **75b-e**. Plates were immersed in 0, 1.3, 2.6, 3.9, and 5.2 M aqueous LiCl solutions and dried prior to analyte application and development with EtOAc.

2.2.2.2 The Retention Mechanism of OEG Derivatives on Silica Stationary Phases

The findings summarized in section 2.2.2 suggest that the retention of OEGs bound to substrates of comparable polarities is dominated by the nature of the interactions of the OEGs with the stationary and mobile phases. The equilibria that may affect the retention of OEG derivatives on silica stationary phases are depicted in Figure 2-9.

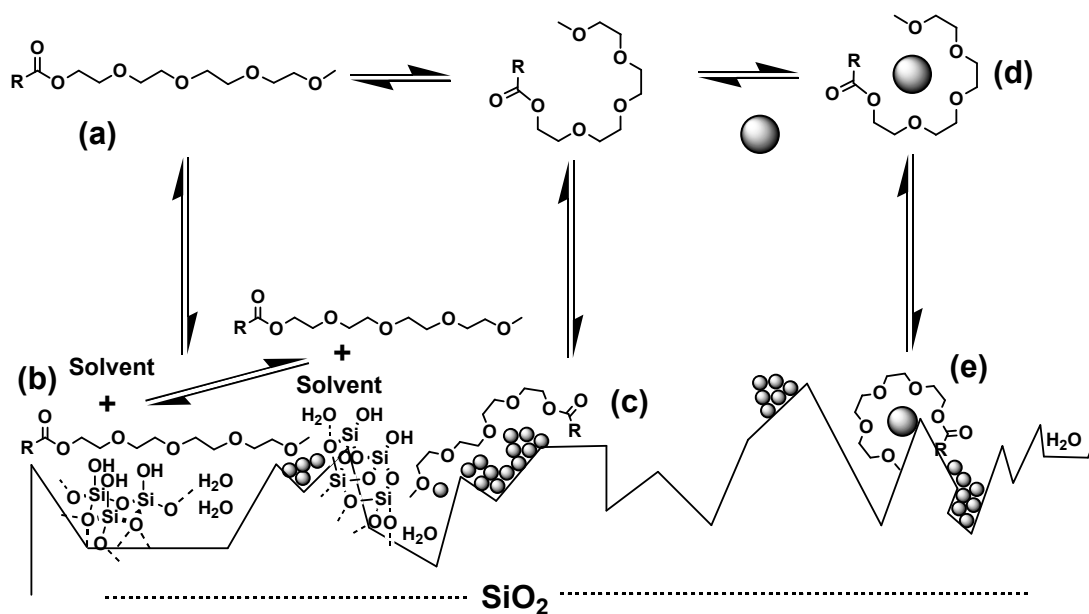


Figure 2-9: Equilibria affecting OEG ester retention on silica.

As suggested by the similarities of retention patterns on silica and cyclodextrin stationary phases, hydrogen bonding of the substrates may be an important factor (equilibrium (a)). Polarity based adsorption can also be a factor. The relative contributions of hydrogen bonding and polar interactions to OEG retention cannot be determined with the data at hand. Use of capped cyclodextrin stationary phases could be useful in that regard. Competition for hydrogen bond donor groups on the silica surface can be regarded as a significant factor in the presence of

hydrogen bond acceptor solvents. This is demonstrated by entries 9-14 in Table 2-4 (equilibrium (b)). Provided they are present on the silica surface, complexation of OEG esters with lithium salts seems to be an important factor in retention, as entries 2-6 in Table 2-4 suggest (equilibrium (c)). This complexation based retention is partially inhibited by the presence of ether-type solvents (entries 11-14). Metal cation-OEG complexes that are soluble in the mobile phase tend to be more mobile than free OEG ligands. Entries 14-17 in Table 2-4 suggest that this complex formation reduces the effect of hydrogen bonding (and/or polar interactions) and metal cation-OEG complex formation on the surface of the stationary phase (equilibria (d), and (e)).

The retention of the compounds within the OEG DP based separatory regions (Figure 2-4) is dependent on the properties of the substrate bound to the OEG group. One such property could be the dipole moments of the non-OEG portion of these esters. The dipole moments of the non-OEG portions of **72b-76e** can be approximated by the dipole moments of the corresponding methyl esters **72a-76a**. The dipole moments for these methyl esters were calculated based on conformations in water that were optimized using MOPAC with AM1 parameters, and the conductor-like screening model (COSMO).⁹ Using water as the solvent that dictates the ambient dielectric constant seems to be the most realistic way of estimating the conformations, and dipole moments of these esters on the surface of the silica stationary phase. There is a qualitative (and perhaps a quantitative) correlation between the elution order of the esters **72a-76a** within each separatory region and their respective dipole moments (Figure 2-10). Moreover within the separatory regions there is also a linear relationship between relative elution times which are calculated in a similar manner as retention factors, and dipole moments ($R^2 \geq 0.95$, Figure 2-11).

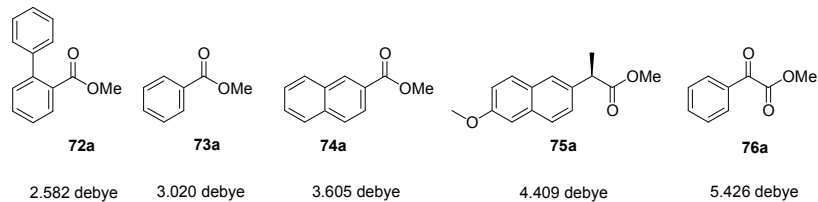


Figure 2-10: Dipole moments for methyl esters 72-76a

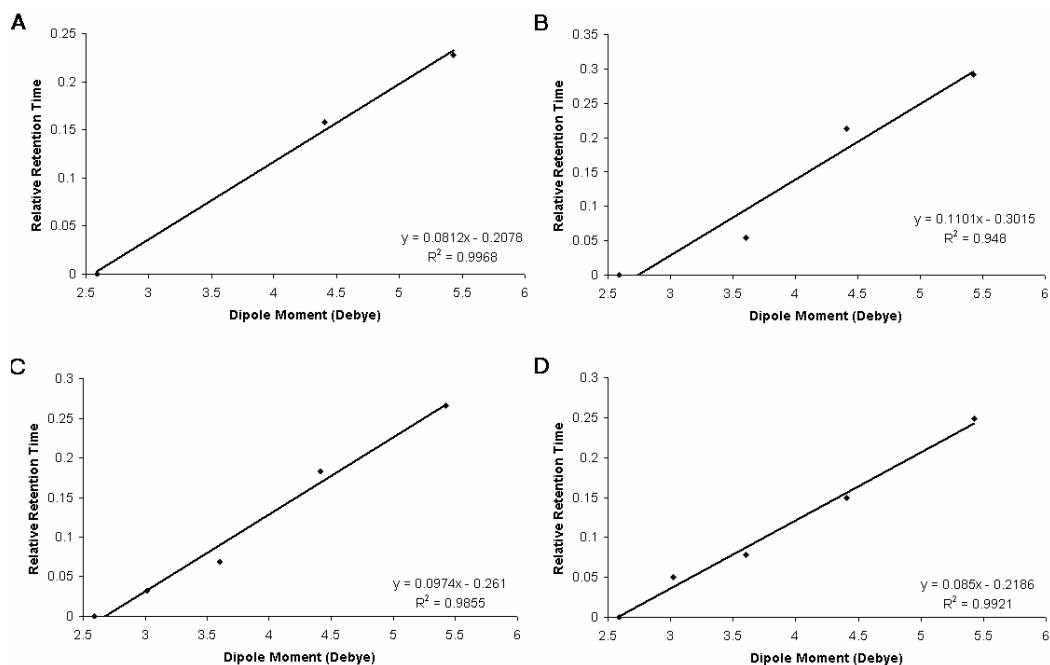


Figure 2-11: Dipole moment versus relative retention time plots for peaks within each separatory region 1-4 (A-D) for the chromatogram in Figure 2-4.

We do not wish to imply that dipole moments of the substrates alone are responsible for retention times within the separatory regions. Entropic change associated with the change in solvation upon interaction with silica, reorganization of the substrates, and other factors could also be involved with the retention process. But it can be said that dipole-dipole interactions make a large contribution to the energetics of retention. Based on the correlations demonstrated in Figure 2-11, one might be inclined to speculate that a difference in dipole moments of the

substrates that is equal or, larger than 0.5 Debye are required for baseline separation. Determination of whether this crude approach for the prediction of elution order, and separation quality holds true requires more experimentation.

2.3 OEGYLATED PROTECTING GROUPS AND THE EFFECT OF DOUBLE OEGYLATION

2.3.1 Design of Protecting Groups Based on Vanillic Acid

One way of introducing sorting tags into a synthetic scheme is their utilization as protecting groups. Provided that the corresponding single component reactions require the employment of protecting groups as well, this strategy would ensure that the use of sorting tags in mixture synthesis does not introduce unnecessary additional reactions. Candidates for sorting tags disguised as protecting groups are benzyl alcohol, and benzoic acid derivatives. Benzyl alcohol, benzoic acid, and their derivatives have found widespread application as protecting groups for alcohols (as esters, ethers), amines (as amides, carbamates, N-benzylamines), carboxylic acids (as esters), diols (as benzylidene acetals, benzylidene ortho esters), phenols (as ethers, esters), and thiols (as thioethers, thioesters).¹⁰

We surmised that derivatives of vanillic acid (**77**) would be good candidates for OEG-based sorting tags (Figure 2-12). The free 4-hydroxyl group would provide a clear point of attachment for the OEG group, affording OEGylated sorting tags **78**, and **79**. Provided that demethylation of the 3-methoxy group can be achieved, fluororous groups can be attached as well, which would expand the scope of these sorting tags (Chimeric Tags, **80**). Furthermore

additional OEG groups can be attached to such demethylated compounds, providing easy access to sorting tags with DPs of 1-9 (**81**). The OEGylated carboxylic acids (**79**) could also be esterified with OEG alcohols to give simple diOEGylated compounds (**82**), which could be used as models to study the effect of the attachment of two distinct OEG groups on the retention of molecules on chromatographic media, and to determine the potential utility of double OEGylation as a means of mixture synthesis with only one class of sorting tag.

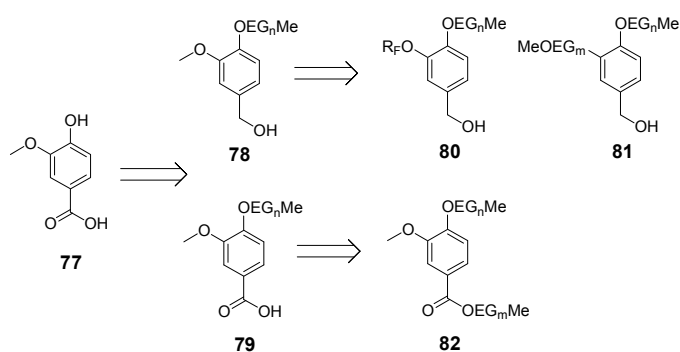


Figure 2-12: Retrosynthetic strategy for sorting tags based on vanillic acid.

As noted in section 2.2.2.1, glyme complexes with cations have much lower K_s values with respect to their crown ether analogues. Introduction of groups which can induce a degree of preorganization of the glyme backbone can enhance those K_s values. Kyba, Helgeson, Madan, Gokel, Tarnowski, Moore, and Cram have studied the tetrabutyl ammonium binding properties of structures **83-85** (Figure 2-13).¹¹ **83** is a benzocrown derivative. **84** is a glyme derivative in which the rigid central naphthalene unit introduces a degree of preorganization, and convergence of the glyme arms. Structure **85** lacks such preorganization. The relative K_s values for **83-85**, derived from extraction studies, are 61000 : 61 : 1. The rigidity and preorganization introduced by the central aromatic group in **84** increases the binding constant significantly with respect to the unrigidized glyme **85**. The structural analogy between **81**, and

84 is self evident. Thus structures like **81** would likely exhibit enhanced cation binding properties, and since chain length can be controlled with facility, would be ligands capable of binding to Li^+ , Na^+ , and K^+ more efficiently than regular OEGs. These properties might make structures like **81** useful on ion-exchange columns where their orderly elution can be controlled by the identity, and concentration of the group IA cation in the mobile phase. Such column packing materials could also potentially be used for solid phase extraction (SPE).

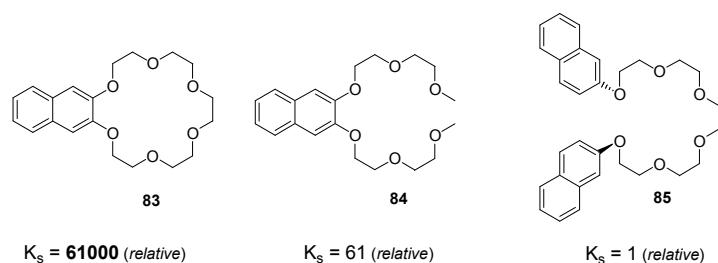


Figure 2-13: Effect of preorganization on the ion binding ability of some OEG derivatives.

2.3.2 Synthetic Work

Since the arguments put forward in Section 2.3.1 seemed to justify further studies, the synthesis of compounds **78-82** has been attempted. One obvious way of attaching the Me-OEG groups to **77** is through an ether bond with 4-hydroxy group of **77**. To this end chlorination of OEG alcohols (**86b-d**) was attempted. SOCl_2 /benzotriazole did not afford the desired chlorinated OEGs (**87b-d**) with sufficient yield.¹² Utilization of SOCl_2 /pyridine seemed to improve the yields of **87b-d** significantly (**87a** is commercially available).¹³ Etherification attempts using a number of conditions ($\text{TEA}/\text{CH}_2\text{Cl}_2$, $\text{K}_3\text{PO}_4/\text{DMSO}$, NaH/THF).¹⁴ It was found that $\text{K}_2\text{CO}_3/\text{KI}/\text{DMF}$ afforded the desired ethers, albeit in low yields. Optimization of reaction

temperature and time improved the yield. Further experimentation revealed that the quality of the DMF used, and our initial workup procedure were lowering the yields. Using distilled DMF stored over molecular sieves, and employing a modified workup procedure yielded the desired ethers **89a-g** in very good yield (Figure 2-14). Yield does not vary significantly whether the etherifications are done as single component, or mixture reactions.

Saponification of **89a-d** employing LiOH/H₂O/dioxane did not furnish the desired carboxylic acids **79a-d** in good yield, but using harsher conditions (KOH (aq)/EtOH/THF/reflux) afforded them in excellent yields. LiAlH₄ reduction of esters **89a-d** to afford **78a-d** proceeded with excellent yield (Figure 2-15). The utility of these benzylic OEG tags (**78a-d**) in mixture synthesis has been tested in Professor Dennis P. Curran's group (Department of Chemistry, University of Pittsburgh, Pittsburgh, PA). His coworkers have used these, along with simultaneous employment of their fluororous tags in a solution phase mixture synthesis of 16 stereoisomers of murisolin (Figure 2-16).¹⁵

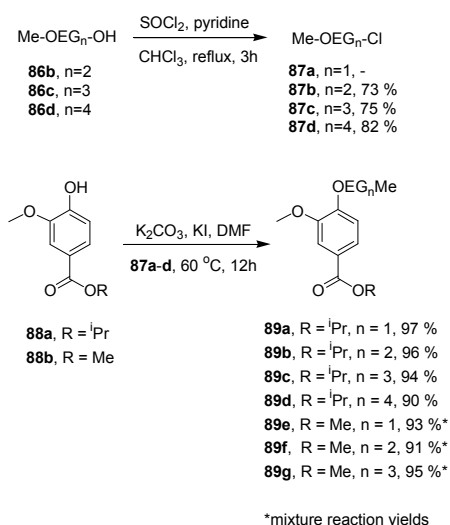


Figure 2-14: Preparation of **87b-d** and **89a-g**.

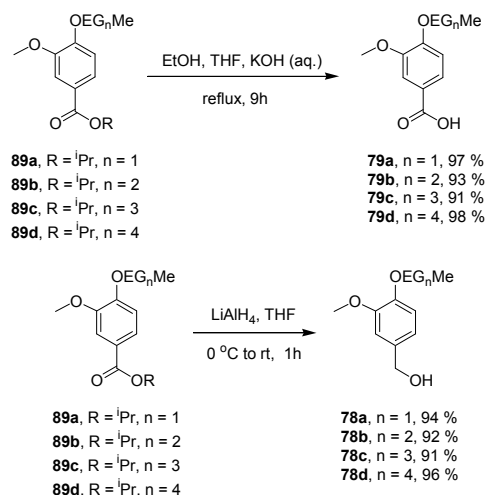


Figure 2-15: Preparation of **79a-d** and **78a-d**.

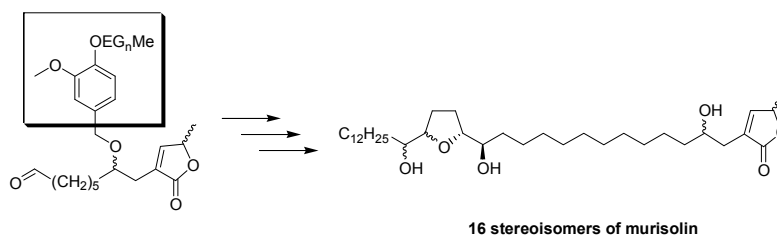


Figure 2-16: Employment of **78a-d** in the mixture synthesis of stereoisomers of murisolin.

TBDMS protection of the benzylic alcohols similarly proceeded with excellent yield to afford silyl ethers **90a-d**. Initial attempts at demethylation of the 3-methoxy group of **90a** employing $\text{BBr}_3/\text{CH}_2\text{Cl}_2$ failed to afford the demethylated product **91a**.¹⁶ These conditions seem to induce decomposition of the starting material. However, it was found that using $\text{LiPPh}_2/\text{THF}$ **91a**, and **91c** (**91b**, and **91d** were also prepared in similar yields, but are not reported here due to the lack of some spectral data) can be obtained in moderate to good yields (Figure 2-17).¹⁷ We tried to obtain a chimeric tag (**80**) by attempting to etherify **91a** with $\text{C}_4\text{F}_9\text{CH}_2\text{CH}_2\text{I}$ under conditions optimized for the preparation of **89a-g**. These attempts, and variations in base, temperature, and reaction time were fruitless. While the reasons for this failure are unknown,

similar difficulties in formation of these fluorous phenyl ethers have been reported.¹⁸ It was observed that such ethers were not formed if the methylene spacer on the fluorous arm was less than 4 subunits long. This problem can be remedied by etherification of **91** using fluoroalkyl bromides, or iodides which bear 4 methylene groups, or alternatively etherification of **91** with 4-bromo-1-butene, and radical addition of C₄F₉I followed by LiAlH₄ reduction (Figure 2-17).^{19a-}

c, 18

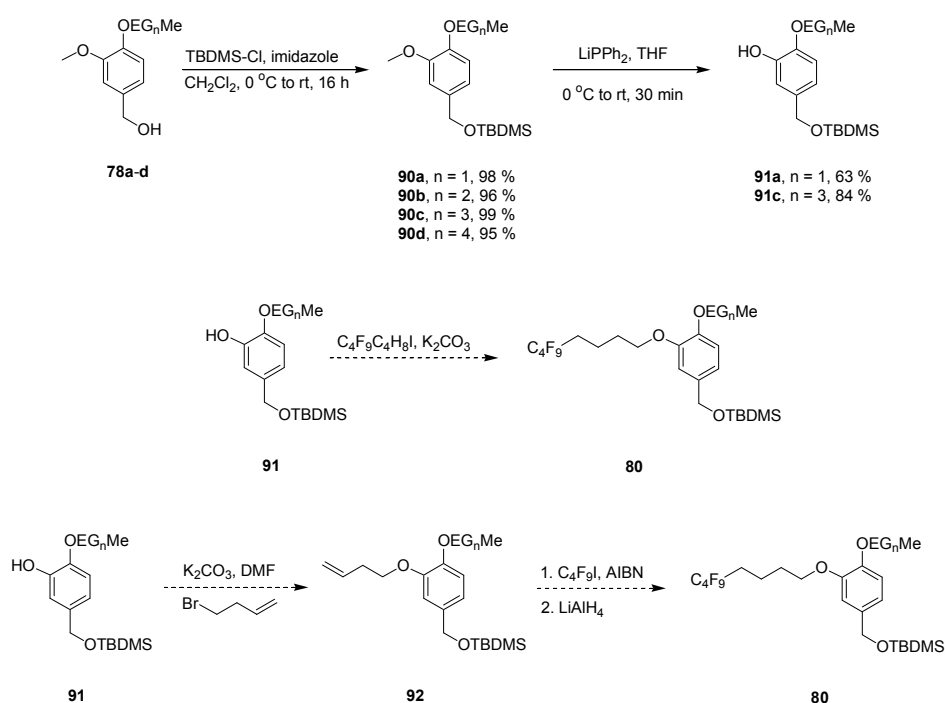


Figure 2-17: Preparation of **90a-d**, **91a**, and **91c**.

The desired double OEGylated compounds **93a-95c** were obtained through esterification of carboxylic acids **79a-c** and OEG alcohols **86a-c** using EDCI/DMAP/CH₂Cl₂. These esterifications were done by reacting each carboxylic acid with a mixture of 3 the OEG alcohols (**86a-c**) and the yields were good to excellent.

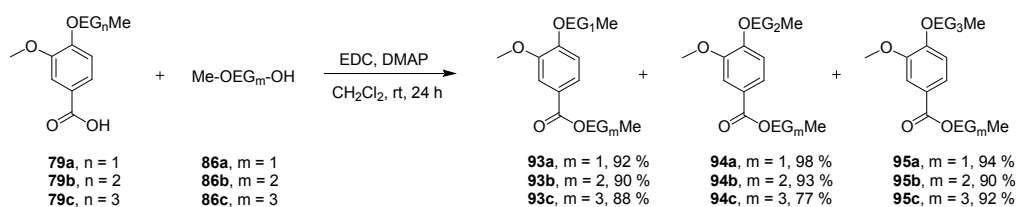


Figure 2-18: Preparation of **93a-c**, **94a-c**, and **95a-c**.

2.3.3 Separation of Double OEGylated Esters using NPLC and Li-TLC

The ability to perform cross reactions where each reactant set is tagged with the same set of OEG tags, or otherwise having the ability of tagging a larger number of substrates with the same set of OEG tags would be quite beneficial. To test this possibility a sample containing equimolar amounts of **89e-g**, and **93a-95c** was prepared. NPLC analysis of this mixture of esters has been done using a VersaPak™ silica column (250 x 4.6 mm, 10μ particle size, 100 Å pore size). The identities of the peaks were determined by comparing the elution times of ester sets {**89e**, **93a-c**}, {**89f**, **94a-c**}, {**89g**, **95a-c**} to those of the original mixture. Purity of the peaks was assigned based on real time UV-Vis spectra of the peaks. The relevant chromatogram is reproduced in Figure 2-19 (where n is the number of EG subunits attached through an ether bond, and m is the number of EG subunits attached through an ester bond), elution order of the double OEGylated esters is provided in Figure 2-20, and relevant chromatographic parameters are given in Table 2-5.

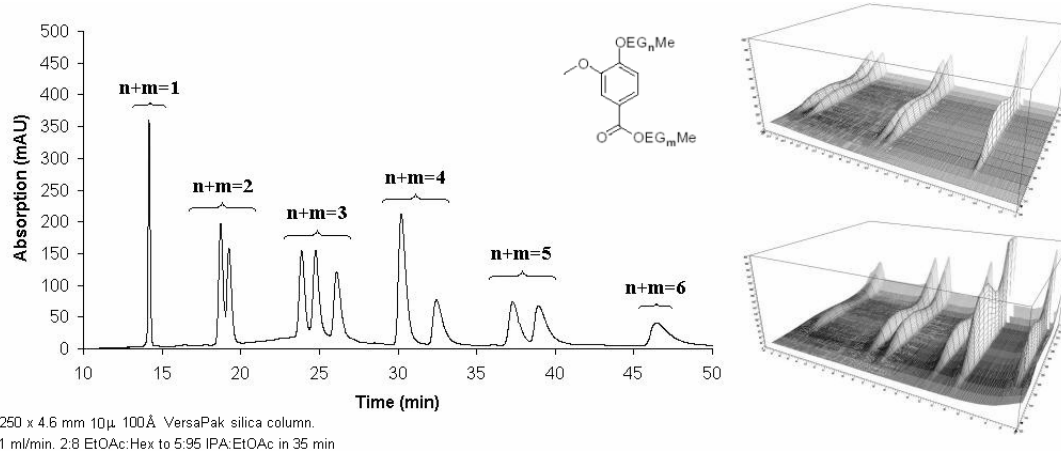


Figure 2-19: Chromatogram for the elution of a mixture of double OEGylated esters.

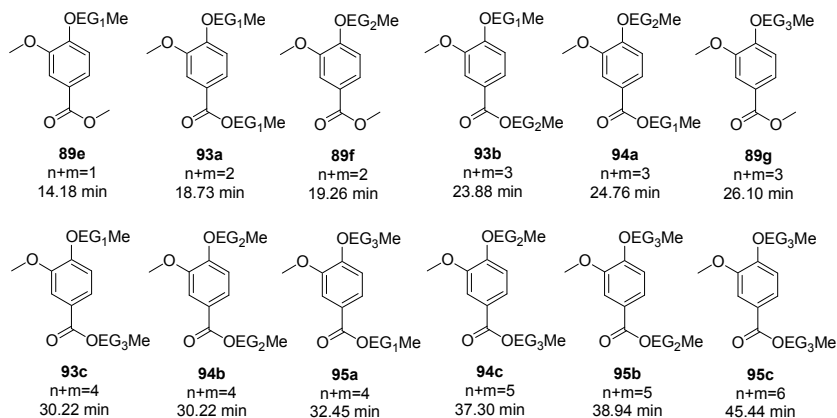


Figure 2-20: Retention times for **89e-g**, **93a-c**, **94a-c**, and **95a-c**.

Table 2-5: Chromatographic parameters for Figure 2-19

Peak #	ID	m+ n	t _R (min)	k'	R _s	N
1	89e	1	14.18	4.45	-	55200
2	93a	2	18.73	6.20	10.94	22200
3	89f	2	19.26	6.41	0.89	19900
4	93b	3	23.88	8.18	6.82	18500
5	94a	3	24.76	8.52	1.14	17100
6	89g	3	26.10	9.04	1.54	14600
7	93c/94b	4	30.22	10.62	4.38	20400
8	95a	4	32.45	11.48	2.04	14600
9	94c	5	37.30	13.35	3.84	17300
10	95b	5	38.94	13.98	1.15	13900
11	95c	6	45.44	16.48	3.92	11600

The chromatographic behavior of the double OEGylated esters is quite remarkable. A total of 11 peaks were observed for 12 compounds. 9 of these peaks exhibited baseline, or close-to-baseline separation, and only two had poor resolution, esters **93c**, and **94b** completely overlapped. One would normally expect these esters to elute as 6 peaks, separated based on the total number of OEG subunits they bear (i.e. $n + m$). This is clearly not the case. The peaks were separated into 6 groups based on the total number of OEG subunits. Within these groups, elution order was determined by the number of OEG subunits attached to the aromatic ring as ethers. It would seem that the per EG retention energy is larger for OEGs that are linked as ethers, than those linked as esters. This could be due to the diminished hydrogen bonding ability of the first oxygen of the OEG portions attached as esters.

Separation of these esters can further be enhanced on silica TLC plates treated with LiCl (Table 2-6). Particularly noteworthy is the enhanced separation of **93a/89f**, and **93c/94b** which partially, or completely overlapped in the chromatogram reproduced in Figure 2-19. These findings suggest that within the $m+n$ based groups, the OEG groups attached as ethers have a more pronounced role in retention due to complexation with Li^+ on the surface of silica. This could be due to a number of factors. The aromatic ring in the ether linked OEGs might introduce a level of preorganization which enhances ion-binding capability. Reduced electron density on the first oxygen of the OEG groups attached as esters could render their cation-binding ability weaker.

Table 2-6: R_f values for esters **89e-g** and **93a-95c** on LiCl treated and untreated silica TLC plates.

Entry	ID	n ^a	m ^b	m + n	R _f (0 M Li ⁺) ^c	R _f (2.6 M Li ⁺) ^d
1	89e	1	0	1	0.61	0.51
2	93a	1	1	2	<u>0.51</u>	<u>0.43</u>
3	89f	2	0	2	<u>0.47</u>	<u>0.36</u>
4	93b	1	2	3	0.42	0.36
5	94a	2	1	3	0.37	0.31
6	89g	3	0	3	0.32	0.21
7	93c	1	3	4	<u>0.31</u>	<u>0.20</u>
8	94b	2	2	4	<u>0.31</u>	<u>0.28</u>
9	95a	3	1	4	0.31	0.20
10	94c	2	3	5	0.24	0.12
11	95b	3	2	5	0.23	0.10
12	95c	3	3	6	0.20	0.08

^aNumber of EGs attached as ether. ^bNumber of EGs as ester. ^cPlate dipped into deionized water then dried. ^dPlate dipped into 2.6 M LiCl solution then dried.

These initial findings suggest that mixture synthesis employing only OEG-based tags could be feasible, provided that the mode of attachment of the two groups of OEG tags is different. This would ensure a slight modification of hydrogen bonding, and/or ion-binding ability which could be exploited to maximize separation between the substrates. It should be noted that the non-OEG portions of esters **89e-g**, and **93a-95c** are identical, thus do not have a contribution to the overall separation of the esters. In real-life applications, the non-OEG portions would be different, and judicious choice of substrate-OEG tag pairings could also enhance separation. Concurrent employment of fluororous tags would further enhance the number of substrates that can be simultaneously tagged in mixture syntheses.

3.0 REVERSED PHASE CHROMATOGRAPHY OF OEGYLATED ESTERS

Our work on the normal phase (NPLC), and complexation chromatography of OEGylated esters (Chapter 2) demonstrated retention behavior which origins lies in specific, and easily determinable modes of interaction. Hydrogen bonding (and to a lesser extent other polar interactions) in the former, and complexation with Li^+ ions in the latter. While OEGylated esters demonstrate excellent separatory power in NPLC, this mode of chromatography has its share of problems. Reproducibility problems exist which can mostly be blamed on the moisture content of the organic solvents, on pH, and on surface silanol density differences from one batch of silica to another. Some very polar substrates are retained too long and some substrates cannot be solubilized in the solvents most commonly employed in NPLC. Separation of nonpolar homologues series (for instance methylene homologues) is difficult or impossible.

Reversed phase liquid chromatography (RPLC) has emerged as a means of overcoming such problems associated with NPLC. Over a time span of 30 years RPLC has gained widespread acceptance and more than 80 % of HPLC applications are performed in the reversed phase mode. Thus examining the behavior of OEGylated esters in RPLC is important for this project.

In this study a Microsorb MVTM C18 column was used. The column dimensions were 250 X 4.6 mm. Particle size was 5 μ and average pore diameter was 100 Å. Further characteristics of the column are given later in this chapter. The OEGylated substrates employed

in this study were OEGylated esters **72a-75e** (Figure 3-1). These esters form homologues series. Thus it is possible to determine the effect of the length of OEG chains on retention, and the effect of the nature of the parent methyl ester on the energetics of retention of the OEG groups.

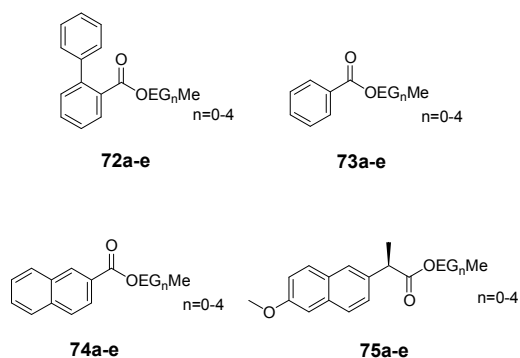


Figure 3-1: Esters employed in RPLC studies.

In this study the question of the nature of the retention of OEGylated esters in RPLC has been approached from a number of angles. The effect of mobile phase composition, and temperature has been investigated. The effect of hydrogen bonding with uncapped surface silanols and the effect of complexation with Li⁺ ions in the mobile phase have been addressed. The data were analyzed to shed light the mechanism of retention.

3.1 GENERAL CONSIDERATIONS

As had been noted earlier, the retention factor for an analyte (k') is defined as

$$k' = \frac{t_R - t_M}{t_M} \quad (1)$$

where t_R is the retention time of the analyte and t_M is the retention time of the solvent on the column of interest. It should be noted that the total time an analyte spends in the mobile phase on the column is also t_M . Thus k' can also be defined as $\frac{t_S}{t_M}$, where t_S is the total time the analyte spends on the stationary phase. This ratio can also be redefined as the ratio of the number of molecules of the analyte in the stationary phase, N_S , to the number of molecules of the analyte in the mobile phase, N_M , at any given time (5). In partition chromatography N_S would then be equal to the product of the stationary phase volume, V_S , and the concentration of the analyte in the stationary phase, c_S . c_M , and V_M can be similarly defined for the mobile phase (5).

$$k' = \frac{N_S}{N_M} = \frac{c_S V_S}{c_M V_M} \quad (5)$$

The ratio of V_S , and V_M is defined as the phase ratio, β (6). The ratio of c_S , and c_M can be defined as the partition coefficient, K (7). Thus k' can be written as the product of the phase ratio, β , and the partition coefficient, K (8). A similar argumentation will give equivalent relationships for other modes of chromatographic retention such as adsorption, and ion exchange.

$$\beta = \frac{V_S}{V_M} \quad (6)$$

$$K = \frac{c_S}{c_M} \quad (7)$$

$$k' = \beta K \quad (8)$$

Based on the Gibbs free energy relationship, (8) can be rewritten as (9):

$$\ln k' = \ln \beta - \frac{\Delta G^o}{RT} \quad (9)$$

(9) can be used to investigate the effect of a number of factors on the energetics of retention of substrates. Relevant enthalpy, and entropy values can be calculated using the Van't Hoff equation (10):

$$-\frac{\Delta G^o}{RT} = -\frac{\Delta H^o}{RT} + \frac{\Delta S}{R} \quad (10)$$

where a plot of ΔG^o versus $1/T$ gives a linear function which slope equals to $-\frac{\Delta H^o}{R}$, and intercept equals to $\frac{\Delta S}{R}$. Knowledge of these values can be used to understand the mechanism of retention.

Application of Van't Hoff analysis to (9), gives (11)

$$\ln k' = -\frac{\Delta H^0}{RT} + \frac{\Delta S^0}{R} + \ln \beta \quad (11)$$

Thus a plot of $\ln k'$ versus $\frac{1}{T}$ will give a slope equal to $-\frac{\Delta H^0}{R}$, and intercept equal to

$\left(\frac{\Delta S^0}{R} + \ln \beta\right)$. While ΔH^0 can be determined without knowledge of the magnitude of β ,

ΔS^0 can not. An approach for calculating β is presented in section 3.2.

Assuming that the retention of OEGylated compounds is the sum of the parent compound, and the OEG portion, (9) can be rewritten as (12)

$$\ln k' = -\frac{\Delta G_s^0}{RT} - n \frac{\Delta G_{EG}^0}{RT} + \ln \beta \quad (12)$$

where ΔG_s^0 is the free energy associated with the retention process of the OEG bound substrate, n is the number of EG monomers in the molecule, and ΔG_{EG}^0 is the free energy associated with the retention process of one EG subunit. The contribution of each EG subunit to the overall retention of the OEGylated molecule is expected to be the same.

Depending on the quality, contamination level, and age of the column, distortions of peak shape in the form of tailing can be observed. This phenomenon reduces the integration quality of peaks, and makes the baseline resolution of analytes more difficult. The extend of peak tailing is referred to as peak asymmetry, A_s , and can be defined as (13)

$$A_s = \frac{t_p}{f_p} \quad (13)$$

where t_p is the width of the tail measured from the maximum at a predefined height, and f_p is the width of the front.² In our case the height from which these widths were measured was chosen to be 10 % from the baseline.

Relative retention (α) can be defined as (14)

$$\alpha = \frac{k_2'}{k_1'} \quad (14)$$

where k_1' , and k_2' are the capacity factors of two adjacent peaks, and $k_2' > k_1'$. (9), and (14) can be combined to give (15)

$$\Delta\Delta G^\circ = RT \ln \alpha \quad (15)$$

where $\Delta\Delta G^\circ$ is the difference in free energy of retention between the said peaks. A minimum α value of 1.1 is needed for baseline separation and this corresponds to a free energy difference of approximately 60 cal/mol.

3.2 CALCULATION OF THE PHASE RATIO (β)

As can be seen in equation (11), while it is possible to obtain the ΔH° values for retention using a Van't Hoff plot ($\ln k'$ vs. $1/T$), it is impossible to determine ΔS° from such a plot without knowing the magnitude of the phase ratio (β). The determination of β requires knowledge of the volume of the mobile phase (V_M), and the volume of the ligands attached to the surface of the packing material (V_S). β would then be V_S/V_M . V_M can be readily determined as the dead volume of the column. The determination of V_S requires detailed information regarding the column structure. Once this information is obtained, V_S can be calculated using (16)

$$V_S = \frac{(\%C)(M)(W_p)}{(100)(12.011)(n_c)(\rho)} \quad (16)$$

where $\%C$ is the percentage of carbon for each ligand as determined by CHN analysis, M is the molecular weight of the ligand (g/mol), W_p is the weight of the bonded packing per column, n_c is the number of carbons in the ligand, and ρ is the density of the alkyl ligand.³

The particular column used in this study is a 250 X 4.6 mm, 5 μ particle size, 100 Å pore diameter Microsorb MV C18 column. This column is produced by attachment of octadecylsilyl groups to the surface silanols of silica particles. Excess silanols are then capped with trimethylsilyl groups. This method of preparation in this particular case gives a surface octadecylsilyl concentration of 2.8 $\mu\text{mol}/\text{m}^2$, and a trimethylsilyl concentration of 0.6 $\mu\text{mol}/\text{m}^2$. There is 3.5 g of the bonded packing per 250 X 4.6 mm column. CHN analysis indicates that 12

% of the mass of bonded packing is carbon.⁴ The mole ratio of the octadecylsilyl groups to the trimethylsilyl groups is approximately 5:1. Thus approximately 11.6 % of the mass of the stationary phase is composed of the carbons in the octadecyl ligands, and 0.4 % due to those of the TMS ligands. The density of the octadecylsilyl groups has been determined to be 0.8607 g/cm³, and that of the TMS groups has been determined to be 0.8638 g/cm³.⁵ V_s is the sum of the volumes of the two ligands. Using equation (14) V_s can be calculated to be 0.57 cm³. Since V_M has been determined to be 2.16 cm³, β would then be 0.264..

3.3 THE QUESTION OF SILANOL ACTIVITY

Our earlier findings suggest that the excellent separatory power of OEGs on silica under normal phase conditions is most likely the result of hydrogen bonding with surface silanols. We suspected that hydrogen bonding with surface silanols would be a factor affecting retention of OEG esters in RPLC employing bonded silica as well. Establishing the presence or absence of such hydrogen bonding effects could aid us in elucidating the retention mechanism of OEG esters. We surmised that hydrogen bonding under such circumstances would reduce the resolution of OEGylated substrates as it would have an effect of increasing the retention time of longer OEG chains, whereas the partition mechanism would have the opposite effect.

Surface concentration of silanols in typical silica is approximately 8 $\mu\text{mol}/\text{m}^2$.^{6a} Under the best of circumstances, derivatization of these silanols reduces their surface concentration to about 4 $\mu\text{mol}/\text{m}^2$, as the steric interaction between the ligands prevents further derivatization.^{6a, b} During this derivatization process, first the main ligand is attached (i.e. octadecyl silyl), and then

excess silanols are capped with smaller ligands (for instance trimethylsilyl). The column used in this study, as mentioned before, has a surface octadecyl concentration of $2.8 \mu\text{mol}/\text{m}^2$, and a trimethylsilyl group concentration of $0.6 \mu\text{mol}/\text{m}^2$.⁴

There are three types of surface silanols: Isolated, geminal, and vicinal (Figure 3-2). These silanol groups have been implicated as being the main source of retention, and peak shape irreproducibility of some solutes, particularly basic ones.⁷ Interestingly, full hydroxylation of the silica prior to derivatization gives the best results in terms of silanol activity reduction. This treatment ensures maximum surface homogeneity, and bridged (i.e. vicinal) silanols are less acidic (Figure 3-2).

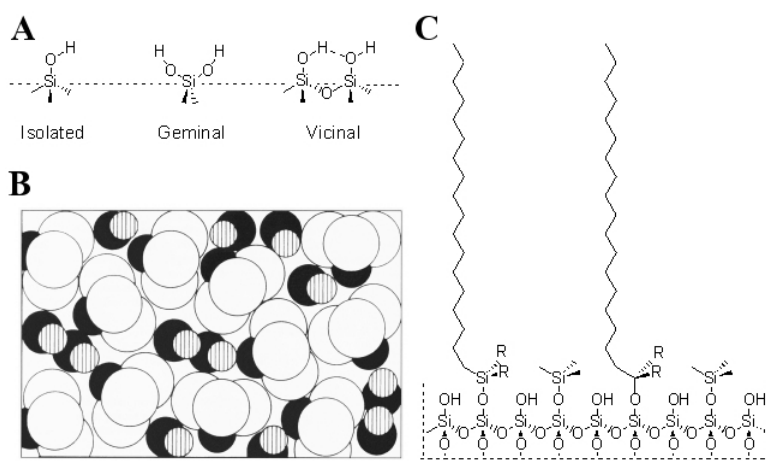


Figure 3-2: A. Types of surface silanols in silica. B. CPK model of TMS derivatized silica.⁸ C. Structure of a typical TMS-capped C18 column.

A number of tests have been developed to address this question.^{6a, b} Engelhardt, and Jungheim used phenol, aniline, toluidine isomers, *N,N*-dimethylaniline, and ethylbenzene as probes for silanol activity.⁹ If the following criteria are met, the silanol activity can be regarded as negligible: i. Aniline should elute before phenol, and the ratio of their symmetries (i.e. $A_S^{Aniline} / A_S^{Phenol}$) should be less than 1.3, ii. Toluidine isomers should be inseparable, iii. *N,N*-

dimethylaniline should elute before ethylbenzene. We have found that aniline elutes after phenol, and that $A_S^{Aniline} / A_S^{Phenol} = 1.98$ (Figure 3-3). *o*-, and *p*-toluidine (*m*-toluidine was not used) were separable, and ethylbenzene eluted before *N,N*-dimethylaniline. Thus we concluded that silanol activity could possibly be a factor affecting the retention of OEGylated compounds on this particular column.

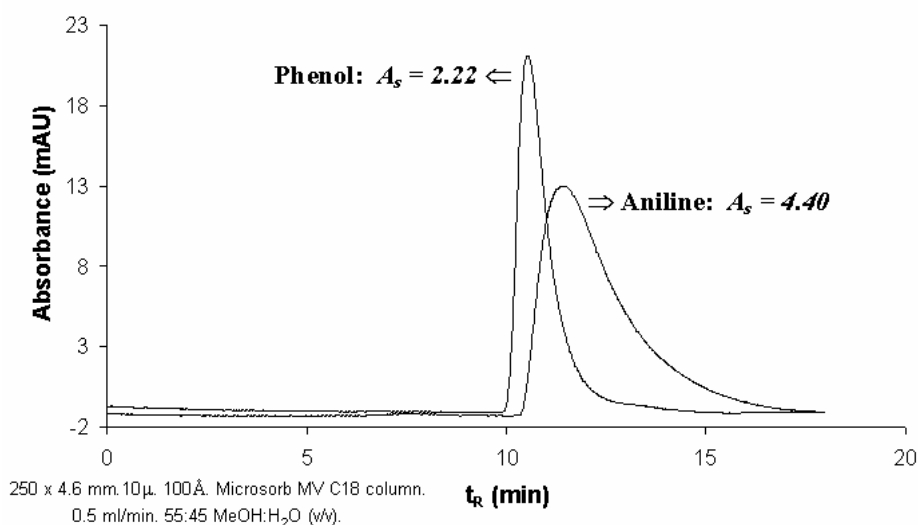


Figure 3-3: Elution of phenol and aniline on a Microsorb MV C18 column.

The question of whether any given solute (particularly ones that are not basic, or very polar) is subject to hydrogen bonding, and whether that bonding has a significant effect on retention cannot necessarily be answered by such column characterizations only. The absence, or presence of such effects can be ascertained by examination of the dependency of k' on the mobile phase composition (i.e. $V_{Water} / V_{OrganicModifier}$), and the Van't Hoff plots.

In the presence of silanol activity, the retention of a substrate (k') can be expressed (17) as the sum of retention due to hydrophobic, or partitioning interactions (k'_1), and silanophilic interactions (k'_2).

$$k' = k'_1 + k'_2 \quad (17)$$

The magnitude of k'_1 is controlled by classical RPLC mechanisms, whereas the magnitude of k'_2 is controlled by NPLC mechanisms. The dependency of these capacity factors on the composition of a binary mobile phase can be expressed using (18), and (19), which can be combined to give (20)

$$k'_1 = Ae^{-B\Psi} \quad (18)$$

$$k'_2 = (C + D\Psi)^{-1} \quad (19)$$

$$k' = Ae^{-B\Psi} + (C + D\Psi)^{-1} \quad (20)$$

where Ψ is the composition of the binary phase, A , and B are the slope, and intercept of the linear $\ln k'_1$ versus Ψ plot, C^{-1} is the retention factor for the solute using the organic modifier only, and D is a constant dependent on the nature of the stationary phase. This model can be further extended to give an expression for ΔH^o of retention (21).

$$\Delta H^{\circ} = \frac{k_1' \Delta H_1^{\circ}}{k'} + \frac{k_2' \Delta H_2^{\circ}}{k'} \quad (21)$$

Given the presence of sufficient silanol activity equations (20), and (21) imply that $\ln k'$ versus Ψ , and Van't Hoff plots would be concave (Figure 3-4). This “dual retention mechanism” has indeed been observed. Nahum and Horvath have observed such behavior for dibenzo-18-crown-6, and dibenzo-24-crown-8 on a number of early C18 columns.^{10a, b} Column technology has improved significantly since then, and silanol activity has been reduced. But the aforementioned shapes of the relevant plots could still be taken as indicators of silanol activity.

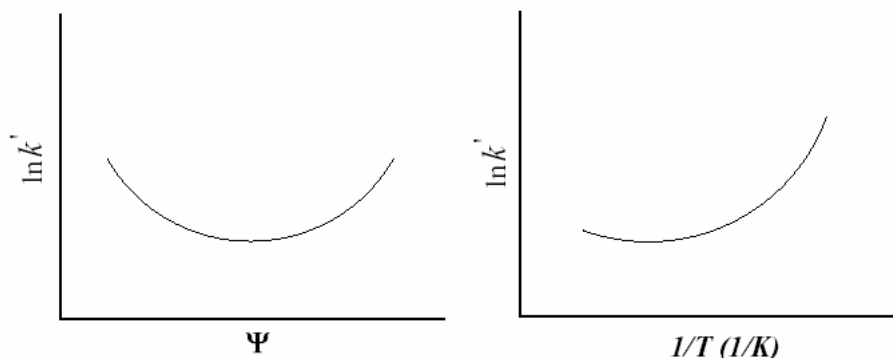


Figure 3-4: Expected shapes of $\ln k'$ versus Ψ (A) and Van't Hoff (B) plots under conditions where significant silanol activity is present.

3.4 EFFECT OF WATER CONCENTRATION ON RETENTION

As mentioned earlier, the effect of water concentration in the mobile phase was investigated by recording the elution times of esters using mobile phases consisting acetonitrile-water with varying water concentrations. Acetonitrile was chosen as the organic modifier as it

represents a midpoint in the elutropic series of solvents commonly utilized in reversed-phased HPLC. The concentration of water was varied between 30, and 50% (v/v). This range represents a reasonable spectrum of solvent composition compatible with most applications, and was a range that gave meaningful capacity factors with convenient elution times for the solutes employed in this study.

A series of chromatograms for esters **75b-e** are provided in Figure 3-5 as examples. It should be noted that the elution order observed for the esters studied is the reverse of that observed for the same esters in normal-phased HPLC. This is expected, as longer OEG chains within each group of esters imply increased polarities for the solutes. Relevant capacity factors (k'), and selectivity factors (α) are provided in Table 3-1.

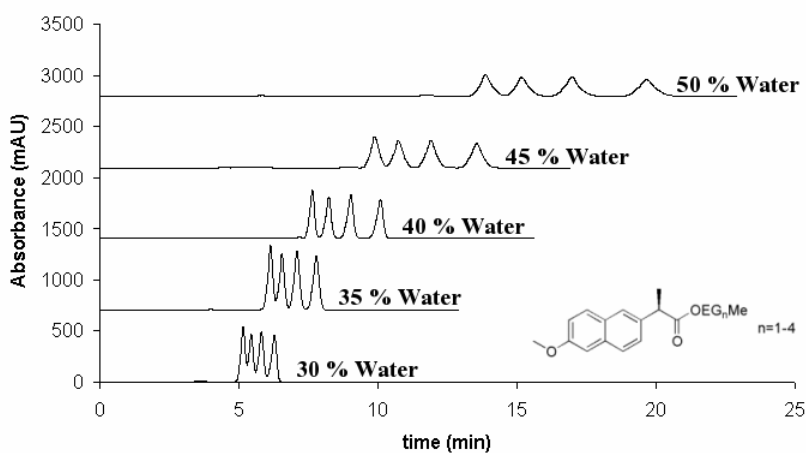


Figure 3-5: Chromatograms for esters **75b-e** for different mobile phase water concentrations (298 K).

Table 3-1: k' and α values for the elution of esters **72a-75e** with varying water concentrations in the mobile phase (298 K).

Ester	DP	30%		35%		40%		45%		50%	
		k'	α								
72a-e	0	1.97	1.10	2.69	1.11	3.74	1.12	5.43	1.13	8.18	1.15
	1	1.79	1.13	2.42	1.14	3.35	1.15	4.79	1.16	7.14	1.17
	2	1.58	1.12	2.11	1.12	2.91	1.13	4.13	1.13	6.12	1.13
	3	1.42	1.11	1.88	1.11	2.58	1.11	3.65	1.12	5.39	1.12
	4	1.28	-	1.69	-	2.32	-	3.26	-	4.82	-
73a-e	0	1.02	1.19	1.28	1.21	1.64	1.20	2.12	1.20	2.84	1.21
	1	0.86	1.15	1.06	1.15	1.37	1.16	1.76	1.17	2.34	1.17
	2	0.75	1.11	0.92	1.12	1.18	1.13	1.51	1.14	2.00	1.14
	3	0.67	1.10	0.83	1.12	1.04	1.11	1.33	1.11	1.76	1.11
	4	0.61	-	0.73	-	0.94	-	1.19	-	1.58	-
74a-e	0	2.23	1.24	2.95	1.25	4.01	1.26	5.71	1.28	8.19	1.27
	1	1.80	1.16	2.37	1.17	3.19	1.18	4.46	1.19	6.43	1.19
	2	1.56	1.13	2.03	1.14	2.71	1.15	3.75	1.15	5.41	1.15
	3	1.38	1.12	1.78	1.12	2.37	1.13	3.26	1.13	4.70	1.13
	4	1.23	-	1.58	-	2.10	-	2.88	-	4.16	-
75a-e	0	2.15	1.13	2.92	1.12	4.13	1.13	6.09	1.15	9.49	1.17
	1	1.90	1.13	2.60	1.14	3.66	1.16	5.28	1.17	8.10	1.18
	2	1.69	1.11	2.28	1.12	3.17	1.13	4.52	1.14	6.86	1.14
	3	1.52	1.10	2.03	1.11	2.80	1.11	3.97	1.11	6.02	1.11
	4	1.38	-	1.84	-	2.53	-	3.57	-	5.42	-

The information provided in Figure 3-5, and Table 3-1 show that the k' values increase as water concentration, and OEG chain length increases, however the α values remain flat, or show very small increases. For OEGylated esters, the elution order was $t_R^{75} > t_R^{72} > t_R^{74} > t_R^{73}$ for all water concentrations (with the exception of **74b** which eluted slightly later than **72b** for 30 % water). The retention of methyl esters was somewhat more complex. **73a** eluted earliest for all mobile phase compositions. **75a** always eluted later than **72a**. **74a** eluted latest for 30 % water, gradually eluting earlier with increasing water concentration until it eluted first (close to **72a**) at 50 % water. This behavior of the methyl esters is strange and seems to differ for the known shape selectivities of the parent aromatic compounds in RPLC.^{11a, b}

Substrates bearing OEG chains of differing lengths could be regarded as constituting homologous series. As expected of homologous series, plots of k' versus DP, and k' versus water concentration are not linear for esters **72a-75e** (Figure 3-6). The trends observed are the opposite of those observed for hydrophilic homologues substrates, such as carbohydrates, in HILIC (hydrophilic interaction liquid chromatography), and are also the opposite of trends observed for hydrophobic (i.e. those series containing alkane chains of varying length) homologous series in reversed-phase HPLC.^{12a, b, c} The free energies of retention (ΔG°) calculated through k' , and β values for esters **72a-75e** are given in Table 3-2.

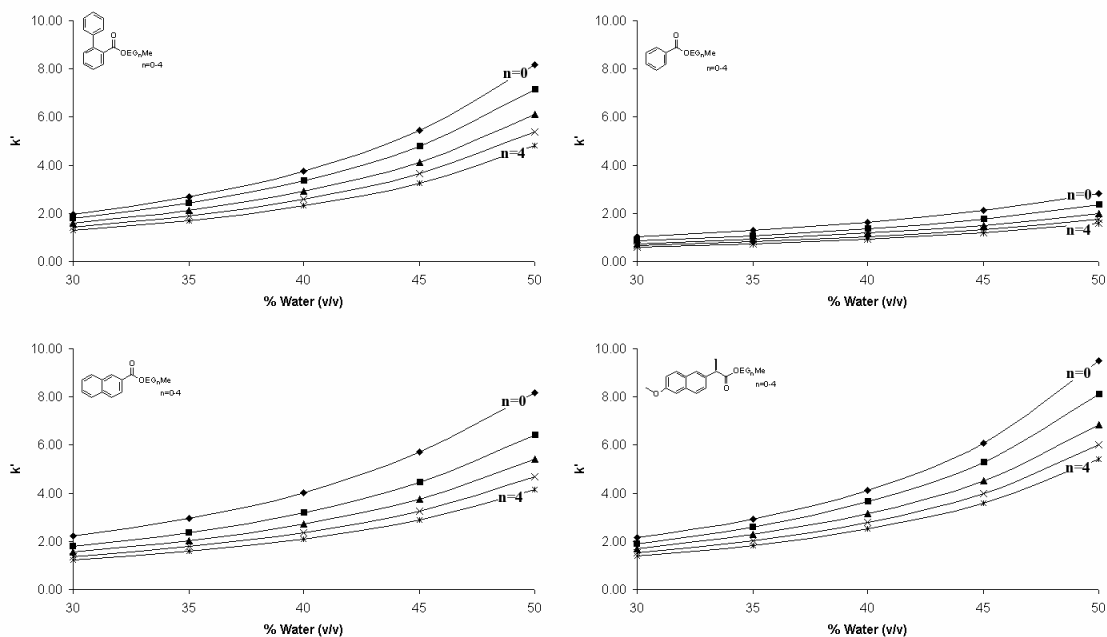


Figure 3-6: $\ln k'$ versus mobile phase water concentration plots for esters **72a-75e** (298 K).

Table 3-2: ΔG° values for the retention of esters **72a-75e**

Ester	DP	ΔG° ^a	ΔG° ^b	ΔG° ^c	ΔG° ^d	ΔG° ^e
72a-e	0	-1190	-1374	-1570	-1791	-2033
	1	-1135	-1311	-1504	-1717	-1953
	2	-1061	-1232	-1421	-1628	-1861
	3	-995	-1163	-1350	-1554	-1787
	4	-935	-1100	-1286	-1488	-1720
73a-e	0	-801	-936	-1081	-1234	-1406
	1	-697	-825	-974	-1124	-1293
	2	-615	-741	-887	-1033	-1200
	3	-551	-675	-813	-956	-1123
	4	-496	-606	-751	-893	-1061
74a-e	0	-1264	-1429	-1611	-1820	-2034
	1	-1138	-1298	-1476	-1674	-1890
	2	-1051	-1207	-1380	-1572	-1788
	3	-978	-1129	-1298	-1488	-1705
	4	-913	-1061	-1227	-1415	-1633
75a-e	0	-1240	-1423	-1629	-1858	-2121
	1	-1170	-1354	-1557	-1774	-2028
	2	-1100	-1276	-1471	-1681	-1929
	3	-1036	-1207	-1399	-1606	-1852
	4	-981	-1148	-1338	-1543	-1789

^a30% water. ^b35% water. ^c40% water. ^d45% water. ^e50% water.

If esters **72a-e**, **73a-e**, **74a-e**, and **75a-e** constitute homologous series, based on (12) it would follow that plots of ΔG° versus degree of polymerization should be linear, with the slopes of the plots being equal to ΔG_{EG}° (the contribution of one EG subunit to the free energy of retention), and the intercepts being ΔG_S° (the free energy of retention of the corresponding methyl ester).^{12a} This seems to be the case in this study (Figure 3-7). Regression parameters for these plots are given Table 3-3.

The observation that the plots of ΔG° versus degree of polymerization were linear seems to indicate that hydrogen-bonding of the solutes with the stationary phase silanols has no, or an insignificant effect on retention. The shapes of the Van't Hoff plots should be examined before arriving at a firmer conclusion.

The slopes of the plots of ΔG^o versus degree of polymerization correspond to ΔG_{EG}^o at any given mobile phase composition. It is noteworthy that these values change relatively little (-7.9 % to +14.8 %) as the mobile phase water content is increased from 30 % to 50 % (v/v). The trends are not clear cut, but it seems that for substrates **72a-e**, **74a-e**, and **75a-e** ΔG_{EG}^o values increase with increasing water content, whereas the opposite is true of substrates **73a-e**. These trends can be assumed to be a function of experimental error, and partitioning in favor of the stationary phase as the polarity of the mobile phase increases. Another conclusion that can be drawn from these plots is that the magnitude of ΔG_{EG}^o is clearly a function of the parent methyl ester. An analysis of ΔG_{EG}^o as function of the properties of the parent methyl ester is presently not available.

Table 3-3: Regression parameters for plots of ΔG^o versus degree of polymerization for esters **72a-75e**.

Ester	% Water (v/v)	30	35	40	45	50
72a-e	Slope	65.00	69.64	72.19	76.84	79.19
	Intercept	-1193	-1375	-1571	-1789	-2029
	R ²	0.998	0.999	0.998	0.998	0.997
73a-e	Slope	75.68	80.97	82.26	84.90	85.99
	Intercept	-783	-918	-1066	-1218	-1389
	R ²	0.988	0.988	0.989	0.988	0.987
74a-e	Slope	86.31	90.54	94.58	99.54	98.63
	Intercept	-1241	-1406	-1588	-1793	-2007
	R ²	0.981	0.983	0.983	0.979	0.980
75a-e	Slope	65.275	69.743	74.003	79.906	83.896
	Intercept	-1235.9	-1421.2	-1626.6	-1852.2	-2111.5
	R ²	0.9974	0.9979	0.9971	0.9951	0.9923

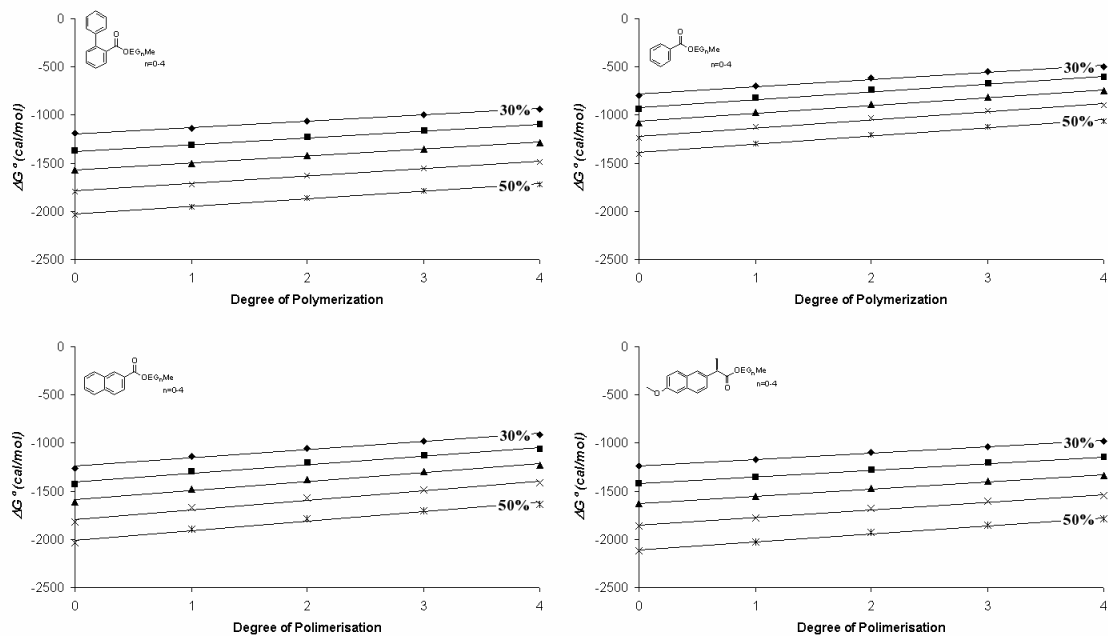


Figure 3-7: Plots of ΔG° versus degree of polymerization for esters **72a-75e**.

One characteristic of homologous series of analytes is a focal point of $\ln k'$ versus DP plots at differing mobile phase compositions. The differences in slopes observed for homologous series of methylene bearing solutes are much steeper than those observed for OEGs.^{12c} For instance certain alkylbenzenes have exhibited a focal point at $DP \approx -4$. The focal points for the OEGylated esters examined in this study were as follows: **72a-e** ≈ 100 , **73a-e** ≈ -90 , **74a-e** ≈ 80 , **75a-e** ≈ 65 . The variation in the focal points seems to be a function of the parent methyl esters. The focal points observed for **72a-75e** were not as clean as those observed for alkylbenzenes. Since the differences in ΔG_{EG}° going from 30% to 50% water (v/v) in the mobile phase were small, the effect of experimental errors is magnified upon extrapolation to distant x-coordinate values. The cause of the anomalous behavior exhibited by **73a-e** is presently unclear.

Plots of ΔG° versus % water in the mobile phase (v/v) were also linear (Table 3-4, Figure 3-8). The change in the slopes going from $DP = 0$ to $DP = 4$ within each homologous

series is very small. The intercepts however changed significantly. These intercepts correspond to the hypothetical free energies of retention that would be observed were pure AcCN to be used as the mobile phase. All intercepts are positive, indicating that retention on the stationary phase would be very unfavorable under such conditions. The magnitudes of the intercepts increase as DP increases, which parallels the hydrophilicities of the corresponding OEGylated esters.

Table 3-4: Regression parameters for plots of ΔG° versus % water (v/v) in mobile the phase for **72a-75e**.

Ester	DP	0	1	2	3	4
72a-e	Slope	-42.04	-40.82	-39.95	-39.48	-39.15
	Intercept	90	109	157	209	260
	R ²	0.997	0.997	0.996	0.996	0.996
73a-e	Slope	-30.14	-29.82	-29.26	-28.50	28.35
	Intercept	114	211	275	317	373
	R ²	0.998	0.998	0.998	0.997	0.995
74a-e	Slope	-38.60	-37.61	-36.77	-36.27	-35.91
	Intercept	-88	9	71	131	186
	R ²	0.997	0.997	0.996	0.995	0.994
75a-e	Slope	-43.91	-42.71	-41.28	-40.60	-40.23
	Intercept	292	322	350	394	439
	R ²	0.995	0.996	0.996	0.995	0.995

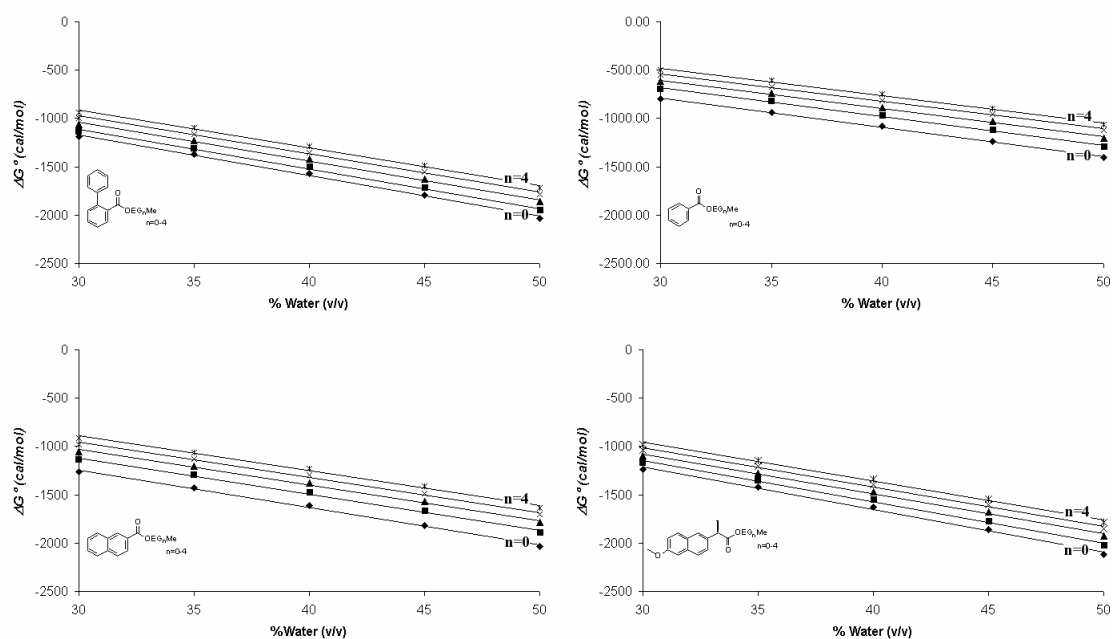


Figure 3-8: Plots of ΔG° versus % water (v/v) in the mobile phase for esters **72a-75e**.

Linear relationships between the logarithm of the octanol-water partitioning coefficients of solutes ($\log P$) and their k' values have frequently been observed.^{13a, b} These observations have been regarded as supporting the partitioning model of RPLC retention mechanism. Thus determination of whether such linear relationships existed for our substrates was of interest.

$\log P$ values were calculated using Molinspiration.^{14a} This software uses a sum of group contributions model that has been compiled based on the experimentally determined $\log P$ values of 12000 drug-like molecules. Those $\log P$ values were similar to values calculated using CaChe.^{14b} Linear relationships between $\log P$ and $\ln k'$ values existed within each and all of homologous series for all mobile phase compositions examined ($R^2 \geq 0.965$ for the cumulative plot, $R^2 \geq 0.980$ for individual homologous series). Regression parameters are given in Table 3-5 and the $\log P$ versus $\ln k'$ plot for all esters are given in Figure 3-9.

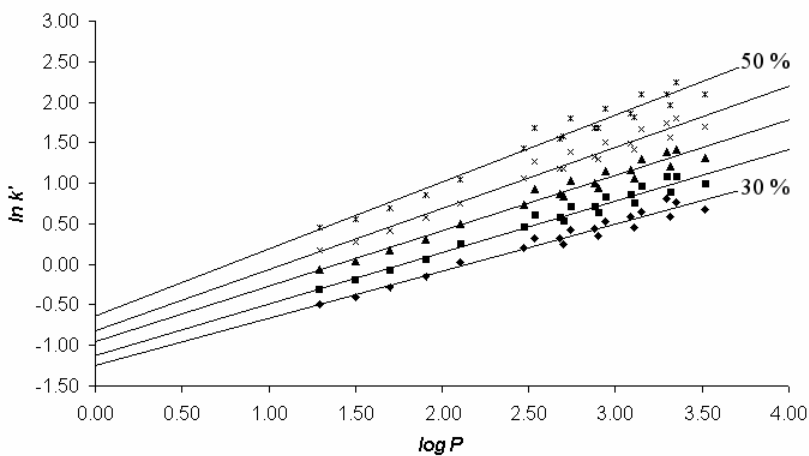


Figure 3-9: $\log P$ versus $\ln k'$ plots for esters 72a-75e.

Table 3-5: Regression parameters for $\log P$ versus $\ln k'$ plots for esters **72a-75e**.

<i>% Water</i>	<i>Ester</i>	<i>slope</i>	<i>intercept</i>	<i>R²</i>	<i>log P</i>
30	All	0.581	-1.244	0.965	3.52
	72a-e	0.538	-1.209	0.998	3.31
	73a-e	0.627	-1.330	0.988	3.11
	74a-e	0.714	-1.585	0.981	2.91
	75a-e	0.540	-1.057	0.997	2.70
35	All	0.636	-1.123	0.969	2.11
	72a-e	0.577	-1.037	0.999	1.90
	73a-e	0.670	-1.194	0.988	1.70
	74a-e	0.749	-1.422	0.983	1.50
	75a-e	0.577	-0.868	0.998	1.29
40	All	0.685	-0.957	0.969	3.29
	72a-e	0.598	-0.781	0.998	3.09
	73a-e	0.681	-0.968	0.989	2.88
	74a-e	0.782	-1.225	0.983	2.68
	75a-e	0.613	-0.640	0.997	2.48
45	All	0.755	-0.820	0.969	3.35
	72a-e	0.636	-0.547	0.998	3.15
	73a-e	0.703	-0.757	0.988	2.95
	74a-e	0.823	1.014	0.980	2.74
	75a-e	0.662	-0.422	0.995	2.54
50	All	0.826	-0.641	0.961	3.52
	72a-e	0.656	-0.211	0.997	3.31
	73a-e	0.712	-0.488	0.987	3.11
	74a-e	0.816	-0.627	0.981	2.91
	75a-e	0.695	-0.095	0.992	2.70

The slope, and intercept values for these plots varied from series to series, but it can still be argued that the partitioning-like mechanism crudely describes the retention patterns. Both hydrophobic, and partitioning models assume a mostly passive stationary phase, and based on these regression data that is obviously not true. These models neglect factors associated with the stationary phase such as hydrogen bonding, shape selectivity, and phase transitions.

3.5 EFFECT OF TEMPERATURE ON RETENTION

In these studies the temperature range examined was 298-318 K (25-45°C). 40 % water (v/v) in AcCN was chosen as the mobile phase as this composition gave acceptable retention times while providing sufficiently separated peaks. Retention times dropped as temperature increased. Similarly a slight reduction in the α values was also observed. Sample chromatograms are reproduced in Figure 3-10, and k' , and α values are given in Table 3-6.

Van't Hoff plots ($\ln k'$ vs. $1/T$) were linear (Figure 3-11). The slopes gave the ΔH° values associated with the retention process. The intercepts equaled $\Delta S^\circ + \ln \beta$, thus entropy values associated with the retention process could be calculated from these slopes using the β value calculated in section 1.2. ΔH° , ΔS° , and $T\Delta S^\circ$ (298 K) values obtained from the Van't Hoff plots are given in Table 3-7.

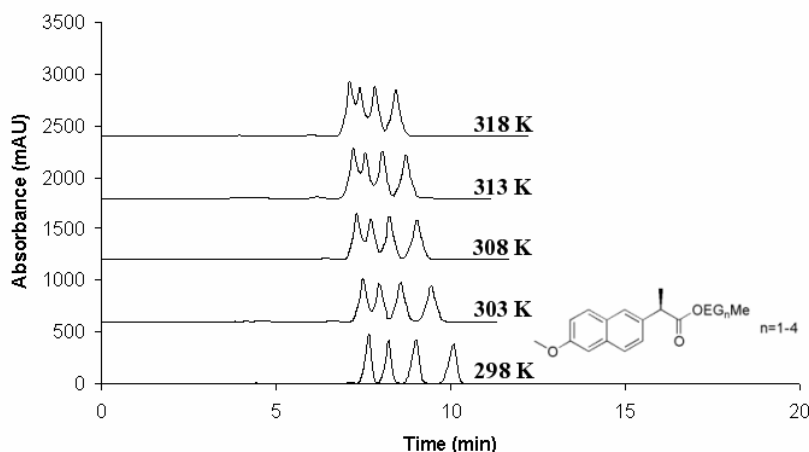


Figure 3-10: Effect of temperature on the retention of esters **75b-e**

Table 3-6: k' and α values for esters **72a-75e** between 298-318 K.

Temp.	DP	72a-e		73a-e		74a-e		75a-e	
		k'	α	k'	α	k'	α	k'	α
298 K	0	3.74	1.12	1.64	1.20	4.01	1.26	4.13	1.13
	1	3.35	1.15	1.37	1.16	3.20	1.18	3.66	1.15
	2	2.91	1.13	1.18	1.13	2.71	1.15	3.17	1.13
	3	2.58	1.11	1.04	-	2.37	1.13	2.81	1.11
	4	2.32	-	-	-	2.10	-	2.54	-
303 K	0	3.48	1.11	1.56	1.19	3.66	1.24	3.80	1.13
	1	3.13	1.14	1.31	1.14	2.94	1.16	3.38	1.14
	2	2.75	1.11	1.15	1.12	2.53	1.13	2.97	1.11
	3	2.47	1.10	1.02	-	2.24	1.11	2.68	1.09
	4	2.25	-	-	-	2.02	-	2.46	-
308 K	0	3.28	1.10	1.48	1.18	3.40	1.23	3.53	1.11
	1	2.97	1.13	1.26	1.13	2.77	1.15	3.19	1.13
	2	2.64	1.10	1.11	1.11	2.42	1.12	2.83	1.10
	3	2.39	1.09	1.01	-	2.16	1.09	2.58	1.08
	4	2.20	-	-	-	1.98	-	2.39	-
313 K	0	3.15	1.10	1.44	1.17	3.24	1.22	3.46	1.13
	1	2.86	1.12	1.23	1.12	2.65	1.14	3.08	1.12
	2	2.55	1.09	1.09	1.10	2.33	1.11	2.75	1.09
	3	2.33	1.08	0.99	-	2.10	1.08	2.52	1.07
	4	2.16	-	-	-	1.94	-	2.36	-
318 K	0	3.05	1.10	1.40	1.16	3.16	1.21	3.33	1.13
	1	2.77	1.11	1.21	1.11	2.60	1.12	2.96	1.11
	2	2.50	1.09	1.08	1.09	2.31	1.10	2.66	1.08
	3	2.31	1.07	1.00	-	2.10	1.08	2.47	1.06
	4	2.15	-	-	-	1.95	-	2.33	-

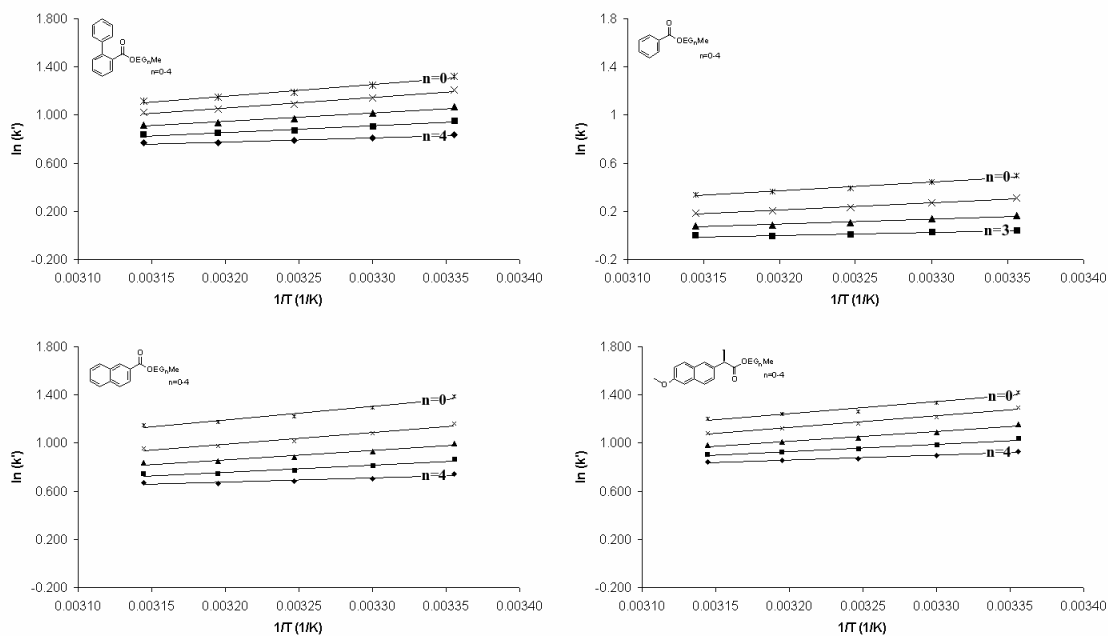


Figure 3-11: Van't Hoff plots for esters 72a-75e.

Table 3-7: ΔH° , ΔS° , and $T\Delta S^\circ$ (at 298 K) values from the Van't Hoff plots of esters 72a-75e.

<i>Ester</i>	ΔH° (cal/mol)	$T\Delta S^\circ$ (cal/mol)	ΔS° (cal/mol-K)	R^2	
72	a	-1917	-354	-1.19	0.979
	b	-1769	-272	-0.91	0.982
	c	-1427	-12	-0.04	0.975
	d	-1074	271	0.91	0.965
	e	-697	584	1.96	0.940
73	a	-1490	-413	-1.39	0.985
	b	-1206	-236	-0.79	0.980
	c	-843	41	0.14	0.970
	d	-457	353	1.19	0.905
	e	-	-	-	-
74	a	-2266	-667	-2.24	0.962
	b	-1959	-493	-1.65	0.957
	c	-1525	-155	-0.52	0.938
	d	-1138	152	0.51	0.913
	e	-693	527	1.77	0.853
75	a	-1980	-364	-1.22	0.946
	b	-1959	-411	-1.38	0.979
	c	-1607	-142	-0.48	0.977
	d	-1216	179	0.60	0.974
	e	-808	528	1.77	0.963

ΔH° can be regarded as a measure of the magnitude interactions of the solute with the stationary phase. These interactions could be partitioning/hydrophobic interactions, shape selectivity of the stationary phase, and hydrogen bonding with the stationary phase.^{11a-b, 6a-b} In a similar manner ΔS° values can be regarded as a measure of the change in the order of the system as a result of those interactions.

The ΔH° values are negative, and their magnitudes get less as the DP increases. These facets of the ΔH° values indicate the preference of the substrates for the stationary phase, and the fact that the partitioning of these esters are reduced with higher DPs as a result of increased polarity of the substrates.

ΔH_{EG}° values (i.e. the contribution of one OEG subunit to the enthalpy) can be determined from ΔH° versus DP plots ($R^2 \geq 0.943$), and relevant regression parameters are given in Table 3-8. The linearity of these plots improved when the parent methyl esters were omitted from the plots ($R^2 \geq 0.999$). The slopes of these plots give the ΔH_{EG}° values. The intercepts on the other hand correspond to the ΔH° values of the parent methyl esters. These ΔH° values for the methyl esters varied from the experimentally determined ones by 2.5-8.0%. The highest deviation was observed for esters **75a-e**. In a similar manner ΔS_{EG}° can also be determined, and relevant regression parameters are also given in Table 3-8. Regression omitting the parent methyl esters gave superior linearity in this case as well ($R^2 \geq 0.997$).

Table 3-8: ΔH_{EG}° , ΔH_S° , ΔS_{EG}° , and ΔS_S° values for **72a-75e** obtained from ΔS_S° versus DP and ΔH° versus DP plots.

Ester	ΔH_{EG}° ^a	ΔH_S° ^a	R^2	ΔS_{EG}° ^b	ΔS_S° ^b	R^2
72a-e	313.4	-2003.4	0.981	0.81	-1.48	0.968
73a-e	346.3	-1518.4	0.995	0.86	-1.51	0.986
74a-e	396.7	-2309.6	0.997	1.02	-2.46	0.987
75a-e	308.7	-2131.6	0.943	0.80	-1.73	0.903
72b-e	356.9	-2133.9	0.999	0.96	-1.91	0.998
73b-e	374.6	-1584.4	0.999	0.99	-1.80	0.999
74b-e	418.3	-2374.5	0.999	1.13	-2.80	0.999
75b-e	384.3	-2358.4	0.999	1.05	-2.51	0.997

^acal/mol. ^bcal/mol·K.

Analogous to the ΔH_{EG}° values obtained in this study, $\Delta H_{CH_2}^{\circ}$ (or $\Delta\Delta H^{\circ}$) values have been determined for methylene homologues by other groups. In one study alkyl benzenes were investigated on a C18 column and a $\Delta H_{CH_2}^{\circ}$ value of -268 cal/mol was obtained.^{12c} The mobile phase was 9:1 MeOH:H₂O, and the C18 column employed in that study was different than the one employed in this study. Thus a direct comparison would not necessarily be quantitatively accurate, but a qualitative comparison is still possible. ΔH_{EG}° values are positive, whereas $\Delta H_{CH_2}^{\circ}$ values are negative. This is to be expected as OEG groups increase the hydrophilicity of the substrates, while methylene groups have the opposite effect. An EG monomer has two methylene groups and an oxygen atom. It is remarkable that one oxygen atom negates the effect of two methylene groups. A rough estimate would put the loss of enthalpy of retention due to one oxygen atom at 900 cal/mol.

Inspection of the ΔH° values in Table 3-7 reveals that going from ester **75a** to **75b** the drop in enthalpy is very small. The same is observed to a lesser extent moving from **72a** to **72b**. For **73a-e** and **74a-e** the effect is small, this is also reflected in their superior R^2 values for plots of ΔH° versus DP. This behavior is probably linked to the structural differences of **72a-e**

(freedom of rotation around the phenyl-phenyl bond) and **75a-e** (presence of a methoxy group, and freedom of rotation around single bonds) from the other two homologues series.

3.6 THE QUESTION OF ENTHALPY ENTROPY COMPENSATION

Extrathermodynamical approaches in physical and physical organic chemistry (also referred to as free-energy relationships) play a significant role in the elucidation of the mechanisms, and energetics of analogous chemical phenomena.¹⁵ One such approach is the famous Hammett equation.¹⁶ Another one is termed enthalpy-entropy compensation (EEC). These approaches are based on the observation that there are similar linear dependencies of rate or equilibrium constants of chemical phenomena on the free energy change associated with those phenomena. Thus it is assumed that all analogous chemical phenomena, provided that they exhibit similar behavior in their free-energy relationships, have the same underlying mechanism.

EEC can be expressed as (22),

$$\Delta H^{\circ} \approx \Theta \Delta S^{\circ} + \Delta G_{\Theta}^{\circ} \quad (22)$$

where $\Delta G_{\Theta}^{\circ}$ is the free energy of a chemical phenomenon at a temperature Θ (i.e. compensation temperature), and ΔH° , and ΔS° are the enthalpies, and entropies associated with the

phenomenon. (22) implies that if a plot of ΔH° versus ΔS° is linear, EEC might be in effect. The slopes of these plots are related to Θ . At temperature Θ the enthalpy gain is offset by the entropy gain and ΔG_Θ° is essentially the same for all analogous species having the same Θ value for a particular chemical phenomenon. In our case this plot is linear as evidenced in Figure 3-12 ($R^2 \geq 0.988$). The slopes of these plots of ΔH° versus ΔS° for esters **72a-75e** are very close (398 for **73a-e**, 379 for **72a-e**, and **74a-75e**).

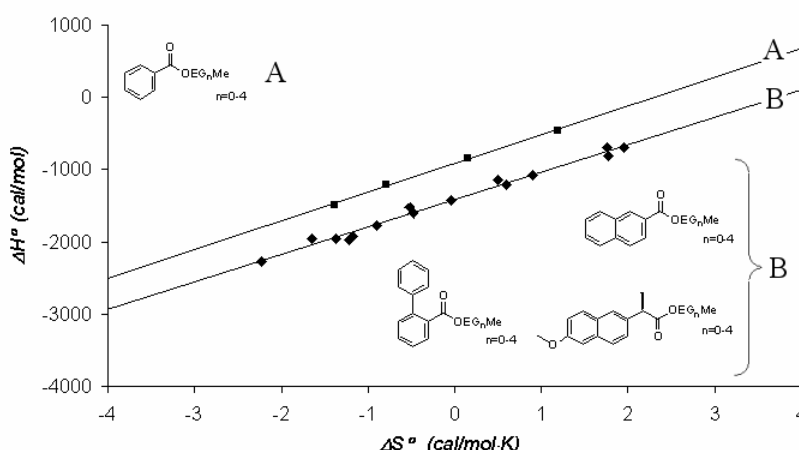


Figure 3-12: Plots of ΔH° versus ΔS° for esters **72a-75e**.

These plots have been the traditional approach to determine EEC. It is interesting to note that many such linear relationships have been observed through the years and they frequently possess better R^2 values than the Arrhenius or Van't Hoff plots they are derived from. This is to be expected since most of these EEC plots are not the result of real chemical phenomena, but are rather a statistical artifact based on the method used for the estimation of both ΔH° and ΔS° .^{17a-c} Unless more rigorous analysis is done these plots and regression parameters derived from them are essentially meaningless.^{17c}

A protocol has been devised for EEC analysis that effectively separates the statistical artifacts from real chemical effects.^{19a, b} Application of this protocol to (22) requires the following analyses be done, and positive outcomes be observed before concluding that EEC is present for a series of solutes in RPLC:

- i. A linear correlation must be observed between ΔH° , and ΔG° at the harmonic mean (T_{hm}) of the temperature range studied. If T_{hm} is not an actual temperature examined in the study, then the closest studied temperature (T_{eval}) should be used. The T_{hm} of a series of experimental temperatures can be defined as (23), where n is the number of temperatures studied, and $T_1 - T_n$ are the temperatures at which the actual experiments were conducted. The slopes of the ΔH° versus ΔG° plots will give a value for Θ .

$$T_{hm} = \frac{n}{\frac{1}{T_1} + \frac{1}{T_2} + \dots + \frac{1}{T_n}} \quad (23)$$

- ii. Statistical analysis (t-test) should be applied to determine whether Θ is significantly different from T_{hm} (or T_{eval}) at the 95% confidence level.
- iii. The relevant Van't Hoff plots should be linear, and should intersect at Θ .
- iv. The probability of intersection of the Van't Hoff plots should be compared the probability of non-intersection using analysis of variance (ANOVA).

Analysis in accordance with (i) revealed that the ΔH° versus ΔG° plots at T_{hm} (308 K) for esters **72a-75e** were linear (Figure 3-13). The relevant regression parameters are given in

Table 10. Slopes and intercepts exhibited variance from homologous series to homologous series. Omission of methyl esters **72a**, **73a**, **74a**, and **75a** yielded plots which linearity was significantly improved (Table 3-9). Using the relationship $\Theta = T_{hm} / (1 - 1/slope)$, the values of Θ for esters **72a-75e** can also be determined (Table 3-9). The average value for the compensation temperature for all esters is found to be 391 K. The values obtained from the plots lacking the methyl esters were lower from those including them. While this does not necessarily imply a radical difference between the retention mechanisms of methyl esters and OEGylated ones, it seems to indicate a slight difference in the relative contributions of the effects leading to retention.

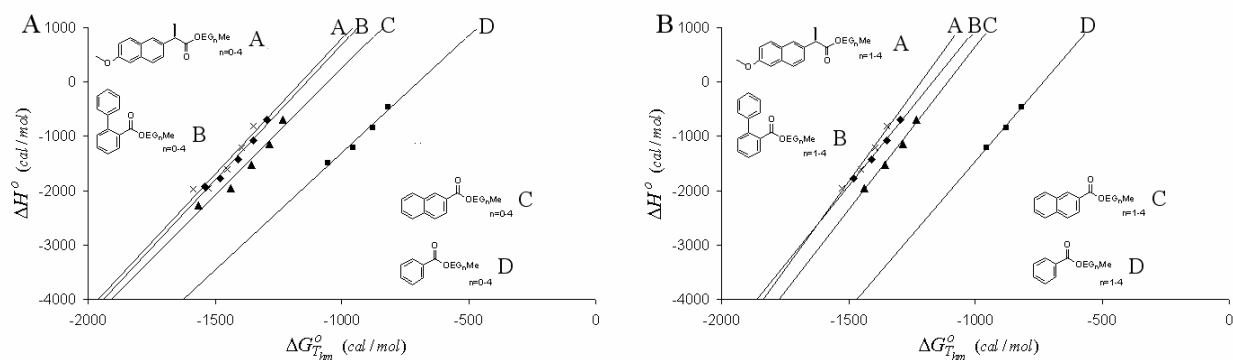


Figure 3-13: ΔH° versus ΔG° plots for esters **72a-75e**.

Table 3-9: Regression parameters of ΔH° versus ΔG° plots and Θ values for esters **72a-75e**.

<i>Ester</i>	<i>slope</i>	<i>intercept</i>	R^2	Θ (K)
72a-e	5.00	5699	0.972	385
73a-e	4.32	3016	0.969	401
74a-e	4.68	4923	0.953	392
75a-e	5.01	5808	0.919	385
72b-e	5.78	6754	0.990	372
73b-e	5.45	3993	0.995	377
74b-e	6.02	6668	0.990	369
75b-e	6.45	7821	0.981	365

(ii) requires that the Van't Hoff plots for esters **72a-75e** intersect at Θ . This is indeed observed, and the regression lines for all esters intersect around 400 K (Figure 3-14). This value is in agreement with the values obtained from the ΔH° versus ΔG° plots at T_{hm} . In addition the Θ values obtained from the slopes of the ΔH° versus ΔS° plots are also similar. Confirmation of the similar compensation temperatures by three different methods seems to be indicating that EEC is observed in this chromatographic system, and that all homologues series examined have the same mechanism of retention. But these conclusions are derived from inspection only, and require statistical analysis.

Statistical analyses have revealed that in most cases of EEC claims the Θ values obtained are not statistically different from T_{hm} (or T_{eval}).¹⁹ Thus a *t*-test is appropriate to check for statistical difference. The null hypothesis is that if T_{hm} (or T_{eval}) falls within the temperature range of Θ at the 95 % confidence level, then EEC is not observed. The temperature range for Θ (Θ_{min} and Θ_{max}) can be found using (24) and (25)

$$\Theta_{min} = \frac{\sum(\Delta H^\circ - \langle \Delta H^\circ \rangle)(\Delta S^\circ - \langle \Delta S^\circ \rangle)}{\sum(\Delta S^\circ - \langle \Delta S^\circ \rangle)^2} - t(3.0.05)\sqrt{V(\Theta)} \quad (24)$$

$$\Theta_{max} = \frac{\sum(\Delta H^\circ - \langle \Delta H^\circ \rangle)(\Delta S^\circ - \langle \Delta S^\circ \rangle)}{\sum(\Delta S^\circ - \langle \Delta S^\circ \rangle)^2} + t(3.0.05)\sqrt{V(\Theta)} \quad (25)$$

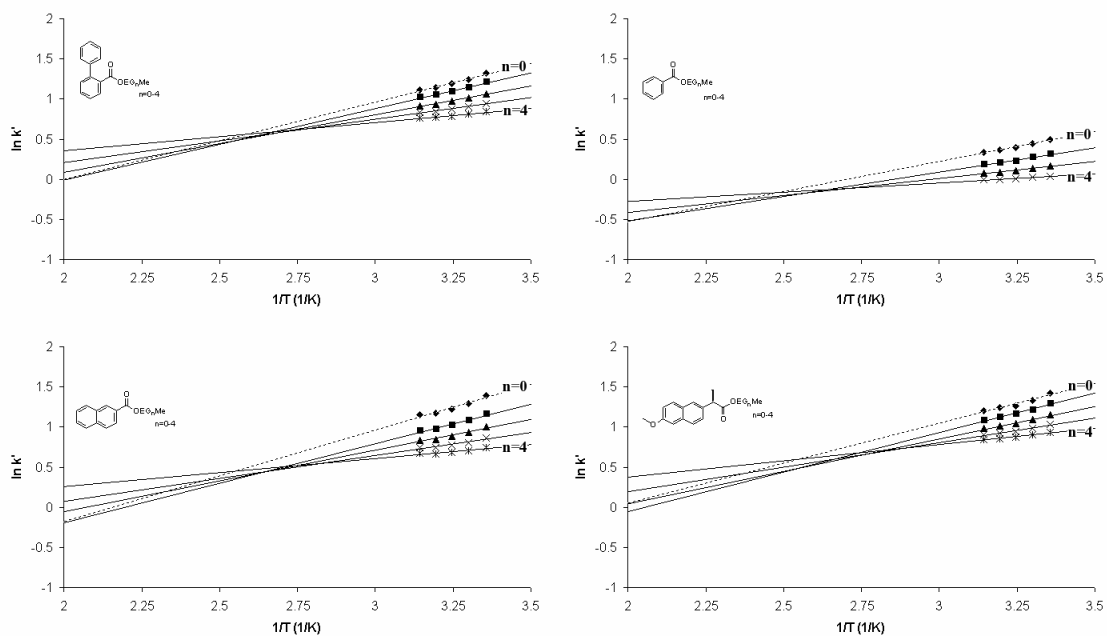


Figure 3-14: Convergence of Van't Hoff plots for esters **72a-75e** at Θ .

where $\langle \Delta H^o \rangle$, and $\langle \Delta S^o \rangle$ are the average enthalpy, and entropy values. $t(3.0.05)$ is the t distribution critical value for 3 degrees of freedom at the 95 % confidence level. In this study the value at 97.5 % was used since this corresponds to a 95 % confidence level as the sum of 2.5 % non-confidence at ends of the assumed Gaussian distribution. This is a common mistake encountered in statistical analysis, the utilization of $t(3.0.05)$ would give a confidence level of 90 %. $V(\Theta)$ is the variance of Θ , and can be calculated using (26).

$$V(\Theta) = \frac{\sum (\Delta H^o - \Delta G_\Theta^o - \Theta \Delta S^o)^2}{3 \sum (\Delta S^o - \langle \Delta S^o \rangle)^2} \quad (26)$$

The t-test was applied, and the range for Θ at the 95 % confidence level, and Θ values obtained from the ΔH° versus ΔS° , and ΔH° versus $\Delta G_{T_{hm}}^\circ$ plots are given in Table 3-10. These Θ_{\min} and Θ_{\max} values are clearly different from T_{hm} (or T_{eval} , 308 K), thus the null hypothesis is rejected. These findings also support the presence of EEC in this chromatographic system.

Table 3-10: Θ ranges for esters **72a-75e** obtained through the *t*-test at the 95 % confidence level.

	<i>Esters</i>	Θ from ΔH° vs. ΔS° (K)	Θ from ΔH° vs. ΔG° (K)	<i>Range (K)</i> (Θ_{\min} - Θ_{\max})
1	72a-e	383	385	353-413
2	73a-d	398	401	360-436
3	74a-e	387	392	346-429
4	75a-e	378	385	324-432
5	72b-e	372	373	355-390
6	73b-d	378	377	367-390
7	74b-e	370	369	357-383
8	75b-e	364	365	348-381

The Θ ranges were wider for homologous series that contained the methyl esters (*entries 1-4*) than those that did not (*entries 5-8*). Inspection of the Van't Hoff plots in Figure 3-14 would suggest the same. The significance of this is not clear. The cause could certainly be experimental errors. Alternatively there could be a slight change in the retention mechanism going from the methyl esters to the corresponding OEGylated esters. Regardless which cause is true, the Θ ranges overlap in all cases. Thus based on the statistical methodology used in separation science we can still regard these findings as supportive of the presence of EEC in our chromatographic system.

The Θ ranges observed varied between 23 and 108 K. These ranges compare favorably to those obtained for methylene homologues, and structurally related halogenated benzylamines (\approx 600 K). For instance for a series of halogenated benzylamines the Θ range was found to be 330-790 K with the calculated Θ value being 560 K.^{19b} For some related aromatic carboxylic

acids the range was 539-897 K, and for substituted benzene derivatives the range was found to be 554-775 K.^{18, 20} The Θ values obtained for OEGylated esters clearly demonstrate that the RPLC retention mechanism of OEGs is different than that for methylene homologues, provided- of course-that EEC is actually observed in our system.

3.7 EFFECT OF LITHIUM CATIONS ON RETENTION

During the normal phase TLC studies it was demonstrated that lithium cations on the surface of the stationary phase and those dissolved in the mobile phase had a significant effect on the retention of OEGylated esters (Chapter 2). Li^+ on the surface of the mobile phase tend to increase retention and the effect is directly proportional to the OEG chain length. This trend parallels the complexation constant of OEGs with Li^+ . This example of complexation chromatography could potentially be exploited to enhance the resolution of closely eluting substrates. Thus it was of interest to study whether similar effects could be achieved in RPLC as well.

It is interesting to consider what the effect of Li^+ in RPLC might be. Complexation with Li^+ could induce a pre-organization of the OEG chains with the ethylene groups facing the solvent. This would facilitate partitioning of the substrates to the stationary phase, thus increasing retention. An alternative mechanism of retention increase could be the “salting out” of the solutes. On the other hand Li^+ could also increase the water solubility of OEGylated substrates and hence reduce retention. It is important to remember that the OEGylated substrates are closely associated with an ionic species in the case of complexation.

In a study that aimed at developing an analytical method for the separation of linear alcohol ethoxylates, Lemr has studied the effect of NaClO₄ on their retention.²¹ The authors optimized the salt concentration and found that 0.01 M gave the most pronounced effect. It was found that addition of NaClO₄ had no effect on the retention of lower OEGs. On the other hand it was observed that the retention time of higher OEGs was reduced considerably.²¹

We performed an experiment using 0.1 M LiCl dissolved in a mobile phase composed of 50:50 AcCN:H₂O. The concentration of the salt and composition of the mobile phase were dictated by the solubility of LiCl in the mobile phase. As demonstrated in Figure 3-15, there was practically no effect of the presence of Li⁺ in the mobile phase on the relative retention of esters **72a-e**. We assume that the complexation constant of Li⁺ with the OEGylated substrates was not large enough in this mobile phase composition to induce a significant effect. But this does not necessarily mean that using ion-exchange columns in the RP mode would not lead to enhanced retention of OEGylated substrates.

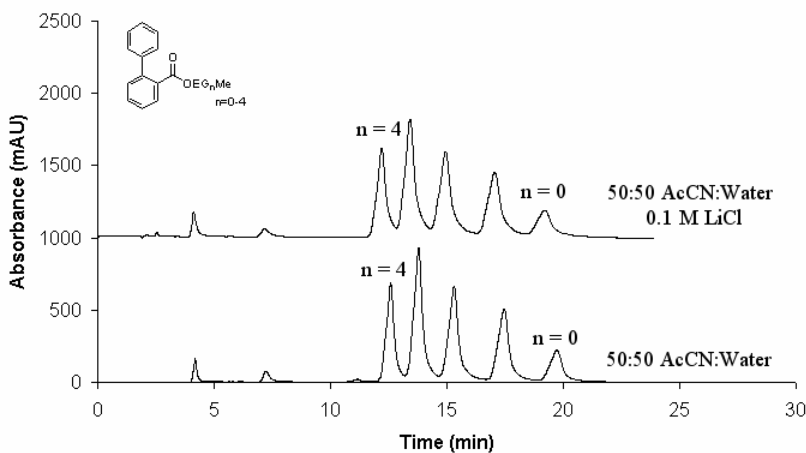


Figure 3-15: The effect of LiCl on the retention of esters **72a-e**.

3.8 MECHANISTIC CONSIDERATIONS AND CONCLUSION

PEGs and their derivatives, have found a wide range of applications in fields ranging from medicine to the textile industry. Therefore a wide variety of HPLC-based analytical methods have been developed for their qualitative and quantitative analysis. The most important application of OEGs and their derivatives is as nonionic surfactants. Therefore the majority of these studies were aimed at such compounds.^{22a-n, 23a-b} A number of studies have been carried out to elucidate the effect of certain chromatographic parameters on the retention of OEGs and to elucidate their retention mechanism in NPLC and RPLC.^{21, 24a-c}

The preceding sections in this chapter detailed our analysis of the chromatographic behavior of OEGylated esters in RPLC. Analysis of the data obtained and comparison of these with information found in the chemical literature regarding the chromatographic behavior of these compounds may help understand this behavior.^{21, 22a-n, 23a-b, 24a-c} A similar comparison with ethylene homologues, which energetics of retention have been examined in detail, could also aid in the mechanistic interpretation of the data we have gathered.^{12d, 13b, 18, 19b, 25}

3.8.1 Effect of Mixture Injections and Hydrogen Bonding with the Stationary Phase on Retention

In these experiments we have injected each homologous series as a mixture to maximize time efficiency. Whether this would change the retention times of the substrates with respect to their single injection retention times is a valid question to ask. We have addressed this question by occasional injections of single substrates. These experiments suggest that mixture injections

do not have a significant effect on retention time with respect to single component injections. This is valid even under circumstances where high degrees of overlap existed between the peaks. Relatively high symmetry of the substrate peaks could be responsible for this.

We have considered the issue of hydrogen bonding with stationary phase silanols as a potential factor affecting the retention of OEGylated esters earlier (Section 3.3). Application of the Engelhardt test demonstrated that hydrogen bonding could be a factor.⁹ Aniline eluted slightly later than phenol. This finding suggests that substrate-accessible (probably acidic) silanols exist in the bonded phase employed in this study. The effect of these seem to be weak, even with a base like aniline. Since we observed linear $\ln k'$ versus % water concentration and $1/T$ (i.e. Van't Hoff plots), we can conclude that hydrogen bonding of **72a-76e** with the stationary phase plays little or no role in their retention.

3.8.2 Effect of the Presence of Capping Groups on Retention Order of OEGylated Compounds

An important aspect of the chromatographic behavior of OEG derivatives is their elution order in RPLC. In our chromatographic system elution times increased with decreasing DP, whereas for uncapped OEGs the elution order was the opposite.^{23b} In another study it was observed that the elution orders of di-DNB (3,5-dinitrobenzene) capped (i.e. both hydroxyl groups capped) OEGs on a RPLC C18 column were the same as the elution orders we observed for OEGylated esters on our C18 RPLC column (Figure 3-16).^{23a} It is interesting to note that in the same study it was also observed that di-DNB capped OEGs exhibited the same elution order on an amine-bonded column under HILIC conditions as our OEGylated esters exhibited on a silica column under NPLC conditions (Section 2.2.2).^{23a} Another point is that the elution times of uncapped

OEGs are much lower than those of capped ones. In other words, $[H_2O]$ in the mobile phase needs to be higher for uncapped OEGs to get capacity factors similar to those of capped ones.

These observations would suggest that the elution order with respect to OEG DP is determined by the presence and nature of capping groups. Elution order would be expected to increase with OEG DP if the hydrophilicity of an EG monomer is less than that of the capping group. This would only be the case for uncapped OEGs, highly charged capping groups, and/or highly polar ones. Most capping groups would be more hydrophilic than an EG monomer, thus the trends observed for **72a-76e** would likely be observed. The differences in total hydrophobic surfaces areas between capped and uncapped OEGs, which are lower for uncapped ones, may explain why uncapped OEGs would elute earlier than their capped counterparts.

In the same manner the relative order of elution of OEGs of the same DP capped with different groups would be dictated by their respective interaction energies with the stationary phase. These energies would be determined by a number of factors such as hydrophilicity/ $\log P$, steric interactions, hydrogen bonding, ionic interactions, and the conformational changes in the OEGylated substrates upon interaction with the stationary phase and mobile phase.²⁶

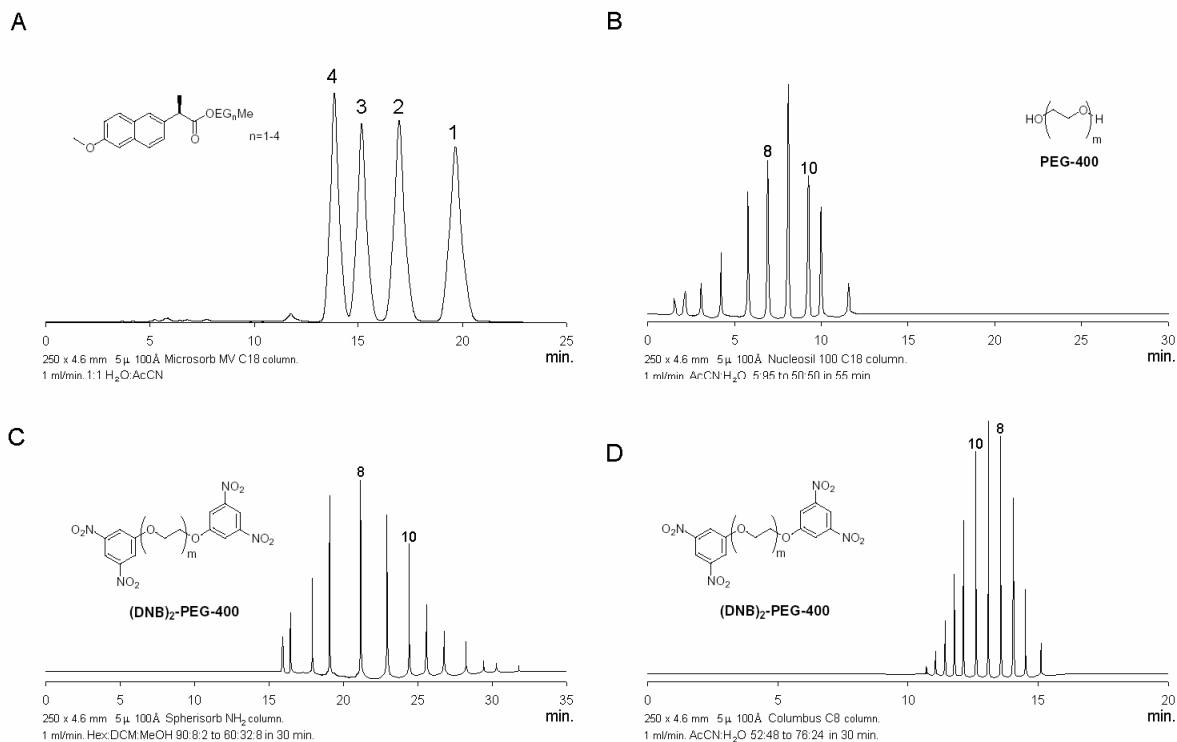


Figure 3-16: Elution orders of a number of capped and uncapped OEGs. A: Esters **75b-d** on a C18 column. B: Peg-400 on a C18 column.^{23c} C: (DNP)₂-PEG-400 on a bonded amine column under HILIC conditions.^{23d} D: (DNP)₂-PEG-400 on a C18 column.^{23d}

3.8.3 Effect of Conformational Changes of the OEG Chains on Retention

Uncapped OEGs are completely miscible with water at moderate temperatures. But elevated temperatures decrease the water solubility of OEGs and phase separation occurs.^{27e} The causes of this phenomenon have been extensively studied. Early on it was postulated that the drop in OEG water solubility at elevated temperatures was the result of a conformational change in the OEG chain. The high-temperature conformation was postulated to be nonpolar whereas the low-temperature conformation was postulated to be polar. The driving force for this conformational change was assumed to be the favorable entropic change upon loss of water. The free energy associated with this process could render OEGs insoluble at elevated temperatures.

Thus the determination of conformations of the OEG chain under various conditions is of importance. Such conformational studies have been done using a number of methods. These methods include IR spectroscopy, quantum chemical calculations, Raman spectroscopy, x-ray crystallography, size exclusion chromatography (SEC), small-angle neutron scattering (SANS), and NMR.^{27a-d, 28a-b, 29, 30a-b, 31, 32b}

Andersson and Karlström have studied the gas and solution phase conformations of 1,2-dimethoxyethane (DME) using quantum mechanics and statistical mechanics.^{28a-b} The workers identified two minima through conformational searches. The lower energy conformer had a geometry where both the C-O and C-C bonds had an anti relationship (a-a-a, Figure 3-17). The higher energy conformer was anti around the C-O bonds and gauche around the C-C bond (a-g-a, Figure 3-17). a-a-a was more stable over a-g-a by 3.2 kJ/mol. The rotational barrier from a-a-a to a-g-a was estimated to be 10 kJ/mol. The respective dipole moments for one EG unit were calculated to be 1.07 (a-a-a) and 1.24 D (a-g-a). This was found to be in agreement with diethyl ether (1.30 D). It was concluded that the geometries of these conformers were dictated by dipole moment interactions. The less polar conformer a-a-a was expected to be dominant in the gas phase. The authors argue that dipole-dipole interactions are responsible for this behavior.^{28a-b} Andersson *et al.* have also theoretically studied the conformers of DME in the solution phase.^{28a-}
^b It was found that a-g-a was more stable than a-a-a. The energy difference between the gauche and anti conformers was found to be in the range of 1.7-3.5 kJ/mol depending on the solvent. The stability of the gauche conformer increased with the polarity of the solvent. It was estimated that solvation stabilized the gauche conformer over the anti conformer by 5.3-6.8 kJ/mol over the gas phase.

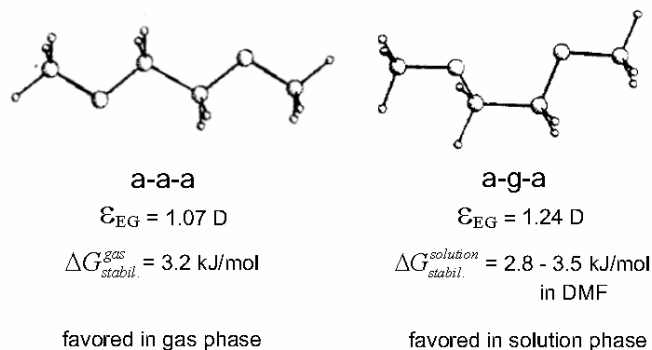


Figure 3-17: The anti and gauche conformers of DME as suggested by theoretical work.^{28c}

Obviously the dipole moments of OEGs depend on the conformations of both the C-C and C-O bonds as well as the nature of the terminal groups (Figure 3-18). Substantial amounts of experimental work have been done to determine the factors that contribute to the conformational change of OEGs and their derivatives. The crystal structures of PEGs are found as 7/2 helices (i.e. 7 EG subunits form 2 turns of a helix).^{30a-b} PEGs with DPs larger than 48 form coils.³¹ Shorter ones may form helices in pure organic acids in the presence of traces of water.³¹ But these studies are irrelevant to our system as the OEGs we employed are rather short. The results of NMR, Raman, and IR studies are more relevant. NMR studies give qualitative and quantitative information, but they are limited to the conformations around the C-C bonds.^{32b} While IR and Raman studies give information about the conformations around both C-C and C-O bonds, this information is of qualitative nature only (Figure 3-18).^{27a-d}

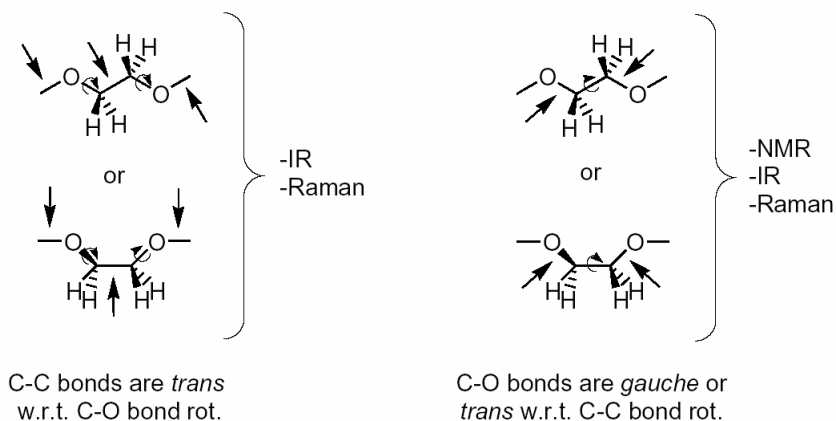


Figure 3-18: Most stable conformers of DME and the experimental methods that can be used to determine them.

Viti, Indovina, Podo, Radics, and Némethy have studied the conformations of 1,2-dimethoxyethane (DME) and 2-methoxyethanol (MOE) using NMR.^{32b} They analyzed the CH₂-CH₂ coupling constants (*gauche* and *trans*) observed in solvents of differing dielectric constants (ϵ) and various temperatures. Their data suggests that in solvents with low ϵ 's DME exists as a mixture of roughly equal amounts of the *trans* and the two *gauche* isomers. MOE on the other hand exists predominantly as the *gauche* isomer. The conformational preference of MOE was explained by intramolecular hydrogen bonding of the terminal hydroxyl group with the adjacent ether oxygen. In higher ϵ solvents the *gauche* population of DME increased, which is consistent with interaction of the solvent dipoles with those of DME. The increase in the *gauche* population was much less for MOE. The difference in the energies between the *trans* and *gauche* isomers was small for DME with respect to MOE ((-0.48 to -0.81 kcal/mol versus -0.89 to 1.04 kcal/mol depending on solvent and temperature). Thus DME had a larger preference for the *trans* conformation around the C-C bond, whereas MOE had a greater preference for the

gauche conformation. In solvents that were good H-bond acceptors the *trans* preference of MOE increased.^{32b}

Results obtained for DME and MOE might not necessarily be completely valid for higher OEGs. The Matsuura group (Hiroshima University Department of Chemistry) has done a number of detailed qualitative conformational studies of capped and uncapped OEG derivatives (DP = 1-4) in various solvents using IR and Raman spectroscopy.^{27a-d, 27f} In OEG-water binary solutions it was found that the *gauche* preference around the C-C bond increased significantly with decreasing OEG mole fraction (χ_{EG}), although evidence exists that a maximum for the *gauche* form exists around $\chi_{EG} = 0.05$.^{27c, 27f} For OEG_nMe₂ (DP = 1-4) the rate of increase of the *gauche* conformer population around the C-C bond was independent of OEG chain length and terminal group identity of R₂OEG (R = -CH₃ through -(CH₂)₃CH₃). For R₂OEGs the change in the *gauche* population varied linearly with χ_{EG} , and the plots were nearly parallel (DP = 1 showed slight deviation at low χ_{EG} 's).^{27c} Interestingly, mono-capped and uncapped OEGs behaved irregularly (i.e. the slopes for different DPs were not parallel). The stabilization of the *gauche* conformer around the C-C bond was explained using dipole-dipole interactions (the *gauche* conformer has a larger dipole moment) and hydrogen bonding with water. One water molecule may form hydrogen bonds such that adjacent ether oxygens or every other are bridged (Figure 3-19). Such bridging may stabilize the *gauche* conformation.^{27c} Loss of water at elevated temperatures may explain the phase separation observed in OEG-water binary mixtures. In contrast to the NMR study of Viti *et al.*, uncapped OEGs showed relatively little increase in the *gauche* conformation around the C-C bond with decreasing χ_{EG} .^{32b, 27c} The authors assumed that the free terminal hydroxyl group induces a perturbation in the solvation sphere which reduces the number of bridging water molecules.^{27c} There was very little change in

the population of the gauche and trans conformers around the C-O bond with decreasing χ_{EG} , although at high water concentrations it is known that around 20% of the OEGs have a *gauche* conformation around the C-O bonds.^{27c} In other studies it was observed that OEG conformations in MeOH and formamide mirrored those in water, whereas opposite trends were observed in CCl₄.^{27a, 27d} It was concluded that OEG conformations in water could be described as being helical, or meandering.^{24a, 27c} The conformation of OEGs in very low ϵ solvents can be described as zig-zag (Figure 3-19).^{24a}

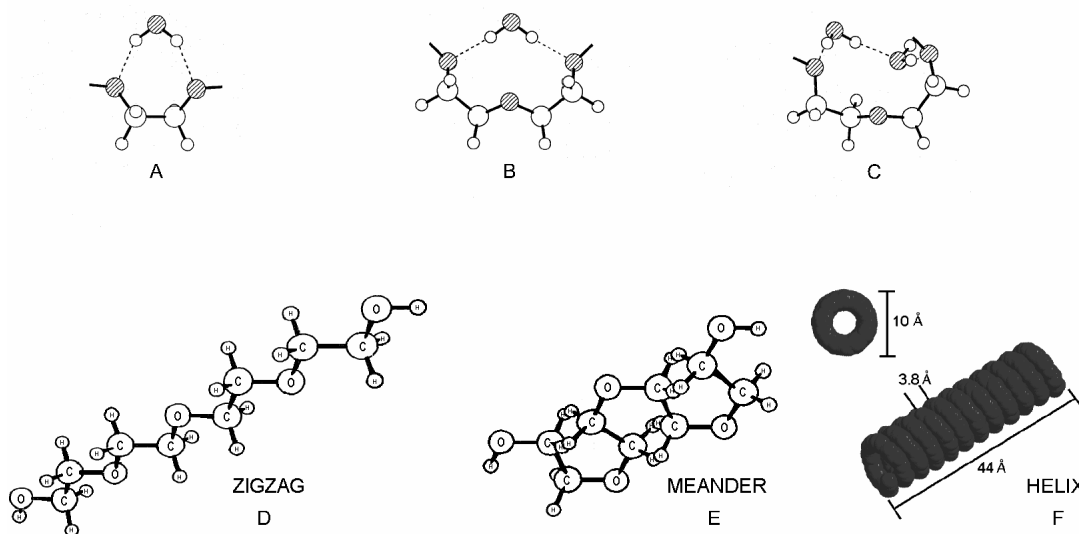


Figure 3-19: Hydrogen bonding structures that may stabilize the gauche configuration around the C-C bond (A-C) and various conformations of OEGs (D-F).^{24d, 31b}

For OEGs to be useful as sorting tags in RPLC their elution with respect to DP should be orderly and predictable. Conformational changes of the OEG chains would change the hydrophobic area of the OEG chains, which in turn would affect the retention times of OEGylated substrates. Such a conformational change would represent an additional mobile phase induced mechanism affecting the retention of OEGylated substrates. The zigzag

conformation tends to increase retention time whereas the meandering/helical conformation tends to reduce it. The per EG surface area for the meandering conformation is approximately 25.1 \AA^2 , whereas that for the zigzag conformation is 27.5 \AA^2 .^{24a}

In an early study which could be regarded as being similar to ours Melander, Nahum, and Horváth studied the effect of conformational change on the retention of uncapped and mono-capped OEGs.^{24a} The authors used these uncapped and mono-capped OEGs as model structures for the study of the effect of conformational changes on retention. The solvent composition, and temperature ranges examined in this study were different that those examined in ours.

Melander *et al.* assumed an equilibrium between the zigzag (A) and meandering/helical (B) conformations of OEGs (27).^{24a} Thus the average capacity factor for the OEG (k'_{av}) can be expressed as (28) and the enthalpy of the retention process governed by this equilibrium can be expressed as (29)



$$k'_{av} = \frac{k'_A + Kk'_B}{1 + K} \quad (28)$$

$$\Delta H^o_{av} = \frac{k'_A \Delta H^o_A}{(k'_A + k'_B K)} + \frac{k'_B K \Delta H^o_B}{(k'_A + k'_B K)} + \frac{K(k'_A - k'_B) \Delta H^o_{eq}}{(k'_A + k'_B K)(1 + K)} \quad (29)$$

where ΔH_A^o , ΔH_B^o , ΔH_{av}^o , and ΔH_{eq}^o correspond to the enthalpies of retention for conformations A, B and their average, and the enthalpy of the conformational equilibrium. The capacity factors are defined similarly. From (29) it can be deduced that Van't Hoff plots should be nonlinear if significant conformational change of the OEG chain occurs in the temperature range studied.^{24a} The authors observed nonlinear Van't Hoff plots for uncapped, mono-phenol, and mono-octylphenol capped OEGs at high water concentrations ($\geq 80\%$ water). A similar theoretical analysis by Melander *et al.* predicts irregular behavior upon change in the mobile phase composition as well. They have demonstrated such behavior experimentally. Retention changes nonlinearly with solvent concentration and even reversal in retention is observed with mono-phenol capped OEGs when water concentration is high ($\geq 80\%$ water).^{24a} Melander *et al.* did not mention how their OEGylated compounds behaved when highly organic eluents were employed.^{24a}

In a more recent study Kamiyuki, Monde, Omae, Morioka and Konakahara have investigated the retention behavior of OEG monolauryl ethers and PEG (DP=5-18) under conditions similar to ours.^{24c} The workers used a Fluofix 120N® fluoros RPLC column, which could be regarded as being similar to a C18 column. For mono-capped OEGs the retention order was the same as ours (45% AcCN). For uncapped PEGs elution order was inverted, as had been observed by Melander *et al.*.^{24a, 24c} Van't Hoff plots were nonlinear, and a breaking point was observed around 40°C (Figure 3-20). At temperatures below this breaking point elution times increased (nonlinearly) with temperature, whereas they decreased at temperatures above it. A convergence point in elution times was observed for DPs 5-8 (no data were presented for lower DPs).^{24c} The authors attribute this breaking point to an increased change in conformation at higher temperatures.

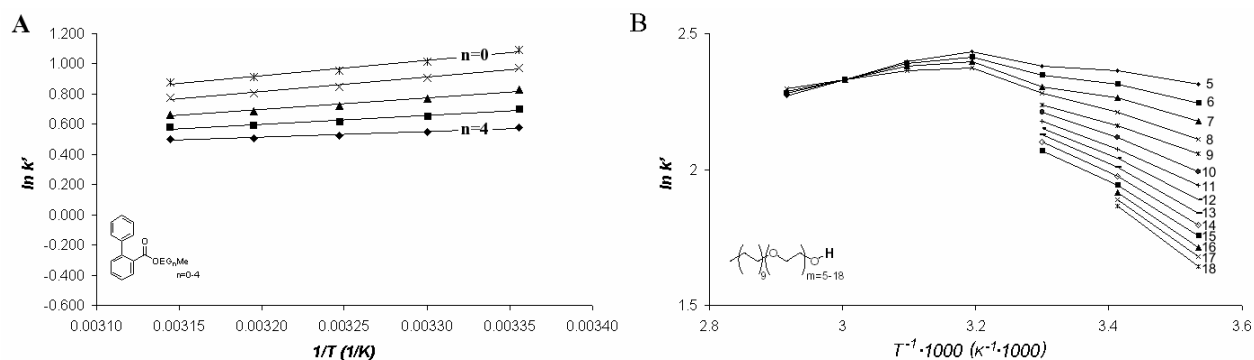


Figure 3-20: Van't Hoff plots for **72a-e** and mono-capped OEGs.^{24c}

Our Van't Hoff plots were linear (Figure 3-20) and no apparent curvature indicating an imminent breaking point is evident. Both ΔH° versus DP and ΔS° versus DP plots were linear in our system (Figure 3-21). Similarly k' versus DP under a number of different mobile phase compositions were linear as well (Figure 3-7). Our chromatographic system is clearly not exhibiting irregular behavior indicative of conformational change of the OEG chain. As the work of Matsuura *et al.* indicates that di-capped OEGs exhibit linear change in conformer populations with increasing or decreasing ϵ (another way of looking at the effect of χ_{EG}) that is uniform for DP = 1-4.^{27c} While there is no doubt that OEG chain conformer populations in our system change with changing mobile phase composition, the rate of change is the same for all DPs and that change is linear with respect to change in ϵ . The net effect is chromatographic behavior that is regular and similar to ethylene homologues.

The studies of Melander *et al.* and Kamiyuki *et al.* covered a wider range of mobile phase composition and temperature than our study.^{24a, 24c} Thus comparison between our findings and theirs does not preclude the possibility that we might observe similar irregularities at higher/lower DPs, temperatures, and/or water concentrations. But the general trends we have observed in our studies suggest that regular behavior could be expected for DPs up to 6, % water

concentrations up to 70, and temperatures up to 60 °C. In our system the elution of **75a-e** at 100% water would require approximately 430-950 minutes at a flow-rate of 1 ml/min. Such long elution times would be difficult with our experimental set-up as the maximum flow rate we can sustain with our C18 column is 1 ml/min and our solvent reservoir volume is only 1 liter. Excessive band broadening could also make the experiments difficult. Furthermore our C18 column is rated only up to 60°C. These factors make expanding the experimental range with our HPLC set-up difficult. Perhaps DSC experiments might be more appropriate for these kinds of studies.²⁵ Such experiments would certainly expand our understanding of the chromatographic and conformational behavior of double-capped OEG derivatives.

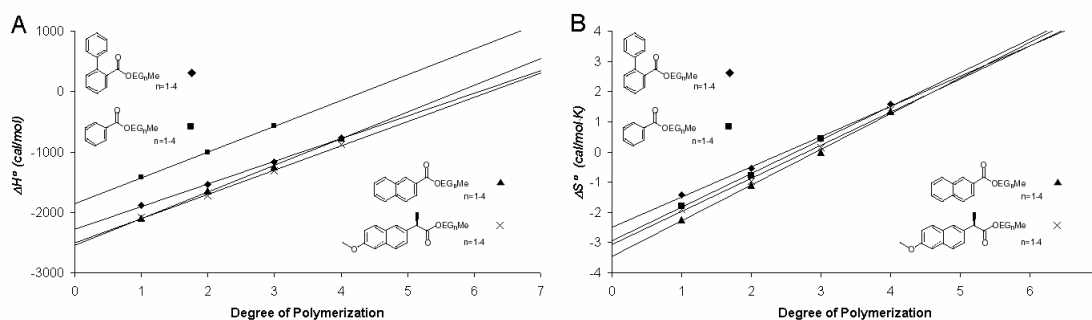


Figure 3-21: ΔH° versus DP and ΔS° versus DP plots for **72b-76e**.

3.8.4 Discussion of ΔH° , ΔS° and EEC Through Comparison with Methylene Homologues

The arguments and findings in Sections 3.8.1-3.8.3 suggest that the effect of mixture injections and hydrogen bonding with stationary phase hydroxyl groups has no or little effect on the retention of OEGylated esters. Conformational changes of the OEG chains of OEGylated

esters **72b-76e** may have an effect, but that effect is linear for all esters and no irregular behavior is observed. Further discussion of the mechanism of retention of **72b-76e** could be aided by comparison with the ΔH^0 , ΔS^0 , T_c , and T_c range values of methylene homologues.

ΔH^0 , ΔS^0 , T_c , and T_c range values for a number of methylene homologues and structurally similar compounds are given in Table 3-11. Generally speaking ΔH^0 and ΔS^0 values increase with increasing bulk of the parent compounds and increasing methylene chain length (Entries 1-11 and 23-28, Table 3-11). In our case ΔH^0 values decreased with increasing OEG DP whereas ΔS^0 values increased. The structural difference between alkyl chains and OEG chains is obviously the presence of one oxygen atom for every two methylene units in the latter. The polarity of OEGylated compounds would be expected to increase as DP increases, this in turn would reduce the affinity of these compounds for the stationary phase. Hydrogen bonding of OEG chains with water can be assumed to play an important role in this regard. Two water molecules can hydrogen bond to the oxygen of an EG unit. When a hydrated EG unit interacts with the stationary phase these water molecules could dissociate resulting in a loss of enthalpy (due to the loss of hydrogen bonds). However such a loss of water would cause an increase in entropy since water has a smaller molecular volume than acetonitrile. The molecular volume of water is $\sim 19 \text{ \AA}^3$ and that for acetonitrile is $\sim 46 \text{ \AA}^3$. Thus the "hole" in the solvation sphere around the solute created by the dissociation of water could only be filled by one acetonitrile molecule (Figure 3-20).

Table 3-11: ΔH° , ΔS° , and T_c values for some methylene homologues and compounds with structural similarity.

#	Structure	$^a\Delta H^{\circ}$	$^b\Delta S^{\circ}$	cT_c	#	Structure	$^a\Delta H^{\circ}$	$^b\Delta S^{\circ}$	cT_c
1 ^{d,e}		-2.06	3.32 ^f		17 ^{l,m}		-13.45 ⁿ	-20.68 ^o	
2 ^{d,e}		-2.46	3.59 ^f		18 ^{l,m}		-14.95 ⁿ	-23.44 ^o	
3 ^{d,e}		-2.99	4.07 ^f		19 ^{l,m}		-18.69 ⁿ	-28.59 ^o	735
4 ^{d,e}		-3.41	4.37 ^f		20 ^{l,m}		-16.29 ⁿ	-23.37 ^o	
5 ^{d,e}		-3.83	4.66 ^f	-	21 ^{l,m}		-23.37 ⁿ	-34.28 ^o	
6 ^{d,e}		-4.08	4.69 ^f		22 ^{l,m}		-20.24 ⁿ	-29.64 ^o	
7 ^{d,e}		-4.34	4.73 ^f		23 ^{p,r}		-2.68	-1.97 ^s	
8 ^{d,e}		-4.88	5.22 ^f		24 ^{p,r}		-3.49	-2.16 ^s	
9 ^{d,e}		-5.36	5.83 ^f		25 ^{p,r}		-4.35	-2.40 ^s	
10 ^{d,e}		-5.75	5.88 ^f		26 ^{p,r}		-5.06	-2.55 ^s	743
11 ^{d,e}		-6.21	6.24 ^f		27 ^{p,r}		-6.09	-2.90 ^s	
12 ^{g,h}		-11.0 ⁱ	1.3 ^j		28 ^{p,r}		-6.84	-3.70 ^s	
13 ^{g,h}		-11.6 ⁱ	1.5 ^j		29 ^{t,u}		-	-	
14 ^{g,h}		-12.1 ⁱ	1.4 ^j	560 ^k	30 ^{t,u}		-	-	
15 ^{g,h}		-9.5 ⁱ	0.3 ^j		31 ^{t,u}		-	-	647 ^v
16 ^{g,h}		-9.1 ⁱ	0.2 ^j		32 ^{t,u}		-	-	

^akcal/mol. ^bkcal/molK. ^cK. ^dReference 12d. ^e500x41 mm, 5 μ , Hypersil C18, 4:1 MeOH:H₂O. ^f $\Delta S^{\circ} + \ln\beta$. ^gReference 19b. ^h150x4.6 mm, 3 μ , Unison-UK C18, 95:5 AcCN:H₂O, 1ml/min. ⁱkJ/mol. ^j(k/molK)-K. ^kRange: 330-790K. ^lReference 13b. ^m300x3.9 mm, μ Bondapak C18, 3:2 MeOH:2.5x10⁻³ M aq. pH 3 phosphate buffer, 1 ml/min. ⁿkJ/mol. ^oJ/molK. ^pReference 25. ^r300x6.4 mm, Nucleosil C18, 80:20 MeOH:H₂O. ^s $\Delta S^{\circ} + \ln\beta$. ^tReference 18. ^u250x4.6 mm, 5 μ , Spherisorb ODS C18, 6:94 AcCN:5x10⁻² M aq. pH 2 NaH₂PO₃ buffer. ^vRange 539-897 K.

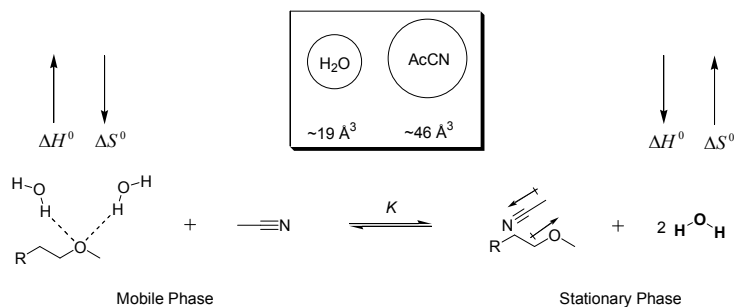


Figure 3-22: Loss of water from an EG unit upon interaction with the stationary phase.

We do not wish to imply that loss of water upon interaction with the stationary phase is the only mechanism that determines the ΔH^0 and ΔS^0 values associated with OEG retention in RPLC. But this is a mechanism which could be present with OEGs, but not with methylene chains. Obviously methylene and OEG homologues would have common mechanisms as well, particularly those that govern the retention of the parent substrates attached to these oligomers. The discussion of these common mechanisms is beyond the scope of this study and can be found elsewhere.^{26a-c}

Comparison of T_c (temperature at which EEC is observed) values and T_c ranges in Table 3-11 reveal that methylene homologues have higher compensation temperatures and wider T_c ranges compared to the corresponding values for the OEGylated esters examined in this study (Table 3-10). This might be the combined result of lower enthalpies of retention (with respect to methylene homologues), drop of retention enthalpy with increasing OEG DP, and increase of retention entropy with increasing OEG DP. The average T_c value found for **72a-76e** is ~ 396 K. Such a T_c value suggests that EEC could actually be experimentally observed (instead of predictions based on Van't Hoff plot extrapolations) if the temperature of the column could be raised up to 150°C (assuming that the OEG chains not loose water and convert to a

predominantly zig-zag conformation). While the RPLC column employed in this study cannot be used at such temperatures, columns that are stable under those conditions are commercially available. Columns such as Blaze200™ C18 (octadecyl bonded silica, Selerity Technologies/Restek), Hamilton PRP-1 (polymeric, Bodman), and Hypercarb™ (porous graphite, Thermo Scientific) are rated up to 200°C.

3.8.5 Conclusion

In this chapter we have described our work regarding the retention behavior of OEGylated esters in RPLC within a limited temperature and solvent composition range. Retention was inversely proportional to OEG DP. The separatory power of OEGs in RPLC was less than that observed in NPLC on silica. The effect of the parent substrates was much more pronounced in RPLC. As a result of their significantly smaller (with respect to **72a**, **74a**, **75a**, and **76a**) parent methyl ester **73a-e** eluted earlier than the rest of the OEGylated esters regardless of the OEG DPs of the latter (Table 3-1). This presents itself as a practical solution to a problem observed in the NPLC study where the **73c-e** peaks overlapped partially or completely with other peaks (Figures 2-4, 2-7, and 6-2). This pronounced parent substrate effect can potentially be used to separate OEGylated compounds based on the size, polarity, acidity, and/or basicity of the parent substrates. Linear DP versus solvent composition and Van't Hoff plots were observed. Based on the focal points of the Van't Hoff plots it was concluded that EEC was observed in this system. The average T_c value found for these esters was ~396 K. Such a low T_c value opens up the possibility of experimental observation of the EEC phenomenon in HPLC. Furthermore, high temperature HPLC could be used to achieve coalescence of the peaks

corresponding to OEGylated substrates which could aid in the separation of these from impurities present in the sample as a result of mixture syntheses.

We have also attempted to construct a retention model based on the Engelhardt silanol activity test and comparison with the retention mechanisms of uncapped OEGs, mono-capped OEGs, and methylene homologues. Our findings suggest that hydrogen bonding with the silanol groups of the column employed in this had little or no effect on retention. The irregular retention of uncapped and mono-capped OEGs note in some reports was not observed with our OEGylated esters under the conditions examined. Our data suggest that we can expect regular retention for temperatures up to 60 °C, water concentrations up to 70 %, and OEG DPs up to 6. The actual limits of regular retention with respect to solvent composition, temperature, and OEG DP should be explored. Hydrogen bonding with water and loss of those upon interaction with the stationary phase (apart from OEG chain conformation considerations) have been suggested as the main difference between the retention mechanisms of OEG and methylene homologues.

4.0 PREPARATION AND APPLICATION OF OEGYLATED EVANS AUXILIARIES

Since its discovery in 1838, the aldol addition reaction has gained considerable importance in organic chemistry as a means for C-C bond formation.¹ This reaction has taken a central role in asymmetric C-C bond formation with the gradual elucidation and control of the factors that affect the stereochemical configuration of the products. Among the methods for stereocontrol of the aldol addition reaction the utilization of boron enolates in conjunction with chiral oxazolidinones as chiral auxiliaries (i.e. Evans auxiliaries: EAs) has found widespread use due to its high yield of aldol adducts with high enantiopurity.^{2a-c} High enantioselectivity in such reactions is achieved through the mechanism depicted in Figure 4-1. Reaction of Bu₂BOTf with the acylated Evans auxiliary (**96**) affords the boron enolate (**97**). Enolization proceeds with high Z-enolate selectivity. The boron enolate (**97**) then reacts with the aldehyde, probably through a Zimmerman-Traxler transition state, to form the desired Evans *syn*-aldol product (**98**) with high enantioselectivity.³

The high synthetic value of the Evans aldol reaction made the preparation and application of Evans auxiliaries a desirable target for us. Evans auxiliaries can also be used for other applications like Diels-Alder cycloadditions, conjugate additions, α -alkylation of carboxylic acids, and Reformatsky reactions.^{4, 5, 6, 7} We believe that OEGylated Evans auxiliaries (OEG-EAs) could speed up syntheses that involve these reactions by enabling mixture synthesis.

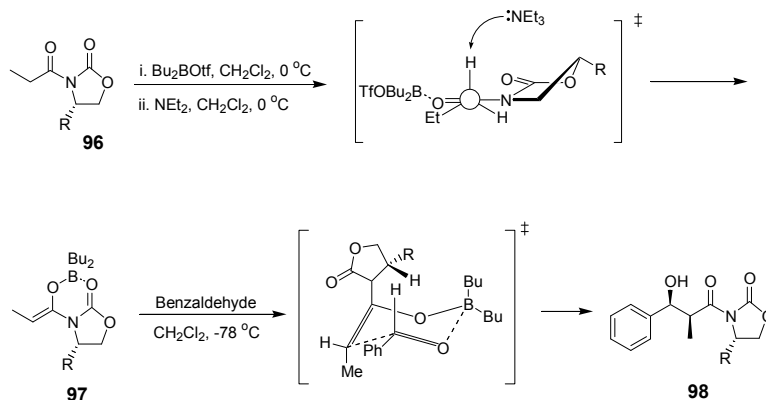


Figure 4-1: Hypothetical transition states for the Evans aldol reaction.

4.1 OBJECTIVES

The objectives of this study are: i. The preparation of OEGylated/acylated Evans auxiliaries (**100**), thus to determine whether the OEG groups are compatible with various conditions and reagents used in the preparation and derivatization of EAs; ii. To optimize and carry out mixture asymmetric aldol reactions with these auxiliaries, thus to test the compatibility of OEGs with such reaction conditions; iii. To investigate the efficiency of OEGs in separating the bound auxiliaries and products (**101**); iv. To examine the yields and stereochemical outcomes of the aldol adducts (**101**, **102**, Figure 4-2).

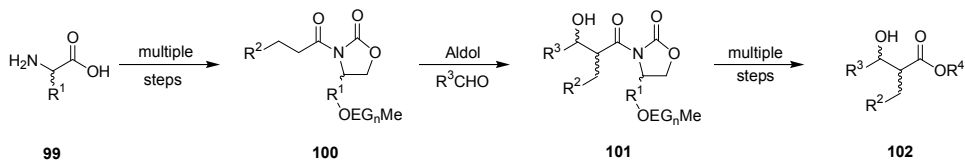


Figure 4-2: The strategy employed in this study.

4.2 PREPARATION AND ACYLATION OF OEGYLATED EVANS AUXILIARIES

Enantiomers of 4-(4-hydroxy-benzyl)-oxazolidin-2-one (**103a** (*R*), **103b** (*S*)) seemed to be good candidates for our study, as they can be derived from the relatively cheap amino acid tyrosine for which both enantiomers are commercially available. The phenol group could be exploited as a site to attach the OEG groups through simple etherification. While a number of other ways could be envisioned for attaching the OEG group to these chiral oxazolidinone, the easiest way for OEGylation of these EAs would be etherification. A similar etherification approach was taken by Ding (Curran group, University of Pittsburgh) in their preparation of fluorinated Evans auxiliaries based on tyrosinol.²⁹ While our strategy was to OEGylate *R*- and *S*-4-(4-hydroxy-benzyl)-oxazolidin-2-one to obtain the OEG-EAs Ding attached fluorinated chains to *R*- and *S*-2-*tert*-butoxycarbonylamino-3-phenyl-propionic acid methyl ester through Mitsunobu reactions and subsequently obtained the fluorinated EAs through ester reduction and cyclization using SOCl₂. Ding obtained fluorinated EAs with two perfluoroalkane groups of differing lengths and applied those to Evans aldol and alkylation reactions.

A number of routes can be envisioned, and have been followed for the preparation of **103b** (Figure 4-3):^{8a-f} An attractive feature of these synthetic routes is that they involve four or fewer steps. On the other hand the use of toxic reagents like phosgene, or its derivatives, is not attractive. Other undesirable qualities of some of these routes became apparent when they were followed. When route A was followed it was found that while the first step proceeded with acceptable yield, attempts at the purification of **104a** by recrystallization proved to be fruitless.^{8b} Attempted protection of nonpurified **104a** as a carbamate using EtOCOCl proceeded with low yield. Thus we tried Evans' route (Route C).^{8d} Reduction of *S*-tyrosine (**106b**) to *S*-tyrosinol (**107b**) using BH₃·SMe₂ proceeded with good yield, but purification of the product proved

impossible, and it was taken to the next step without purification. Attempted oxazolidinone formation using diethyl carbonate, and di-*tert*-butyl carbonate proceeded with unsatisfactory, and unreliable yields. The remaining routes were not attempted.

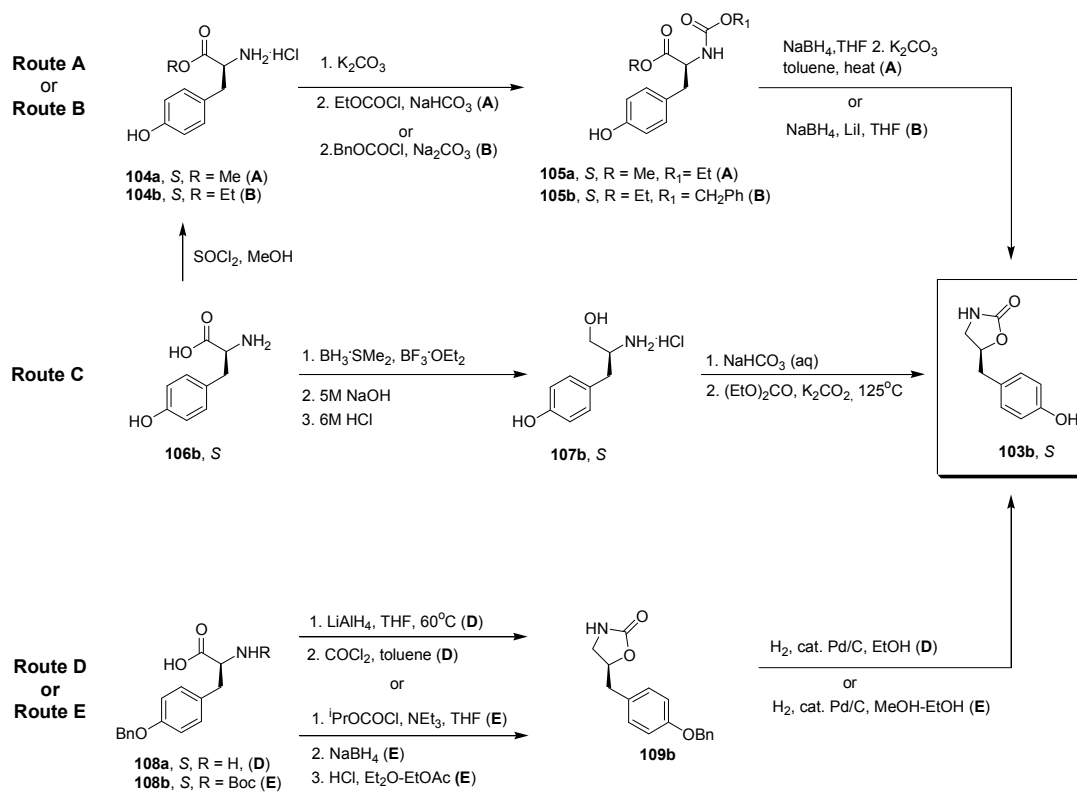


Figure 4-3: Some synthetic routes for the preparation of **103b**.^{8a}

Recently a more reliable synthesis of **103b** that yields intermediates purifiable by recrystallization has been introduced by Green, Taylor, Bull, James, Mahon, and Merritt.^{8a} While this route involves a larger number of reactions and longer reaction times than the previously mentioned ones, in our experience it proved facile, reliable, and high-yielding. We prepared both **103a** and **103b** using this route. The synthesis (Figure 4-4) started with the Boc protection of *R*- and *S*-tyrosine (**106a-b**) using Boc_2O . These products (**110a-b**) were obtained

in good yield and purity, but proved to be foams which were difficult to handle, thus were taken on to the next step without further purification. Simultaneous protection of the phenol and carboxylic acid groups of **110a-b** was accomplished via reaction with BnBr/K₂CO₃/Bu₄NI and proceeded in good yield to give the globally protected tyrosine derivatives **111a-b**, which were purified by recrystallization (the recrystallization solvent had to be modified from the reported one to work properly in our case). LiAlH₄ reduction of **111a-b** afforded the protected tyrosinols **112a-b** in good yield and purity. Cyclization to give the benzyl protected oxazolidinones (**113a-b**) was achieved through deprotonation of the alcohol with NaH. Catalytic hydrogenation of **113a-b** generated the desired oxazolidinones (**103a-b**). The time required for these hydrogenations can be reduced significantly by using a Parr hydrogenation apparatus instead of a hydrogen filled balloon.

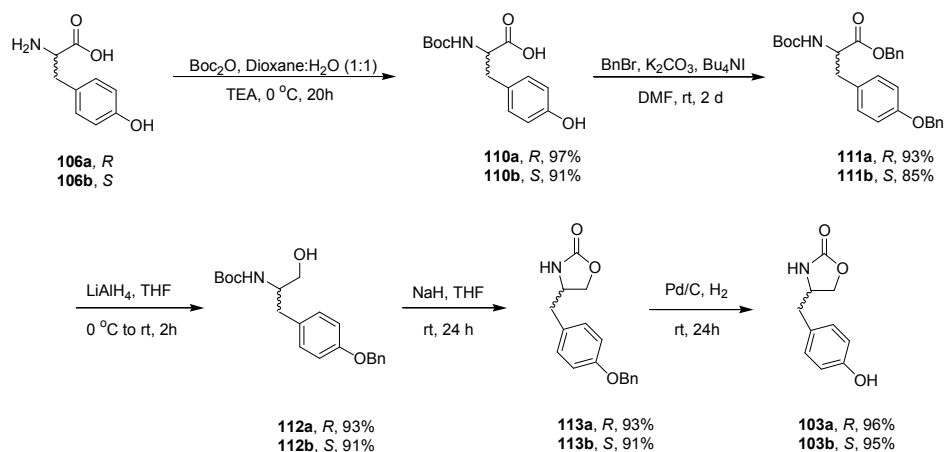


Figure 4-4: Preparation of **103a** and **103b**.

The optical rotation of **103b** was found to be -11.2°, whereas the value found by Green *et al.* was -12.3°, and that of Faita *et al.* was -11.8°. ^{8a, 9a} Our value is within the expected error range for optical rotations, thus sufficient enantiopurity of **103b** was assumed. This assumption

was proven to be correct after the stereochemical analysis of the aldol adducts. **103a** displayed an optical rotation value of +11.2°. The syntheses of **103a-b** were reproducible, and intermediates, and final products were obtained in good yield, purity, and enantiopurity. The overall yield for **103a** was 75%, and 62% for **103b**. Increased familiarity with the reactions over time and differences in care during the recrystallization of **111a** and **111b** (*R*-tyrosine is significantly more expensive than its enantiomer) seem to be the causes of the difference between the overall yields of the two enantiomers.

Hydroxyl group bearing oxazolidinones are of particular interest to solid phase synthesis since they can be attached to resins through etherification reactions. Resins to which **103b** was attached through etherification include Merrifield, Wang, hydroxymethyl/chloromethyl polystyrene, and polystyrene resins obtained through copolymerization of oxazolidinone bound 4-vinylbenzyl alcohol, and styrene.^{4, 5, 8b-e, 9a-d} A number of reagents were used for etherification which include PPh₃/DEAD, NaH/KH, K₂CO₃, and Cs₂CO₃.^{4, 5, 8b-e, 9a-d}

Based on our positive experience with the OEGylation of phenols (Chapter 2), we were inclined to use the K₂CO₃/KI/DMF system. Reactions of **103a-b** with **87a-d** (Me(OEG)_nCl, n = 1–4) did not yield significant amounts of the OEG-EAs (**114a-d**). Variations in reaction temperature, and reaction time did not improve the outcome. OEGylation using Cs₂CO₃/KI initially afforded the desired compounds in moderate yields. Optimization attempts by variation of reaction time/temperature did not improve the yields. However it was found the reaction yield is highly sensitive to the quality of the DMF used. Even use of commercially available anhydrous DMF in SureSeal™ bottles did not result in acceptable yields. Distilled DMF stored over molecular sieves, and under nitrogen is required for the reaction to work properly. We

suggest that dimethylamine produced by the decomposition of DMF, or residual moisture, opens the oxazolidinone ring during the etherification reaction (Figure 3-5).

A number of methods can be used for the acylation of oxazolidinones. Deprotonation of the oxazolidinones with organolithium bases (i.e. *n*-BuLi, LHMDS, LDA), and subsequent reaction with the desired acylchloride is a popular method.^{2, 8d, 8e, 9b} Another frequently applied method is the NEt₃/DMAP mediated acylation of oxazolidinones with the acid anhydride of interest.^{4, 8b, 9a, 9c, 10} Both methods seem to have similar yields. One advantage of procedures employing organolithium reagents is that they require less time. The NEt₃/DMAP method requires 3 days, while the reaction employing organolithium reagents can be completed in hours.^{9a,10}

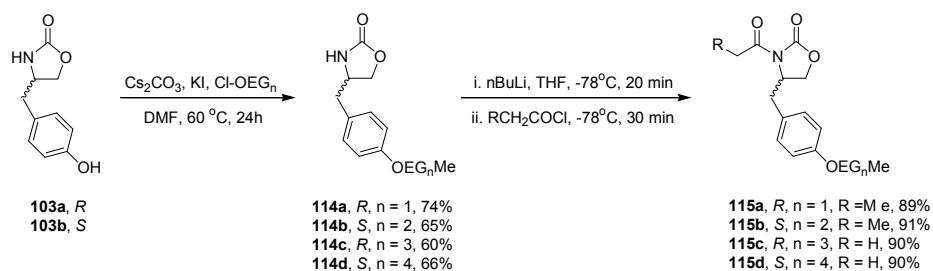


Figure 4-5: Preparation of **114a-d** and **115a-d**.

Due to advantages mentioned above we decided to use *n*-BuLi for the acylation step. The acid chlorides of interest were propionyl chloride and butyryl chloride since the spectroscopic, and stereochemical properties of their aldol adducts with benzaldehyde are known.²¹⁻²⁷ Deprotonation of **114a-d** using *n*-BuLi, and subsequent addition of the desired acyl chlorides afforded the acylated OEG-EAs of interest in good yield. As can be seen in Figure 4-5, the OEG-EAs were acylated such that Me(OEG)₁-, and Me(OEG)₂- tagged auxiliaries would give a pair of enantiomers, and the Me(OEG)₃-, and Me(OEG)₄- tagged ones would give another pair

of enantiomers. The less polar butyryl group was attached to the first two OEG-EAs to enhance the separation of the products. The success of the acylation reactions demonstrates that neither the presence, nor length of the OEG tag affects reactions with *n*-BuLi, and that OEGylated compounds are compatible with organolithium reagents.

4.3 ASYMMETRIC ALDOL REACTIONS USING OEGYLATED EVANS AUXILIARIES

The rationale for the choice of Lewis acid and substrates for the Evans aldol reactions has been explained in Sections 4.0 and 4.2. Bu₂BOTf is the Lewis acid that gives the highest stereoselection in Evans aldol reactions. Reactions of **115a-d** with benzaldehyde will generate known structures. Comparison of the spectroscopic, and stereochemical data obtained as a result of our experiments with the relevant data in the literature could help in the elucidation of the stereochemical outcome of the mixture aldol reactions of OEG-EAs.

To test and optimize the Evans aldol reaction **115a** was investigated (Figure 3-6). Once the reaction was optimized for **115a**, the longest OEG chain bearing auxiliary **115d** could be reacted under the same conditions, and thus it would be possible to determine whether the reaction outcome is affected by the presence of longer OEG chains. In initial experiments 1.1 equivalents of Bu₂BOTf were used, because this seems to give satisfactory yields in reactions of this kind. To our surprise under these conditions the reactions proceeded with very low yields (~20%). Trying different batches of 1 M Bu₂BOTf in either CH₂Cl₂, or Et₂O did not change the reaction outcome.

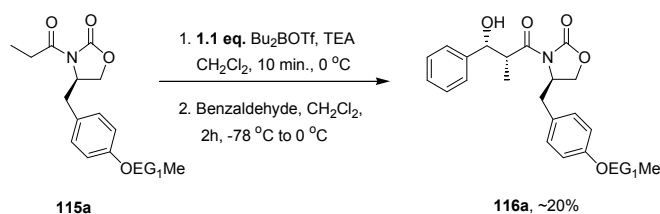


Figure 4-6: Poor yields obtained from the *syn*-aldol reactions of **115a** using 1.1 eq Bu₂BOTf.

The poor yields of the initial aldol reactions could potentially be explained by a number of factors. The concentration of Bu₂OTf could be lower than expected due to decomposition. Residual moisture in **115a**, benzaldehyde, triethylamine, or solvent, could result in the decomposition of Bu₂OTf during the enolization. Bu₂OTf might not be reactive enough to promote the reaction with OEG-EAs or might be interacting with the OEG groups. One other factor might be that simply more equivalents of the Lewis acid were required.

The question of moisture in the reactants can be ruled out. **115a** was dried under vacuum at 60°C for at least 12 hours before the reaction. Triethylamine and CH₂Cl₂ were distilled immediately before the reaction. Benzaldehyde was distilled, and stored over molecular sieves, in a dessicator under nitrogen. The question of the actual concentration of Bu₂BOTf, and its reactivity can be addressed by determination of Bu₂BOTf concentration, and by preparation of Et₂BOTf, and Bu₂BOTf immediately before use.

Determination of Bu₂BOTf concentration could be done using ¹¹B NMR or GC.^{11a-b} Whether Bu₂BOTf would survive during GC analysis is unclear, and as is the reliability of ¹¹B-NMR as a tool for quantitative analysis. While protolysis of B-C bonds and measurement of the amount of alkane generated via use of a gas burette is possible, that method is not applicable to Bu₂BOTf, nor would such an analysis give information about the extent of decomposition of the Lewis acid because B-C bond cleavage is not expected to have occurred as these require

strong acids, and/or elevated temperatures (Figure 4-7).^{11a-b,12a-b} Thus determination of Bu₂BOTf concentration was not attempted.

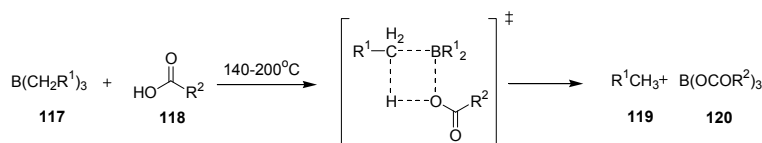


Figure 4-7: Protolysis of the B-C bonds in boranes.

Preparation of fresh Et₂BOTf and Bu₂BOTf was undertaken. Whether or not the use of Et₂BuOTf in aldol reactions has any advantages is unclear, as there are conflicting reports.^{2, 13} These Lewis acids can be prepared by reacting equimolar quantities of the corresponding alkyl borane and trifluoromethanesulfonic acid (Figure 4-8).^{2, 14} During the preparation a procedure found in the literature was followed and the expected gas evolution observed. The only deviation from the procedure was the use of a nitrogen atmosphere instead of an argon atmosphere. It was found that no product was obtained when these “home made” Lewis acids were used in Evans aldol reactions.

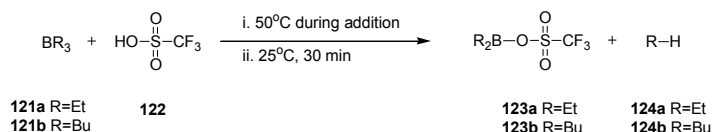


Figure 4-8: Preparation of Et₂BOTf and Bu₂BOTf.

These observations made it necessary to investigate the effect of the equivalents of Lewis acid on the outcome of the aldol reactions. We hesitated to increase the equivalents of Bu₂BOTf since it could potentially change the cyclic transition state to an open one due to the coordination

of excess Lewis acid to the aldehyde and thus result in poor stereoselectivity through generation of the *anti*-aldol product (Figure 4-9).¹⁵ There are reports of such a switch due to the presence of excess Bu₂BOTf. However these reports also suggest that our Bu₂BOTf/NEt₃/CH₂Cl₂ system would not to display such behavior.¹⁵ Switching of transition states occurs when excess Lewis acid is used along with DIPEA (Hünig's base) as the base. Apparently the bulky nature of DIPEA makes its complex with Bu₂BOTf weaker, and thus a small amount of the Lewis acid remains free to catalyze the undesired reaction by coordination to the aldehyde.¹⁵

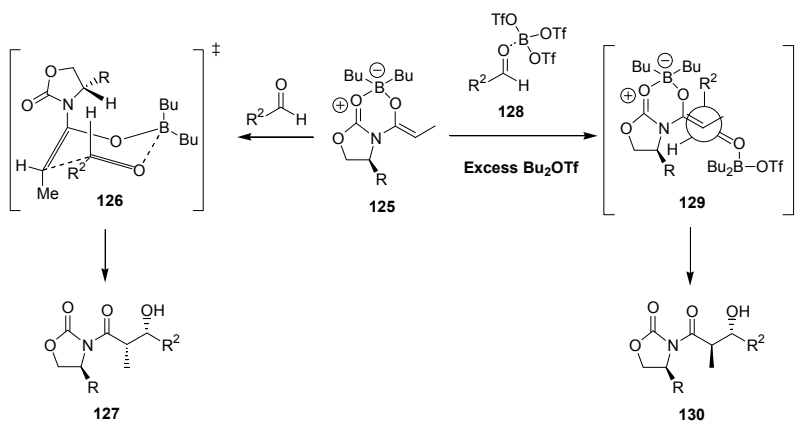


Figure 4-9: Open and closed transition states in Bu₂BOTf promoted aldol reactions.

The extent of conversion of **115a** to **116a** can conveniently be quantified by ¹H-NMR. Comparison of integration values for the benzylic methine proton of the adduct, and one of the equivalent pairs of aromatic protons on the auxiliary portion gives a rough estimate of percent conversion of **115a** (Figure 4-10). As expected, percent conversion increased with increasing amounts of Bu₂BOTf. Evans aldol reactions with **115a**, and **115d** both gave similar yields with the same equivalents of Bu₂BOTf. Thus it was concluded that the reaction was not affected by

the OEG chain length of the OEG-EAs. Based on these experiments it was decided that 1.8 equivalents of Bu₂OTf would give sufficient yields of **116a-b** in mixture aldol reactions.

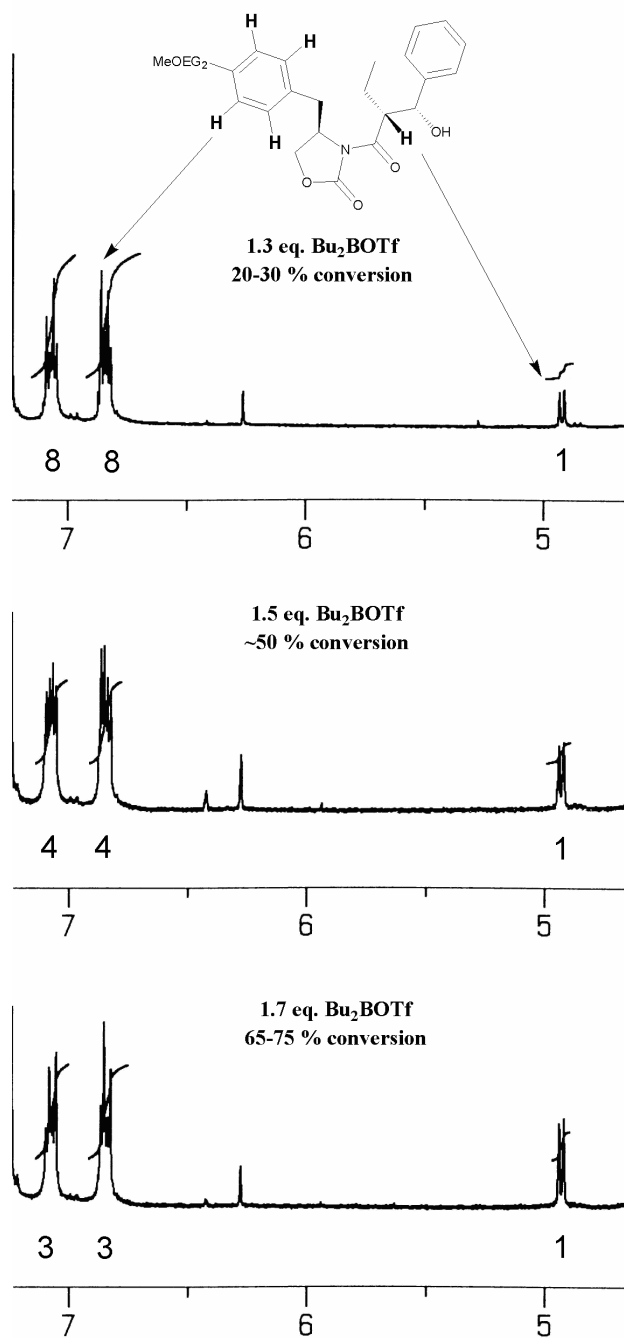


Figure 4-10: Effect of equivalents of Bu₂BOTf on the % conversion of **115a**.

Higher equivalents of Bu₂BOTf were employed. Enolization of a mixture of **115a-d** by use of Bu₂BOTf (1.8 eq.)/NEt₃ (1.9 eq.), and subsequent addition of benzaldehyde afforded the desired aldol adducts **116a-d** in good yield (Figure 4-11). The isolated yields of **116b-d** are lower than that of **116a** since some fractions collected during silica flash columns were rejected due to the observation of co-elution with remaining **115a-d**. This problem can probably be minimized by either higher conversion through employment of more equivalents Bu₂OTf or by purification via preparatory scale HPLC. As a result of the more polar nature of the products, differences in *R_f* values between them were less than the values that have been observed for earlier OEGylated compounds (see Chapter 2). It is interesting to note that despite this, it was possible to separate 9 compounds (products **116a-d**, remaining starting materials **115a-d**, and excess benzaldehyde) at once by employing simple flash column chromatography. The yields of single component aldol reactions were comparable to those of mixture reactions.

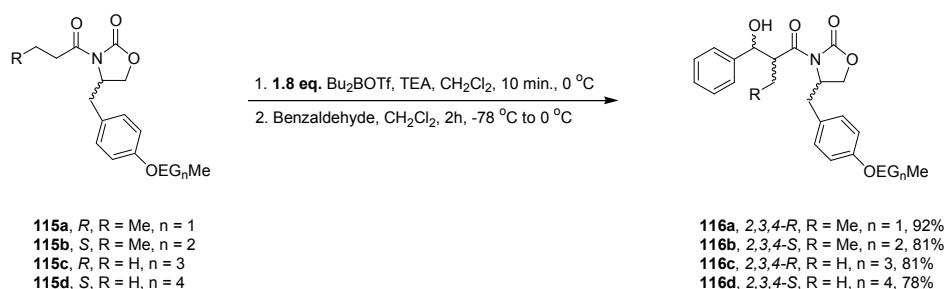


Figure 4-11: Optimized yields for Evans aldol reactions of **115a-d**.

NPLC analysis of **116a-d** was done using the 5 μ , 250 mm x 4.6 mm Supelcosil™ silica column. After some experimentation it was found that a rather steep gradient (1:1 EtOAc:Hexane to EtOAc in 5 min, then EtOAc to 5% IPA in EtOAc in 3 minutes) was required to ensure elution of the peaks in a narrow timeframe (Figure 4-12). The elution order was

directly proportional to the OEG chain length of each compound. Excellent peak separation was observed and relevant chromatographic parameters are given in Table 4-1. The fact that retention time differences between the compounds was large when a less steep gradient was employed seems to suggest that a number of different substrates could be attached to EAs with the same OEG DP and still be purified in preparatory scale HPLC. Thus EST seems possible.

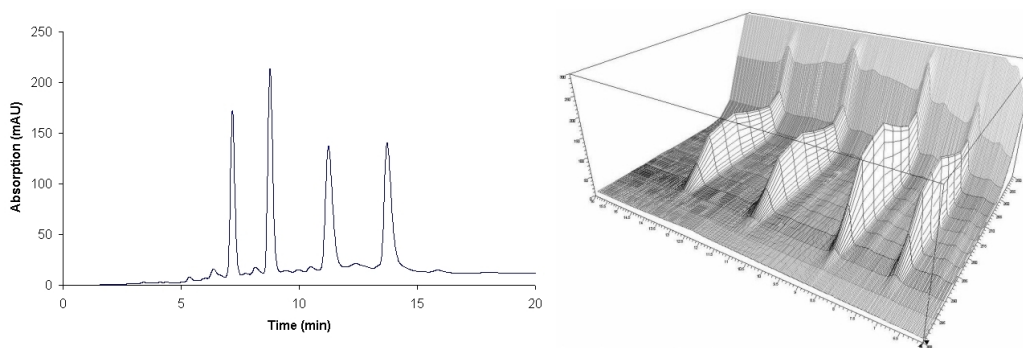


Figure 4-12: Chromatogram and real-time UV-Vis spectrum for a mixture of **116a-d**.

Table 4-1: Chromatographic parameters for the peaks in Figure 4-12.

peak	ID	t_R	k'	N	R_s	Symmetry
1	116a	7.17	2.59	6391	-	0.813
2	116b	8.76	3.38	7862	4.56	0.769
3	116c	11.24	4.62	5606	4.60	0.675
4	116d	13.73	5.86	7728	3.84	0.656

A number of methods can be used for the liberation of aldol products from the OEG-EAs. The Evans laboratory has been quite prolific in this area. Their work has generated methods for removal of aldol adducts through transamination ($\text{Me}_2\text{AlN}(\text{OR})\text{R}$), reduction (LiBH_4), transesterification (LiOBn , $\text{Ti}(\text{OBn})_4$, BrMgOMe), and hydrolysis (LiOH , LiOOH).^{17a-e,6}

Among the hydrolysis reagents, LiOOH is far superior to the rest since it exhibits excellent “exocyclic cleavage regioselectivity”.^{17e}

We were interested in the methyl esters of the aldol adducts, thus transesterification was a natural choice. We decided to use a two step hydrolysis/esterification sequence, since we could purify the hydrolyzed aldol adducts through simple acid/base extraction. The acid then could be easily converted to the methyl ester through a number of methods, Fischer esterification, TMSCHN₂, and CH₂N₂ being some of them.^{18a-b} Hydrolysis of **116a-d** using LiOOH, and purification through acid/base extraction afforded acids **131a-d** in good yield, and purity. Esterification attempts through the use of TMSCHN₂, and employment of Fischer esterification failed to give the desired methyl esters **132a-d** in good yield, and/or purity. On the other hand methyl ester formation through the use of freshly prepared CH₂N₂ was successful, and produced esters **132a-d** in essentially quantitative yield (Figure 4-13).

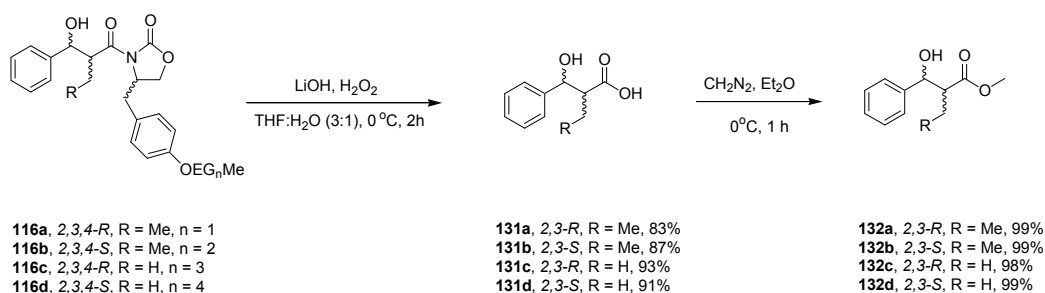


Figure 4-13: Hydrolysis of **116a-d** and preparation of methyl esters from **131a-d**.

4.4 STEREOCHEMICAL ANALYSIS OF ALDOL PRODUCTS

In this study, stereochemical analysis of the aldol products has been done by calculation of α - β hydrogen coupling constants, determination of optical rotation values, and chiral HPLC analysis. Coupling constant calculations aid in the determination of the relative configuration of the chiral carbons, while optical rotation measurements, and chiral HPLC analysis reveal absolute configuration and enantiomeric purity.

In dry, and non-hydrogen bonding solvents it can be assumed that the esters of the aldol products form intramolecular hydrogen bonds. Under those conditions, of the three rotamers of *syn*-aldols two (S_1 and S_2) place the α , and β hydrogens in a gauche position, which reduces their coupling constants ($J_{AB} = 2-6$ Hz). The population of rotamer S_3 can be assumed to be low. For *anti*-aldols however one of the hydrogen bonded rotamers puts the two hydrogens in a gauche position (A_2), while the other puts them in the *anti* position (A_1). The observed coupling constant is the average of those two, and is thus larger than the coupling constant of the *syn*-aldols ($J_{AB} = 7-10$ Hz). This is a simplistic analysis since as the size of R_2 , and R_3 increases the populations of S_3 , and A_2 become larger, and the coupling constant analysis fails. For our substrates this is not a problem (Figure 4-14).¹⁹

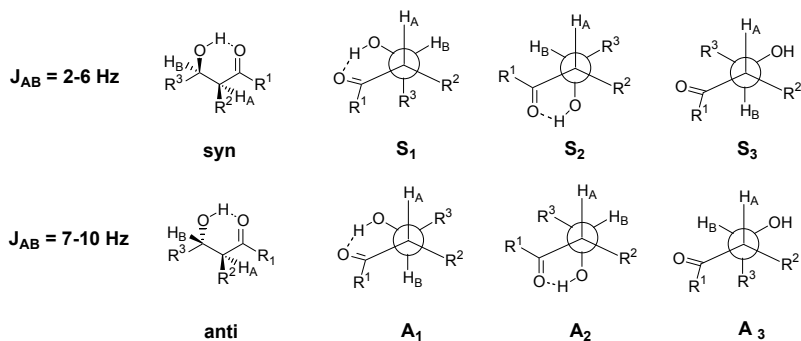
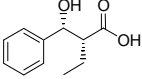
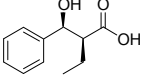
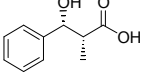
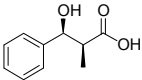
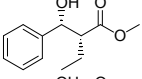
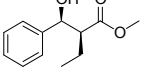
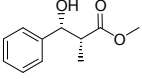
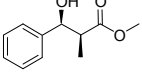


Figure 4-14: Coupling constants for *syn*- and *anti*-aldol products.¹⁹

To determine the relative, and absolute configurations of **131a-d**, and **132a-d** their coupling constants have been calculated, and their optical rotations measured. Comparison with literature values aided in the assignment of absolute configurations. Our findings, and the values in the literature are summarized in Table 4-2.

Table 4-2: Optical Rotation and spin-spin coupling values for **131a-132d**.

Structure	ID	$[\alpha]_D$	$[\alpha]_D$ Lit.	J_{AB} (Hz)	J_{AB} (Hz) Lit.
	131a	+19.68°	-	5.36	-
	131b	-20.0°	-	5.33	-
	131c	+27.5°	+27.5-28.5 ^{o22}	3.97	3.5 ²²
	131d	-29.9°	-24.4 ^{o22} -29.5 ^{o23} -28.7 ^{o24}	4.04	4.0 ²² 3.7 ²³ 3.9 ²⁴
	132a	+13.4°	+12.0 ^{o27} +13.5 ^{o21}	5.33	5.4 ²⁷
	132b	-13.5°	-13.0 ^{o21}	5.33	5.4 ²¹
	132c	+22.6°	+23.5 ^{o21} +23.3 ²²	3.78	3.8 ²²
	132d	-23.3°	-23.5 ^{o25} -22.6 ^{o26}	3.64	4.0 ²⁵

From the coupling constant values listed in Table 4-2 it can be concluded that **132a-d** are *syn*-aldols, since the α - β hydrogen coupling values fall within the expected range, and are also in accord with published values. From the optical rotation values it can be concluded that our samples of **132a-d** are predominantly composed of molecules with the expected absolute configuration.

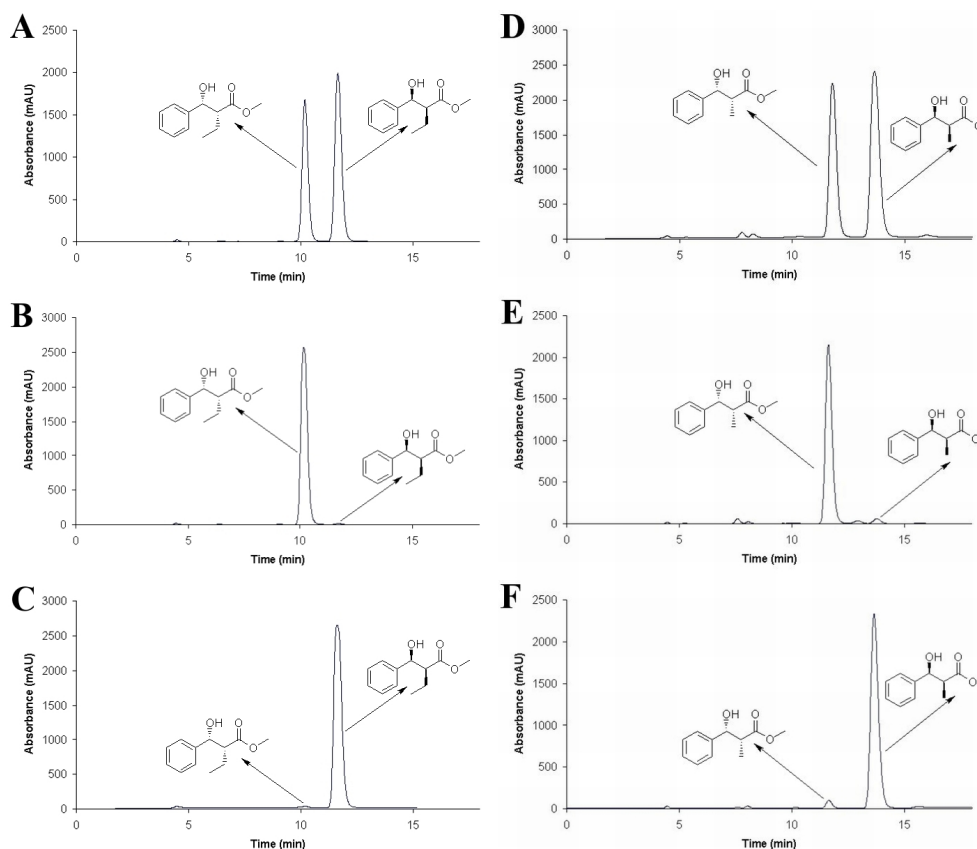


Figure 4-15: Chromatograms for a sample consisting of an equimolar mixture of **132a-b** (A), a sample consisting of **132a** (B), a sample consisting of **132b** (C), a sample consisting of an equimolar mixture of **132c-d** (D), a sample consisting of **132c** (E), and a sample consisting of **132d** (F).

Determination of the enantiomeric purity of aldol addition products can be done with a number of methods, including derivative formation, use of shift reagents, application of chiral GC, and chiral HPLC. As the substrates of interest have relatively strong UV absorption, we chose to use chiral HPLC. Using a Chiralcel OD-H column (5% IPA in Hexanes, 0.75 ml/min.) baseline separation of both enantiomer pairs **132a-b** (t_R for **132a** was 10.2 min., that for **132b** was 11.7 min.), and **132c-d** (t_R for **132c** was 11.7 min., that for **132d** was 13.6 min.) was observed. In both cases the *2R,3R*- isomers eluted first (Figure 4-15). Good baseline separation and peak symmetry was observed for all peaks. Upon integration of the peak areas, it was found that **132a**, and **132** had formed with 99% enantiomeric excess. The enantiomeric excess values

for **132c-d** were found to be 95% each. Relevant chromatographic parameters are given in Table 4-3.

Table 4-3: Relevant chromatographic data for the chromatograms in Figures 4-15.

Peak	ID	t_R	k'	N	R_s	% ee	<i>Symm.</i>
1	23a	10.19	4.10	6900	-	99	0.813
2	23b	11.66	4.83	6700	2.54	99	0.79
1	23c	11.80	4.90	6000	-	95	0.775
2	23d	13.65	5.83	5600	2.58	95	0.692

4.5 CONCLUSION

In this chapter we have demonstrated the preparation of OEGylated Evans auxiliaries based on tyrosine. The use of these OEGylated auxiliaries in parallel aldol addition reactions generated the desired products in good yield and high enantioselectivity. The chemistry used in this chapter furthered the list of reactions compatible with OEG sorting tags. The OEG tags proved to be practically inert under the conditions of the reactions done in this chapter. These OEGylated auxiliaries could potentially be useful in other asymmetric reactions as well.

5.0 CONCLUSION AND FUTURE DIRECTIONS

Chapters 2-4 outline our endeavor towards establishing the utility of OEG based sorting tags as tools for mixture synthesis. We have approached this scientific problem from the perspectives of separation science, and synthetic organic chemistry. Chapters 2, and 3 dealt primarily with the nature, and mechanism of retention of OEGylated compounds on various chromatographic media. Chapter 4 demonstrated an application of OEG-based sorting tags to mixture synthesis.

Sorting tag based solution phase mixture syntheses employing two, or more classes of tags require that each different class of sorting tag be separable under orthogonal conditions with respect to the other. The only preexisting class of sorting tags is based on perfluoroalkanes. We have found that three modes of chromatography in which fluororous sorting tags exhibit little, or no retention can be used to maximize the separation efficiency of OEG-tagged substrates: NPLC (*on silica*), complexation chromatography (*Li-TLC*), and RPLC. Based on these modes of separation under which fluororous tags show little retention, we have suggested that OEG based tags be employed concurrently with fluororous tags to maximize the scope of sorting tag based solution phase mixture synthesis.

NPLC could be regarded as the primary mode of separation for OEGs. OEGs have a natural affinity towards silica due to hydrogen bonding with surface silanols. The nature of the substrates attached to OEGs also plays a role, albeit a lesser one. The retention based on the nature of the parent substrates enables Excess Substrate Tagging (*EST*). *EST* allows for the

tagging of multiple substrates with the same sorting tag. This approach would enable mixture synthesis with a larger number of substrates. We have demonstrated EST through the one-step NPLC separation of 17 (*out of 18*) OEGylated esters with excellent resolution ($R_s \geq 1.5$, *Chapter 2*). We have used the complexation of OEGs to Li^+ to enhance separation. To the best of our knowledge, this is the first example of complexation chromatography applied to OEGs, and related structures. Through the use of Li-TLC (*lithium salt containing TLC*), remarkable enhancement in resolution has been achieved.

In course of the NPLC, and Li-TLC studies we have designed, and synthesized OEGylated benzyl protecting groups based on vanillic acid (**78a-d**, and **79a-d**, *Chapter 2*). **78a-d** have been used along with fluororous sorting tags in the mixture synthesis of 16 stereoisomers of murisinol by the Curran group. These protecting groups are flexible, and could be further elaborated to give two classes of novel sorting tags: Chimeric tags which have both OEG, and perfluoroalkane groups (**80**, *Chapter 2*), and diOEGylated protecting groups (**81**, *Chapter 2*). While neither has been realized as yet, we have made critical progress towards their preparation, and have identified a synthetic strategy that is most likely to afford them. In course of the studies, we have also investigated the possibility of cross-reactions involving substrates tagged with the same series of OEG tags. Our findings based on NPLC, and Li-TLC studies suggest this is indeed possible.

We have studied the retention of OEGylated esters on RPLC in detail (*Chapter 3*). To the best of our knowledge this is the first study of its kind involving OEGs. Through EEC (enthalpy-entropy compensation) analysis we have found that all 20 esters studied have the same retention mechanism. Thus it might be possible to predict the elution order of OEGylated esters

on RPLC. RPLC has some attractive features, such as separation based on molecular size, shape, polarity, charge, and pH-dependent modulation of elution order.

We have prepared a series of OEGylated Evans auxiliaries (OEG-EAs). These were based on tyrosine and could be synthesized on a large scale (≥ 1 g). The OEG-EAs were successfully applied to mixture Evans aldol reactions. These reactions afforded the desired products in good yield and excellent enantioselectivity. The reactions involved in this and earlier syntheses demonstrated the compatibility of OEGs with a number of common reagents such as organolithium reagents and Lewis acids. Furthermore it has been shown that OEGs did not interfere with the $^1\text{H-NMR}$ analysis of aldol products. It would seem that the synthetic route employed in the preparation of OEG-EAs can be exploited to afford fluororous EAs as well and this would be an alternative route to that taken by Ding in the preparation of fluororous EAs.²⁹ The only requirement would be that the necessary etherifications be done using fluoroalkanes having at least a 3 unit methylene spacer.

These findings seem to suggest that sorting tags based on OEGs would have significant utility in solution phase mixture synthesis. The scope of OEGs can certainly be further enhanced. As suggested earlier chimeric and diOEGylated tags are close to being realized. These would enable the tagging of a larger number of substrates and improve their separation using complexation chromatography. With the synthesis and application of OEG-EAs being demonstrated, they could be used for further studies involving aldol and other reactions EAs are known to be useful in.

It would be interesting to study the retention behavior of OEGylated substrates in HILIC (*hydrophilic interaction liquid chromatography*). HILIC involves hydroxyl bearing stationary phases that are employed with mobile phases consisting of water, and organic modifiers.

Stationary phases such as bonded/polymeric diols, silica, and bonded cyclodextrin have been employed in HILIC. HILIC has the advantage of allowing for NPLC-like separation using mobile phases usually associated with RPLC. This allows for adjusting of the pH of the mobile phase such that acidic/basic substrates can be eluted earlier or later. This would enhance the structural diversity of substrates that could be tagged with OEGs and allow for the HPLC of substrates not suitable for NPLC.

6.0 EXPERIMENTAL

6.1 GENERAL

Proton (^1H NMR) and carbon (^{13}C NMR) nuclear resonance spectra were recorded on Bruker Avance 300 spectrometers at 300 MHz and 75 MHz respectively. The chemical shifts are given in parts per million (ppm) on the delta scale (δ). The solvent peak was used as the reference value. For ^1H NMR: $\text{CDCl}_3 = 7.27$ ppm. For ^{13}C NMR: $\text{CDCl}_3 = 77.23$ ppm. For the proton data: s = singlet; d = doublet, t = triplet; q = quartet; dd = doublet of doublets; dq = doublet of quartets; m = multiplet; b = broad; app = apparent.

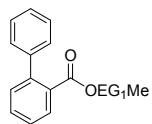
High resolution, and low resolution mass spectra were recorded on a VG 7070 spectrometer. Infrared (IR) spectra were collected on a Nicolet Avatar 360 spectrometer. Samples for IR were prepared as a thin film on a NaCl plate by dissolving the sample in CH_2Cl_2 and then evaporating the CH_2Cl_2 (neat), as a KBr pellet (KBr), or as a suspension in light mineral oil (nujol). Melting points were determined using a Thomas Hoover capillary melting point apparatus and are uncorrected. Analytical TLC was performed on E. Merck pre-coated (25 mm) silica gel 60F-254 plates. Visualization was done under UV (254 nm) or using CAM staining. For HPLC experiments a HP 1090 HPLC system with diode array detection (System 1), or a system consisting of a Waters 616 pump, Waters 600S flow controller and a HP 1050

DAD (System 2) were employed. The following columns were used: 5 μ particle size, 250 x 4.6 mm Supelco Supelcosil silica column; Astec Cyclobond-I column; Alltech/Applied Science 10 μ , 300 x 4.1 mm VersaPak silica column. Separations were attempted at room temperature (22 \pm 5 $^{\circ}$ C), and solvents were purged with helium for 20 minutes before first elution. Flash chromatography was done by using oven-dried E. Merck silica gel 60 (mesh 230-400). Solvents used for chromatography or reactions were dried and purified as follows: Ethyl acetate (EtOAc) was dried over 4 \AA molecular sieves for at least 24 h prior to use. Reagent grade methylene chloride (CH₂Cl₂) was distilled from CaH₂ prior to use. Hexanes (the commercial mixture was used) were stirred over concentrated sulfuric acid for at least 24 h, decanted, stirred over anhydrous sodium carbonate for at least 12 h, decanted, and then distilled. Diethyl ether (Et₂O) and tetrahydrofuran (THF) were distilled from benzophenone ketyl.

6.2 SYNTHETIC PROCEDURES

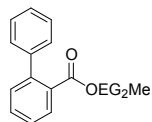
OEG Esters 72b-76e: 2.66 mmol of the respective organic acid, 612 mg (3.20 mmol) EDCI, 391 mg (3.2 mmol) DMAP, 36 mg (0.475 mmol) ethylene glycol monomethyl ether (**86a**), 57 mg (0.475 mmol) diethylene glycol monomethyl ether (**86b**), 78 mg (0.475 mmol) triethylene glycol monomethyl ether (**86c**), 99 mg (0.475 mmol) tetraethylene glycol monomethyl ether (**86d**), and 391 mg (3.2 mmol) DMAP were placed under N₂ atmosphere in an oven-dried vessel, and dissolved in 25 ml freshly distilled CH₂Cl₂. The reaction was stirred under nitrogen atmosphere at room temperature for 24 h. The solvent was evaporated, the residue dissolved in 50 mL EtOAc, and washed with (2x) 50 ml 1.0N HCl, (2x) sat. NaHCO₃, and (1x) saturated NaCl solution. The organic phase was dried with anhydrous MgSO₄. The solvent was removed

in vacuo. The residue was purified by flash column chromatography (SiO_2 , 3:7 *EtOAc:Hexane* to *EtOAc*).



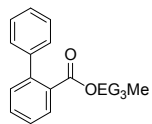
Biphenyl-2-carboxylic acid 2-methoxy-ethyl ester (72b): 111 mg (91% yield)

product was obtained as a colorless oil. R_f : 0.41 (*SiO₂*, 3:7 *EtOAc:Hexane*); IR (*neat*, cm^{-1}): 3057, 1623, 1475, 1444, 1280, 1075, 743, 697; 1H NMR (300 MHz, $CDCl_3$): δ 7.83 (1H, *dd*, $J_1 = 7.54$ Hz, $J_2 = 1.38$ Hz), 7.50 (1H, *dt*, $J_1 = 7.56$ Hz, $J_2 = 1.40$ Hz), 7.36 (7H, *m*), 4.17 (2H, *m*), 3.29 (2H, *m*), 3.22 (3H, *s*); ^{13}C NMR (75 MHz, $CDCl_3$): δ 168.8, 142.7, 141.6, 131.4, 130.9, 130.8, 130.0, 128.5, 128.1, 127.3, 70.1, 64.0, 59.0; MS (*EI+*), m/e calculated for $C_{16}H_{16}O_3$ (M^+) 256.1099, found 256.1111



Biphenyl-2-carboxylic acid 2-(2-methoxy-ethoxy)-ethyl ester (72c): 134 mg

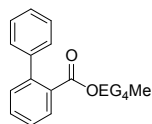
(94% yield) product was obtained as a colorless oil. R_f : 0.24 (*SiO₂*, 3:7 *EtOAc:Hexane*); IR (*neat*, cm^{-1}): 3060, 2874, 2816, 1720, 1590, 1441, 1475, 1231, 1111, 1093, 748, 695; 1H NMR (300 MHz, $CDCl_3$): δ 7.83 (1H, *dd*, $J_1 = 7.54$ Hz, $J_2 = 1.38$ Hz), 7.50 (1H, *dt*, $J_1 = 7.56$ Hz, $J_2 = 1.40$ Hz), 7.36 (7H, *m*), 4.17 (2H, *m*), 3.60 (2H, *m*), 3.46 (2H, *s*), 3.29 (2H, *m*), 3.22 (3H, *s*); ^{13}C NMR (75 MHz, $CDCl_3$): δ 168.7, 142.6, 141.6, 131.4, 131.0, 130.8, 130.0, 128.6, 128.2, 127.3, 71.9, 70.5, 68.8, 64.2, 59.2; MS (*EI+*), m/e calculated for $C_{18}H_{20}O_4$ (M^+) 300.1362, found 300.1374



Biphenyl-2-carboxylic acid 2-[2-(2-methoxy-ethoxy)-ethoxy]-ethyl ester (72d):

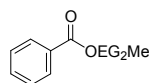
155 mg (95% yield) product was obtained as a colorless oil. R_f : 0.15 (*SiO₂*, 3:7 *EtOAc:Hexane*); IR (*neat*, cm^{-1}) 3057, 1623, 1475, 1444, 1280, 1075, 743, 697; 1H NMR

(300 MHz, $CDCl_3$): δ 7.82 (1H, dd, $J_1 = 7.54$ Hz, $J_2 = 1.38$ Hz), 7.51 (1H, dt, $J_1 = 7.56$ Hz, $J_2 = 1.40$ Hz), 7.37 (7H, m), 4.17 (2H, m), 3.58 (4H, m), 3.49 (4H, m), 3.40 (2H, m), 3.34 (3H, s); ^{13}C NMR (75 MHz, $CDCl_3$): δ 168.7, 142.6, 141.6, 131.4, 131.0, 130.8, 130.0, 128.5, 128.1, 127.3, 72.0, 70.66, 70.63, 70.59, 68.8, 64.2, 59.1; MS (EI+), m/e calculated for $C_{17}H_{18}O_4$ ($M^+ - CH_2CH_2OMe^+$) 286.1205, found 286.1208



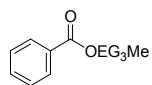
Biphenyl-2-carboxylic acid 2-{2-[2-(2-methoxy-ethoxy)-ethoxy]-ethoxy}-ethyl

ester (72e): 170 mg (92% yield) of the product was obtained as a colorless oil. R_f : 0.37 (SiO_2 , $EtOAc$); IR (neat, cm^{-1}): 3057, 1623, 1475, 1444, 1280, 1075, 743, 697; 1H NMR (300 MHz, $CDCl_3$): δ 7.82 (1H, dd, $J_1 = 7.54$ Hz, $J_2 = 1.38$ Hz), 7.51 (1H, dt, $J_1 = 7.56$ Hz, $J_2 = 1.40$ Hz), 7.37 (7H, m), 4.17 (2H, m), 3.51 (14H, m), 3.35 (3H, s); ^{13}C NMR (75 MHz, $CDCl_3$): δ 168.7, 142.6, 141.6, 131.4, 131.0, 130.8, 130.0, 128.5, 128.1, 127.3, 72.0, 70.70, 70.67, 70.62, 70.57, 68.8, 64.2, 59.1; MS (EI+), m/e calculated for $C_{18}H_{20}O_4$ ($M^+ - CH_2CH_2OMe^+$) 300.1362, found 300.1362

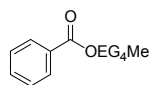


Benzoic Acid 2-(2-Methoxy-Ethoxy)-Ethyl Ester (73c): 100 mg (94% yield) of the product was obtained as a colorless liquid. R_f : 0.30 (SiO_2 , 3:7

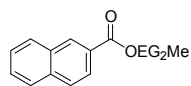
$EtOAc$:Hexane); IR (neat, cm^{-1}): 3058, 2884, 2817, 1716, 1603, 1450, 1281, 1112, 938, 856, 702; 1H -NMR (300 MHz, $CDCl_3$): δ 8.05 (2H, m), 7.54 (1H, m), 7.42 (2H, m), 4.47 (2H, m), 3.83 (2H, m), 3.68 (2H, m), 3.55 (2H, m), 3.37 (3H, s); ^{13}C NMR (75 MHz, $CDCl_3$): δ 166.5, 133.0, 129.9, 129.8, 129.7, 128.4, 71.9, 70.6, 69.3, 64.1, 59.0; MS (EI+), m/e calculated for $C_{12}H_{16}O_4$ (M^+) 224.1049, found 224.1040



Benzoic Acid 2-(2-(2-methoxy-ethoxy)-ethoxy)-Ethyl Ester (73d): 123 mg (96% yield) of the product was obtained as a colorless liquid. R_f : 0.11 (SiO_2 , 3:7 *EtOAc:Hexane*); IR (*neat*, cm^{-1}): 3068, 2873, 1721, 1598, 1445, 1276, 1112, 1325, 948, 851, 717; 1H NMR (300 MHz, $CDCl_3$): δ 8.04 (2H, m), 7.54 (1H, m), 7.42 (2H, m), 4.46 (2H, m), 3.83 (2H, m), 3.67 (6H, m), 3.51 (2H, m), 3.35 (3H, s); ^{13}C NMR (75 MHz, $CDCl_3$): δ 166.7, 133.1, 130.2, 129.8, 128.5, 72.0, 70.8, 70.7, 70.6, 69.3, 64.2, 59.1; MS (*EI+*), m/e calculated for $C_{15}H_{21}O_5$ (M^+) 269.1389, found 269.1382

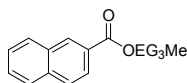


Benzoic acid 2-{2-[2-(2-methoxy-ethoxy)-ethoxy]-ethoxy}-ethyl ester (73e): 136 mg (92% yield) product was obtained as a colorless liquid. R_f : 0.35 (SiO_2 , *EtOAc*); IR (*neat*, cm^{-1}) 3068, 2868, 1711, 1445, 1265, 1107, 938, 840, 712; 1H NMR (300 MHz, $CDCl_3$): δ 8.04 (2H, m), 7.54 (1H, m), 7.42 (2H, m), 4.46 (2H, m), 3.83 (2H, m), 3.67 (10H, m), 3.51 (2H, m), 3.35 (3H, s); ^{13}C NMR (75 MHz, $CDCl_3$): δ 166.5, 133.1, 130.2, 129.8, 128.5, 72.0, 70.8, 70.7, 70.6, 69.3, 64.2, 59.2; MS (*EI+*), m/e calculated for $C_{15}H_{21}O_5$ ($M^+ - CH_3O$) 281.1389, found 281.1384.



Naphthalene-2-carboxylic acid 2-(2-methoxy-ethoxy)-ethyl ester (74c): 128 mg (98% yield) of the desired ester was obtained as a colorless oil. R_f : 0.23 (SiO_2 , 3:7 *EtOAc:Hexane*); IR (*neat*, cm^{-1}): 3053, 2811, 1715, 1468, 1348, 1280, 1184, 1121, 1087, 773, 763; 300; 1H NMR (300 MHz, $CDCl_3$): δ 8.62 (1H, *app. s*), 8.06 (1H, *dd*, $J_1 = 8.66$, $J_2 = 1.67$ Hz), 7.94 (1H, *app. d*, $J = 8.83$ Hz), 7.86 (2H, *app. d*, $J = 8.49$ Hz), 7.56 (2H, m), 4.54 (2H, m), 3.88 (2H, m), 3.72 (2H, m), 3.57 (2H, m), 3.38 (3H, s); ^{13}C NMR (75 MHz, $CDCl_3$) δ 166.8, 135.7, 132.6, 131.3, 129.5, 128.4, 128.2, 127.9, 127.5,

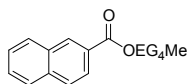
126.7, 125.4, 72.1, 70.7, 69.5, 64.3, 59.2; MS (*EI*+), *m/e* calculated for C₁₆H₁₈O₄ (*M*⁺) 274.1205, found 274.1216.



Naphthalene-2-carboxylic acid 2-[2-(2-methoxy-ethoxy)-ethoxy]-ethyl ester

(74d): 145 mg (96% yield) of the desired ester was obtained as a colorless oil.

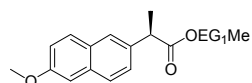
R_f: 0.094 (*SiO*₂, 3:7 *EtOAc*:*Hexane*); IR (*neat*, *cm*⁻¹): 3053, 2879, 2821, 1710, 1618, 1459, 1353, 1280, 1184, 1130, 1087, 773, 754; ¹H NMR (300 MHz, *CDCl*₃): δ 8.61 (1*H*, *app. s*), 8.06 (1*H*, *dd*, *J*₁ = 8.66, *J*₂ = 1.67 Hz), 7.94 (1*H*, *app. d*, *J* = 8.83 Hz), 7.86 (2*H*, *app. d*, *J* = 8.49 Hz), 7.56 (2*H*, *m*), 4.53 (2*H*, *m*), 3.87 (2*H*, *m*), 3.74 (2*H*, *m*), 3.66 (4*H*, *m*), 3.51 (2*H*, *m*), 3.34 (3*H*, *s*); ¹³C NMR (75 MHz, *CDCl*₃): δ 166.8, 135.7, 132.6, 131.3, 129.5, 128.4, 128.2, 127.9, 127.5, 126.7, 125.4, 72.0, 70.85, 70.79, 70.73, 69.4, 64.4, 59.1; MS (*EI*+), *m/e* calculated for C₁₈H₂₂O₅ (*M*⁺) 318.1467, found 318.1464



Naphthalene-2-carboxylic acid 2-{2-[2-(2-methoxy-ethoxy)-ethoxy]-ethoxy}-

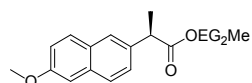
ethyl ester (74e): 160 mg (93% yield) of the desired ester was obtained as a

colorless oil. R_f: 0.38 (*SiO*₂, *EtOAc*); IR (*neat*, *cm*⁻¹): 3053, 2874, 2806, 1720, 1628, 1464, 1357, 1270, 1227, 1193, 1082, 768, 763; ¹H NMR (300 MHz, *CDCl*₃): δ 8.61 (1*H*, *app. s*), 8.06 (1*H*, *dd*, *J*₁ = 8.66 Hz, *J*₂ = 1.67 Hz), 7.94 (1*H*, *app. d*, *J* = 8.83 Hz), 7.87 (2*H*, *app. d*, *J* = 8.49 Hz), 7.54 (2*H*, *m*), 4.53 (2*H*, *m*), 3.87 (2*H*, *m*), 3.65 (10*H*, *m*), 3.50 (2*H*, *m*), 3.34 (3*H*, *s*); ¹³C NMR (75 MHz, *CDCl*₃): δ 166.8, 135.7, 132.6, 131.3, 129.5, 128.4, 128.2, 127.9, 127.5, 126.7, 125.4, 72.0, 70.82, 70.76, 70.72, 70.61, 69.4, 64.4, 59.1; MS (*EI*+), *m/e* calculated for C₂₀H₂₆O₆ (*M*⁺) 362.1729, found 362.1714



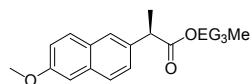
2-(6-Methoxy-naphthalen-2-yl)-propionic acid 2-methoxy-ethyl ester

(75b): 130 mg (95% yield) of the desired ester was obtained as a crystalline white solid. Mp: 94-95°C; R_f: 0.37 (SiO₂, 3:7 EtOAc:Hexane); IR (nujol, cm⁻¹): 3058, 2919, 1716, 1609, 1455, 1312, 1189, 1091, 1030, 861, 820; ¹H NMR (300 MHz, CDCl₃): δ 7.68 (3H, m), 7.39 (1H, dd, J₁ = 8.4 Hz, J₂ = 1.9 Hz), 7.1 (2H, m), 4.21 (2H, m), 3.88 (4H, m), 3.51 (2H, m), 3.28 (3H, s), 1.56 (3H, d, J = 8.36 Hz); ¹³C NMR (75 MHz, CDCl₃): δ 174.8, 157.7, 135.7, 133.8, 129.4, 129.0, 127.2, 126.4, 126.1, 119.1, 105.7, 70.5, 63.9, 59.1, 55.4, 45.4, 18.8; MS (EI+), m/e calculated for C₁₇H₂₀O₄ (M⁺) 288.1362, found 288.1359



2-(6-Methoxy-naphthalen-2-yl)-propionic acid 2-(2-methoxy-ethoxy)-ethyl ester (75c): 152 mg (96% yield) of the desired ester was obtained as

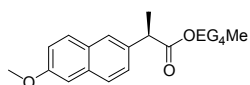
a colorless oil. R_f: 0.20 (SiO₂, 3:7 EtOAc:Hexane); IR (neat, cm⁻¹): 3063, 2930, 1726, 1634, 1593, 1445, 1265, 1173, 1102, 922, 856, 805; ¹H NMR (300 MHz, CDCl₃): δ 7.67 (3H, m), 7.39 (1H, dd, J₁ = 8.4 Hz, J₂ = 1.9 Hz), 7.1 (2H, m), 4.22 (2H, m), 3.86 (4H, m), 3.61 (2H, m), 3.46 (2H, m), 3.38 (2H, m), 3.29 (3H, s), 1.56 (3H, d, J = 7.2 Hz); ¹³C NMR (75 MHz, CDCl₃): δ 174.7, 157.7, 135.7, 133.8, 129.4, 129.0, 127.2, 126.4, 126.1, 119.1, 105.7, 71.9, 70.5, 69.2, 64.1, 59.1, 55.4, 53.5, 45.4, 18.6; MS (EI+), m/e calculated for C₁₉H₂₄O₅ (M⁺) 332.1624, found 332.1640



2-(6-Methoxy-naphthalen-2-yl)-propionic acid 2-[2-(2-methoxy-ethoxy)-ethoxy]-ethyl ester (75d): 173 mg (97% yield) of material was

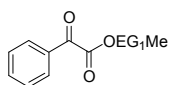
obtained as a colorless oil. R_f: 0.085 (SiO₂, 3:7 EtOAc:Hex); IR (neat, cm⁻¹) 3055, 2916,

2844, 1727, 1626, 1607, 1459, 1253, 1171, 1099, 1022, 922, 850, 802; ^1H NMR (300 MHz, CDCl_3): δ 7.66 (3H, m), 7.39 (1H, dd, $J_1=8.4$ Hz, $J_2=1.9$ Hz), 7.1 (2H, m), 4.21 (2H, m), 3.87 (4H, m), 3.60 (2H, m), 3.50 (8H, m), 3.34 (3H, s), 1.56 (3H, d, $J=7.15$ Hz); ^{13}C NMR (75 MHz, CDCl_3): δ 174.7, 157.7, 135.7, 133.8, 129.4, 129.0, 127.2, 126.4, 126.1, 119.1, 105.7, 72.0, 70.63, 70.60, 69.1, 64.1, 59.1, 55.4, 45.4, 18.6; MS (EI+), m/e calculated for $\text{C}_{21}\text{H}_{28}\text{O}_6$ (M^+) 376.1886, found 376.1903



2-(6-Methoxy-naphthalen-2-yl)-propionic acid 2-{2-[2-(2-methoxyethoxy)-ethoxy]-ethoxy}-ethyl ester (75e): 190 mg (95% yield) of the

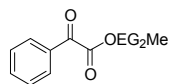
desired ester was obtained as a colorless oil. R_f : 0.029 (SiO_2 , 3:7 EtOAc:Hex); IR (neat, cm^{-1}) 3055, 2873, 1732, 1626, 1487, 1392, 1272, 1176, 1109, 1022, 936, 855, 812; ^1H NMR (300 MHz, CDCl_3): δ 7.67 (3H, m), 7.39 (1H, dd, $J_1 = 8.4$ Hz, $J_2 = 1.9$ Hz), 7.1 (2H, m), 4.21 (2H, m), 3.87 (4H, m), 3.56 (14H, m), 3.35 (3H, s), 1.56 (3H, d, $J = 7.14$ Hz); ^{13}C NMR (75 MHz, CDCl_3): δ 174.7, 157.7, 135.8, 129.4, 129.0, 127.2, 126.4, 126.4, 126.0, 119.1, 105.7, 72.0, 70.63, 69.1, 64.1, 59.1, 55.4, 45.4, 18.6; MS (EI+), m/e calculated for $\text{C}_{23}\text{H}_{32}\text{O}_7$ (M^+) 420.2148, found 420.2155



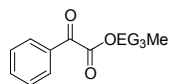
Oxo-phenyl-acetic acid 2-methoxy-ethyl ester (76b): 60 mg (61% yield) of the desired ester was obtained as a pale yellow oil. R_f : 0.32 (SiO_2 , 3:7

EtOAc:Hexane); IR (neat, cm^{-1}): 3057, 2934, 1737, 1684, 1452, 1257, 1200, 1100, 1024, 858; ^1H NMR (300 MHz, CDCl_3): δ 8.01 (2H, m), 7.64 (1H, m), 7.50 (2H, m), 4.54 (2H, m), 3.72 (2H, m), 3.40 (3H, s); ^{13}C NMR (75 MHz, CDCl_3): δ 186.3, 163.9, 135.0, 132.5,

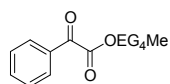
130.2, 129.0, 70.0, 65.0, 59.2; MS (*EI*+), *m/e* calculated for C₁₁H₁₂O₄ (*M*⁺) 208.0736, found 208.0376



Oxo-phenyl-acetic acid 2-(2-methoxy-ethoxy)-ethyl ester (76c): 70 mg (58% yield) of the desired ester was obtained as a pale yellow oil. *R_f*: 0.13 (*SiO*₂, 3:7 *EtOAc:Hexane*); IR (*neat*, *cm*⁻¹) 3066, 2881, 1737, 1684, 1589, 1457, 1247, 1200, 1110, 844, 692; ¹H NMR (300 MHz, *CDCl*₃): δ 8.02 (2*H*, *m*), 7.65 (1*H*, *m*), 7.49 (2*H*, *m*), 4.54 (2*H*, *m*), 3.83 (2*H*, *m*), 3.69 (2*H*, *m*), 3.54 (2*H*, *m*), 3.36 (1*H*, *s*); ¹³C NMR (75 MHz, *CDCl*₃) δ 186.3, 163.9, 135.04, 132.05, 130.3, 129.0, 72.0, 70.7, 68.8, 65.0, 59.2; MS (*EI*+), *m/e* calculated for C₁₂H₁₂O₄ (*M*⁺-*CH*₃*OH*) 220.0736, found 220.0740

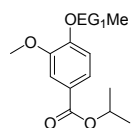


Oxo-phenyl-acetic acid 2-[2-(2-methoxy-ethoxy)-ethoxy]-ethyl ester (76d): 60 mg (43% yield) of product was obtained as a yellow oil. *R_f*: 0.11 (*SiO*₂, 3:7 *EtOAc:Hexane*); IR (*neat*, *cm*⁻¹): 3057, 2877, 1737, 1689, 1447, 1262, 1195, 1100, 849, 701; ¹H NMR (300 MHz, *CDCl*₃): δ 8.01 (2*H*, *m*), 7.64 (1*H*, *m*), 7.50 (2*H*, *m*), 4.53 (2*H*, *m*), 3.64 (6*H*, *m*), 3.51 (2*H*, *m*), 3.34 (1*H*, *s*); ¹³C NMR (75 MHz, *CDCl*₃): δ 186.3, 163.9, 135.0, 132.5, 130.2, 129.0, 72.0, 70.8, 70.7, 70.6, 68.7, 65.1, 59.1; MS (*EI*+), *m/e* calculated for C₁₂H₁₂O₄ (*M*⁺-*OCH*₂*CH*₂*OCH*₃) 220.0736, found 220.0736

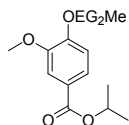


Oxo-phenyl-acetic acid 2-{2-[2-(2-methoxy-ethoxy)-ethoxy]-ethoxy}-ethyl ester (76e): 75 mg (46 % yield) of the desired ester was obtained as a yellow oil.

R_f: 0.28 (*SiO*₂, 8:2 *EtOAc:Hexane*); IR (*neat*, *cm*⁻¹): 3057, 2886, 1737, 1689, 1452, 1262, 1110, 849, 711; ¹H NMR (300 MHz, *CDCl*₃): δ 8.01 (2H, *m*), 7.64 (1H, *m*), 7.50 (2H, *m*), 4.53 (2H, *m*), 3.65 (10H, *m*), 3.52 (2H, *m*), 3.35 (1H, *s*); ¹³C NMR (75 MHz, *CDCl*₃): δ 186.3, 163.9, 135.1, 132.5, 130.2, 129.0, 72.0, 70.76, 70.72, 70.66, 70.56, 70.53, 68.7, 65.1, 59.1; MS (*EI*⁺), *m/e* calculated for C₁₅H₁₉O₆ (*M*⁺ - *CH*₂*OCH*₃) 295.1182, found 295.1184

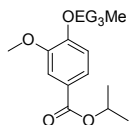


3-Methoxy-4-(2-methoxy-ethoxy)-benzoic acid isopropyl ester (89a): To a mixture of 1.97 g (14.3 mmol) K₂CO₃, 60 mg (0.357 mmol) KI, and 1.5 g (7.13 mmol) isopropyl vanillate was added 25 ml anhydrous DMF. To this mixture was added 1.35 g (1.31 ml, 0.0143 mol) 1-chloro-2-methoxyethane (87a). The reaction was stirred at 60 °C under N₂ atmosphere overnight. The DMF was removed *in vacuo*, and the resulting solid was partitioned between water (50 ml) and EtOAc (50 ml). The aqueous portion was discarded, and the organic phase was washed with 50 ml water, 50 ml 0.1 N HCl, and 50 ml saturated brine. The desired product was obtained via flash column chromatography (*SiO*₂, 3:7 *EtOAc:Hex*) as a pale yellow oil (1.85 g, 97 % yield). R_f: 0.26 (*SiO*₂, 3:7 *EtOAc:Hexane*); IR (*neat*, *cm*⁻¹): 2981, 2935, 2873, 1701, 1598, 1511, 1460, 1419, 1352, 1265, 1219, 1107, 1025, 943, 769; ¹H NMR (*CDCl*₃, 300 MHz): δ 1.34 (6H, *d*, *J* = 6.44 Hz), 3.43 (3H, *s*), 4.20 (2H, *app. t*, *J* = 4.81), 5.20 (1H, *sp.*, *J* = 6.18 Hz), 6.88 (1H, *d*, *J* = 8.53), 7.51 (1H, *d*, *J* = 1.83 Hz), 7.62 (1H, *dd*, *J*₁ = 8.45, *J*₂ = 2.10); ¹³C NMR (*CDCl*₃, 75 MHz): δ 22.05, 56.08, 59.40, 68.24, 70.85, 111.96, 123.31, 123.84, 149.07, 152.22, 166.01; MS (*EI*⁺): *m/e* calculated for C₁₄H₂₀O₅ (*M*⁺) 268.1311, found 268.1315



3-Methoxy-4-[2-(2-methoxy-ethoxy)-ethoxy]-benzoic acid isopropyl ester (89b):

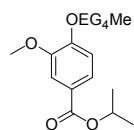
To a mixture of 1.32 g (9.62 mmol) K_2CO_3 , 40 mg (0.238 mmol) KI, and 1.0 g (4.76 mmol) isopropyl vanillate was added 18 ml anhydrous DMF. To this mixture was added 1.31 g (1.31 ml, 9.62 mmol) 1-(2-Chloro-ethoxy)-2-methoxy-ethane (87b). The reaction was stirred at 60°C under a N_2 atmosphere overnight. The DMF was removed *in vacuo*, and the resulting solid was partitioned between water (50 ml), and EtOAc (50 ml). The aqueous portion was discarded, and the organic phase was washed with 50 ml water, 50 ml 0.1 N HCl, and 50 ml saturated brine. The desired product was obtained via flash column chromatography (SiO_2 , 3:7 EtOAc:Hex) as a pale yellow oil (1.43 g, 96 % yield). R_f : 0.11 (SiO_2 , 3:7 EtOAc:Hexane); IR (neat, cm^{-1}): 2981, 2935, 2873, 1701, 1598, 1511, 1460, 1419, 1352, 1265, 1219, 1107, 1025, 943, 769; 1H NMR ($CDCl_3$, 300 MHz): δ 1.37 (6H, d, $J = 6.26$ Hz), 3.40 (3H, s), 3.58 (2H, m), 3.75 (2H, m), 3.92 (5H, m), 4.26 (2H, m), 5.21 (1H, sp., 6.20 H), 6.91 (1H, d, $J = 8.44$ Hz), 7.54 (1H, d, $J = 1.86$ Hz), 7.65 (1H, dd, $J_1 = 8.41$ Hz, $J_2 = 1.87$ Hz); ^{13}C NMR ($CDCl_3$, 75 MHz): δ 22.10, 56.10, 59.18, 68.25, 68.38, 69.53, 70.91, 72.01, 111.94, 112.47, 123.37, 123.80, 149.02, 152.20, 166.02; MS (EI+): m/e calculated for $C_{16}H_{24}O_6$ (M^+) 312.1573, found 312.1559



3-Methoxy-4-{2-[2-(2-methoxy-ethoxy)-ethoxy]-ethoxy}-benzoic acid isopropyl ester (89c):

To a mixture of 1.97 g (0.0143 mol) K_2CO_3 , 60 mg (0.357 mmol) KI, and 1.5 g (7.14 mmol) isopropyl vanillate was added 25 ml anhydrous DMF. To this mixture was added 2.60 g (0.053 mol) 1-[2-(2-Chloro-ethoxy)-ethoxy]-2-methoxy-ethane (87c). The reaction was stirred at 60°C under a N_2 atmosphere overnight. The DMF was removed *in vacuo*, and the resulting solid was partitioned between water (100 ml), and EtOAc (100 ml). The

aqueous portion was discarded, and the organic phase was washed with 100 ml water, 100 ml 0.1 N HCl, 100 ml saturated NaHCO₃, 100 ml saturated brine, and dried with MgSO₄. The solvent was evaporated *in vacuo*, and the yellow liquid subjected to flash column chromatography (SiO₂, gradient: 1:1 EtOAc:Hexane to EtOAc) to give 2.37 g (94% yield) of the desired product as a pale yellow liquid. R_f: 0.31 (SiO₂, EtOAc); IR (*neat*, cm⁻¹): 2986, 2873, 1701, 1593, 1521, 1460, 1409, 1347, 1265, 1219, 1102, 1025, 948, 881, 835, 758; ¹H NMR (CDCl₃, 300 MHz): δ 1.33 (6H, d, J = 6.26 Hz), 3.35 (3H, s), 3.52 (2H, m), 3.64 (4H, m), 3.72 (2H, m), 3.89 (5H, m), 4.21 (2H, *app. t*, J = 5.71 Hz), 5.20 (1H, *sp*, J = 6.26 Hz), 6.89 (1H, d, J = 8.45 Hz), 7.51 (1H, d, J = 1.97 Hz), 7.61 (1H, *dd*, J₁ = 8.44 Hz, J₂ = 1.97 Hz); ¹³C NMR (CDCl₃, 75 MHz): δ 22.12, 56.09, 59.13, 68.23, 68.37, 69.49, 70.60, 70.72, 70.97, 71.97, 112.00, 123.31, 123.79, 148.96, 153.23, 166.00; MS (*EI*⁺): *m/e* calculated for C₁₈H₂₈O₇ (*M*⁺) 356.1835, found 356.1848

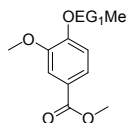


3-Methoxy-4-(2-{2-[2-(2-methoxy-ethoxy)-ethoxy]-ethoxy}-ethoxy)-benzoic acid

isopropyl ester (89d): To a mixture of 0.66 g (4.76 mmol) K₂CO₃, 20 mg (0.119 mmol) KI, and 0.5 g (2.38 mmol) isopropyl vanillate was added 8 ml anhydrous DMF. To this mixture was added 1.08 g (1.08ml, 4.76 mmol) 1-[2-(2-Chloro-ethoxy)-ethoxy]-2-(2-methoxy-ethoxy)-ethane (87d). The reaction was stirred at 60°C under a N₂ atmosphere overnight. The DMF was removed *in vacuo*, and the resulting solid was partitioned between water (100 ml), and EtOAc (100 ml). The aqueous portion was discarded, and the organic phase was washed with 100 ml water, 100 ml 0.1 N HCl, 100 ml saturated NaHCO₃, 100 ml saturated brine, and dried with MgSO₄. The solvent was evaporated *in vacuo*, and the residue purified by flash chromatography (SiO₂, EtOAc) to give 0.86 g (90 % yield) of the desired product as a pale

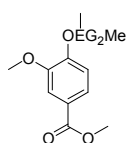
yellow liquid. R_f : 0.23 (SiO_2 , $EtOAc$); IR (*neat*, cm^{-1}): 2976, 2879, 1696, 1603, 1511, 1460, 1419, 1271, 1096, 1035, 943, 881, 830, 758; 1H NMR ($CDCl_3$, 300 MHz): δ 1.33 (6H, *d*, $J = 6.42$ Hz), 3.55 (3H, *s*), 3.51 (2H, *m*), 3.63 (8H, *m*), 3.71 (2H, *m*), 3.89 (5H, *m*), 4.21 (2H, *app. t*, $J = 4.91$ Hz), 5.20 (1H, *sp*, $J = 6.32$ Hz), 6.88 (1H, *d*, $J = 8.56$ Hz), 7.51 (1H, *d*, $J = 1.86$ Hz), 7.62 (1H, *dd*, $J_1 = 8.44$ Hz, $J_2 = 1.85$ Hz); ^{13}C NMR ($CDCl_3$, 75 MHz): δ 22.08, 55.09, 59.12, 68.22, 68.44, 69.52, 70.53, 70.57, 70.94, 72.01, 112.02, 112.51, 123.35, 123.83, 149.02, 152.26, 165.99; MS (*EI+*): m/e calculated for $C_{20}H_{32}O_8$ (M^+) 400.2097, found 400.2097

Mixture Preparation of 89e-g: To a mixture of 3.04 g (22 mmol) K_2CO_3 , 91 mg (0.55 mmol) KI, and 2.0 g (11.0 mmol) methyl vanillate in 25 ml of anhydrous DMF was added 0.24 ml (0.25 g, 3.3 mmol) 1-chloro-2-methoxyethane (**87a**), 0.40 g (0.40 ml, 3.3 mmol) 1-(2-Chloro-ethoxy)-2-methoxy-ethane (**87b**), and 0.52 ml (0.54 g, 3.3 mmol) 1-[2-(2-chloro-ethoxy)-ethoxy]-2-methoxy-ethane (**87c**). The reaction was stirred at 60°C under a N_2 atmosphere overnight. The reaction was diluted with 50 ml CH_2Cl_2 , and washed with (3x) 50 ml of 1M HCl, saturated $NaHCO_3$, and brine. The solvent was removed under reduced pressure, and the residue was subjected to flash column chromatography (SiO_2 , 3:7 $EtOAc:Hex$ to $EtOAc$).



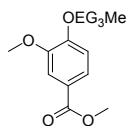
3-Methoxy-4-(2-methoxy-ethoxy)-benzoic acid methyl ester (89e): 0.74 g (93 % yield) of the desired material was obtained as a colorless oil. R_f : 0.63 (SiO_2 , $EtOAc$); IR (*neat*, cm^{-1}): 3082, 2955, 2884, 2841, 1713, 1598, 1511, 1424, 1337, 1270, 1123, 1025, 985, 882, 763; 1H NMR ($CDCl_3$, 300 MHz): δ 3.41 (3H, *s*), 3.79 (2H, *app. t*, $J = 4.98$ Hz), 3.85 (3H, *s*), 3.88 (3H, *s*), 4.20 (2H, *app. t*, $J = 4.71$ Hz), 6.89 (1H, *d*, $J = 8.46$

Hz), 7.52 (1H, d, $J = 1.86$ Hz), 7.62 (1H, dd, $J_1 = 8.45$ Hz, $J_2 = 2.04$ Hz); ^{13}C NMR (CDCl_3 , 75 MHz): δ 51.91, 55.93, 59.18, 68.24, 70.72, 111.93, 112.35, 122.95, 123.35, 149.01, 152.32, 166.79; MS (ES^+): m/e calculated for $\text{C}_{12}\text{H}_{16}\text{O}_5$ (M^+) 240.0998, found 240.0989



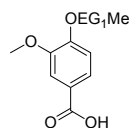
3-Methoxy-4-[2-(2-methoxy-ethoxy)-ethoxy]-benzoic acid methyl ester (89f):

0.85 g (91 % yield) of the desired material was obtained as a colorless oil. R_f : 0.45 (SiO_2 , EtOAc); IR (*neat*, cm^{-1}): 3093, 2946, 2872, 1716, 1601, 1511, 1340, 1270, 1221, 1136, 1099, 1021, 988, 870, 760; ^1H NMR (CDCl_3 , 300 MHz): δ 3.35 (3H, s), 3.54 (2H, m), 3.70 (2H, m), 3.86 (3H, s), 3.87 (3H, s), 3.88 (2H, m), 4.22 (2H, *app. t*, $J = 4.92$ Hz), 6.89 (1H, d, $J = 8.46$ Hz), 7.51 (1H, $J = 1.92$ Hz), 7.61 (1H, dd, $J_1 = 8.37$ Hz, $J_2 = 1.89$ Hz); ^{13}C NMR (CDCl_3 , 75 MHz): δ 51.85, 55.91, 58.93, 68.34, 69.40, 70.49, 70.75, 71.87, 112.01, 112.41, 122.86, 123.36, 148.96, 152.31, 166.71; MS (ES^+): m/e calculated for $\text{C}_{14}\text{H}_{20}\text{O}_6$ (M^+) 284.1260, found 284.1271. **Single Component Preparation:** To a mixture of 1.06 g (7.68 mmol) K_2CO_3 , 33 mg (0.192 mmol) KI, and 0.7 g (3.84 mmol) methyl vanillate in 10 ml of anhydrous DMF was added 1.07 g (1.07 ml, 7.68 mmol) 1-(2-Chloro-ethoxy)-2-methoxyethane. The reaction was stirred under N_2 atmosphere overnight. The reaction was diluted with 50 ml CH_2Cl_2 , and washed with 3x 50 ml of 1M HCl, saturated NaHCO_3 , and brine. The crude product was subjected to flash column chromatography (SiO_2 , 3:7 $\text{EtOAc}:\text{Hex}$). 1.04 mg (95 % yield) of the desired material was obtained as a colorless oil. *Spectral data matched those of the mixture reaction product.*

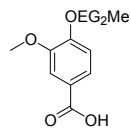


3-Methoxy-4-{2-[2-(2-methoxy-ethoxy)-ethoxy]-ethoxy}-benzoic acid methyl ester (89g): 1.04 g (96 % yield) of the desired material was obtained as a colorless

oil. R_f : 0.33 (SiO_2 , $EtOAc$); IR (*neat*, cm^{-1}): 3093, 2946, 2872, 1720, 15393, 1511, 1430, 1340, 1279, 1111, 1029, 993, 874; 1H NMR ($CDCl_3$, 300 MHz): δ 3.35 (3H, s), 3.52 (2H, m), 3.64 (6H, m), 3.73 (2H, m), 3.86 (3H, s), 3.87 (3H, s), 3.90 (2H, *app. t*, $J = 5.61$ Hz), 4.22 (2H, *app. t*, $J = 4.86$ Hz), 6.90 (1H, d, $J = 8.64$ Hz), 7.51 (1H, d, $J = 1.89$ Hz), 7.62 (1H, dd, $J_1 = 8.46$ Hz, $J_2 = 1.89$ Hz); ^{13}C NMR ($CDCl_3$, 75 MHz): δ 51.75, 55.80, 58.80, 68.29, 69.34, 70.40, 70.51, 70.75, 71.80, 111.96, 112.32, 122.74, 123.27, 148.89, 152.29, 166.55; MS (ES^+): m/e calculated for $C_{16}H_{24}O_7$ (M^+) 328.1522, found (*file is somewhere*)

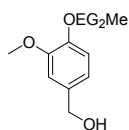


3-Methoxy-4-(2-methoxy-ethoxy)-benzoic acid (79a): To 600 mg (2.34 mmol) 3-Methoxy-4-(2-methoxy-ethoxy)-benzoic acid isopropyl ester (**89a**) in a mixture of 9 ml EtOH, and 4 ml THF was added 7.05 ml 2.6 M aq. KOH. The reaction was refluxed for 9h. The reaction was brought to pH \sim 1 with 1 N HCl, and the carboxylic acid was extracted with 4x20 ml portions of EtOAc. The organic layers were combined, washed with a 30 ml portion of saturated NaCl, and dried with anhydrous $MgSO_4$. The solvent was evaporated *in vacuo*, and 513 mg (97 % yield) product was obtained as a white solid. R_f : 0.36 (SiO_2 , $EtOAc$); 1H NMR ($CDCl_3$, 300 MHz): δ 3.44 (3H, s), 3.84 (2H, m), 3.90 (3H, s), 4.23 (2H, m), 6.92 (2H, d, $J = 8.51$ Hz), 7.56 (1H, d, $J = 1.85$ Hz), 7.71 (2H, $J_1 = 8.45$ Hz, $J_2 = 2.33$ Hz); ^{13}C NMR ($CDCl_3$, 75 MHz): δ 56.09, 59.39, 68.36, 70.80, 111.96, 112.76, 122.10, 124.48, 149.15, 153.17, 171.85; MS (EI^+): m/e calculated for $C_{11}H_{14}O_5$ (M^+) 226.0841, found 226.0846



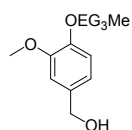
3-Methoxy-4-[2-(2-methoxy-ethoxy)-ethoxy]-benzoic acid (79b): To 600 mg 3-Methoxy-4-[2-(2-methoxy-ethoxy)-ethoxy]-benzoic acid isopropyl ester (**89b**) was added 5.36 ml 2.6 M KOH (*aq.*), 7 ml EtOH, and 3 ml THF. The reaction was refluxed for 9h.

15% NaOH solution (*aq.*). Formation of gray precipitate was observed. The mixture was dried by addition of Na₂SO₄. The mixture was filtered through celite, and the solids were washed with copious amounts of EtOAc. The organic phase was dried with MgSO₄, and the solvent was removed *in vacuo*. 670 mg (94 % yield) of the desired alcohol was obtained as a colorless oil. R_f: 0.40 (*SiO*₂, *EtOAc*); IR (*neat*, *cm*⁻¹): 3401, 2940, 2868, 1588, 1516, 1455, 1409, 1265, 1224, 1132, 1015, 851, 805; ¹H NMR (*CDCl*₃, 300 MHz): δ 3.42 (3H, *s*), 3.76 (2H, *app. t*, *J* = 4.07 Hz), 3.85 (3H, *s*), 4.14 (2H, *app. t*, *J* = 4.67 Hz), 4.60 (2H, *s*), 6.89 (3H, *m*); ¹³C NMR (*CDCl*₃, 75 MHz): δ 55.92, 59.29, 65.25, 68.59, 71.11, 110.92, 113.75, 119.37, 134.46, 147.80, 149.80



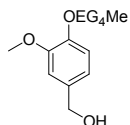
{3-Methoxy-4-[2-(2-methoxy-ethoxy)-ethoxy]-phenyl}-methanol (78b): To a suspension of 97 mg (2.56 mmol) LiAlH₄ in 2 ml freshly distilled THF at 0 °C was added a solution of 200 mg (0.64 mmol) 3-Methoxy-4-[2-(2-methoxy-ethoxy)-ethoxy]-benzoic acid isopropyl ester (**89b**) in 3 ml dry. After completion of addition the reaction was allowed to heat to room temperature, and stirred at room temperature for an additional 40 min. The reaction was again cooled to 0 °C, and quenched by careful drop-wise addition of 0.5 ml water, and 0.5 ml 15% NaOH solution (*aq.*). Formation of gray precipitate was observed. The mixture was dried by addition of Na₂SO₄. The mixture was filtered through Celite, and the solids were washed with copious amounts of EtOAc. The organic phase was dried with MgSO₄, and the solvent was removed *in vacuo*. 151 mg (92% yield) of the desired alcohol was obtained as a colorless oil. R_f: 0.27 (*SiO*₂, *EtOAc*); IR (*neat*, *cm*⁻¹): 3391, 2930, 2879, 1588, 1511, 1455, 1414, 1260, 1132, 1030, 938, 856, 799; ¹H NMR (*CDCl*₃, 300 MHz): δ 3.37 (3H, *s*), 3.57 (2H, *m*), 3.69 (2H, *m*), 3.87 (5H, *m*), 4.18 (2H, *m*), 4.60 (2H, *s*), 6.87 (3H, *m*); ¹³C NMR

($CDCl_3$, 75 MHz): δ 56.00, 59.21, 65.39, 68.68, 69.77, 70.82, 72.06, 110.99, 113.73, 119.64, 134.31, 147.86, 149.75; MS (EI+): m/e calculated for $C_{13}H_{20}O_5$ (M^+) 256.1311, found 256.1308



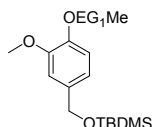
(3-Methoxy-4-{2-[2-(2-methoxy-ethoxy)-ethoxy]-ethoxy}-phenyl)-methanol

(78c): To a suspension of 532 mg (0.0140 mol) $LiAlH_4$ in 10 ml freshly distilled THF was added drop-wise a solution of 1.25 g (3.51 mmol) 3-Methoxy-4-{2-[2-(2-methoxy-ethoxy)-ethoxy]-ethoxy}-benzoic acid isopropyl ester (**89c**) in 15 ml dry THF. After completion of addition the reaction was allowed to heat to room temperature, and stirred at room temperature for an additional 40 min. The reaction was again cooled to $0^\circ C$, and quenched by careful drop-wise addition of 1 ml water, and 1 ml 15% NaOH solution (aq.). Formation of gray precipitate was observed. The mixture was dried by addition of Na_2SO_4 . The mixture was filtered through Celite, and the solids were washed with copious amounts of EtOAc. The organic phase was dried with $MgSO_4$, and the solvent was removed *in vacuo*. 955 mg of the desired alcohol was obtained (91% yield) as a pale yellow oil. R_f : 0.19 (SiO_2 , 3:7 EtOAc:Hexane); IR (neat, cm^{-1}): 3426, 2930, 2868, 1593, 1516, 1455, 1419, 1271, 1230, 1132, 1040, 948, 851, 805; 1H NMR ($CDCl_3$, 300 MHz): δ 3.35 (3H, s), 3.52 (2H, m), 3.60 (4H, m), 3.84 (5H, m), 4.16 (2H, app. t, $J = 4.97$ Hz), 4.60 (2H, s), 6.87 (3H, m); ^{13}C NMR ($CDCl_3$, 75 MHz): δ 55.94, 59.13, 65.23, 68.62, 69.72, 70.60, 70.70, 70.88, 71.99, 110.96, 113.93, 119.41, 134.44, 147.79, 149.71; MS (EI+): m/e calculated for $C_{15}H_{24}O_6$ (M^+) 300.1573, found 300.1564



[3-Methoxy-4-(2-{2-[2-(2-methoxy-ethoxy)-ethoxy]-ethoxy}-ethoxy)-phenyl]-

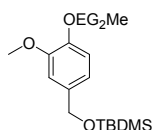
methanol (78d): To a suspension of 380 mg (0.01 mol) LiAlH₄ in 5 ml freshly distilled THF at 0°C was added drop-wise a solution of 1 g (2.5 mmol) 3-Methoxy-4-{2-[2-(2-methoxy-ethoxy)-ethoxy]-ethoxy}-benzoic acid isopropyl ester (**89d**) in 15 ml dry. After completion of addition the reaction was allowed to heat to room temperature, and stirred at room temperature for an additional 40 min. The reaction was again cooled to 0°C, and quenched by careful drop-wise addition of 1 ml water, and 1 ml 15% NaOH solution (aq.). Formation of gray precipitate was observed. The mixture was dried by addition of Na₂SO₄. The mixture was filtered through Celite, and the solids were washed with copious amounts of EtOAc. The organic phase was dried with MgSO₄, and the solvent was removed *in vacuo*. 822 mg (96% yield) of the desired alcohol was obtained as a colorless oil. R_f: 0.14 (SiO₂, EtOAc), IR (neat, cm⁻¹): 3462, 2873, 1588, 1516, 1414, 1347, 1137, 1035, 948, 861, 810; ¹H NMR (CDCl₃, 300 MHz): δ 3.38 (3H, s), 3.54 (2H, m), 3.66 (8H, m), 3.73 (2H, m), 3.89 (5H, m), 4.19 (2H, app. t, J = 5.31 Hz), 4.62 (2H, s), 6.90 (3H, m); ¹³C NMR (CDCl₃, 75 MHz): δ 55.95, 59.13, 65.24, 68.66, 69.77, 70.57, 70.68, 70.93, 72.03, 110.97, 113.73, 119.41, 134.42, 147.81, 149.74; MS (EI+): *m/e* calculated for C₁₇H₂₈O₇ (M⁺) 344.1835, found 344.1835



tert-Butyl-[3-methoxy-4-(2-methoxy-ethoxy)-benzyloxy]-dimethyl-silane (90a):

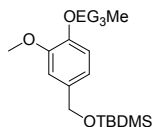
610 mg (2.88 mmol) 4-(2-methoxyethyl)vanillyl alcohol (**78a**), and 240 mg (3.46 mmol) imidazole were dissolved in 25 ml dry CH₂Cl₂ under N₂. The mixture was cooled to 0°C, and a solution of 551 mg (3.46 mmol) TBDMS-Cl in 25 ml dry CH₂Cl₂ was added drop-wise. Formation of a white precipitate was observed. The reaction was stirred under a N₂ atmosphere for an additional 16 hours. The reaction was diluted with 100 ml ether, filtered, washed with 50

ml 1 N HCl, saturated NaHCO₃, and brine. The solution was dried with MgSO₄, and the solvent removed *in vacuo* to give 900 mg (98% yield) of the desired silyl ether as pale yellow liquid. R_f: 0.39 (SiO₂, 3:7 EtOAc:Hexanes); ¹H NMR (CDCl₃, 300 MHz): δ 0.069 (6H, s), 0.92 (9H, s), 3.43 (3H, s), 3.75 (2H, app. t, J = 5.33Hz), 3.83 (3H, s), 4.14 (2H, app. t, J = 4.62 Hz), 4.66 (2H, s), 6.84 (4H, m); ¹³C NMR (CDCl₃, 75 MHz): δ -5.04, 18.56, 25.95, 55.87, 59.28, 64.91, 68.70, 71.14, 110.15, 113.88, 135.00, 147.30, 149.72; MS (EI+): *m/e* calculated for C₁₇H₃₀O₄Si (M⁺) 326.1913, found 326.1915



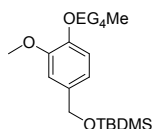
tert-Butyl-{3-methoxy-4-[2-(2-methoxy-ethoxy)-ethoxy]-benzyloxy}-dimethylsilane (90b): To a solution of 890 mg (3.47 mmol) 4-(2-methoxyethyl)vanillyl

alcohol (**78b**), and 283 mg (4.16 mmol) imidazole in 25 ml dry CH₂Cl₂ at 0°C was added dropwise a solution of 628 mg (4.16 mmol) TBDMS-Cl in 25 ml dry CH₂Cl₂. Formation of a white precipitate was observed. The reaction was stirred at room temperature for 16 hours. The reaction was diluted with 100 ml ether, filtered, washed with 50 ml each of 1 N HCl, saturated NaHCO₃, and brine. The solution was dried with MgSO₄, the solvent removed *in vacuo* to give 1.25 g (96% yield) of the title compound as a pale yellow liquid. R_f: 0.56 (SiO₂, EtOAc); IR (neat, cm⁻¹): ***; ¹H NMR (CDCl₃, 300 MHz): δ 0.07 (6H, s), 0.91 (9H, s), 3.37 (3H, s), 3.57 (2H, m), 3.69 (2H, m), 3.86 (3H, s), 3.88 (2H, m), 4.15 (2H, m), 4.65 (2H, s), 6.79 (1H, m), 6.87 (2H, m); ¹³C NMR (CDCl₃, 75 MHz): δ -5.73, 18.53, 26.02, 55.90, 59.18, 64.90, 68.68, 69.78, 70.86, 72.04, 110.15, 113.70, 118.26, 134.87, 147.21, 149.58; MS (EI+): *m/e* calculated for C₁₉H₃₄O₅Si (M⁺) 370.2176, found 370.2169



tert-Butyl-(3-methoxy-4-{2-[2-(2-methoxy-ethoxy)-ethoxy]-ethoxy}-benzyloxy)-dimethyl-silane (90c): 1.456 g (4.85 mmol) (3-Methoxy-4-{2-[2-(2-methoxy-

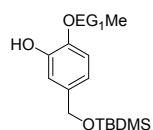
ethoxy)-ethoxy]-ethoxy}-phenyl)-methanol (78c), and 396 mg (5.82 mmol) imidazole were placed in a reaction vessel under N₂ atmosphere, and dissolved in 50 ml dry CH₂Cl₂. The mixture was cooled to 0°C, and a solution of 877 mg (5.82 mmol) TBDMS-Cl in 25 ml dry CH₂Cl₂ was added drop-wise. Formation of a white precipitate was observed. The reaction was stirred under N₂ atmosphere for an additional 16 hours. The reaction was diluted with 100 ml ether, filtered, washed with 50 ml 1 N HCl, saturated NaHCO₃, and brine. The solution was dried with MgSO₄, the solvent removed *in vacuo*, to give 2.0 g (99% yield) of the desired silyl ether as pale yellow liquid. R_f: 0.46 (SiO₂, EtOAc); IR (*neat*, cm⁻¹): 2925, 2853, 1593, 1516, 1460, 1250, 1143, 943, 840, 769; ¹H NMR (CDCl₃, 300 MHz): δ 0.07 (6H, s), 0.91 (9H, s), 3.36 (3H, s), 3.52 (2H, m), 3.65 (4H, m), 3.72 (2H, s), 3.84 (5H, m), 4.15 (2H, *app. t*, J = 5.00 Hz), 4.65 (2H, s), 6.83 (3H, m); ¹³C NMR (CDCl₃, 75 MHz): δ -5.70, 25.75, 55.88, 59.16, 64.90, 68.69, 69.76, 70.65, 70.74, 70.90, 72.03, 110.14, 113.72, 118.24, 134.86, 147.22, 149.58; MS (EI⁺): *m/e* calculated for C₂₁H₃₈O₆Si (M⁺) 414.2438, found 414.2422



tert-Butyl-[3-methoxy-4-(2-{2-[2-(2-methoxy-ethoxy)-ethoxy]-ethoxy}-ethoxy)-benzyloxy]-dimethyl-silane (90d): To a solution of 1.2 g (3.48 mmol) [3-

Methoxy-4-(2-{2-[2-(2-methoxy-ethoxy)-ethoxy]-ethoxy}-ethoxy)-phenyl]-methanol (78d), and 248 mg (4.18 mmol) imidazole in 50 ml dry CH₂Cl₂ at 0 °C, was added drop-wise a solution of 630 mg (4.18 mmol) TBDMS-Cl in 25 ml dry CH₂Cl₂. Formation of a white precipitate was observed. The reaction was stirred at room temperature 16 hours. The reaction was diluted with

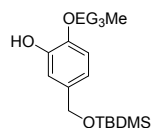
100 ml ether, filtered, washed with 50 ml each of 1 N HCl, saturated NaHCO₃, and brine. The solution was dried with MgSO₄, and the solvent removed *in vacuo* to give 1.52 g (95% yield) of the title compound as a colorless liquid. R_f: 0.36 (SiO₂, EtOAc); IR (*neat*, cm⁻¹): 2940, 2853, 1588, 1516, 1460, 1424, 1250, 1127, 938, 835, 774, 733, 671; ¹H NMR (CDCl₃, 300 MHz): δ 0.07 (6H, s), 0.92 (9H, s), 3.35 (3H, s), 3.53 (2H, m), 3.65 (10H, m), 3.70 (2H, m), 3.84 (5H, m), 4.15 (2H, *app. t*, J = 4.97 Hz), 4.65 (2H, s), 6.83 (3H, m); ¹³C NMR (CDCl₃, 75 MHz): δ -5.08, 18.52, 26.06, 55.89, 59.14, 64.90, 68.74, 69.76, 70.61, 70.71, 70.90, 72.03, 110.19, 113.78, 118.26, 134.88, 147.25, 149.62; MS (EI⁺): *m/e* calculated for C₂₃H₄₂O₇Si (M⁺) 458.2670, found 458.2586



5-(*tert*-Butyl-dimethyl-silyloxymethyl)-2-(2-methoxy-ethoxy)-phenol (91a):

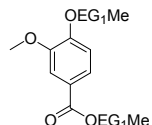
To 672 mg (0.628 ml, 3.61 × 10⁻³ mol) diphenylphosphine dissolved in 3 ml dry THF at 0°C was added drop-wise 2.57 ml (3.91 mol, 1.3 M in hexanes) *n*-BuLi (1.3 M in hexanes). Formation of an orange-red color was observed. The reaction was allowed to heat to room temperature, and was stirred for an additional half hour. 980 mg (3.01 mmol) of the TBS ether (90a) dissolved in 12 ml dry THF was added to this solution, and the reaction was stirred for 3 h at room temperature. The reaction was quenched with 5 ml 0.1 N HCl. The reaction was partitioned between 30 ml 0.1 N HCl, and 50 ml EtOAc, the organic phase washed with 30 ml saturated NaCl solution, and dried with MgSO₄. The solvent was removed under reduced pressure, and the residue subjected to flash column chromatography (SiO₂, 3:7 EtOAc:Hex) to give 592 mg (63% yield) of the title compound as a colorless oil. R_f: 0.30 (SiO₂, 3:7 EtOAc:Hexane); ¹H NMR (CDCl₃, 300 MHz): δ 0.05 (6H, s), 0.91 (9H, s), 3.44 (3H, s), 3.67 (2H, m), 4.13 (2H, m), 4.62 (2H, s), 6.76 (1H, m), 6.88 (2H, m); ¹³C NMR (CDCl₃,

75 MHz): δ -5.70, 18.58, 26.16, 59.12, 64.75, 70.42, 71.02, 113.70, 115.65, 117.58, 136.77, 144.88, 147.46; MS (EI+): m/e calculated for C₁₆H₂₈O₄Si (M^+) 312.1769, found 312.1760



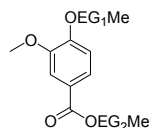
5-(tert-Butyl-dimethyl-silyloxyethyl)-2-{2-[2-(2-methoxy-ethoxy)-ethoxy]-ethoxy}-phenol (91c): To 1.06 g (0.990 ml, 5.68 mmol) diphenylphosphine in 5 ml dry THF at 0°C under N₂, was added drop-wise 4.05 ml (6.15 mmol) *n*-BuLi (1.52 M in *hexanes*). Formation of an orange-red color was observed. The reaction was allowed to heat to room temperature, and was stirred for an additional half hour. 1.96 g (4.73 mmol) of the *tert*-butyl-(3-methoxy-4-{2-[2-(2-methoxy-ethoxy)-ethoxy]-ethoxy}-benzyloxy)-dimethyl-silane (90c) dissolved in 20 ml dry THF was added to this solution, and the reaction was stirred for 3 h at room temperature. Fading of the color to give a clear colorless solution was observed. The reaction was quenched with 5 ml 0.1 N HCl. The reaction was partitioned between 30 ml 0.1 N HCl, and 50 ml EtOAc. The organic phase was washed with 30 ml saturated NaCl solution, and dried with MgSO₄. The solvent removed under reduced pressure, and the residue subjected to flash column chromatography (*SiO*₂, 1:1 EtOAc:Hex) to give 1.58 g (84% yield) of the title compound as a pale yellow liquid. R_f : 0.16 (*SiO*₂, 1:1 EtOAc:Hexane); ¹H NMR (CDCl₃, 300 MHz): δ 0.06 (6H, *m*), 0.91 (9H, *m*), 3.36 (3H, *m*), 3.54 (2H, *m*), 3.68 (6H, *m*), 3.79 (2H, *m*), 4.13 (2H, *m*), 4.61 (2H, *m*), 6.82 (3H, *m*); ¹³C NMR (CDCl₃, 75 MHz): δ -5.76, 18.54, 26.13, 59.13, 64.78, 69.65, 70.40, 70.56, 70.59, 70.69, 72.01, 113.73, 115.45, 117.52, 136.58, 144.96, 147.53

Preparation of DiOEGylated Esters 93a-93c: To a solution of 450 mg (2.0 mmol) 3-Methoxy-4-(2-methoxy-ethoxy)-benzoic acid (**79a**), 507 mg (2.64 mmol) EDC, and 323 mg (2.64 mmol) DMAP in 15 ml CH₂Cl₂ was added a solution of 45 mg (0.597 mmol) 2-methoxy-ethanol (**86a**), 72 mg (0.597 mmol) 2-(2-methoxy-ethoxy)-ethanol (**86b**), and 98 mg (0.597 mmol) 2-[2-(2-Methoxy-ethoxy)-ethoxy]-ethanol (**86c**) in 5 ml CH₂Cl₂. The reaction was stirred at rt for 24 h, after which it was diluted with 30 ml CH₂Cl₂, washed with (2x) 20 ml each of 0.1 M HCl, saturated NaHCO₃, and brine. Drying with MgSO₄, and *in vacuo* removal of the solvent afforded a yellow liquid which was subjected to flash column chromatography (SiO₂, 1:1 EtOAc:Hexane to EtOAc).



3-Methoxy-4-(2-methoxy-ethoxy)-benzoic acid 2-methoxy-ethyl ester (93a):

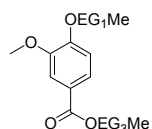
156 mg (92% yield) of the desired material was obtained as a white oil. R_f: 0.54 (SiO₂, EtOAc); IR (neat, cm⁻¹): 3085, 2938, 2815, 1704, 1601, 1511, 1454, 1413, 1262, 1123, 1025, 744, 714; ¹H NMR (CDCl₃, 300 MHz): δ 3.41 (3H, s), 3.43 (3H, s), 3.70 (2H, m), 3.79 (2H, m), 3.88 (3H, s), 4.20 (2H, m), 4.43 (2H, m), 6.89 (1H, d, J = 8.46 Hz), 7.53 (1H, d, J = 1.95 Hz), 7.66 (1H, dd, J₁ = 8.42 Hz, J₂ = 2.02 Hz); ¹³C NMR (CDCl₃, 75 MHz): 55.88, 58.90, 59.10, 63.80, 68.16, 70.55, 70.65, 111.82, 112.39, 122.78, 123.49, 148.93, 152.36, 166.23; MS (ES⁺): *m/e* calculated for C₁₄H₂₀O₆ (M⁺) 284.1260, found 284.1267



3-Methoxy-4-(2-methoxy-ethoxy)-benzoic acid 2-(2-methoxy-ethoxy)-ethyl ester (93b): 176 mg (90% yield) of the desired ester was obtained as a white oil.

R_f: 0.41 (SiO₂, EtOAc); IR (neat, cm⁻¹): 2970, 2884, 1699, 1593, 1516, 1450, 1270, 1209,

1095, 1017, 751; $^1\text{H NMR}$ (CDCl_3 , 300 MHz): δ 3.36 (3H, s), 3.43 (3H, s), 3.54 (2H, m), 3.66 (2H, m), 3.79 (4H, m), 3.88 (3H, s), 4.21 (2H, m), 4.44 (2H, m), 6.89 (1H, d, $J = 8.46$ Hz), 7.54 (1H, d, $J = 1.96$ Hz), 7.65 (1H, dd, $J_1 = 8.41$ Hz, $J_2 = 2.00$ Hz); $^{13}\text{C NMR}$ (CDCl_3 , 75 MHz): δ 55.90, 58.95, 59.12, 63.88, 68.19, 69.26, 70.49, 70.66, 71.85, 111.88, 112.45, 122.86, 123.49, 148.95, 152.35, 166.20; MS (ES^+): m/e calculated for $\text{C}_{16}\text{H}_{24}\text{O}_7$ (M^+) 328.1522, found 328.1514

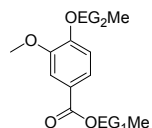


3-Methoxy-4-(2-methoxy-ethoxy)-benzoic acid 2-[2-(2-methoxy-ethoxy)-ethoxy]-ethyl ester (93c): 196 mg (88% yield) of the desired ester was obtained as

a white oil. R_f : 0.28 (SiO_2 , EtOAc); IR (*neat*, cm^{-1}): 3076, 2925, 2876, 1704, 1605, 1507, 1454, 1405, 1270, 1115, 1049, 764, 723; $^1\text{H NMR}$ (CDCl_3 , 300 MHz): δ 3.35 (3H, s), 3.43 (3H, s), 3.51 (2H, m), 3.65 (6H, m), 3.81 (4H, m), 3.88 (3H, s), 4.20 (2H, m), 4.43 (2H, m), 6.89 (1H, d, $J = 8.49$ Hz), 7.53 (1H, d, $J = 1.88$ Hz), 7.65 (1H, dd, $J_1 = 8.44$ Hz, $J_2 = 1.97$ Hz); $^{13}\text{C NMR}$ (CDCl_3 , 75 MHz): δ 55.93, 58.89, 59.12, 63.89, 68.20, 69.21, 70.48, 70.55, 70.61, 70.66, 71.84, 111.92, 112.46, 122.88, 123.47, 148.97, 152.35, 166.18; MS (TOF-MS ES^+): m/e calculated for $\text{C}_{18}\text{H}_{28}\text{O}_8\text{Na}$ (MNa^+) 395.1682, found 395.1652

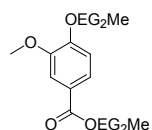
Mixture Preparation of esters 94a-94c: To a solution of 180 mg (0.666 mmol) 3-methoxy-4-[2-(2-methoxy-ethoxy)-ethoxy]-benzoic acid (**79b**), 169 mg (0.879 mmol) EDC, and 107 mg (0.879 mmol) DMAP in 5 ml CH_2Cl_2 was added a solution of 15 mg (0.202 mmol) 2-methoxy-ethanol (**86a**), 24 mg (0.202 mmol) 2-(2-methoxy-ethoxy)-ethanol (**86b**), and 33 mg (0.202 mmol) 2-[2-(2-Methoxy-ethoxy)-ethoxy]-ethanol (**86c**) in 5 ml CH_2Cl_2 . The reaction was stirred at rt for 24 h, after which it was diluted with 10 ml CH_2Cl_2 , washed with 2x10 ml each of 0.1 M

HCl, saturated NaHCO₃, and brine. Drying with MgSO₄, and *in vacuo* removal of the solvent afforded a yellow liquid which was subjected to flash column chromatography (*SiO*₂, 1:1 *EtOAc:Hexane* to 5:95 *MeOH:EtOAc*).



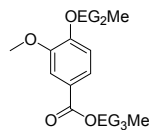
3-Methoxy-4-[2-(2-methoxy-ethoxy)-ethoxy]-benzoic acid 2-methoxy-ethyl ester (94a): 65 mg (98% yield) of the desired material was obtained as a white oil.

R_f: 0.39 (*SiO*₂, *EtOAc*); IR (*neat*, cm⁻¹): 2983, 2937, 2876, 1708, 1601, 1507, 1454, 1409, 1262, 1225, 1103, 1025, 764; ¹H NMR (*CDCl*₃, 300 MHz): δ 3.37 (3H, s), 3.41 (3H, s), 3.55 (2H, m), 3.70 (4H, m), 3.88 (3H, s), 3.91 (2H, m), 4.23 (2H, m), 4.43 (2H, m), 6.89 (1H, d, *J* = 8.48 Hz), 7.53 (1H, d, *J* = 198 Hz), 7.66 (1H, dd, *J*₁ = 8.38 Hz, *J*₂ = 2.04); ¹³C NMR (*CDCl*₃, 75 MHz): 56.00, 59.01, 63.86, 68.32, 69.41, 70.62, 70.78, 71.90, 111.95, 112.58, 122.63, 123.61, 148.96, 152.41, 166.33; MS (*ES*⁺): *m/e* calculated for C₁₆H₂₄O₇ (*M*⁺) 328.1522, found 328.1535



3-Methoxy-4-[2-(2-methoxy-ethoxy)-ethoxy]-benzoic acid 2-(2-methoxy-ethoxy)-ethyl ester (94b): 70 mg (93% yield) of the desired ester was obtained as a white oil.

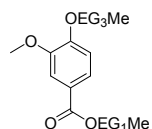
R_f: 0.27 (*SiO*₂, *EtOAc*); IR (*neat*, cm⁻¹): 3082, 2927, 2878, 1711, 1597, 1507, 1459, 1266, 1214, 1103, 1031, 751; ¹H NMR (*CDCl*₃, 300 MHz): δ 3.37 (6H, s), 3.55 (4H, m), 3.70 (4H, m), 3.82 (2H, m), 3.89 (3H, s), 3.92 (2H, m), 4.24 (2H, *app. t*, *J* = 4.94 Hz), 4.41 (2H, m), 6.90 (1H, d, *J* = 8.47 Hz), 7.54 (1H, d, *J* = 1.95 Hz), 7.66 (1H, dd, *J*₁ = 8.42 Hz, *J*₂ = 2.01 Hz); ¹³C NMR (*CDCl*₃, 75 MHz): δ 56.98, 59.02, 63.92, 68.33, 69.31, 69.41, 70.54, 70.77, 71.89, 111.97, 112.58, 122.87, 123.58, 148.95, 152.38, 166.28; MS (*TOF-MS ES*⁺): *m/e* calculated for C₁₈H₂₈O₈Na (*MNa*⁺) 395.1682, found 395.1660



3-Methoxy-4-[2-(2-methoxy-ethoxy)-ethoxy]-benzoic acid 2-[2-(2-methoxy-ethoxy)-ethoxy]-ethyl ester (94c): 65 mg (77% yield) of the desired ester was

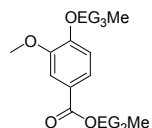
obtained as a white oil. R_f : 0.17 (SiO_2 , $EtOAc$); IR (*neat*, cm^{-1}): 3076, 2926, 2870, 1714, 1598, 1511, 1447, 1417, 1267, 1218, 1132, 1102, 1035, 772; 1H NMR ($CDCl_3$, 300 MHz): δ 3.35 (3H, s), 3.37 (3H, s), 3.51 (4H, m), 3.63 (4H, m), 3.70 (4H, m), 3.81 (2H, *app. t*, $J = 4.92$ Hz), 3.88 (3H, s), 3.90 (2H, *app. t*, $J = 5.40$ Hz), 4.23 (2H, *app. t*, 4.88 H), 4.43 (2H, *app. t*, $J = 4.72$ Hz), 6.89 (1H, *d*, $J = 8.48$), 7.53 (1H, *d*, $J = 1.88$ Hz), 7.65 (1H, *dd*, $J_1 = 8.42$ Hz, $J_2 = 1.97$ Hz); ^{13}C NMR ($CDCl_3$, 75 MHz): δ 56.10, 59.11, 64.05, 68.41, 69.38, 69.50, 70.64, 70.70, 70.75, 70.87, 71.99, 112.02, 112.64, 122.95, 123.67, 149.03, 152.47, 166.38; MS (ES^+): m/e calculated for $C_{20}H_{32}O_9Na^+$ (MNa^+) 439.1944, found 439.1901

Mixture Preparation of esters 95a-95c: To a solution of 235 mg (0.75 mmol) 3-methoxy-4-{2-[2-(2-methoxy-ethoxy)-ethoxy]-ethoxy}-benzoic acid (79c), 171 mg (0.224 mmol) EDC, and 109 mg (0.89 mmol) DMAP in 5 ml CH_2Cl_2 was added a solution of 17 mg (0.224 mmol) 2-methoxy-ethanol (86a), 27 mg (0.224 mmol) 2-(2-methoxy-ethoxy)-ethanol (86b), and 37 mg (0.224 mmol) 2-[2-(2-methoxy-ethoxy)-ethoxy]-ethanol (86c) in 5 ml CH_2Cl_2 . The reaction was stirred at rt for 24 h, after which it was diluted with 30 ml CH_2Cl_2 , washed with 2x20 ml each of 0.1 M HCl, saturated $NaHCO_3$, and brine. Drying with $MgSO_4$, and *in vacuo* removal of the solvent afforded a yellow liquid which was subjected to flash column chromatography (SiO_2 , 7:3 $EtOAc$:Hexane to 95:5 $EtOAc$: MeOH).



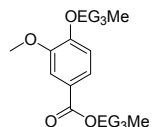
3-Methoxy-4-{2-[2-(2-methoxy-ethoxy)-ethoxy]-ethoxy}-benzoic acid 2-methoxy-ethyl ester (95a): 78 mg (94% yield) of the desired material was

obtained as a colorless oil. R_f : 0.30 (SiO_2 , $EtOAc$); IR (*neat*, cm^{-1}): 3080, 2926, 2878, 2821, 1706, 1594, 1504, 1462, 1410, 1267, 1215, 1102, 1027, 761, 727; 1H NMR ($CDCl_3$, 300 MHz): δ 3.36 (3H, s), 3.41 (3H, s), 3.52 (2H, m), 3.64 (4H, m), 3.71 (4H, m), 3.88 (3H, s), 3.89 (2H, m), 4.22 (2H, *app. t*, $J = 4.87$ Hz), 4.43 (2H, *app. t*, 4.74 Hz), 6.89 (1H, $J = 8.50$ Hz), 7.53 (1H, *d*, 1.83 Hz), 7.66 (1H, *dd*, $J_1 = 8.42$ Hz, $J_2 = 2.0$ Hz); ^{13}C NMR ($CDCl_3$, 75 MHz): 55.98, 58.98, 63.84, 68.34, 69.40, 70.56, 70.60, 70.86, 71.89, 111.99, 112.59, 122.80, 123.60, 148.96, 152.43, 166.30; MS (ES^+): m/e calculated for $C_{18}H_{28}O_8$ (M^+) 372.1784, found 372.1777



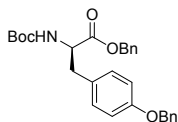
3-Methoxy-4-{2-[2-(2-methoxy-ethoxy)-ethoxy]-ethoxy}-benzoic acid 2-(2-methoxy-ethoxy)-ethyl ester (95b): 84 mg (90% yield) of the desired material was

obtained as a colorless oil. R_f : 0.22 (SiO_2 , $EtOAc$); IR (*neat*, cm^{-1}): 3086, 2942, 2880, 1716, 1597, 1524, 1430, 1332, 1274, 1103, 1033, 968, 874, 751; 1H NMR ($CDCl_3$, 300 MHz): δ 3.35 (3H, s), 3.36 (3H, s), 3.55 (4H, m), 3.66 (8H, m), 3.72 (2H, *app. t*, $J = 4.82$ Hz), 3.79 (3H, s), 3.89 (2H, *app. t*, $J = 4.90$ Hz), 4.22 (2H, *app. t*, $J = 5.07$ Hz), 4.44 (2H, *app. t*, $J = 5.07$ Hz), 6.89 (1H, *d*, $J = 8.43$ Hz), 7.53 (1H, *d*, $J = 1.86$ Hz), 7.64 (1H, *dd*, $J_1 = 8.37$ Hz, $J_2 = 1.86$ Hz); ^{13}C NMR ($CDCl_3$, 75 MHz): δ 56.05, 59.06, 59.10, 63.98, 68.38, 69.37, 69.46, 70.59, 70.66, 70.92, 71.94, 111.98, 112.57, 122.88, 123.61, 148.96, 152.43, 166.33; MS (ES^+): m/e calculated for $C_{20}H_{32}O_9$ (M^+) 416.2046, found 416.2047



3-Methoxy-4-{2-[2-(2-methoxy-ethoxy)-ethoxy]-ethoxy}-benzoic acid 2-[2-(2-methoxy-ethoxy)-ethoxy]-ethyl ester (95c): 95 mg (92% yield) of the desired

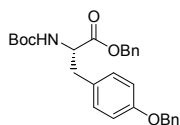
material was obtained as a colorless oil. R_f : 0.20 (SiO_2 , $EtOAc$); IR (*neat*, cm^{-1}): 2915, 2885, 1714, 1590, 1500, 1455, 1417, 1271, 1215, 1113, 1016, 768, 730; 1H NMR ($CDCl_3$, 300 MHz): δ 3.35 (3H, s), 3.36 (3H, s), 3.52 (4H, m), 3.69 (12H, m), 3.81 (2H, m), 3.88 (3H, s), 3.90 (2H, *app. t*, $J = 5.41$ Hz), 4.23 (2H, *app. t*, $J = 4.82$ Hz), 4.44 (2H, *app. t*, $J = 4.85$ Hz), 6.90 (1H, *d*, $J = 8.52$ Hz), 7.53 (1H, *d*, $J = 1.89$ Hz), 7.65 (1H, *dd*, $J_1 = 8.42$ Hz, $J_2 = 2.01$ Hz); ^{13}C NMR ($CDCl_3$, 75 MHz): δ 56.05, 59.02, 63.98, 68.39, 69.31, 69.44, 70.55, 70.58, 70.64, 70.68, 70.90, 71.92, 112.00, 112.58, 112.87, 123.59, 148.97, 152.41, 166.27; MS (ES^+): m/e calculated for $C_{22}H_{36}O_{10}Na^+$ (MNa^+) 483.2206, found 483.2224



R-3- (4-Benzyloxy- phenyl)-2-tert- butoxycarbonylamino-propionic acid benzyl ester (111a): A mixture consisting of 7.5 g (0.0267 mol) Boc-*R*-tyrosine

(**106a**), 10 g (7 ml, 0.0587 mol) benzyl bromide, 11.05 g (0.0801 mol) K_2CO_3 , and 1.18 g (0.004 mol) tetrabutylammonium iodide in 100 ml distilled DMF was stirred under N_2 at room temperature for 48 hours. The solvent was removed *in vacuo*, and the residue partitioned between 100 ml each of $EtOAc$, and water. The organic layer was washed with two 50 ml portions each of 1 N HCl, saturated $NaHCO_3$, and saturated brine. Drying with $MgSO_4$, and reduced pressure evaporation of the solvent afforded an orange oil, which was recrystallized from $EtOAc$ /hexanes. 11.5 g (93%) of the desired product was obtained as short, white crystals. R_f : 0.49 (SiO_2 , 3:7 $EtOAc$:Hex); mp: 79-80°C; $[\alpha]_D$: +7.7° (c : 0.5, $CHCl_3$); IR (KBr , cm^{-1}): 3359, 3067, 3034, 2977, 2928, 2929, 1741, 1719, 1606, 1505, 1453, 1363, 1247, 1161, 1056, 1015, 741; 1H NMR ($CDCl_3$, 300 MHz): δ 1.39 (9H, s), 3.00 (2H, *d*, $J = 5.52$ Hz),

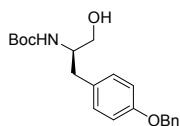
4.50 (1H, s), 4.94 (1H, d, $J = 8.11$ Hz), 5.00 (2H, s), 5.10 (2H, m), 6.81 (2H, d, $J = 8.66$ Hz), 6.92 (2H, d, $J = 8.42$ Hz), 7.35 (10H, m); ^{13}C NMR (CDCl_3 , 75 MHz): δ 28.44, 37.43, 54.80, 67.06, 69.74, 70.00, 79.86, 114.99, 127.55, 128.04, 128.32, 128.41, 128.51, 128.67, 130.49, 135.38, 135.49, 137.2, 155.3, 157.98, 171.91; MS (MNa^+): m/e calculated for $\text{C}_{28}\text{H}_{31}\text{NO}_5\text{Na}$ (MNa^+) 484.2100, found 484.2076



S-3-(4-Benzyloxy-phenyl)-2-tert-butoxycarbonylamino-propionic acid benzyl

ester (111b): A mixture consisting of 29 g (0.103 mol) Boc-*S*-tyrosine (**106b**),

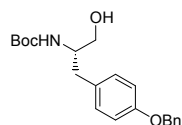
35.2 g (24.5 ml, 0.206 mol) benzyl bromide, 42.6 g (0.206 mol) K_2CO_3 , and 5.7 g (0.0155 mol) tetrabutylammonium iodide in 500 ml distilled DMF was stirred under N_2 at room temperature for 48 hours. The solvent was removed *in vacuo*, and the residue partitioned between 500 ml each of EtOAc, and water. The organic layer was washed with two 50 ml portions each of 1 N HCl, saturated NaHCO_3 , and saturated brine. Drying with MgSO_4 , and reduced pressure evaporation of the solvent afforded an orange oil, which was recrystallized from ether/hexanes. 40.1 g (85 %) of the title compound was obtained as short, white crystals. R_f : 0.49 (SiO_2 , 3:7 EtOAc:Hexane); $[\alpha]_D$: -7.5° (c : 0.5, CDCl_3); ^1H NMR (CDCl_3 , 300 MHz): δ 1.36 (9H, s), 3.00 (2H, d, $J = 5.63$ Hz), 4.58 (1H, m), 4.94 (1H, d, $J = 6.64$ Hz), 5.00 (2H, s), 5.11 (2H, dd, $J_1 = 24.46$, $J_2 = 12.37$ Hz), 6.81 (2H, d, $J = 8.60$ Hz), 6.92 (2H, d, $J = 8.42$ Hz), 7.34 (10H, m); MS (TOF-MS): m/e calculated for $\text{C}_{28}\text{H}_{31}\text{NO}_5\text{Na}$ (MS^+) 484.2100, found 484.2107



R-[1-(4-Benzyloxy-benzyl)-2-hydroxy-ethyl]-carbamic acid tert-butyl ester

(112a): 10.0 g (0.021 mol) of *R*-3-(4-benzyloxy -phenyl)- 2-tert-

butoxycarbonylamino-propionic acid benzyl ester (**111a**) dissolved in 60 ml dry THF was added drop-wise over 45 min to a suspension of 2.39 g (0.063 mol) LiAlH₄ at 0 °C under an N₂ atmosphere. After the addition is complete, the reaction is allowed to heat to room temperature, after which the reaction was stirred for an additional hour. The reaction was quenched by careful addition of 100 ml 10% KOH. The mixture was filtered through Celite™, and extracted with (3x) 30 ml EtOAc. The organic layer was washed with 50 ml each of 5% HCl, saturated NaHCO₃, and saturated brine. Drying with MgSO₄, and *in vacuo* removal of the solvent afforded 7.0 g (93% yield) of the desired product as a white powder. R_f: 0.5 (SiO₂, 1:3 EtOAc:Hexane); mp: 112-113°C; [α]_D: +19.74° (c: 0.2, CHCl₃); IR (neat, cm⁻¹): 3356, 3030, 2974, 29.29, 28.61, 1700, 1517, 1449, 1239, 1161, 1003, 730; ¹H NMR (CDCl₃, 300 MHz): δ 1.4 (9H, s), 2.76 (2H, d, J = 7.11 Hz), 3.53 (1H, dd, J₁ = 11.0 Hz, J₂ = 5.4 Hz), 3.65 (1H, dd, J₁ = 11.0 Hz, J₂ = 3.67 Hz), 3.79 (1H, m), 4.69 (1H, s), 5.02 (2H, s), 6.90 (2H, d, J = 8.6 Hz), 7.10 (2H, d, J = 8.6 Hz), 7.35 (5H, m); ¹³C NMR (CDCl₃, 75 MHz): δ 28.50, 36.76, 53.99, 63.98, 70.14, 79.74, 115.02, 127.57, 128.03, 128.67, 130.16, 137.21, 156.34, 157.60; MS (MNa⁺): *m/e* calculated for C₂₁H₂₇NO₄Na (MNa⁺) 380.1838, found 380.1838

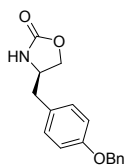


S-[1-(4-Benzyloxy-benzyl)-2-hydroxy-ethyl]-carbamic acid tert-butyl ester

(112b): 32.0 g (0.069 mol) of S-3-(4-Benzyloxy-phenyl)- 2-tert-

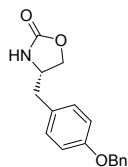
butoxycarbonylamino-propionic acid benzyl ester (**111b**) dissolved in 200 ml dry THF was added drop-wise over 45 min to a suspension of 2.39 g (0.063 mol) LiAlH₄ in 100 ml THF at 0°C under a N₂ atmosphere. After the addition is complete, the reaction is allowed to heat to room temperature, after which it was stirred for an additional hour. The reaction was quenched

by careful addition of 300 ml 10% NaOH. The mixture was filtered through Celite™, and extracted with (3x) 90 ml EtOAc. The organic layer was washed with 150 ml each of 5% HCl, saturated NaHCO₃, and saturated brine. Drying with MgSO₄, and *in vacuo* removal of the solvent afforded 22.3 g (91%) of the title compound as a white powder. R_f: 0.5 (SiO₂, 1:3 EtOAc:Hexanes); mp: 110-111 °C; [α]^D = -19.20° (c: 0.20, CHCl₃); ¹H NMR (CDCl₃, 300 MHz): δ 1.40 (9H, s); 2.75 (2H, d, J = 7.11 Hz), 3.52 (1H, dd, J₁ = 10.99 Hz, J₂ = 5.38 Hz), 3.64 (1H, dd, J₁ = 10.99, J₂ = 3.75 Hz), 3.79 (1H, m), 4.68 (1H, s), 5.02 (2H, s), 6.89 (2H, d, J = 9.59 Hz), 7.10 (2H, d, J = 8.55 Hz), 7.34 (5H, m); MS (EI+ MS): m/e calculated for C₂₁H₂₇NO₄ (M⁺) 357.1940, found 357.1927

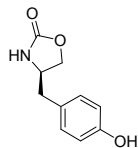


R-4-(4-Benzyloxy-benzyl)-oxazolidin-2-one (113a): 6.8 g (19.0 mmol) R-[1-(4-benzyloxy-benzyl)-2-hydroxy-ethyl]-carbamic acid *tert*-butyl ester (**112a**) dissolved in 50 ml freshly distilled THF was added drop-wise at room temperature to a suspension of 1.37 g (57.0 mmol) NaH under N₂ atmosphere over 20 minutes. The reaction was stirred for 24 h, after which it was cooled to 0°C, and carefully quenched with 100 ml saturated aqueous NH₄Cl (*Caution: H₂ evolution!*). The resulting mixture was filtered through Celite™, and extracted with (3x) 50 ml portions of EtOAc. The organic layer was washed with (2x) 100 ml portions each of 1N HCl, saturated aqueous NaHCO₃, and saturated brine. The organic phase was dried with MgSO₄, and the solvent was removed *in vacuo* to yield 5 g (93% yield) of the desired product as a pale yellow crystalline solid. R_f: 0.45 (SiO₂, EtOAc); mp: 139-141°C; [α]_D: +83.0° (c: 0.016, CDCl₃); IR (film, cm⁻¹): 3273, 2910, 2857, 1753, 1700, 1505, 1397, 1232, 1090, 1015, 936, 734; ¹H NMR (CDCl₃, 300 MHz): δ 2.79 (2H, m), 4.01 (1H, m), 4.12 (1H, dd, J₁ = 8.6 Hz, J₂ = 5.5 Hz), 4.45 (1H, app. t, J = 8.5 Hz), 5.04 (2H, s), 6.92

(2H, d, $J = 8.7$ Hz), 7.07 (2H, d, $J = 8.7$ Hz), 7.36 (5H, m); ^{13}C NMR (CDCl_3 , 75 MHz): δ 40.52, 53.90, 69.58, 70.07, 115.36, 127.48, 128.04, 128.20, 128.63, 130.10, 158.00, 160.01; MS (EI^+): m/e calculated for $\text{C}_{17}\text{H}_{17}\text{NO}_3$ (M^+) 283.3208, found 283.1217

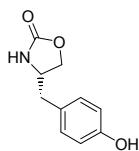


S-4-(4-Benzyloxy-benzyl)-oxazolidin-2-one (113b): 7.0 g (20.0 mmol) *S*-[1-(4-benzyloxy-benzyl)-2-hydroxy-ethyl]-carbamic acid *tert*-butyl ester (**112b**) dissolved in 50 ml freshly distilled THF was added drop-wise at room temperature to a suspension of 1.44 g (60.0 mmol) NaH under N_2 atmosphere over 20 minutes. The reaction was stirred for 24 h, after which it was cooled to 0°C , and carefully quenched with 100 ml saturated aqueous NH_4Cl (*Caution: H₂ evolution*). The resulting mixture was extracted with 60 ml portions (3x) of EtOAc. The organic layer was washed with 100 ml portions (3x) each of 1N HCl, saturated aqueous NaHCO_3 , and saturated brine. The organic phase was dried with MgSO_4 , and the solvent was removed *in vacuo*. 5.15 g (91% yield) of the title compound was obtained as a white, crystalline solid. R_f : 0.45 (SiO_2 , EtOAc); $[\alpha]_D$: -84.5° (c: 0.016, CHCl_3); ^1H NMR (CDCl_3 , 300 MHz): δ 2.79 (2H, m), 4.01 (1H, m), 4.12 (1H, dd, $J_1 = 8.63$ Hz, $J_2 = 5.51$ Hz), 4.45 (1H, app. t, $J = 8.37$ Hz), 5.04 (2H, s), 6.92 (2H, d, $J = 8.48$ Hz), 7.07 (2H, d, $J = 8.47$ Hz), 7.35 (5H, m); MS (EI^+): m/e calculated for $\text{C}_{17}\text{H}_{17}\text{NO}_3$ (M^+) 283.1208, found 283.1217

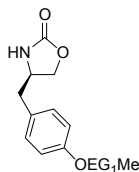


(R)-4-(4-Hydroxy-benzyl)-oxazolidin-2-one (103a): To a solution of 1.37 g (8.83 mmol) *R*-4-(4-Benzyloxy-benzyl)-oxazolidin-2-one (**113a**) in 40 ml anhydrous EtOH was added 0.515 g (0.48 mmol Pd) of 10% Pd on activated carbon. The reaction was carried out under a H_2 atmosphere (*balloon*) at room temperature for 24 h (*alternatively the reaction can be*

carried out in a Parr Reactor at 40 psi H₂ pressure, is complete in 12 h, and gives similar yield). Filtering through Celite™, and *in vacuo* removal of the solvent afforded 0.894 g (96% yield) of the desired compound as a white solid. R_f: 0.55 (SiO₂, EtOAc); mp: 182-184°C; [α]_D: -11.2° (c: 1.0, EtOH); IR (KBr, cm⁻¹): 3550, 3080, 2877, 1765, 1601, 1511, 1246, 1100, 1000, 949, 850, 767; ¹H NMR (CDCl₃, 300 MHz): δ 2.66 (2H, m), 3.99 (2H, m), 4.27 (1H, m), 6.64 (2H, d, J = 8.62 Hz), 6.95 (2H, d, 8.66 Hz); ¹³C NMR (CDCl₃, 75 MHz): δ 39.60, 53.08, 69.27, 115.09, 126.88, 129.98, 156.01, 160.78; MS (EI+): m/e calculated for C₁₀H₁₁NO₃ (M⁺) 193.0739, found 193.0745

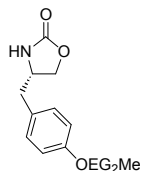


S-4-(4-Hydroxy-benzyl)-oxazolidin-2-one (103b): To a solution of 0.5 g (1.77 mmol) S-4-(4-benzyloxy-benzyl)-oxazolidin-2-one (**113b**) in 10 ml anhydrous EtOH was added 0.187 g (0.177 mmol Pd) of 10% Pd on activated carbon. The reaction was carried out under a H₂ atmosphere (balloon) at room temperature for 24 h (alternatively the reaction can be carried out in a Parr Reactor at 40 psi H₂ pressure, is complete in 12 h, and gives similar yield). Filtering through Celite™, and *in vacuo* removal of the solvent afforded 0.323 g (94% yield) of the desired compound as a white solid. R_f: 0.55 (SiO₂, EtOAc); mp: 181-184°C; [α]_D: +11.8° (c: 1.0, EtOH); ¹H NMR (MeOD, 300 MHz): δ 2.67 (2H, m), 4.02 (2H, m), 4.29 (1H, m), 6.65 (2H, d, J = 8.32 Hz), 6.97 (2H, d, J = 8.35 Hz); MS (EI+): m/e calculated for C₁₀H₁₁NO₃ (M⁺) 193.0739, found 193.0734



R-4-[4-(2-Methoxy-ethoxy)-benzyl]-oxazolidin-2-one (114a): To a mixture of 500 mg (2.59 mmol) R-4-(4-hydroxy-benzyl)-oxazolidin-2-one (**103a**), 1.69 g (5.18

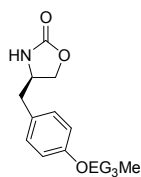
mmol) Cs₂CO₃, and 25 mg (*0.13 mmol*) KI in 10 ml anhydrous DMF was added 270 mg (*0.27 ml*, *2.85 mmol*) 2-methoxyethyl chloride (**87a**). The reaction was stirred at 60°C for 12h. The solvent was removed *in vacuo*, and the residue partitioned between water (*50 ml*) and EtOAc (*50 ml*). The organic phase was washed with (*3x*) 30 ml 1 N HCl, (*3x*) 30 ml saturated aqueous NaHCO₃, and (*1x*) 30 ml saturated brine. The organic phase was dried with MgSO₄, and the solvent removed under reduced pressure. Flash column chromatography (*SiO₂*, *EtOAc*) afforded 480 mg (*74% yield*) of the title compound as a white solid. R_f: 0.45 (*SiO₂*, *EtOAc*); [α]_D: +34.4° (*c*: 1.0, CHCl₃); IR (*neat*, cm⁻¹): 3056, 2935, 2897, 1750, 1614, 1515, 1465, 1402, 1250, 1108, 1070, 1020, 935, 845, 778; ¹H NMR (CDCl₃, 300 MHz): δ 2.79 (2H, *m*), 3.43 (3H, *s*), 3.73 (2H, *m*), 3.99 (1H, *m*), 4.09 (2H, *m*), 4.44 (1H, *app. t*, *J* = 8.5 Hz), 4.95 (1H, *s*), 6.88 (2H, *d*, *J* = 8.6 Hz), 7.06 (2H, *d*, *J* = 8.5 Hz); ¹³C NMR (CDCl₃, 75 MHz): δ 40.18, 53.69, 59.03, 67.22, 69.30, 70.75, 114.88, 128.21, 130.05, 158.25, 159.80; MS (*EI*⁺): *m/e* calculated for C₁₃H₁₇NO₄ (*M*⁺) 251.1158, found 251.1159



S-4-{4-[2-(2-Methoxy-ethoxy)-ethoxy]-benzyl}-oxazolidin-2-one (114b): To a mixture of 560 mg (*2.90 mmol*) *S*-4-(4-hydroxy-benzyl)-oxazolidin-2-one (**103b**), 1.89 g (*5.8 mmol*) Cs₂CO₃, and 24 mg (*0.145 mmol*) KI in 10 ml anhydrous DMF

was added 440 mg (*3.19 mmol*) 1-(2-chloro-ethoxy)-2-methoxy-ethane (**87b**). The reaction was stirred at 60°C for 24h. The reaction was partitioned between water (*50 ml*), and CH₂Cl₂ (*50 ml*). The organic phase was washed with (*3x*) 30 ml 1 N HCl, (*3x*) 30 ml saturated aqueous NaHCO₃, and 30 ml saturated brine. The organic phase was dried with MgSO₄, and the solvent removed under reduced pressure. Flash column chromatography (*SiO₂*, *EtOAc*) afforded 560 mg (*65% yield*) of the title compound as a yellow oil. R_f: 0.31 (*SiO₂*, *EtOAc*); [α]_D: -44.5° (*c*:

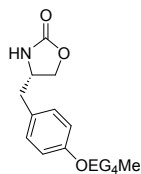
1.0, CHCl_3); IR (*neat*, cm^{-1}): 3322, 2924, 2893, 1760, 1624, 1507, 1457, 1480, 1399, 1243, 1103, 1061, 1022, 929, 851, 770; ^1H NMR (CDCl_3 , 300 MHz): δ 2.77 (2H, *m*), 3.37 (3H, *s*), 3.56 (2H, *m*), 3.70 (2H, *m*), 3.84 (2H, *m*), 4.00 (2H, *m*), 4.10 (2H, *m*), 4.22 (1H, *app. t*, $J = 8.07$ Hz), 5.21 (1H, *b s*), 6.86 (2H, *d*, $J = 8.70$ Hz), 7.05 (2H, *d*, $J = 8.73$ Hz); ^{13}C NMR (CDCl_3 , 75 MHz): δ 40.15, 53.68, 58.86, 67.35, 69.26, 69.59, 70.49, 71.79, 114.86, 128.17, 130.08, 157.74, 159.81; MS (*EI+*): m/e calculated for $\text{C}_{15}\text{H}_{21}\text{NO}_5$ (M^+) 295.1420, found 295.1411



R-4-(4-{2-[2-(2-Methoxy-ethoxy)-ethoxy]-ethoxy}-benzyl)-oxazolidin-2-one

(114c): To a mixture of 500 mg (2.59 mmol) R-4-(4-hydroxy-benzyl)-oxazolidin-2-one (**103a**), 1.69 g (2.85 mmol) Cs_2CO_3 , and 21 mg (0.021 mmol) KI in 5 ml anhydrous DMF was added 519 mg (2.85 mmol) 1-[2-(2-chloro-ethoxy)-ethoxy]-2-methoxyethane (**87c**). The reaction was stirred at 60°C for 12h. The reaction was partitioned between water (50 ml), and CH_2Cl_2 (50 ml). The organic phase was washed with (3x) 30 ml 1 N HCl, (3x) 30 ml saturated aqueous NaHCO_3 , and 30 ml saturated brine. The organic phase was dried with MgSO_4 , and the solvent removed under reduced pressure. Flash column chromatography (SiO_2 , *EtOAc*) afforded 530 mg (60% yield) of the title compound as a pale yellow oil. R_f : 0.31 (SiO_2 , 5:95 *MeOH:EtOAc*); $[\alpha]_D$: $+36.31^\circ$ (c : 1.0, CDCl_3); IR (*neat*, cm^{-1}): 2867, 1759, 1608, 1507, 1241, 1105, 1004, 929, 853, 763; ^1H NMR (CDCl_3 , 300 MHz): δ 2.76 (2H, *m*), 3.36 (3H, *s*), 3.53 (2H, *m*), 3.65 (4H, *m*), 3.72 (2H, *m*), 3.83 (2H, *m*), 4.00 (2H, *m*), 4.10 (2H, *m*), 4.43 (1H, *app. t*, $J = 8.2$ Hz), 5.13 (1H, *b s*, *m*), 6.86 (2H, *d*, $J = 8.69$ Hz), 7.05 (2H, *d*, $J = 8.7$ Hz); ^{13}C NMR (CDCl_3 , 75 MHz): δ 40.27, 53.78, 58.97, 67.46, 69.36, 69.68, 70.37, 70.53, 70.74, 71.88, 114.97, 128.30,

130.16, 157.94, 159.89; MS (*EI*⁺): *m/e* calculated for C₁₇H₂₅NO₆ (*M*⁺) 339.1682, found 339.1672



S-4-[4-(2-{2-[2-(2-Methoxy-ethoxy)-ethoxy]-ethoxy}-ethoxy)-benzyl]-oxazolidin-

2-one (114d): To a mixture of 500 mg (2.59 mmol) *S*-4-(4-hydroxy-benzyl)-

oxazolidin-2-one (**103b**), 1.69 g (5.18 mmol) Cs₂CO₃, and 25 mg (0.13 mmol) KI in

10 ml anhydrous DMF was added 644 mg (2.85 mmol) 1-[2-(2-chloro-ethoxy)-ethoxy]-2-(2-

methoxy-ethoxy)-ethane (**87d**). The reaction was stirred at 60°C for 12h. The reaction was

partitioned between water (50 ml), and CH₂Cl₂ (50 ml). The organic phase was washed with

(3x) 30 ml 1 N HCl, (3x) 30 ml saturated aqueous NaHCO₃, and 30 ml saturated brine. The

organic phase was dried with MgSO₄, and the solvent removed under reduced pressure. Flash

column chromatography (*SiO*₂, *EtOAc*) afforded 650 mg (66% yield) of the title compound as a

colorless oil. *R*_f: 0.27 (*SiO*₂, 5:95 *MeOH*:*EtOAc*); [*α*]_D: -34.99° (*c*: 1.0, CHCl₃); IR (*neat*,

cm⁻¹): 2873, 1751, 1603, 1511, 1450, 1399, 1245, 1102, 1020, 938, 846, 769; ¹H NMR

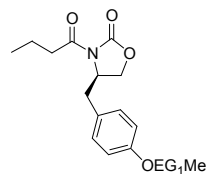
(CDCl₃, 300 MHz): δ 2.78 (2H, *m*), 3.35 (3H, *s*), 3.52 (2H, *m*), 3.67 (10H, *m*), 3.83 (2H,

m), 4.01 (1H, *m*), 4.11 (3H, *m*), 4.44 (1H, *app. t*, *J* = 8.3 Hz), 4.98 (1H, *b s*), 6.86 (2H, *d*,

J = 8.5 Hz), 7.06 (2H, *d*, *J* = 8.5 Hz); ¹³C NMR (CDCl₃, 75 MHz): δ 40.22, 53.73, 53.80,

58.92, 67.40, 69.28, 69.62, 70.34, 70.54, 70.68, 71.79, 114.88, 128.18, 130.14, 157.80,

159.80; MS (*EI*⁺): *m/e* calculated for C₁₉H₂₉NO₇ (*M*⁺) 383.1944, found 383.1944

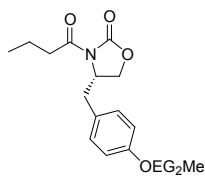


R-3-Butyryl-4-[4-(2-methoxy-ethoxy)-benzyl]-oxazolidin-2-one (115a): 1.36

ml (1.55 mmol) of 1.14 M *n*-BuLi in hexanes was added slowly to a solution of

300 mg (1.19 mmol) *R*-4-[4-(2-Methoxy-ethoxy)-benzyl]-oxazolidin-2-one

(**114a**) in 10 ml anhydrous THF at -78 °C. The reaction was stirred at -78 °C for 20 min, and 178 mg (0.173 ml, 0.167 mmol) of butyryl chloride was added slowly. The reaction was stirred at -78°C for 30 min, and was quenched with saturated aqueous NH₄Cl (5 ml). The solution was extracted with 20 ml EtOAc, and the organic phase was washed with saturated brine (20 ml). The organic phase was dried with MgSO₄, and the solvent removed under reduced pressure. Flash column chromatography (SiO₂, 1:1 EtOAc:Hexane) afforded 341 mg (89% yield) of the title compound as a colorless oil. R_f: 0.37 (SiO₂, 1:1 EtOAc:Hexane); [α]_D: -34.24° (c: 1.0, CHCl₃); IR (neat, cm⁻¹): 2919, 1781, 1698, 1608, 1496, 1446, 1377, 1234, 1131, 1087, 1047, 855, 806, 757; ¹H NMR (CDCl₃, 300 MHz): δ 0.90 (3H, t, J = 7.34 Hz), 1.71 (2H, qt, J₁ = 7.5 Hz, J₂ = 20.7), 2.69 (1H, m), 2.89 (2H, m), 3.19 (1H, m), 3.42 (3H, s), 3.72 (2H, m), 4.08 (2H, m), 4.16 (2H, m), 4.60 (1H, m), 6.87 (2H, d, J = 8.6 Hz), 7.09 (2H, d, J = 8.6 Hz); ¹³C NMR (CDCl₃, 75 MHz): δ 13.73, 17.34, 36.94, 37.37, 55.13, 59.14, 66.19, 67.31, 71.05, 115.01, 127.52, 130.49, 153.33, 158.13, 173.15; MS (EI+): m/e calculated for C₁₇H₂₃NO₅ (M⁺) 321.1576, found 321.1560

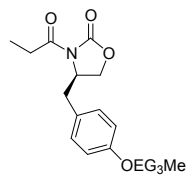


S-3-Butyryl-4-{4-[2-(2-methoxy-ethoxy)-ethoxy]-benzyl}-oxazolidin-2-one

(**115b**): 1.8 ml (2.47 mmol) of 1.40 M *n*-BuLi in hexanes was added slowly to

a solution of 560 mg (1.90 mmol) *S*-4-{4-[2-(2-Methoxy-ethoxy)-ethoxy]-benzyl}-oxazolidin-2-one (**114b**) in 10 ml anhydrous THF at -78 °C. The reaction was stirred at -78 °C for 20 min, and 283 mg (0.276 ml, 2.66 mmol) of butyryl chloride was added slowly. The reaction was stirred at -78°C for 30 min, and was quenched with saturated aqueous NH₄Cl (5 ml). The solution was extracted with 20 ml EtOAc, and the organic phase was washed with saturated brine (20 ml). The organic phase was dried with MgSO₄, and the solvent removed

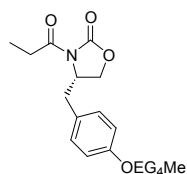
under reduced pressure. Flash column chromatography (SiO_2 , $EtOAc$) afforded 633 mg (91% yield) of the title compound as a colorless oil. R_f : 0.59 (SiO_2 , $EtOAc$); $[\alpha]_D$: +43.49° (c : 1.0, $CHCl_3$); IR (*neat*, cm^{-1}) 2966, 2933, 2872, 1781, 1699, 1605, 1507, 1405, 1389, 1287, 1258, 1123, 1066, 858, 817, 756; 1H NMR ($CDCl_3$, 300 MHz): δ ; 0.99 (3H, *t*, $J = 7.35$ Hz), 1.71 (2H, *dd*, $J_1 = 7.5$ Hz, $J_2 = 20.7$ Hz), 2.69 (1H, *dd*, $J_1 = 9.49$ Hz, $J_2 = 13.5$ Hz), 2.89 (2H, *m*), 3.19 (1H, *dd*, $J_1 = 3.1$ Hz, $J_2 = 13.4$ Hz), 3.37 (3H, *s*), 3.56 (2H, *m*), 3.70 (2H, *m*), 3.83 (2H, *m*), 4.14 (4H, *m*), 4.60 (1H, *m*), 6.85 (2H, *d*, $J = 8.7$ Hz), 7.08 (2H, *d*, $J = 8.6$ Hz); ^{13}C NMR ($CDCl_3$, 75 MHz): δ 13.58, 17.62, 36.84, 37.24, 58.91, 66.07, 67.34, 69.61, 70.61, 71.84, 114.97, 127.34, 130.33, 153.41, 157.98, 173.00; MS (EI^+): m/e calculated for $C_{19}H_{27}NO_6$ (M^+) 365.1838, found 365.1827



R-4-(4-{2-[2-(2-Methoxy-ethoxy)-ethoxy]-ethoxy}-benzyl)-3-propionyl-oxazolidin-2-one (115c): 2 ml (2.68 mmol) of 1.33 M *n*-BuLi in hexanes was added slowly to a solution of 698 (2.06 mol) R-4-(4-{2-[2-(2-methoxy-ethoxy)-

ethoxy]-ethoxy}-benzyl)-oxazolidin-2-one (**114c**) in 10 ml anhydrous THF at -78°C. The reaction was stirred at -78 °C for 20 min, and 266 mg (0.252 ml, 2.88 mmol) of propionyl chloride was added slowly. The reaction was stirred at -78°C for 30 min, and was quenched with saturated aqueous NH_4Cl (5 ml). The solution was extracted with 20 ml $EtOAc$, and the organic phase was washed with saturated brine (20 ml). The organic phase was dried with $MgSO_4$, and the solvent removed under reduced pressure. Flash column chromatography (SiO_2 , 1:1 $EtOAc$: $Hexane$) afforded 733 mg (90% yield) of the title compound as a colorless oil. R_f : 0.46 (SiO_2 , $EtOAc$); $[\alpha]_D$: -40.59° (c : 1.0, $CDCl_3$); IR (*neat*, cm^{-1}): 2987, 2933, 2872, 1781, 1691, 1524, 1360, 1242, 1123, 952, 845, 805, 760; 1H NMR ($CDCl_3$, 300 MHz): δ 1.18

(3H, t, $J = 7.31$ Hz), 2.69 (1H, dd, $J_1 = 13.50$ Hz, $J_2 = 9.47$), 2.93 (2H, m), 3.19 (1H, dd, $J_1 = 13.47$, $J_2 = 3.13$), 3.36 (3H, s), 3.53 (2H, m), 3.65 (4H, m), 3.72 (2H, m), 3.83 (2H, m), 4.09 (2H, m), 4.16 (2H, m), 4.60 (1H, m), 6.85 (2H, d, $J = 8.70$ Hz), 7.08 (2H, d, $J = 8.63$); ^{13}C NMR (CDCl_3 , 75 MHz): δ 8.27, 29.11, 36.94, 55.15, 58.96, 66.16, 67.42, 69.66, 70.51, 70.64, 70.73, 71.89, 115.02, 127.35, 130.55, 153.49, 158.06, 173.97; MS (ES+): m/e calculated for $\text{C}_{20}\text{H}_{29}\text{N}_1\text{O}_7$ (M^+) 395.1944, found 395.1943



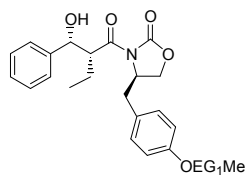
S-4-[4-(2-{2-[2-(2-Methoxy-ethoxy)-ethoxy]-ethoxy}-ethoxy)-benzyl]-3-

propionyl-oxazolidin-2-one (115d): 0.68 ml (1.09 mmol) of 1.6 M *n*-BuLi in

hexanes was added slowly to a solution of 320 mg (0.835 mmol) S-4-[4-(2-{2-[2-(2-methoxy-ethoxy)-ethoxy]-ethoxy}-ethoxy)-benzyl]-oxazolidin-2-one (114d) in 5 ml anhydrous THF at -78°C . The reaction was stirred at -78°C for 20 min, and 108 mg (0.104 ml, 0.117 mmol) of propionyl chloride was added slowly. The reaction was stirred at -78°C for 30 min, and was quenched with saturated aqueous NH_4Cl (5 ml). The solution was extracted with 20 ml EtOAc, and the organic phase was washed with saturated brine (20 ml). The organic phase was dried with MgSO_4 , and the solvent removed under reduced pressure. Flash column chromatography (SiO_2 , EtOAc) afforded 330 mg (90% yield) of the title compound as a pale yellow oil. R_f : 0.32 (SiO_2 , EtOAc); $[\alpha]_D$: $+41.74^\circ$ (c : 1.0, CDCl_3); IR (neat, cm^{-1}): 2980, 2926, 2865, 1785, 1685, 1520, 1350, 1232, 1115, 954, 8395, 801, 756; ^1H NMR (CDCl_3 , 300 MHz): δ 1.18 (3H, t, $J = 7.35$ Hz), 2.69 (1H, m), 2.93 (2H, m), 3.19 (1H, m), 3.35 (3H, s), 3.51 (2H, m), 3.66 (10H, m), 3.82 (2H, m), 4.14 (4H, m), 4.60 (1H, m), 6.85 (2H, d, $J = 8.5$ Hz), 7.08 (2H, d, $J = 8.5$ Hz); ^{13}C NMR (CDCl_3 , 75 MHz): δ 8.35, 29.14, 36.92, 55.15, 58.97, 66.22, 67.45, 69.68, 70.59, 70.78, 71.92, 115.06, 127.52, 130.38, 153.53,

158.12, 173.98; MS (TOF-MS⁺): *m/e* calculated for C₂₂H₃₃NO₈Na (*M*⁺) 462.2104, found 462.2101

Mixture Aldol Reaction of 115a-115d: To a solution of 110 mg (0.342 mmol) *R*-3-Butyryl-4-[4-(2-methoxy-ethoxy)-benzyl]-oxazolidin-2-one (**115a**), 125 mg (0.342 mmol) *S*-3-Butyryl-4-{4-[2-(2-methoxy-ethoxy)-ethoxy]-benzyl}-oxazolidin-2-one (**115b**), 135 mg (0.342 mmol) *R*-4-(4-{2-[2-(2-Methoxy-ethoxy)-ethoxy]-ethoxy}-benzyl)-3-propionyl-oxazolidin-2-one (**115c**), and 150 mg (0.342 mmol) *S*-4-[4-(2-{2-[2-(2-Methoxy-ethoxy)-ethoxy]-ethoxy}-ethoxy)-benzyl]-3-(2-methyl-3-phenyl-butyryl)-oxazolidin-2-one (**115d**) in 12 ml CH₂Cl₂ at 0 °C, was added 2.46 ml (2.46 mmol) of a 1 M solution of dibutylboron triflate in CH₂Cl₂. After stirring the solution for 5 min at 0 °C, 263 mg (0.362 ml, 2.60 mmol) freshly distilled triethylamine was added carefully, and the reaction was stirred for another 5 min after which the reaction was cooled to -78 °C. 276 mg (0.264 ml, 2.60 mmol) benzaldehyde was added to the reaction, and the reaction was allowed to heat to 0 °C after stirring at -78 °C for 30 min. After 2h at 0 °C the reaction was quenched with 10 ml 2:1 MeOH:pH 7 phosphate buffer. Subsequently 10 ml of 2:1 MeOH:30% aqueous H₂O₂ was added to the reaction, and stirred at 0 °C for 1 h. The volatiles were removed under reduced pressure and the reaction diluted with 20 ml EtOAc. The reaction was washed with 20 ml saturated aqueous NaHCO₃. The aqueous layer was back extracted with 10 ml EtOAc, and the combined organic phases were dried with MgSO₄. The residue was subjected to gradient flash column chromatography (*SiO*₂, 1:1 EtOAc:Hexanes to 5:95 MeOH:EtOAc).

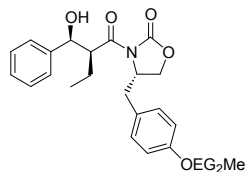


3-[2-(Hydroxy-phenyl-methyl)-butyryl]-4-[4-(2-methoxy-ethoxy)-benzyl]-oxazolidin-2-one (116a): 135 mg (92% yield) of the title

compound was obtained as a colorless oil. $R_f = 0.27$ (SiO_2 , 1:1 EtOAc: Hexanes); $R_f = 0.63$ (SiO_2 , EtOAc), $[\alpha]_D^{25} = -59.2^\circ$ ($c = 1.0$, $CHCl_3$). IR (neat, cm^{-1}): 3461, 2958, 2933, 2864, 1773, 1683, 1601, 1511, 1450, 1385, 1238, 1193, 1115, 1054, 764, 706; 1H NMR ($CDCl_3$, 300 MHz): δ 0.90 (3H, t, $J = 7.42$ Hz), 1.77 (2H, m), 1.90 (2H, m), 2.59 (1H, dd, $J_1 = 9.93$ Hz, $J_2 = 13.43$ Hz), 3.18 (1H, dd, $J_1 = 3.43$ Hz, $J_2 = 13.4$ Hz), 3.43 (3H, s), 3.72 (2H, m), 3.79 (1H, app. t, $J = 8.0$ Hz), 4.00 (1H, dd, $J_1 = 2.34$ Hz, $J_2 = 8.97$ Hz), 4.07 (2H, m), 4.30 (1H, m), 4.34 (1H, m), 4.92 (1H, d, $J = 5.87$ Hz), 6.85 (2H, d, $J = 8.48$ Hz), 7.08 (2H, d, $J = 8.57$ Hz), 7.32 (5H, m); ^{13}C NMR ($CDCl_3$, 75 MHz): 11.85, 20.94, 37.22, 51.59, 55.80, 59.35, 66.00, 67.38, 71.10, 74.97, 115.13, 126.41, 127.45, 127.84, 128.37, 130.48, 141.83, 153.26, 158.17, 175.33; MS (ES⁺): m/e calculated for $C_{24}H_{29}NO_6Na$ (MNa⁺) 450.1893, found 450.1884. **Single Component Aldol Reaction of**

115a: To a solution of 100 mg (0.311 mmol) *R*-3-butyryl-4-[4-(2-methoxy-ethoxy)-benzyl]-oxazolidin-2-one (115a) in 4 ml CH_2Cl_2 at 0 °C, was added 0.560 ml (0.560 mmol) of a 1 M solution of dibutylboron triflate in CH_2Cl_2 . After stirring the solution for 5 min at 0 °C, 60.0 mg (0.082 ml, 0.591 mmol) freshly distilled triethylamine was added carefully, and the reaction was stirred for another 5 min after which the reaction was cooled to -78 °C. 63.0 mg (0.060 ml, 0.591 mmol) benzaldehyde was added to the reaction, and the reaction was allowed to heat to 0°C after stirring at -78 °C for 30 min. After 2h at 0°C the reaction was quenched with 3 ml 2:1 MeOH:pH 7 phosphate buffer. Subsequently 3 ml of 2:1 MeOH:30% aqueous H_2O_2 was added to the reaction, and stirred at 0°C for 1 h. The volatiles were removed under reduced pressure and the reaction diluted with 10 ml EtOAc. The reaction was washed with 10 ml saturated

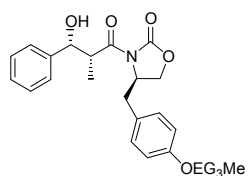
aqueous NaHCO₃. The aqueous layer was back extracted with 10 ml EtOAc, and the combined organic phases were dried with MgSO₄. The residue was subjected to gradient flash column chromatography (SiO₂, 1:1 EtOAc:Hexanes) to give 110 mg (83% yield) of the title compound as a colorless oil. *Characterization data match those of the mixture reaction product.*



3-[2-(Hydroxy-phenyl-methyl)-butyryl]-4-{4-[2-(2-methoxy-ethoxy)-ethoxy]-benzyl}-oxazolidin-2-one (116b): 131 mg (81% yield) of the title compound was obtained as a colorless oil. $R_f = 0.13$ (SiO₂, 1:1 EtOAc:

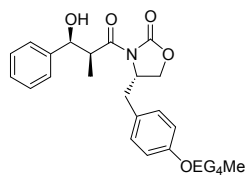
Hexanes); $R_f = 0.55$ (SiO₂, EtOAc); $[\alpha]_D^{25} = +54.31^\circ$ ($c = 0.0262$, CHCl₃); IR (neat, cm⁻¹): 3473, 2925, 2872, 1777, 1679, 1610, 1507, 1458, 1389, 1246, 1103, 805, 751, 694; ¹H NMR (CDCl₃, 300 MHz): δ 0.90 (3H, t, $J = 7.40$ Hz), 1.80 (1H, m), 1.90 (1H, m), 2.59 (1H, dd, $J_1 = 13.32$, $J_2 = 10.05$ Hz), 3.17 (1H, dd, $J_1 = 13.49$, $J_2 = 2.96$ Hz), 3.37 (3H, s), 3.57 (2H, m), 3.69 (2H, m), 3.81 (3H, m), 4.00 (1H, d, $J_1 = 9.03$ Hz, $J_2 = 2.32$ Hz), 4.10 (2H, m), 4.32 (2H, m), 4.92 (1H, d, $J = 5.78$ Hz), 6.84 (2H, d, $J = 8.56$ Hz), 7.07 (2H, d, $J = 8.52$ Hz), 7.33 (5H, m); ¹³C NMR (CDCl₃, 75 MHz): δ 11.73, 14.17, 20.98, 51.73, 55.67, 58.99, 60.38, 65.85, 67.41, 69.68, 70.67, 71.90, 74.97, 115.03, 126.35, 127.33, 127.64, 128.17, 130.35, 142.03, 153.11, 158.04, 175.05; MS (EI⁺): m/e calculated for C₂₆H₃₃NO₇ (M^+) 471.2257, found 471.2263. **Single Component Reaction of 116b:** To 125 mg (0.353 mmol) *S*-3-bButyryl-4-{4-[2-(2-methoxy-ethoxy)-ethoxy]-benzyl}-oxazolidin-2-one (115b) in 4 ml CH₂Cl₂ at 0 °C, was added 0.636 ml (0.636 mmol) of a 1 M solution of dibutylboron triflate in CH₂Cl₂. After stirring the solution for 5 min at 0 °C, 67.9 mg (0.093 ml, 0.671 mmol) freshly distilled triethylamine was added carefully, and the reaction was stirred for another 5 min after which the reaction was cooled to -78°C. 71.2 mg (0.068 ml, 0.671 mmol) benzaldehyde was

added to the reaction, and the reaction was allowed to heat to 0°C after stirring at -78 °C for 30 min. After 2h at 0 °C the reaction was quenched with 3 ml 2:1 MeOH:pH 7 phosphate buffer. Subsequently 3 ml of 2:1 MeOH:30% aqueous H₂O₂ was added to the reaction, and stirred at 0°C for 1 h. The volatiles were removed under reduced pressure and the reaction diluted with 10 ml EtOAc. The reaction was washed with 10 ml saturated aqueous NaHCO₃. The aqueous layer was back extracted with 10 ml EtOAc, and the combined organic phases were dried with MgSO₄. The residue was subjected to gradient flash column chromatography (*SiO*₂, 1:1 *EtOAc:Hexanes*) to give 135 mg (81% yield) of the title compound as a colorless oil. Characterization data match those of the mixture reaction product.



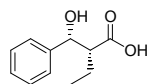
3-(3-Hydroxy-2-methyl-3-phenyl-propionyl)-4-(4-{2-[2-(2-methoxyethoxy)-ethoxy]-ethoxy}-benzyl)-oxazolidin-2-one (116c): 138 mg (81% yield) of the title compound was obtained as a colorless oil. $R_f = 0.40$ (*SiO*₂,

EtOAc); $[\alpha]_D^{25} = -40.6^\circ$ ($c = 1.0$, *CHCl*₃); IR (*neat*, cm^{-1}): 3469, 2942, 2872, 1765, 1691, 1614, 1511, 1446, 1368, 1242, 1103, 854, 756, 690; ¹H NMR (*CDCl*₃, 300 MHz): δ 1.54 (3H, *d*, $J = 6.96$ Hz), 2.70 (1H, *dd*, $J_1 = 13.63$, $J_2 = 9.29$ Hz), 3.14 (1H, *dd*, $J_1 = 13.52$ Hz, $J_2 = 3.16$ Hz), 3.53 (2H, *m*), 3.65 (4H, *m*), 3.72 (2H, *m*), 4.08 (6H, *m*), 4.53 (1H, *m*), 5.08 (1H, *d*, $J = 3.86$ Hz), 6.85 (2H, *d*, $J = 8.58$ Hz), 7.07 (2H, *d*, $J = 8.57$ Hz), 7.33 (5H, *m*); ¹³C NMR (*CDCl*₃, 75 MHz): δ 11.06, 36.84, 44.59, 55.31, 59.01, 66.13, 67.46, 69.99, 70.51, 70.54, 70.81, 71.92, 73.89, 115.08, 126.15, 127.10, 127.51, 128.23, 130.41, 141.45, 152.95, 158.16, 176.61; MS (*EI*⁺): m/e calculated for C₂₇H₃₅NO₈ (M^+) 501.2363, found 501.2344



3-(3-Hydroxy-2-methyl-3-phenyl-propionyl)-4-[4-(2-{2-[2-(2-methoxy-ethoxy)-ethoxy]-ethoxy}-ethoxy)-benzyl]-oxazolidin-2-one (116d): 146

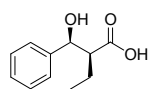
mg (78% yield) of the title compound was obtained as a colorless oil. $R_f = 0.26$ (*SiO*₂, *EtOAc*); $[\alpha]_D^{25} = +41.6^\circ$ ($c = 1.0$, *CHCl*₃); IR (*neat*, cm^{-1}): 3465, 2921, 2880, 1781, 1699, 1613, 1507, 1450, 1381, 1250, 1115, 862, 813, 760, 702; ¹H NMR (*CDCl*₃, 300 MHz): δ 1.20 (3H, *d*, $J = 7.15$), 2.70 (1H, *dd*, $J_1 = 13.54$ Hz, $J_2 = 9.39$ Hz), 3.14 (1H, *dd*, $J_1 = 13.53$ Hz, $J_2 = 3.30$ Hz), 3.35 (3H, *s*), 3.54 (2H, *m*), 3.65 (10H, *m*), 3.82 (2H, *app. t*, $J = 5.04$ Hz), 4.08 (6H, *m*), 4.53 (1H, *m*), 5.08 (1H, *d*, $J = 3.95$ Hz), 6.85 (2H, *d*, $J = 8.67$ Hz), 7.07 (2H, *d*, $J = 8.92$ Hz), 7.31 (5H, *m*); ¹³C NMR (*CDCl*₃, 75 MHz): δ 11.07, 14.18, 21.03, 36.80, 44.60, 55.29, 58.99, 66.11, 67.44, 69.63, 70.36, 70.49, 70.59, 70.68, 71.81, 73.86, 115.06, 126.13, 127.13, 127.48, 128.19, 130.45, 141.50, 152.94, 158.09, 176.52; MS (*ES*⁺): m/e calculated for C₂₉H₃₉NO₉Na (*TOF-MS*, *ES*⁺) 545.2625, found 568.2482



(2R,3R)-2-(Hydroxy-phenyl-methyl)-butyric acid (131a): To 93 mg (0.218 mmol) 3-[2-(Hydroxy-phenyl-methyl)-butyryl]-4-[4-(2-methoxy-ethoxy)-benzyl]-

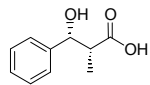
oxazolidin-2-one (**116a**) dissolved in 3.5 ml 3:1 THF:H₂O, and cooled to 0°C was added in succession 0.262 ml 30% H₂O₂ (2.18 mmol), and 10.5 mg (0.436 mmol) LiOH. The reaction was allowed to heat to room temperature. After 2h the reaction was cooled to 0°C, and 1.75 ml 1.5 M Na₂SO₃ (2.62 mmol) was added to quench excess H₂O₂. After removal of THF under reduced pressure, the cleaved auxiliary was removed by extraction with 2x5 ml CH₂Cl₂. The aqueous phase was cooled to 0°C, brought to pH ~1 with 1 N HCl, and saturated with NaCl. Extraction with EtOAc, drying with MgSO₄, and *in vacuo* removal of the solvent afforded 35 mg (83 %

yield) of (2*R*,3*R*)-2-(Hydroxy-phenyl-methyl)-butyric acid as a white crystalline solid. $[\alpha]_D$: +19.68° (*c*: 1.0, *CHCl*₃); ¹H NMR (*CDCl*₃, 300 MHz): δ 0.92 (3*H*, *t*, *J* = 7.44 Hz), 1.70 (3*H*, *m*), 2.69 (1*H*, *m*), 5.01 (1*H*, *d*, *J* = 5.36 Hz), 7.30 (5*H*, *m*); MS (*ES*⁺): *m/e* calculated for C₁₁H₁₄O₃ (*M*⁺) 194.0943, found 194.0947



(2*S*,3*S*)-2-(Hydroxy-phenyl-methyl)-butyric acid (131*b*): To 100 mg (0.212 mmol) 3-[2-(Hydroxy-phenyl-methyl)-butyryl]-4-{4-[2-(2-methoxy-ethoxy)-

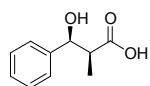
ethoxy]-benzyl}-oxazolidin-2-one (**116*b***) dissolved in 3.3 ml 3:1 THF:H₂O, and cooled to 0°C was added in succession 0.219 ml 30% H₂O₂ (2.12 mmol), and 10 mg (0.424 mmol) LiOH. The reaction was allowed to heat to room temperature. After 2h the reaction was cooled to 0°C, and 1.70 ml 1.5 M Na₂SO₃ (2.54 mmol) was added to quench excess H₂O₂. After removal of THF under reduced pressure, the cleaved auxiliary was removed by extraction with 2x5 ml CH₂Cl₂. The aqueous phase was cooled to 0°C, brought to pH ~1 with 1 N HCl, and saturated with NaCl. Extraction with EtOAc, drying with MgSO₄, and *in vacuo* removal of the solvent afforded 34 mg (83% yield) of (2*S*,3*S*)-(-)-2-(Hydroxy-phenyl-methyl)-butyric acid as a white crystalline solid. *R*_f: 0.52 (*SiO*₂, *EtOAc*); $[\alpha]_D$: +20.0° (*c*: 1.0, *CDCl*₃); ¹H NMR (*CDCl*₃, 300 MHz): δ 0.92 (3*H*, *t*, *J* = 7.45 Hz), 1.71 (2*H*, *m*), 2.70 (1*H*, *m*), 5.01 (1*H*, *d*, 5.39 Hz), 7.30 (5*H*, *m*); MS (*ES*⁺): *m/e* calculated for C₁₁H₁₄O₃ (*M*⁺) 194.0943, found 194.0935



(2*R*,3*R*)-2-(Hydroxy-phenyl-methyl)-butyric acid (131*c*): To 110 mg (0.219 mmol) 3-(3-Hydroxy-2-methyl-3-phenyl-propionyl)-4-[4-(2-{2-[2-(2-

methoxy-ethoxy)-ethoxy]-ethoxy}-ethoxy)-benzyl]-oxazolidin-2-one (**116*c***) dissolved in 3.5 ml 3:1 THF:H₂O, and cooled to 0°C was added in succession 0.226 ml 30% H₂O₂ (2.19 mmol), and

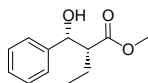
10.5 mg (0.438 mmol) LiOH. The reaction was allowed to heat to room temperature. After 2h the reaction was cooled to 0°C, and 1.75 ml 1.5 M Na₂SO₃ (2.63 mmol) was added to quench excess H₂O₂. After removal of THF under reduced pressure, the cleaved auxiliary was removed by extraction with 2x5 ml CH₂Cl₂. The aqueous phase was cooled to 0°C, brought to pH ~1 with 1 N HCl, and saturated with NaCl. Extraction with EtOAc, drying with MgSO₄, and *in vacuo* removal of the solvent afforded 36 mg (93% yield) of (2*R*,3*R*)-(+)-3-Hydroxy-2-methyl-3-phenyl-propionic acid as a white crystalline solid. R_f: 0.52 (1:1 EtOAc:Hexane); [α]_D: +27.5° (*c*: 1.0, CHCl₃); ¹H NMR (CDCl₃, 300 MHz): δ 1.14 (2*H*, *d*, *J* = 7.17 Hz), 2.84 (1*H*, *dq*, *J*₁ = 3.93 Hz, *J*₂ = 7.17 Hz), 5.16 (1*H*, *d*, 3.97 Hz), 7.30 (5*H*, *m*); MS (ES⁺): *m/e* calculated for C₁₀H₁₂O₃ (*M*⁺) 180.0786, found 180.0791



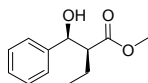
(2*S*,3*S*)-2-(Hydroxy-phenyl-methyl)-butyric acid (131*d*): To 112 mg (0.205 mmol) 3-(3-Hydroxy-2-methyl-3-phenyl-propionyl)-4-[4-(2-{2-[2-(2-methoxy-

ethoxy)-ethoxy]-ethoxy}-ethoxy)-benzyl]-oxazolidin-2-one (**116*d***) dissolved in 3.5 ml 3:1 THF:H₂O, and cooled to 0°C was added in succession 0.221 ml 30% H₂O₂ (2.05 mmol), and 10 mg (0.410 mmol) LiOH. The reaction was allowed to heat to room temperature. After 2h the reaction was cooled to 0°C, and 1.64 ml 1.5 M Na₂SO₃ (2.46 mmol) was added to quench excess H₂O₂. After removal of THF under reduced pressure, the cleaved auxiliary was removed by extraction with 2x5 ml CH₂Cl₂. The aqueous phase was cooled to 0°C, brought to pH ~1 with 1 N HCl, and saturated with NaCl. Extraction with EtOAc, drying with MgSO₄, and *in vacuo* removal of the solvent afforded 33.7 mg (91 % yield) of (2*S*,3*S*)-3-Hydroxy-2-methyl-3-phenyl-propionic acid as a white crystalline solid. R_f: 0.52 (1:1 EtOAc:Hexane); [α]_D: -29.9° (*c*: 1.0, CHCl₃); ¹H NMR (CDCl₃, 300 MHz): δ 1.14 (2*H*, *d*, *J* = 7.18 Hz), 2.84 (1*H*, *m*), 5.16 (1*H*,

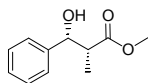
d, 4.04 Hz), 7.30 (5H, *m*); MS (*ES*⁺): *m/e* calculated for C₁₀H₁₂O₃ (*M*⁺) 180.0786, found 180.0785



(2R,3R)-2-(Hydroxy-phenyl-methyl)-butyric acid methyl ester (132a): To a solution of 32 mg (0.165 mmol) (2R,3R)-2-(Hydroxy-phenyl-methyl)-butyric acid (**131a**) in 2 ml Et₂O at 0 °C was added drop-wise 2.20 ml (0.66 mmol) of a solution of 0.3 M CH₂N₂ in Et₂O. The reaction was stirred at 0 °C for 1 h, and *in vacuo* removal of volatiles afforded 31.7 mg (99%) of the desired ester as a colorless oil. R_f: 0.58 (SiO₂, 1:1 EtOAc:Hex); [α]_D: +13.4° (*c*: 1.0, CHCl₃); ¹H NMR (CDCl₃, 300 MHz): δ 0.85 (3H, *t*, *J* = 7.49 Hz), 1.69 (2H, *m*), 2.64 (1H, *td*, *J*₁ = 5.03 Hz, *J*₂ = 4.72 Hz), 4.95 (1H, *d*, *J* = 5.33 Hz), 7.32 (5H, *m*); MS (*ES*⁺): *m/e* calculated for C₁₂H₁₆O₃ (*M*⁺) 208.1099, found 208.1108

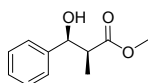


(2S,3S)-2-(Hydroxy-phenyl-methyl)-butyric acid methyl ester (132b): To a solution of 32 mg (0.165 mmol) (2S,3S)-2-(Hydroxy-phenyl-methyl)-butyric acid (**131b**) in 2 ml Et₂O at 0 °C was added drop-wise 2.20 ml (0.66 mmol) of 0.3 M CH₂N₂ in Et₂O. The reaction was stirred at 0 °C for 1 h, and *in vacuo* removal of volatiles afforded 34.2 mg (99%) of the desired ester as a colorless oil. R_f: 0.58 (SiO₂, 1:1 EtOAc:Hex); [α]_D: -13.5° (*c*: 1.0, CHCl₃); ¹H NMR (CDCl₃, 300 MHz): δ 0.85 (3H, *t*, *J* = 7.49 Hz), 1.69 (2H, *m*), 2.64 (1H, *td*, *J*₁ = 5.03 Hz, *J*₂ = 4.72 Hz), 4.95 (1H, *d*, *J* = 5.33 Hz), 7.32 (5H, *m*); MS (*ES*⁺): *m/e* calculated for C₁₂H₁₆O₃ (*M*⁺) 208.1099, found 208.1110



(2R,3R)-3-Hydroxy-2-methyl-3-phenyl-propionic acid methyl ester (132c): To a solution of 20 mg (0.111 mmol) (2R,3R)-3-Hydroxy-2-methyl-3-phenyl-propionic

acid (**131c**) in 2 ml Et₂O at 0 °C was added drop-wise 0.148 ml (0.44 mmol) of a solution of 0.3 M CH₂N₂ in Et₂O. The reaction was stirred at 0 °C for 1 h, and *in vacuo* removal of volatiles afforded 21 mg (98%) of the desired ester as a colorless oil. R_f: 0.56 (SiO₂, 1:1 EtOAc:Hex); [α]_D: +22.6° (c: 1.0, CHCl₃); ¹H NMR (CDCl₃, 300 MHz): δ 1.11 (3H, d, J = 7.19 Hz), 2.78 (1H, dq, J₁ = 7.22 Hz, J₂ = 3.99 Hz), 2.88 (1H, d, J = 3.08 Hz), 5.1 (1H, app. t, J = 3.78 Hz), 7.30 (5H, m); MS (ES⁺): *m/e* calculated for C₁₁H₁₄O₃ (M⁺)194.0943, found 194.0945



(2S,3S)-2-Hydroxy-2-methyl-3-phenylpropionic acid methyl ester (132d): To a solution of 31 mg (0.172 mmol) (2S,3S)-3-Hydroxy-2-methyl-3-phenyl-propionic acid (**131d**) in 2 ml Et₂O at 0 °C was added drop-wise 0.213 ml (0.69 mmol) of a solution of 0.3 M CH₂N₂ in Et₂O. The reaction was stirred at 0 °C for 1 h, and *in vacuo* removal of volatiles afforded 33.1 mg (99%) of the desired ester as a colorless oil. R_f: 0.56 (SiO₂, 1:1 EtOAc:Hex); [α]_D: -23.3° (c: 1.0, CHCl₃); ¹H NMR (CDCl₃, 300 MHz): δ 1.11 (3H, d, J = 7.17 Hz), 2.78 (1H, dq, J₁ = 7.19 Hz, J₂ = 3.98 Hz), 2.88 (1H, s), 5.10 (1H, d, J = 3.64 Hz); MS (ES⁺): *m/e* calculated for C₁₁H₁₄O₃ (M⁺)194.0943, found 194.0952

6.3 HPLC EXPERIMENTS

6.3.1 General

For HPLC experiments a HP 1090 HPLC system with diode array detection (System 1), or a system consisting of a Waters 616 pump, Waters 600S flow controller, and a HP 1050 DAD (System 2) were employed. These instruments were controlled, the data collected, and

analyzed using HP ChemStations (Hewlett Packard, Rev. A06.03 [509], 1998). The following columns were used: 5 μ particle size, 250 x 4.6 mm Supelco Supelcosil silica column, Astec Cyclobond-I column, and Alltech/Applied Science 10 μ , 300 x 4.1 mm VersaPak silica column. Separations were attempted at room temperature (22 \pm 5 $^{\circ}$ C), and solvents were purged with helium for 20 minutes before the first elution. The columns were allowed to equilibrate with the solvent system for 20 minutes prior to sample injection.

Chromatographic parameters k'_A (retention factor), N (number of theoretical plates), R_s (resolution factor), and α (selectivity factor) were calculated using:

$$k'_A = \frac{t_R - t_M}{t_M} \quad (1)$$

$$N = \frac{5.55t_R^2}{w_{1/2}^2} \quad (2)$$

$$R_s = \frac{2[(t_R)_B - (t_R)_A]}{W_A + W_B} \quad (3)$$

$$\alpha = \frac{k'_B}{k'_A} \quad (4)$$

where t_R is the retention time for the solute ((tR)_B > (tR)_A), t_M is the retention time for the mobile phase, $w_{1/2}$ is the peak width at half height, and W_A is the peak width at baseline for solute A. t_R , W_A (using the “tangents to point of inflections” method), and $w_{1/2}$ can be determined from the chromatogram as depicted in Figure 6-1. The symmetry of the peaks was calculated automatically by HP ChemStations.

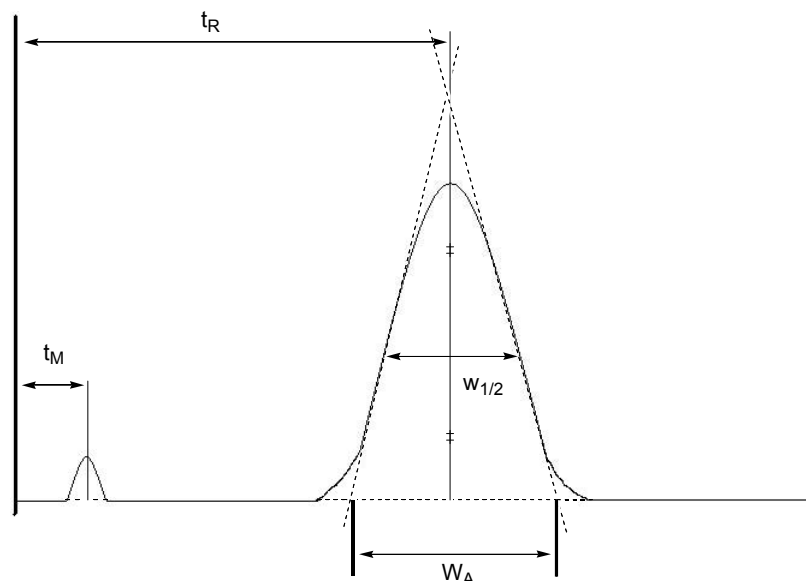


Figure 6-1: Definition of terms t_R , t_M , W_A , and $w_{1/2}$

6.3.2 NPLC Retention of OEG Esters

6.3.2.1 Supelcosil Silica Column

The general procedure outlined in section 6.3.1 was followed. HPLC system 1 was employed. A 5μ particle size, 250 x 4.6 mm Supelco Supelcosil silica column was used. The samples contained 10^{-2} M each of esters **72b-76e**. The flow rate was 1 ml/min. Detection was at 265 nm. The following gradient elution protocol was developed: 3:7 EtOAc: Hex to 8:2 EtOAc:Hex in 20 minutes. HPLC experiments were done in triplicate. The relative elution order was determined by injection of single component samples, and comparison of real-time UV-vis spectra of the separatory regions. Relevant chromatographic parameters are given in Table 6-1 and standard deviations of retention times are given in Table 6-2.

Table 6-1: t_R (retention time), k' (retention factor), N (number of theoretical plates), R_s (resolution factor), and symmetry values for the chromatogram obtained with the 5 μ Supelcosil column (*Gradient: 3:7 EtOAc: Hex to 8:2 EtOAc:Hex in 20 min, 10⁻² M sample, flow-rate: 1ml/min*) ^a R_s is defined with respect to the precedent peak. ^bNot present in sample. ^cOverlaps with 72c.

	b	c	d	e	
72	t_R	4.56	6.89	11.37	18.53
	k'	0.75	1.65	3.37	6.13
	N	26100	27700	43000	35300
	R_s	- ^a	8.71	12.11	15.95
	<i>symm.</i>	0.784	0.669	0.517	0.303
73	t_R	- ^b	- ^c	11.74	19.45
	k'	- ^b	- ^c	3.52	6.48
	N	- ^b	- ^c	33500	34100
	R_s	- ^b	- ^c	1.57	2.52
	<i>symm.</i>	- ^b	- ^b	0.449	0.271
74	t_R	- ^b	7.26	12.16	19.99
	k'	- ^b	1.79	3.68	6.69
	N	- ^b	30800	42400	27300
	R_s	- ^b	2.17	1.57	0.96
	<i>symm.</i>	- ^b	0.744	0.462	0.311
75	t_R	5.28	8.36	13.45	21.30
	k'	1.03	2.22	4.17	7.19
	N	28400	37700	55600	31500
	R_s	5.28	6.04	4.60	2.18
	<i>symm.</i>	0.781	0.747	0.468	0.243
76	t_R	5.60	8.90	14.39	23.13
	k'	1.15	2.42	4.53	7.90
	N	27600	35300	63700	30400
	R_s	2.32	2.85	3.54	3.21
	<i>symm.</i>	0.754	0.695	0.460	0.205

Table 6-2: Standard deviation for retention times of OEG esters **72b-75e** on the Supelcosil column. ^aminutes; ^btrial #1, ^ctrial #2, ^dtrial #3. Average % standard deviation for the retention times was found to be 3.75 %.

Peak	ID	#1 ^{a,b}	#2 ^{a,c}	#3 ^{a,d}	Average ^a	Std ^a	% Std
1	72b	4.60	4.55	4.33	4.49	0.14	3.09
2	75b	5.28	5.22	4.95	5.15	0.18	3.44
3	76b	5.60	5.53	5.23	5.46	0.20	3.59
4	72c	6.89	6.80	6.38	6.69	0.27	4.08
5	74c	7.26	7.15	6.67	7.03	0.31	4.45
6	75c	8.36	8.25	7.70	8.10	0.35	4.37
7	76c	8.90	8.77	8.18	8.62	0.38	4.45
8	72d	11.37	11.17	10.39	10.98	0.52	4.70
9	73d	11.73	11.50	10.65	11.29	0.57	5.04
10	74d	12.16	11.89	11.03	11.70	0.59	5.04
11	75d	13.45	13.16	12.44	13.02	0.52	3.98
12	76d	14.39	14.20	13.48	14.02	0.48	3.42
13	72e	18.53	18.45	17.58	18.19	0.52	2.88
14	73e	19.45	19.37	18.41	19.08	0.58	3.04
15	74e	19.99	19.90	18.95	19.61	0.57	2.92
16	75e	21.30	21.22	20.33	20.95	0.54	2.57
17	76e	23.13	23.03	22.04	22.73	0.60	2.66

6.3.2.2 VersaPak Silica Column

The general procedure outlined in section 6.3.1 was followed. HPLC system 1 was employed. An Alltech/Applied Science 10 μ , 300 x 4.1 mm VersaPak silica column was used. The samples contained 10⁻² M each of esters **72b-76e**. The flow rate was 1 ml/min. Detection was at 265 nm. The following gradient elution protocol was developed: 3:7 EtOAc: Hex to 8:2 EtOAc:Hex in 20 minutes. This protocol was not optimized for this particular column. The relative elution order was determined by injection of single component samples, and comparison of real-time UV-vis spectra of the separatory regions. Relevant chromatographic parameters are given in Table 6-3. A single HPLC experiment was performed.

Table 6-3: t_R , k' , N , R_s , W_a , $w_{1/2}$, and symmetry values for the chromatogram obtained with the Alltech/Applied Science 10 μ , 300 x 4.1 mm VersaPak silica column (Gradient: 3:7 EtOAc: Hex to 8:2 EtOAc:Hex in 20 min, 10^{-2} M sample, flow-rate: 1ml/min). ^a R_s is defined with respect to the precedent peak, ^boverlaps with 73c, ^coverlaps with 73d, ^doverlaps with 73e.

Peak	Identity	t_R	k'	N	R_s^a	W_a	$W_{1/2}$	symmetry
1	72b	1.09	1.72	7986	-	0.27	0.14	0.79
2	75b	1.52	2.27	9366	3.76	0.31	0.16	0.87
3	76b	1.62	2.41	9410	0.84	0.34	0.17	0.80
4	72c ^b	2.36	3.37	5899	4.56	0.50	0.27	0.76
5	74c	2.55	3.61	10092	1.06	0.42	0.22	0.85
6	75c	3.10	4.33	13203	3.20	0.48	0.22	0.98
7	76c	3.23	4.49	12627	0.68	0.50	0.23	0.86
8	72dc	4.32	5.92	14776	5.61	0.52	0.27	0.82
9	74d ^c	4.68	6.38	10576	1.63	0.60	0.34	1.16
10	75d	5.25	7.12	16696	2.57	0.56	0.30	0.80
11	76d	5.51	7.46	18745	1.23	0.55	0.29	0.82
12	72e	6.82	9.16	15097	5.30	0.73	0.39	0.71
13	74e ^d	7.37	9.88	9812	1.65	1.02	0.52	0.85
14	75e	7.87	10.52	16824	1.41	0.80	0.42	0.67
15	76e	8.32	11.11	15112	1.41	0.88	0.46	0.65

6.3.2.3 Cyclobond-I Cyclodextrin Column

The general procedure outlined in section 6.3.1 was followed. HPLC system 1 was employed. An Astec Cyclobond-I column was used. The samples contained 10^{-2} M each of esters **72b-76e**. The flow rate was 1 ml/min. Detection was at 265 nm. The following gradient elution protocol was developed: 3:7 EtOAc: Hex to 8:2 EtOAc:Hex in 20 minutes. This protocol was not optimized for this particular column. The relative elution order was determined by injection of single component samples, and comparison of real-time UV-vis spectra of the separatory regions. The chromatogram is reproduced in Figure 6-2, along with a comparison of real-time UV-vis spectra of analytes eluting in separatory region 3 on the Supelcosil, and Cyclobond-I columns. Chromatographic parameters were not calculated. A single HPLC experiment was performed. The only difference in the elution order was observed for OEG esters **73b-e**, which eluted first in their respective separatory regions.

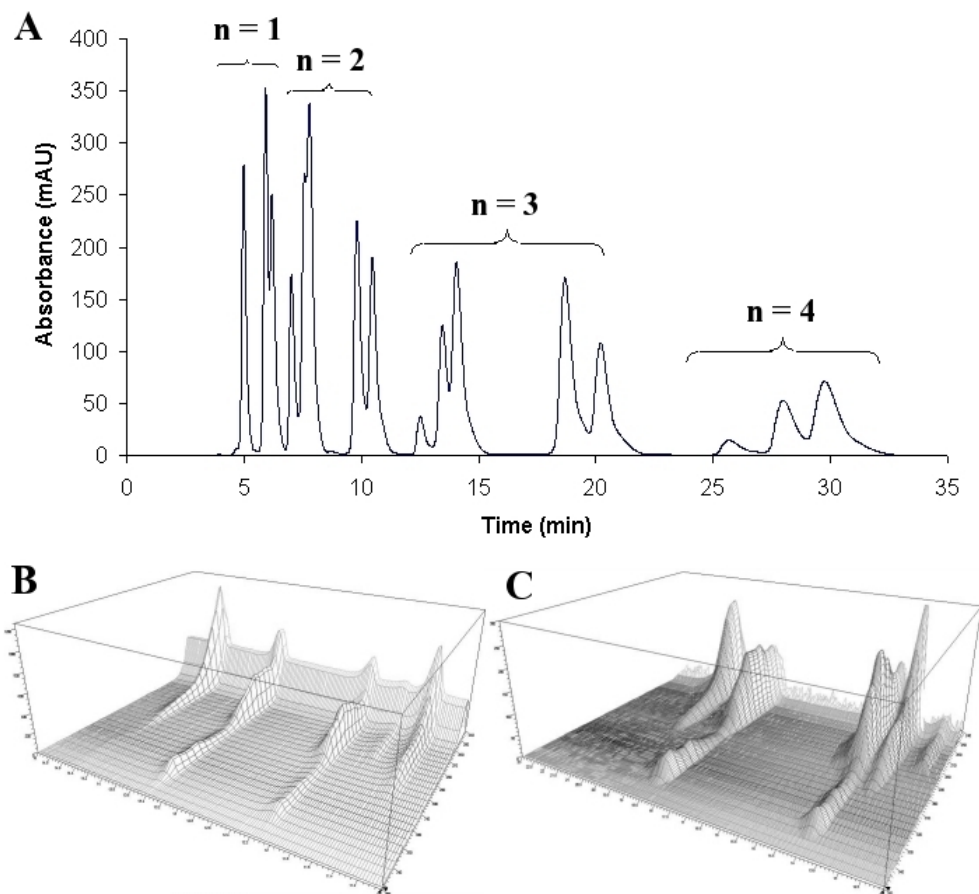


Figure 6-2: Chromatogram for samples **72b-76e** on an Astec Cyclobond-I column (3:7 EtOAc: Hex to 8:2 EtOAc:Hex in 20 minutes, 1ml/min, 10 μ l injection, 10^{-2} M each of 72e-76e, detection at 265 nm). B. Real-time UV-vis spectra of analytes eluting in separatory region 3 on the Supelcosil column. C. Real-time UV-vis spectra of analytes eluting in separatory region 3 on the Cyclobond column. Comparison of A, and C establishes elution order.

6.3.3 Retention of DiOEGylated Esters on Silica

The general procedure outlined in section 6.3.1 was followed. HPLC system 2 was employed. An Alltech/Applied Science 10 μ particle size, 100 \AA pore size, 300 x 4.1 mm VersaPak silica column was used. The samples contained 10^{-3} M each of esters **89e-g**, and **93a-95c**. A flow-rate of 1 ml/min was employed, and for each run 10 μ l of the sample was injected. Gradient elution was required for optimum separation. The gradient was 2:8 EtOAc:Hexane to

5% IPA in EtOAc in 35 minutes. Detection was done at 295 nm. The identities of the peaks were determined by comparing the elution times of ester sets {89e, 93a-c}, {89f, 94a-c}, {89g, 95a-c} to those of the original mixture. Purity of the peaks was assigned based on real time UV-vis spectra of the peaks. The elution order of the diOEGylated esters is provided in Figure 6-3, the relevant chromatogram is reproduced in Figure 6-4, relevant chromatographic parameters are given in Table 6-4, and standard deviations for retention times are given in Table 6-5.

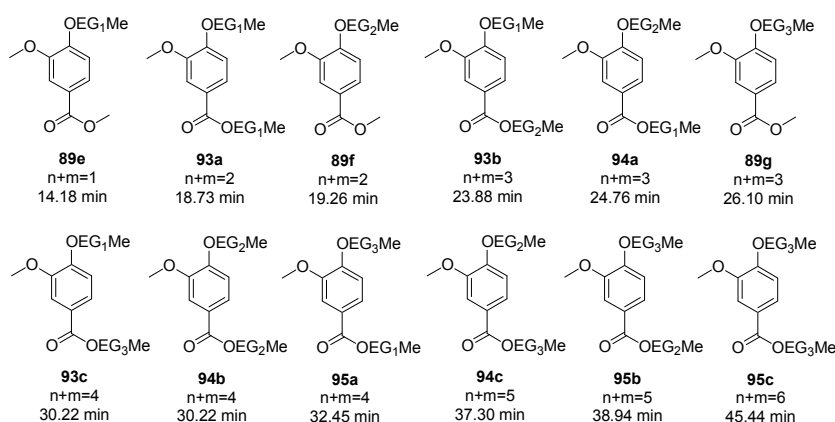


Figure 6-3: Elution times of diOEGylated vanillic acid derivatives.

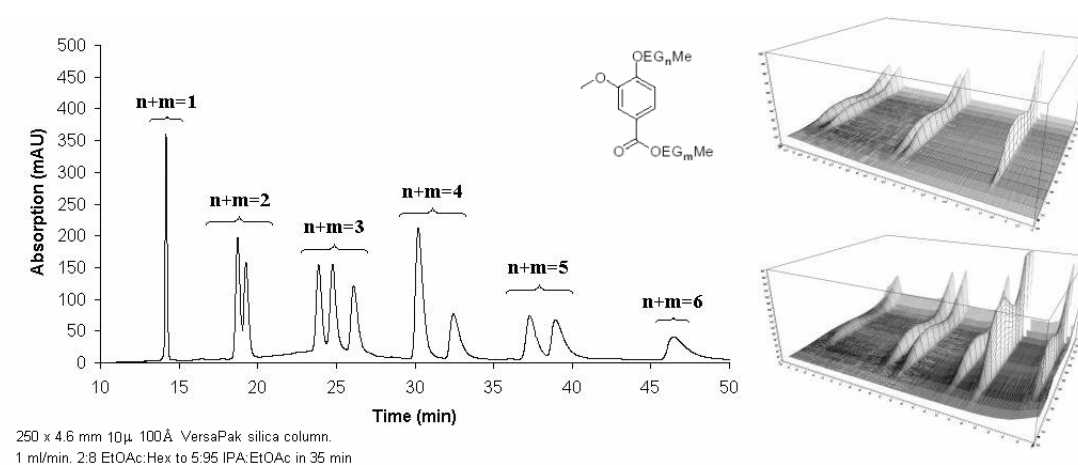


Figure 6-4: (Left) Elution of a mixture of 89e-g, and 93a-95c (10 μ VersaPak silica column, 10⁻³ M, 10 μ l injection, 2:8 EtOAc:Hexane to 5:95 IPA:EtOAc in 35 min, 295 nm). (Right) Real-time UV-Vis spectra of the peaks.

Table 6-4: t_R , k' , R_s , N , and symmetry values for the chromatogram in Figure 8. ^a**93c**, and **94b** overlap completely.

Peak #	ID	m+ n	t_R (min)	k'	R_s	N	Symmetry
1	89e	1	14.18	4.45	-	55200	0.818
2	93a	2	18.73	6.20	10.94	22200	0.849
3	89f	2	19.26	6.41	0.89	19900	0.776
4	93b	3	23.88	8.18	6.82	18500	0.893
5	94a	3	24.76	8.52	1.14	17100	0.632
6	89g	3	26.10	9.04	1.54	14600	0.567
7	93c^a	4	30.22	10.62	4.38	20400	0.572
8	95a	4	32.45	11.48	2.04	14600	0.467
9	94c	5	37.30	13.35	3.84	17300	0.532
10	95b	5	38.94	13.98	1.15	13900	4.439
11	95c	6	45.44	16.48	3.92	11600	0.402

Table 6-5: Determination of elution order of **89e-g**, and **93a-95c** through averaging of a number of HPLC experiments. ^amin; ^b**89e-g**, and **93a-95c**; ^c**89e**, and **93a-c**; ^d**89g**, and **94a-c**; ^e**89f**, and **95a-c**; ^faverage of retention times (min); ^gstandard deviation of retention times (min); ^h% standard deviation of retention times. Average standard deviation of retention times was found to be ~1.5 %.

ID	#1 ^{a,b}	#2 ^{a,b}	#3 ^{a,b}	#4 ^{a,c}	#5 ^{a,d}	#6 ^{a,b}	#7 ^{a,c}	#8 ^{a,e}	#9 ^{a,d}	#10 ^{a,e}	Av. ^f	STD ^g	%STD ^h
89e	14.18	13.75	13.74	13.85	-	13.8	14.14	-	-	-	13.91	0.20	1.42
93a	18.73	18.22	18.2	18.05	-	18.35	18.63	-	-	-	18.36	0.26	1.44
89f	19.26	18.56	18.53	-	-	18.64	-	18.88	-	19.05	18.82	0.29	1.57
93b	23.88	23.29	23.25	23.74	-	23.45	23.73	-	-	-	23.56	0.26	1.11
94a	24.76	24.1	24.04	-	-	24.27	-	24	-	24.9	24.34	0.39	1.60
89g	26.1	25.4	25.31	-	25.74	25.58	-	-	24.89	-	25.50	0.41	1.61
93c	30.22	29.55	29.41	29.83	-	29.62	29.74	-	-	-	29.73	0.28	0.95
94b	30.22	29.55	29.41	-	-	29.62	-	29.79	-	30.5	29.85	0.42	1.42
95a	32.45	31.89	31.68	-	31.91	31.94	-	-	31.05	-	31.82	0.46	1.43
94c	37.3	36.72	36.38	-	-	36.14	-	35.5	-	36.3	36.39	0.60	1.65
95b	38.94	38.52	38.09	-	37.76	37.69	-	-	37.37	-	38.06	0.58	1.53
95c	46.41	46.41	45.76	-	44.81	44.76	-	-	44.82	-	45.50	0.80	1.76

6.3.4 NPLC Analysis of OEGylated Aldol Adducts

The general procedure outlined in section 6.3.1 was followed. HPLC system 1 was employed. A 5 μ particle size, 250 x 4.6 mm Supelco Supelcosil silica column was used. The samples contained 10⁻³ M each of OEGylated aldol adducts **132a-d**. The flow rate was 1 ml/min.

Detection was at 275 nm. After some experimentation it was found that a rather steep gradient (1:1 EtOAc:Hexane to EtOAc in 5 min, then EtOAc to 5% IPA in EtOAc in 3 minutes) was required to ensure elution of the peaks in a narrow timeframe. HPLC experiments were done in triplicate. The relative elution order was determined by injection of single component samples, and comparison of real-time UV-vis spectra of the separatory regions. The chromatogram is reproduced in Figure 6-5, and relevant chromatographic parameters are given in Table 6-6.

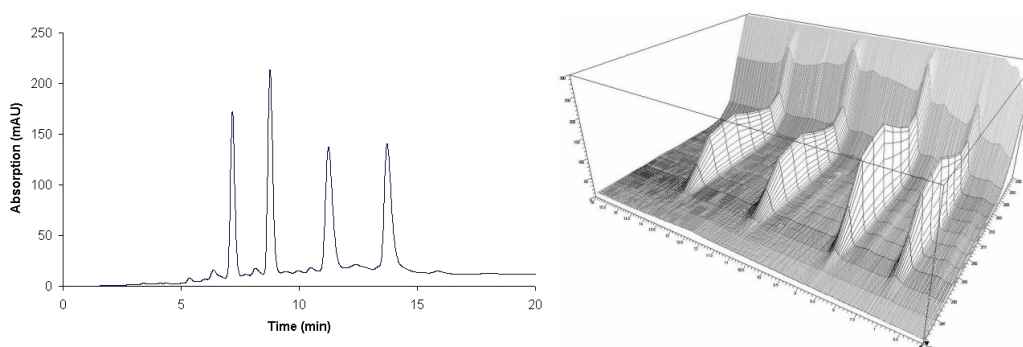


Figure 6-5: Chromatogram for a mixture of 10^{-3} M each of **132a-d**. 1 ml/min flow-rate, 10 μ l injection, 1:1 EtOAc:Hexane to EtOAc in 5 min, then EtOAc to 5% IPA in EtOAc in 3 minutes. 275 nm detection.

Table 6-6: Chromatographic parameters for the peaks in Figure 6-5.

peak	ID	t_R	k'	N	R_s	W_A	$w_{1/2}$	Symmetry
1	132a	7.17	2.59	6391	-	0.265	0.211	0.813
2	132b	8.76	3.38	7862	4.56	0.434	0.233	0.769
3	132c	11.24	4.62	5606	4.60	0.643	0.354	0.675
4	132d	13.73	5.86	7728	3.84	0.650	0.368	0.656

6.3.5 Chiral HPLC Analysis of **132a-d**

The general procedure outlined in section 6.3.1 was followed. HPLC system 2 was employed. An Chiral Technologies 5 μ , 250 mm x 4.6 mm Chiracel OD-H chiral column was used. The samples contained 10^{-2} M each of **132a-132d**. A flow-rate of 0.75 ml/min was employed, and for each run 10 μ l of the sample was injected. Isocratic elution with 5% (v/v) IPA in Hexanes was found to give optimal separation. Detection was done at 210 nm. The identities of the peaks were determined by comparing the elution times of single component samples of **132a-d** to those of binary mixtures of the enantiomeric pairs. Purity of the peaks was assigned based on real-time UV-Vis spectra of the peaks. The reported % ee values were based on the average of % ee's determined at 210 nm, and 254 nm. The chromatograms, and real-time UV-Vis spectra for these compounds are reproduced in Figures 6-6, and 6-7. Relevant chromatographic parameters are given in Table 6-7.

Table 6-7: Chromatographic parameters for the chiral separation of **132a-d**.

Peak	ID	t_R	k'	N	R_s	% ee	<i>Symm.</i>	W_A	$w_{1/2}$
1	132a	10.19	4.10	6900	-	99	0.813	0.541	0.289
2	132b	11.66	4.83	6700	2.54	99	0.79	0.618	0.337
1	132c	11.80	4.90	6000	-	95	0.775	0.660	0.360
2	132d	13.65	5.83	5600	2.58	95	0.692	0.777	0.428

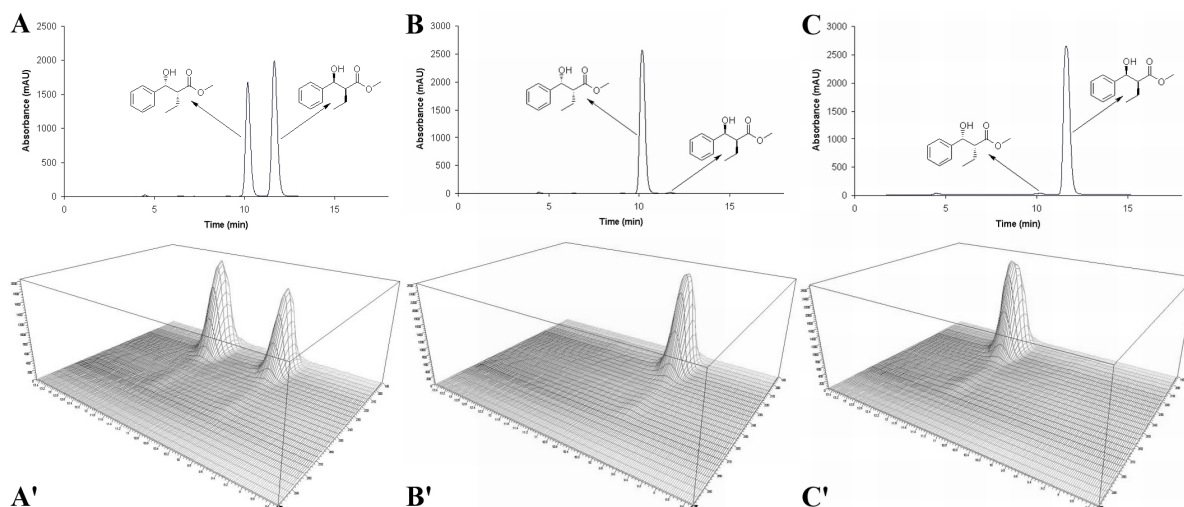


Figure 6-6: Chromatograms and real-time UV-vis spectra for a sample containing approximately equimolar amounts of **132a-b** (*A, A'*), for a sample of **132a** obtained as a product of the synthetic work (*B, B'*), and for a sample of **132b** obtained as a product of the synthetic work (*C, C'*). Chiracel OD-H column, 0.75 ml/min, 10^{-2} M samples, 10 μ l injections, isocratic elution with 5 % (*v/v*) IPA in hexane.

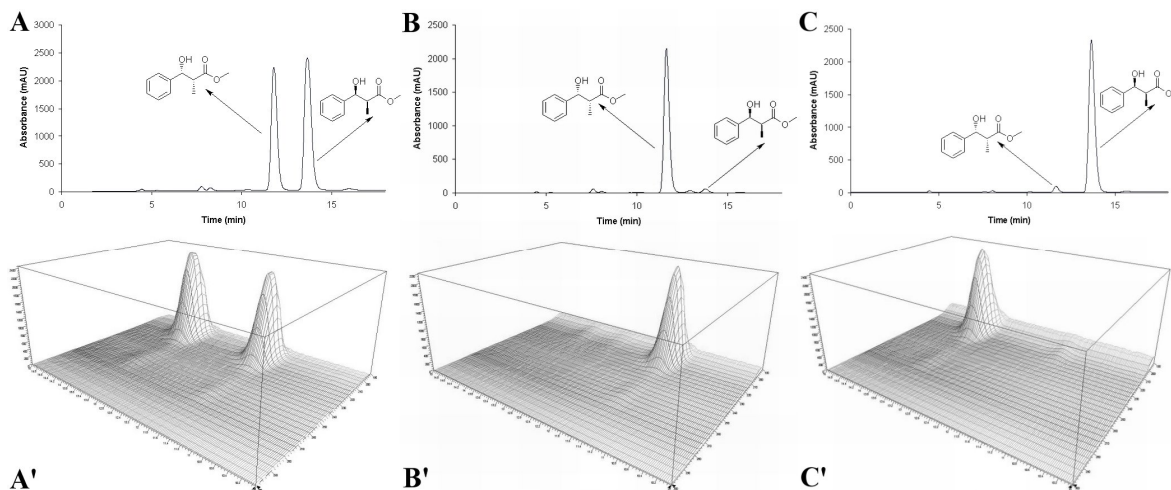


Figure 6-7: Chromatograms, and real-time UV-vis spectra for a sample containing approximately equimolar amounts of **132c-d** (*A, A'*), for a sample of **132c** obtained as a product of the synthetic work (*B, B'*), and for a sample of **132d** obtained as a product of the synthetic work (*C, C'*). Chiracel OD-H column, 0.75 ml/min, 10^{-2} M samples, 10 μ l injections, isocratic elution with 5 % (*v/v*) IPA in hexane.

6.4 TLC EXPERIMENTS

6.4.1 Preparation of TLC Plates and Method of Data Acquisition

The TLC plates (*Analytical E. Merck precoated (25 mm) silica gel 60F-254, cut to dimensions of 50 mm X 25 mm*) were dried in an oven at 150 °C for at least 12 hours. After being cooled in a desiccator, they were dipped into aqueous solutions of LiCl of desired molarity, or into aqueous saturated solutions of NaCl or KCl. Control plates were dipped into distilled water. The dipped plates were wiped with Kimwipes to remove excess liquid, air dried for 4 hours, and then further dried in an oven at 150 °C for 12 hours, after which they were cooled in a desiccator. The TLC plates were developed to a solvent front of 4 cm, and visualization was done by UV lamp (254 nm), and CAM staining.

6.4.2 Determination of Salt Concentration on TLC Plates

The amount of metal salts deposited on the TLC plates was determined by the difference of weight between dried TLC plates containing no metal salts, and those which were treated with metal salts. Three measurements for each class of TLC plate were averaged. The w/w concentration of metal salts was calculated based on the weight of the silica scraped off dried, untreated TLC plates. Care was taken to ensure that the TLC plates were cut in identical dimensions. It was found that the silica concentration on TLC plates was 11.52 mg/cm², or 144 mg per 50 mm X 25 mm silica plate. Metal ion concentrations on the TLC plates are given in Table 1.

Table 6-8: Salt concentrations on TLC plates. ^aConcentration of LiCl in dipping solution; ^bdipping solution was saturated aqueous NaCl; ^cdipping solution was saturated aqueous KCl; ^dquantity per TLC plate; ^evalues per cm² of TLC plate; ^fsilica density on TLC plates is approximately 11.52 mg/cm²

Entry	[Salt]	W ₀ (g)	W _f (g)	W _{salt} (mg)	Av. W _{Salt} (mg) ^d	Av. [Salt] (mg/cm ²) ^e	Av. [Salt] (mol/cm ²) ^e	% Salt (w/w) ^f
1	1.3 ^a	4.1269	4.1374	10.5				
2	1.3 ^a	3.9534	3.9605	7.1	9.07	0.73	1.72 x 10 ⁻⁵	6.0
3	1.3 ^a	4.1332	4.1428	9.6				
4	2.6 ^a	4.0616	4.0820	20.4				
5	2.6 ^a	3.8243	3.8448	20.5	19.73	1.58	3.73 x 10 ⁻⁵	12.1
6	2.6 ^a	4.0795	4.0978	18.3				
7	3.9 ^a	4.1877	4.2238	36.1				
8	3.9 ^a	3.8238	3.8578	34.0	35.13	2.81	6.63 x 10 ⁻⁵	19.6
9	3.9 ^a	4.1383	4.1736	35.3				
10	5.2 ^a	4.0518	4.1011	49.3				
11	5.2 ^a	4.1190	4.1643	45.3	46.3	3.7	8.73 x 10 ⁻⁵	24.3
12	5.2 ^a	3.8484	3.8927	44.3				
13	6.5 ^a	3.8143	3.8756	61.3				
14	6.5a	3.9354	3.9917	56.3	57.93	4.63	1.09 x 10 ⁻⁴	28.7
15	6.5a	4.0306	4.0868	56.2				
16	7.8a	3.9824	4.0572	74.8				
17	7.8 ^a	4.1716	4.2428	71.2	72.2	5.78	1.36 x 10 ⁻⁴	33.4
18	7.8 ^a	3.9323	4.0028	70.5				
19	- ^b	3.8005	3.8625	62				
20	- ^b	3.8695	3.9397	70.2	65.1	5.2	8.9 x 10 ⁻⁵	31.1
21	- ^b	3.9860	4.0493	63				
22	- ^c	3.8475	3.9044	57				
23	- ^c	4.0550	4.1122	57.2	56.7	4.54	6.1 x 10 ⁻⁵	28.3
24	- ^c	3.9205	3.9767	56.2				

6.4.3 Optimization of LiCl Concentration on TLC Plates

Table 6-9: Optimization of [LiCl] for optimum separation of OEG esters. Esters **75b-e** were used in this study. Average values for 3 measurements are given. Standard deviation was ± 5 %.

Entry	[LiCl] in Solution	[LiCl] on Silica (mg/cm ²)	[LiCl] on Silica (mol/cm ²)	75b	75c	75d	75e
1	0	0	0	0.7	0.6	0.46	0.34
2	1.3	0.73	1.72 x 10 ⁻⁵	0.75	0.64	0.33	0.18
3	2.6	1.58	3.73 x 10 ⁻⁵	0.76	0.63	0.34	0.19
4	3.9	2.81	6.63 x 10 ⁻⁵	0.70	0.60	0.34	0.16
5	5.2	3.7	8.73 x 10 ⁻⁵	0.71	0.59	0.22	0.11
6	6.5	4.63	1.09 x 10 ⁻⁴	0.70	0.59	0.22	0.10

6.4.4 Effect of Cation Identity, and Solvent Composition on Retention of OEG Esters on Silica TLC Plates

Table 6-10: Separation of esters **75b-e** by TLC under various conditions. R_f values are an average of 3 measurements. ^aConc. of metal ions on the surface of the TLC plate; ^b R_f values; ^c1:1 EtOAc:Hex; ^d1:1 DME:Hex; ^e1:1 THF:Hex; ^f0.1 M LiClO₄ in EtOAc; ^g1 M LiClO₄ in EtOAc; ^hVariation in R_f values was \pm 5%.

Entry	[M ⁺] (mol/cm ²) ^a	75b ^{b,h}	75c ^{b,h}	75d ^{b,h}	75e ^{b,h}	Eluent
1	0	0.70	0.60	0.46	0.34	EtOAc
2	8.73 x 10 ⁻⁵ (Li ⁺)	0.71	0.59	0.22	0.11	EtOAc
3	8.9 x 10 ⁻⁵ (Na ⁺)	0.75	0.63	0.48	0.38	EtOAc
4	6.1 x 10 ⁻⁵ (K ⁺)	0.78	0.68	0.53	0.33	EtOAc
5	0	0.50	0.29	0.15	0.08	^c
6	8.73 x 10 ⁻⁵ (Li ⁺)	0.56	0.34	0.08	0.03	^c
7	8.73 x 10 ⁻⁵ (Li ⁺)	0.59	0.48	0.30	0.20	^d
8	8.73 x 10 ⁻⁵ (Li ⁺)	0.78	0.75	0.68	0.62	DME
9	8.73 x 10 ⁻⁵ (Li ⁺)	0.58	0.45	0.23	0.11	^e
10	8.73 x 10 ⁻⁵ (Li ⁺)	0.64	0.58	0.50	0.39	THF
11	0	0.73	0.65	0.51	0.38	^f
12	0	0.75	0.64	0.61	0.58	^g
13	3.73 x 10 ⁻⁵ (Li ⁺)	0.78	0.65	0.43	0.30	^g

6.4.5 Effect of LiCl on the Retention of DiOEGylated Esters

Table 6-11: R_f values, standard deviations and % standard deviations for esters **89e-g**, and **93a-95c** on silica TLC plates dried after immersion into 0 M and 2.6 M aqueous LiCl solutions. Note the enhanced separation (*underlined*) of **93a/89f**, and **93c/94b** with respect to the chromatogram in Figure 8. Average standard deviation was \pm ~4 %.

ID	m + n	R_f (0 M Li ⁺)						R_f (2.6 M Li ⁺)							
		1st	2nd	3rd	Av.	Std.	% Std.	1st	2nd	3rd	Av.	Std.	% Std.		
89e	1	0.62	0.60	0.60	0.61	0.012	1.97	0.51	0.49	0.53	0.51	0.02	3.92		
93a	2	0.53	0.49	0.53	0.51	0.023	4.51	0.43	0.44	0.43	0.43	0.006	1.4		
89f	2	0.48	0.46	0.48	0.47	0.012	2.55	0.35	0.38	0.35	0.36	0.017	4.72		
93b	3	0.43	0.41	0.43	0.42	0.012	2.86	0.37	0.37	0.35	0.36	0.012	3.33		
94a	3	0.36	0.37	0.37	0.37	0.006	1.62	0.32	0.32	0.30	0.31	0.011	3.55		
89g	3	0.31	0.33	0.33	0.32	0.012	3.75	0.20	0.22	0.20	0.21	0.012	5.71		
93c	4	0.30	0.30	0.32	0.31	0.012	3.87	0.21	0.19	0.19	0.20	0.012	6		
94b	4	0.30	0.30	0.32	0.31	0.012	3.87	0.29	0.28	0.28	0.28	0.006	2.14		
95a	4	0.30	0.30	0.32	0.31	0.012	3.87	0.21	0.19	0.19	0.20	0.012	6		
94c	5	0.22	0.26	0.23	0.24	0.021	8.75	0.12	0.13	0.13	0.12	0.006	5		
95b	5	0.22	0.25	0.23	0.23	0.015	6.52	0.10	0.10	0.10	0.10	0	0		
95c	6	0.20	0.21	0.18	0.20	0.015	7.5	0.07	0.08	0.08	0.08	0.006	7.5		
						Av. % Std.	4.3							Av. % Std.	4.11

APPENDIX A

ABBREVIATIONS

AAC	Acyl halide-aldehyde cyclocondensation
AIBN	2,2'-azobisisobutyronitrile
AM1	Austin Model 1
ANOVA	Analysis of variance
Bfp	Bisfluorous chain type propanoyl
Boc	<i>tert</i> -Butoxycarbonyl
BTF	Benzyltrifluoride
COSMO	Conductor-like screening model
DEAD	Diethyl azodicarboxylate
DIPEA	Diisopropylethylamine
DMAP	4-Dimethylaminopyridine
DME	Dimethoxyethane
DMF	Dimethylformamide
DMSO	Dimethyl sulfoxide
DP	Degree of polymerization
dppp	1,3-bis(diphenylphosphino)propane (F-dppp is the fluororous analogue)
DSC	Differential scanning calorimetry
EA	Evans auxiliary
EDCI	1-ethyl-3-[-(dimethylamino)propyl]-carbodiimide hydrochloride
EEC	Enthalpy-entropy compensation
EG	Ethylene glycol (monomer of OEG)
EST	Excess substrate tagging
F-DEAD	Fluorous analogue of DEAD
F-HPLC	Fluorous HPLC
F-LLE	Fluorous liquid-liquid extraction
FMOC	(9H-Fluoren-9-yl)-methyl (F ^t FMOC is the fluororous analogue)
FMS	Fluorous mixture synthesis
FRP	Fluorous reversed phase
F-SPE	Fluorous solid phase extraction
HILIC	Hydrophobic interaction liquid chromatography
HPLC	High performance (or pressure) liquid chromatography
ICL	Indexed combinatorial library
ILSS	Ionic liquid supported synthesis
IPA	Isopropyl alcohol
LCMS	Liquid chromatography-mass spectrometry

LCNMR	Liquid chromatography-nuclear magnetic resonance spectroscopy
LCPS	Liquid phase combinatorial synthesis
LDA	Lithium diisopropylamide
LHMDS	Lithium 1,1,1,3,3,3-hexamethyldisilazane
Li-TLC	Lithium thin layer chromatography
LPS	Liquid phase synthesis
MOE	2-methoxyethanol
MOM	methoxymethyl
MPEG	Poly(ethyleneglycol) ω -monomethyl ether
NMR	Nuclear magnetic resonance
NPLC	Normal phase liquid chromatography
OEG	Oligomeric ethylene glycol
OEG-EA	Oligomeric ethylene glycol appended Evans auxiliary
PEG	Polyethylene glycol
PFMC	Perfluoromethylcyclohexane
PMB	<i>p</i> -Methoxybenzyl
PVA	Polyvinylalcohol
PyBOP	1-Yl-oxytritypyrrolidinophosphonium hexafluoride
RD	Recursive deconvolution
RPLC	Reversed phase liquid chromatography
SANS	Small-angle neutron scattering
SEC	Size exclusion liquid chromatography
SPOS	Solid phase organic synthesis
TEA	Triethylamine
THF	Tetrahydrofuran
TLC	Thin layer chromatography

BIBLIOGRAPHY

Chapter 1

1. Merrifield, R. B., *J. Am. Chem. Soc.*, **1963**, *85*, 2149-54
2. Furka, A.; Sebastyen, F.; Asgedom, M., and Dibo, G., *Abstr. 14th Int. Congr. Biochem. Prague, Czechoslovakia*, **1988**, *5*, 47
3. ^aLam, K. S.; Salmon, S. E.; Hersch, E. M.; Hruby, V. J.; Kazmierski, W. M.; Knapp, R. J., *Nature*, **1991**, *354*, 82-84 ;^bHoughten, R. A.; Pinilla, C.; Blondelle, C.; Appel, J. R.; Dooley, C. T.; Cuervo, J. H., *Nature*, **1991**, *354*, 84-86
4. ^aGravet, D. J.; Janda, K. D., *Chem. Rev.*, **1997**, *97*, 489-509; ^bToy, P. H.; Janda, K. D. *Acc. Chem. Res.*, **2000**, *33*, 546-554
5. ^aTerrett, N. K., *Combinatorial Chemistry*, 1998, Oxford University Press, New York, p. 64-66; ^b*ibid.*, p. 55-76; ^c*ibid.*, p. 77-94
6. Weishi, M.; Chan, T. H., *Acc. Chem. Res.*, **2006**, *39*, 897-908
7. Han, H.; Wolfe, M. M.; Brenner, S.; Janda, K. K., *Proc. Natl. Acad. Sci. USA*, **1995**, *92*, 6419-6423
8. ^aDouglas, P. D.; Whitfield, D. M.; Krepsinski, J. J., *J. Am. Chem. Soc.*, **1995**, *117*, 2116-2117; ^bTjogen, F-S.; Tong, E. K.; Hodges, R. S., *J. Org. Chem.*, **1978**, *43*, 4190; ^cBonora, G. M.; Scremin, C. L.; Colonna, F. P.; Garbesi, A., *Nucleic Acids Res.*, **1990**, *18*, 3155;

- ^dBonora, G. M.; Maffine, M.; Scremin, C. L., *Nucleic Acids Res.*, **1993**, *21*, 1213; ^eHan, H.; Janda, K. M., *J. Am. Chem. Soc.*, **1996**, *118*, 2539-2544
9. Erb, E.; Janda, K. K.; Brenner, S., *Proc. Natl. Acad. Sci. USA*, **1994**, *91*, 11422-11426
10. ^aHuang, K-T.; Sun, C-H., *Bioorg. Med. Chem. Lett.*, **2002**, *12*, 1001-1003; ^b Cheng, M-F.; Fang, J-M., *J. Comb. Chem.*, **2004**, *6*, 99-104; ^cRacker, R.; Doring, K.; Reiser, O. *J. Org. Chem.* **2000**, *65*, 6932-6939
11. Pirrung, M. C. *Chem. Rev.*, **1997**, *97*, 473-498
12. ^aPirrung, M. C.; Chen, J. *J. Am. Chem. Soc.*, **1995**, *117*, 1240-1245; ^bReprinted with permission from Pirrung, M. C.; Chen, J. *J. Am. Chem. Soc.*, **1995**, *117*, 1240-1245. Copyright 1995 American Chemical Society.
13. ^aAndrus, M. B.; Turner, T. M.; Sauna, Z. E.; Ambudkar, S. V. *J. Org. Chem.* **2000**, *65*, 4973-4983; ^bAndrus, M. B.; Asgari, D.; Wenke, L. *J. Org. Chem.* **1999**, *64*, 2978; ^cReprinted with permission from Andrus, M. B.; Turner, T. M.; Sauna, Z. E.; Ambudkar, S. V. *J. Org. Chem.* **2000**, *65*, 4973-4983. Copyright 2000 American Chemical Society.
14. Boger, D. L.; Tarby, C. M.; Myers, P. L.; Caporale, L. H. *J. Am. Chem. Soc.*, **1996**, *118*, 2109-2110
15. Cheng, S.; Comer, D. D.; Williams, J. P.; Myers, P.L.; Boger, D. L. *J. Am. Chem. Soc.*, **1996**, *118*, 2567-2573
16. ^aCarell, T.; Wintner, E. A.; Rebek, J. *Angew. Chem. Int. Ed. Engl.*, **1994**, *33*, 2061-2064;
17. For some reviews see: ^aHorváth, I. T. *Acc. Chem. Res.*, **1998**, *31*, 641-650; ^bBarthel-Rosa, L. P., Gladysz, J. A. *Coor. Chem. Rev.*, **1999**, *190-192*, 597-605; ^cCurran, D. P. *Angew. Chem. Int. Ed. Engl.*, **1998**, *37*, 1174-1196; ^dGladysz, J. A.; Curran, D. P. *Tetrahedron*,

- 2002**, 58, 3823-3825; ^eZhang, W. *Tetrahedron*, **2003**, 59, 4475-4489; ^fZhang, W., Curran, D. P. *Tetrahedron*, **2006**, 62, 11837-11865
18. Scott, R. L. *J. Am. Chem. Soc.*, **1948**, 70, 4090-4093
19. ^aHorváth, I. T.; Rábai, J. *Science*, **1994**, 266, 72-75; ^bFrom Horváth, I. T.; Rábai, J. *Science*, **1994**, 266, 72-75. Reprinted with permission from AAAS.
20. ^aCurran, D. P.; Hadida, S. *J. Am. Chem. Soc.*, **1996**, 118, 2531-2532; ^bCurran, D. P.; Hadida, S.; He, M. *J. Org. Chem.*, **1997**, 62, 6714-6715; ^cRyu, I.; Kreimerman, S.; Niguma, T.; Minakata, S.; Komatsu, M.; Lui, Z.; Curran, D. P. *Tetrahedron Lett.*, **2001**, 42, 947-950; ^dCurran, D. P. *Synlett.*, **2001**, 9, 1488-1496
21. ^aHoshino, M.; Degenkolb, P.; Curran, D. P. *J. Org. Chem.*, **1997**, 62, 8341-8349; ^bLarhed, M.; Hoshino, M.; Hadida, S.; Curran, D. P.; Halberg, A. *J. Org. Chem.*, **1997**, 62, 5583-5587; ^cOlofsson, K.; Kim, S-Y.; Larhed, M.; Curran, D. P.; Halberg, A. *J. Org. Chem.*, **1999**, 64, 4539-4541;
22. ^aDandapani, S.; Curran, D. P. *Tetrahedron*, **2002**, 58, 3855-3864; ^bCurran, D. P., Bajpai, R.; Sanger, E. *Adv. Synth. Catal.*, **2006**, 348, 1621-1624; ^cDandapani, S.; Curran, D. P. *J. Org. Chem.*, **2002**, 69, 8751-8757; ^dCurran, D. P., Wang, X. Zhang, Q. *J. Org. Chem.*, **2005**, 70, 3716-3719; ^eRocaboy, C.; Gladsyz, J. A. *Chem. Eur. J.*, **2003**, 9, 88-95; ^fKaleta, Z.; Makowski, B. T.; Soós, T.; Dembinski, R. *Org. Lett.*, **2006**, 8, 1625-1628; ^gVallin, K. S. A.; Zhang, Q.; Larhed, M.; Curran, D.P.; Hallberg, A. *J. Org. Chem.*, **2003**, 68, 6639-6645; ^hMatsugi, M., Curran, D. P. *J. Org. Chem.*, **2004**, 69, 1636-1642; ⁱChu, Q.; Zhang, W.; Curran, D. P. *Tetrahedron, Lett.*, **2006**, 47, 9287-9290; ^jZu, L.; Li, H.; Wang, J.; Yu., X.; Wang, W. *Tetrahedron, Lett.*, **2006**, 47, 5131-5134; ^kLinclau, B.; Sing, A. K.; Curran, D. P. *J. Org. Chem.*, **1999**, 64, 2835-2842

23. ^aStuder, A.; Curran, D. P. *Tetrahedron*, **1997**, *53*, 6681-6696; ^bStuder, A.; Hadida, S.; Ferritto, R.; Kim, S-Y.; Jeger, P.; Wipf, P.; Curran, D. P., *Science*, **1997**, *275*, 823-826; ^cPalmacci, E. R.; Hewitt, M. C.; Seeberger, P. H. *Angew. Chem. Int. Ed. Eng.*, **2001**, *40*, 4433-4437; ^dMiura, T.; Hirose, Y.; Ohmae, M.; Inazu, T. *Org. Lett.*, **2001**, *3*, 3957-3950; ^eCurran, D. P.; Ogoe, C. *QSAR Comb. Sci.*, **2006**, *25*, 732-735; ^fLuo, Z.; Williams, J.; Read, R. W.; Curran, D. P. *J. Org. Chem.*, **2001**, *66*, 4261-4266; ^gSchwinn, D.; Bannwarth, W. *Helv. Chim. Acta*, **2002**, *85*, 255-264; ^hMatsugi, M.; Yamanaka, K.; Inomata, I.; Takekoshi, N.; Hasegawa, M.; Curran, D. P. *QSAR Comb. Sci.*, **2006**, *25*, 713-715; ⁱVillard, A-L.; Warrington, B. H.; Ladlow, M. *J. Comb. Chem.*, **2004**, *6*, 611-622
24. ^aNeue, U. D. HPLC Columns: Theory, Technology, and Practice; Wiley-VCH; New York; 1997; p.189-190; ^bMiyabe, K.; Nomura, N.; Morishita, F.; Kurata, S.; Asamura, H.; Imaya, Y. *Anal. Sci.*, **1998**, *14*, 355-359
25. ^aBerendsen, G. E.; Galan, L. D. *J. Liquid Chromatogr.*, **1978**, *1*, 403; ^bDanielson, N. D.; Beaver, L. G.; Wangsa, J. *J. Chromatogr.*, **1991**, *544*, 187-199
26. ^aBerendsen, G. E.; Pikaart, K. A.; de Galan, L. *Anal. Chem.*, **1980**, *52*, 1990-1993; ^bBilliet, H. A. H.; Schoenmakers, P. J.; de Galan, L. *J. Chromatogr.*, **1981**, *218*, 443-454; ^cSadek, P. C.; Carr, P. W. *J. Chromatogr.*, **1984**, *288*, 25-41; ^dReprinted from Billiet, H. A. H.; Schoenmakers, P. J.; de Galan, L. *J. Chromatogr.*, **1981**, *218*, 443-454, Copyright 1981, with permission from Elsevier.
27. ^aLuo, Z.; Zhang, Q.; Oderaotshi, Y.; Curran, D. P. *Science*, **2001**, *291*, 1766-1769; ^bZhang, W.; Luo, Z.; Chen, C. H-T.; Curran, D. P. *J. Am. Chem. Soc.*, **2002**, *124*, 10443-10450; ^cCurran, D. P.; Oderaotshi, Y. *Tetrahedron*, **2001**, *57*, 5243-5253; ^dFrom Luo,

Z.; Zhang, Q.; Oderatoshi, Y.; Curran, D. P. *Science*, **2001**, *291*, 1766-1769. Reprinted with permission from AAAS.

28. ^aCurran, D. P.; Furukawa, T. *Org. Lett.*, **2002**, *4*, 2233-2235; ^bZhang, Q.; Rivkin, A.; Curran, D. P. *J. Am. Chem. Soc.*, **2002**, *124*, 5774-5781; ^cFukui, Y.; Bruckner, A. M.; Shin, Y.; Balachandran, R.; Day, B. W.; Curran, D. P. *Org. Lett.*, **2006**, *8*, 301-304; ^dManku, S.; Curran, D. P. *J. Org. Chem.*, **2005**, *70*, 4470-4473; ^eCurran, D. P.; Moura-Letts, G.; Pohlman, M. *Angew. Chem. Int. Ed. Eng.*, **2006**, *45*, 2423-2436; ^fYang, F.; Newsome, J. J.; Curran, D. P. *J. Am. Chem. Soc.*, **2006**, *128*, 14200-14205; ^gDandapani, S.; Jeske, M.; Curran, D. P. *J. Org. Chem.*, **2005**, *70*, 9447-9462
29. ^aWang, X.; Nelson, S.G.; Curran, D. P. *Tetrahedron*, **2007**, doi:10.1016/j.tet.2007.03.034 (article in press); ^bNelson, S. G.; Spencer, K. L.; Cheung, W. S.; Mamie, S. J. *Tetrahedron*, **2002**, *58*, 7081-7091

Chapter 2

1. Some of the results in this chapter have been published. Wilcox, C.S.; Turkyilmaz, S. *Tetrahedron Lett.*, **2005**, *46*, 1827-1829
2. ^aBerthod, A.; Chang, S. C. C.; Kullman, J. P. S.; Armstrong, D. W. *Talanta*, **1998**, *47*, 1001-1012 ^bZeng, X.; Osseo-Asare, K. *Colloids and Surfaces A: Eng. Aspects*, **2003**, *226*, 45-54; ^cFuchs, G.; Rupprecht, H. *Colloids and Surfaces*, **1983**, *6*, 175-187; ^dBianchini, C.; Barbaro, P.; Santo, V. D.; Gobetto, R.; Meli, A.; Oberhauser, W.; Psaro, R.; Vizza, F. *Adv. Synth. Catal.*, **2001**, *343*, 41-45
3. ^aJursic, B. S. *Synth. Comm.*, **1993**, *23*, 361-364; ^bKadaba, P. K. *Synthesis*, **1973**, 71

4. For a general review of podands see: Gokel, G. W.; Murillo, O. "Podands" in *Supramolecular Chemistry*, eds, Atwood, J. L.; Davies, J. E. D.; Macnicol, D. D.; Vogtle, F., Elsevier, New York, 1996, vol.1, p.1
5. For a general review see: Vogtle, F.; Weber, E. *Angew. Chem. Int. Ed. Eng.*, **1979**, *18*, 753-776
6. Frensdorff, H. K. *J. Am. Chem. Soc.*, **1971**, *93*, 600-606
7. ^aCabiness, D. K.; Margerum, D. W. *J. Am. Chem. Soc.*, **1969**, *91*, 6540; ^bKodama, M. *J. Chem. Soc. Chem. Comm.*, **1975**, 891; ^cJones, T. E.; Zimmer, L. L.; Diaddario, L. L.; Rorabacher, D. B.; Ochrymowicz, L. A. *J. Am. Chem. Soc.*, **1975**, *97*, 7163
8. ^aChan, L. L.; Wong, K. H.; Smid, J. *J. Am. Chem. Soc.*, **1970**, *92*, 1955-1963; ^bTakaki, U.; Smid J. *J. Am. Chem. Soc.*, **1974**, *96*, 2588-2593; ^cChan, L. L.; Smid, J. *J. Am. Chem. Soc.*, **1968**, *90*, 4654-4661; ^dChan, L. L.; Smid, J. *J. Am. Chem. Soc.*, **1967**, *89*, 4547-4549
9. Klamt, A.; Shuuman, G. *J. Chem. Soc. Perkin Trans. 2*, **1991**, 799
10. Greene, T. W. in *Protective Groups in Organic Synthesis*, John Wiley & Sons, 1981, New York, p. 29-32, 61-64, 239-247, 261-264, 272-274, 171-178, 79-82, 83, 97, 195-202, 209-215
11. Kyba, P. K.; Helgeson, R. C.; Madan, K.; Gokel, G. W.; Tarnowski, T. L.; Moore, S. S.; Cram, D. J. *J. Am. Chem. Soc.*, **1977**, *99*, 2564-2571
12. Chaudhari, S. S.; Akamanchi, K. G. *Synlett*. **1999**, *11*, 1763-1765
13. Hamaide, T. *Synth. Comm.* **1990**, *20 (18)*, 2913-2920
14. Wada; Akimori; Shoichi; Nagai; Sotoo *Chem. Phar. Bull.* **1985**, *33 (3)*, 1016-1022

15. Wilcox, C.S.; Gudipati, V; Lu, H.J.; Turkeyilmaz, S.; Curran, D.P. *Angew. Chem. Int. Ed. Eng.*, **2005**, *44*, 6938-6940
16. *Synth. Comm.* **1992**, *22*, 1673
17. *Org. Synth.* **1988**, *IV*, 567
18. Kaleta, Z.; Makowski, B. T.; Soos, T.; Dembinski, R. *Org. Lett.*, **2006**, *8*, 1625-1628
19. ^aJohansson, G.; Percec, V.; Ungar, G.; Smith, K. *Chem. Mater.*, **1997**, *9*, 164-175;
^bMarkowicz, M. W.; Dembinski, R. *Org. Lett.*, **2002**, *4*, 3785-3787

Chapter 3

1. For a good introduction see: Neue, U. D. *HPLC Columns: Theory, Technology, and Practice*, 1997, Wiley-VCH, New York, p: 35-39
2. *ibid.*, p: 13-14
3. Cole, L. A.; Dorsay, J. G. *Anal. Chem.*, **1992**, *64*, 1317-1323
4. Correspondence with Golnar Javadi, Varian Inc.
5. Cheng, W. *Anal. Chem.*, **1985**, *57*, 2409-2412
6. ^aNeue, U. D., *HPLC Columns: Theory, Technology, and Practice*, Wiley-VCH, New York, 1997, p:107-108; ^bRogers, S. D.; Dorsey, J. G. *J. Chromatogr. A*, **2000**, *892*, 57-65
7. Cox, G. B. *J. Chromatogr. A.*, **1993**, *656*, 353
8. Berendsen, G. E.; de Galan, L. *J. Liq. Chromatogr. A.*, **1978**, *1*, 403-426
9. Engelhardt, H.; Jungheim, M. *Chromatographia*, **1990**, *29*, 59-68

10. ^aNahum, A.; Horvath, C. *J. Chromatogr.*, **1981**, *203*, 53-63; ^bBij, K. E.; Horvath, C.; Melander, W. E.; Nahum, A.; *J. Chromatogr.*, **1981**, *203*, 65-84
11. ^aMartire, D. E.; Boehm, R. E. *J. Phys. Chem.* **1983**, *87*, 1045-1062; ^bLochmuller, C. H.; Hunnicutt, M. L.; Mullaney, J. F. *J. Phys. Chem.* **1985**, *89*, 5770-5772
12. ^aBerthod, A.; Chang, S. S. C., Kullman, J. P. S.; Armstrong, D. W. *Talanta*, **1998**, *47*, 1001-1012; ^bKoizumi, K.; Utamura, T.; Okada, Y. *J. Chromatogr.*, **1985**, *321*, 145-157; ^cGrushka, E.; Colin, H.; Guiochon, G. *J. Chromatogr.*, **1982**, *248*, 325-339
13. ^aNeue, U. D. *HPLC Columns: Theory, Technology, and Practice*, 1997, Wiley-VCH, New York, p: 186-187; ^bKuchar, M.; Rejholec, V.; Miller, V.; Kraus, E., *J. Chromatogr.*, **1983**, *280*, 289-295
14. ^a<http://www.molinspiration.com>; ^bReference given in the CaChe calculation suite
15. Pross, Addy *Theoretical and Physical Principles of Organic Reactivity*, 1995, John Wiley & Sons Inc., New York, p: 159-182
16. Hammett, L. P. *J. Am. Chem. Soc.* **1937**, *59*, 96
17. ^aExner, O. *Coll. Czech. Chem. Comm.*, **1964**, *26*, 1094-1113; ^bKrug, R. R.; Hunter, W. G.; Grieger, R. A. *J. Phys. Chem.*, **1976**, *80*, 2335-2341; ^cCornish-Bowden, A. *J. Biosci.*, **2002**, *27*, 121-126
18. Melander, W.; Campbell, D. E.; Horvath, C. *J. Chromatogr.*, **1978**, *158*, 215-225
19. ^aKrug, R. R.; Hunter, W. G.; Grieger, R. A. *J. Phys. Chem.*, **1976**, *80*, 2341-2351; ^bKazusaki, M.; Yamaguchi, T. *Chromatography*, **2006**, *27*, 57-62
20. Kikta, Jr., E. J.; Gruschka, E. *Anal. Chem.*, **1976**, *48*, 1098
21. Lemr, K. *J. Chromatogr. A*, **1996**, *732*, 299-305

22. ^aSchwarzenbach, R. *J. Chromatogr.*, **1977**, *140*, 304-309; ^bVan der Maeden, F. P. B.; Biemond, M. E. F.; Janssen, P. C. G. M. *J. Chromatogr.*, **1978**, *149*, 539-552; ^cNozawa, A.; Ohnuma, T. *J. Chromatogr.*, **1980**, *187*, 261-263; ^dHendrix, J.; Lee, Jr., R. E.; James, H. *J. Chromatogr.*, **1981**, *210*, 45-53; ^eKudoh, M.; Konami, S.; Fudano, S.; Yamaguchi, S. *J. Chromatogr.*, **1982**, *234*, 219-213; ^fEscott, R. E. A.; Brinkworth, S. J., Steedman, T. A. *J. Chromatogr.*, **1983**, *282*, 655-661; ^gKudoh, M.; Kotsui, M.; Fudano, S.; Tsuji, K. *J. Chromatogr.*, **1984**, *295*, 187-191; ^hMarcomini, A.; Capri, S.; Giger, W. *J. Chromatogr.*, **1987**, *403*, 243-252; ⁱBear, G. R. *J. Chromatogr.*, **1988**, *459*, 91-107; ^jDesbene, P. L.; Desmazieres, B.; Basselier, J. J.; Desbene-Monvernay, A. *J. Chromatogr.*, **1989**, *461*, 305-313; ^kRissler, K.; Kunzi, H. P.; Grether, H-J. *J. Chromatogr.*, **1993**, *635*, 89-101; ^lBerek, D.; Mendichi, R. *J. Chromatogr. B*, **2004**, *800*, 69-74; ^mKarakasyan, C.; Millot, M-C.; Jaulmes, A.; Vidal-Madjar, C. *J. Chromatogr. A*, **2006**, *1127*, 108-116; ⁿTrathnigg, B.; Jamelnik, B. *J. Chromatogr. A*, **2007**, *1146*, 78-84
23. ^aSun, C; Baird, M.; Simpson, J. *J. Chromatogr. A*, **1998**, *800*, 231-238; ^bRissler, K. *Chromatographia*, **1998**, *49 (11/12)*, 615-620; ^cChromatogram generated from data in ref. 23b; ^dChromatogram generated from data in ref. 23a
24. ^aMelander, W. R.; Naoum, A.; Horváth, C. *J. Chromatogr.* **1979**, *185*, 129-152; ^bIbrahim, N. M. A.; Wheals, B. B. *J. Chromatogr. A*, **1996**, *731*, 171-177; ^cKamiusuki, T.; Monde, T.; Omae, K.; Morioka, K.; Konakahara, T. *Chromatographia* **2000**, *51*, 390-396; ^dReprinted from Melander, W. R.; Naoum, A.; Horváth, C. *J. Chromatogr.* **1979**, *185*, 129-152 (Figures 3-19-D and 3-19-E only), Copyright 1979, with permission from Elsevier.; ^eVan't Hoff plot generated from data in ref. 24c.
25. Vigh, Gy.; Varga-Puchony, Z. *J. Chromatogr.* **1980**, *196*, 1-9

26. ^aSnyder, L. R.; Dolan, J. W.; Carr, P. W. *J. Chromatogr. A*, **2004**, *1060*, 77-166;
^bJaroniec, M. *J. Chromatogr. A*, **1993**, *656*, 37-50; ^cMartire, D. E. *J. Phys. Chem.* **1983**,
87, 1045-1062
27. ^aBegum, R.; Masatoki, S.; Matsuura, H. *J. Mol. Struct.* **1996**, *384*, 115-120 and references
therein; ^bBegum, R.; Sagawa, T.; Masatoki, S.; Matsuura, H. *J. Mol. Struct.* **1998**, *442*,
243-250; ^cBegum, R.; Matsuura, H. *J. Chem. Soc. Faraday Trans.* **1997**, *93(21)*, 3839-
3848; ^dBegum, R.; Yonemitsu, T.; Matsuura, H. *J. Mol. Struct.* **1998**, *447*, 111-117;
^eSaeki, S.; Kuwahara, N.; Nakata, M.; Kaneko, M. *Polymer*, **1976**, *17*, 685-689;
^fMasatoki, S.; Takamura, M.; Matsuura, H.; Kamogawa, K. Kitagawa, T. *Chem. Lett.*
1995, 991
28. ^aAndersson, M.; Karlström, G. *J. Phys. Chem.* **1985**, *89*, 4957-4962; ^bKarlström, G. *J.*
Phys. Chem. **1985**, *89*, 4962-4964; ^cReprinted with permission from Andersson, M.;
Karlström, G. *J. Phys. Chem.* **1985**, *89*, 4957-4962. Copyright 1985 American Chemical
Society.
29. Kalyanasundaram, K.; Thomas, J. K. *J. Phys. Chem.* **1976**, *80*, 1452-1473;
30. ^aTakahashi, Y.; Tadokoro, H. *Macromolecules*, **1973**, *6*, 672-675; ^bYang, R.; Yang, X.
R.; Evans, D. F.; Hendrikson, W. A. *J. Phys. Chem.*, **1990**, *94*, 6123-6125
31. ^aNorman, A. I.; Fei, Y.; Ho, D. L.; Greer, S. C. *Macromolecules*, **2007**, *40*, 2559-2567;
^bReprinted with permission from Norman, A. I.; Fei, Y.; Ho, D. L.; Greer, S. C.
Macromolecules, **2007**, *40*, 2559-2567 (Figure 3-19-F only). Copyright 2007 American
Chemical Society.
32. ^aViti, V.; Zampetti, P. *Chem. Phys.* **1973**, *2*, 233; ^bViti, V.; Indovina, P. L.; Podo, F.;
Radics, L.; Nemety, G. *Mol. Phys.*, **1974**, *27*, 541

Chapter 4

1. Kane, R. *Ann. Physik. Chem.*, **1838**, *44*, 475; Kane, R., *J. Prakt. Chem.*, **1838**, *15*, 219
2. Evans, D. A.; Nelson, J. V.; Vogel, E.; Taner, T. R. *J. Am. Chem. Soc.*, **1981**, *103*, 3099-3111; Evans, D. A.; Bartroli, J.; Shih, T. L., *J. Am. Chem. Soc.*, **1981**, *103*, 2127-2129; Evans, D. A., Takacs, J. M.; McGee, L. R.; Ennis, M. D.; Mathre, D. J.; *Pure & Appl. Chem.*, **1981**, *53*, 1109-1127
3. Zimmerman, Traxler, *J. Am. Chem. Soc.*, **1957**, *79*, 1920
4. Desimoni, G.; Faita, G.; Galbiati, A.; Pasini, D.; Quadrelli, P.; Rancati, F., *Tetrahedron Asymmetry*, **2002**, *13*, 333-337
5. Phoon, C. W.; Abell, C., *Tetrahedron Lett.*, **1998**, *39*, 2655-2658
6. Evans, D.A.; Emins, M.D.; Mathre, D.J., *J. Am. Chem. Soc.*, **1982**, *104*, 1737-1739
7. Kagoshima, H.; Hashimoto, Y.; Oguro, D.; Saigo, K., *J. Org. Chem.*, **1998**, *63*, 691-697
8. a. Green, R.; Taylor, P.J.M.; Bull, S.D.; James, T.D.; Mahon, M.F.; Merritt, A.T., *Tetrahedron Asymm.*, **2003**, *14*, 2619-2623; b. Faita, G.; Paio, A; Quadrelli, P.; Rancati, F.; Seneci, P., *Tetrahedron Lett.*, **2000**, *41*, 1265; c. Sudharsan, M.; Hultin, P.G., *Synlett.*, **1997**, 171, Gage, J.R.; Evans, D.A., *Org. Synth.*, **1990**, 68-78; d. Phoon, C.W.; Abell, C., *Tetrahedron Lett.*, **1998**, *39*, 2655; e. Purandare, A.V.; Natarajan, S., *Tetrahedron Lett.*, **1997**, *38*, 8777; f. Burgess, K.; Lim, D.J., *Chem. Comm.*, **1997**, 785
9. a. Faita, G.; Paio, A; Quadrelli, P.; Rancati, F.; Seneci, P., *Tetrahedron*, **2001**, *57*, 8313-8322; b. Ganguly, A.K.; Seah, N.; Popov, V.; Wang, C.H.; Kuang, R.; Saksena, A.K.; Pramanik, B.N.; Chan, T.M.; McPhail, A.T., *Tetrahedron Lett.*, **2002**, *43*, 8981-8083; c.

- Allin, M.S., Shuttleworth, S.J., *Tetrahedron Lett.*, **1996**, *37*, 8023-8026; d. Richter, L.S., Gadek, T.R., *Tetrahedron Lett.*, **1994**, *35*, 4705-4706
10. Ager, D.J.; Prakash, I.; Schaad, D.R., *Chem. Rev.*, **1996**, *96*, 835-875
11. a. Mikhailov, B.M.; Bubnov Y.N. in *Organoboron Compounds in Organic Synthesis*, OPA Amsterdam B.V., 1984, pp 255-278; b. Brown, H.C. in *Organic Synthesis Via Boranes*, John Wiley & Sons, New York, 1975, pp 239-261
12. a. Koster, R.; Frenzl, W., *Liebigs Ann. Chem*, **1974**, 69-100; b. Koster, R.; Frenzl, W.; Seidel, G., *Liebigs Ann. Chem*, **1975**, 352-372
13. Baker, R.; Castro, J.L.; Swain, C.J., *Tetrahedron Lett.*, **1988**, *29*, 2247-2250
14. Inoue, T.; Mukaiyama, T., *Bull. Chem. Soc. Jpn.*, **1980**, *53*, 174-178
15. Danda, H., Hansen, M.H., Heathcock, C.H., *J. Org. Chem.*, **1990**, *55*, 173-181
16. *J. Org. Chem.*, **2001**, *66*, 8463-8469
17. a. Evans, D.A.; Bender, S.L., *Tetrahedron Lett.*, **1986**, *27*, 799-802; b. Evans, D.A.; Sjogren, E.B.; Bartoli, J.; Dow, R.L., *Tetrahedron Lett.*, **1986**, *27*, 4957-4960; c. Evans, D.A.; Ellman, J.A.; Dow, R.L., *Tetrahedron Lett.*, **1987**, *28*, 1123-1126; d. Evans, D.A.; Morrissey, M.M.; Dow, R.L., *J. Am. Chem. Soc.*, **1985**, *107*, 4346-4348; e. Evans, D.A.; Britton, T.C.; Ellman, J.A., *Tetrahedron Lett.*, **1987**, *28*, 6141-6144
18. a. Hashimoto, N.; Aoyama, T.; Shioiri, T., *Chem. Pharm. Bull.*, **1981**, *29*, 1475-1478; b. Hudlicky, M., *J. Org. Chem.*, **1980**, *45*, 5377-5378
19. Heathcock, C.H. in *Asymmetric Synthesis*, Academic Press, New York, NY, **1984**, Vol. 3, pp 111-212
20. Oppolzer, W.; Blagg, J.; Rodriguez, I.; Walther, E., *J. Am. Chem. Soc.*, **1990**, *112*, 2767-2772

21. *J. Org. Chem.* **2000**, *65*, 3754-3760
22. Kim, M-S.; Jun, J-G., *Synth. Comm.*, **2002**, *32*, 3851-3864
23. Casper, D.M.; Burgeson, J.R.; Esken, J.M.; Ferrence, G.M.; Hitchcock, S.R., *Org. Lett.*, **2002**, *4*, 3739-3742
24. Banks, M.R.; Cadogan, J.I.G.; Gosney, I.; Gould, R.O.; Hodgson, P.K.G.; McDougall, D., *Tetrahedron*, **1998**, *54*, 9765-9784
25. Yan, T-H.; Tan, C-W.; Lee, H-C.; Lo, H-C.; Huang, T-Y., *J. Am. Chem. Soc.*, **1993**, *115*, 2613-2621
26. Ahn, K.Y.; Yoo, J.J.; Kim, J.S., *Tetrahedron Lett.*, **1992**, *33*, 6661-6664
27. Hsiao, C-N.; Liu, L.; Miller, M.J., *J. Org. Chem.*, **1987**, *52*, 2201-2206
28. ^aHein, E. H.; Hultin, P. G. *Synlett.* **2003**, *5*, 635-638; ^bHein, E. H.; Hultin, P. G. *Tetrahedron Asymm.* **2005**, *16*, 2341-2347
29. Ding, X. M.S. Thesis, University of Pittsburgh, Pittsburgh, PA 15260, 2006